



Terms and Conditions of Use of Digitised Theses from Trinity College Library Dublin

Copyright statement

All material supplied by Trinity College Library is protected by copyright (under the Copyright and Related Rights Act, 2000 as amended) and other relevant Intellectual Property Rights. By accessing and using a Digitised Thesis from Trinity College Library you acknowledge that all Intellectual Property Rights in any Works supplied are the sole and exclusive property of the copyright and/or other IPR holder. Specific copyright holders may not be explicitly identified. Use of materials from other sources within a thesis should not be construed as a claim over them.

A non-exclusive, non-transferable licence is hereby granted to those using or reproducing, in whole or in part, the material for valid purposes, providing the copyright owners are acknowledged using the normal conventions. Where specific permission to use material is required, this is identified and such permission must be sought from the copyright holder or agency cited.

Liability statement

By using a Digitised Thesis, I accept that Trinity College Dublin bears no legal responsibility for the accuracy, legality or comprehensiveness of materials contained within the thesis, and that Trinity College Dublin accepts no liability for indirect, consequential, or incidental, damages or losses arising from use of the thesis for whatever reason. Information located in a thesis may be subject to specific use constraints, details of which may not be explicitly described. It is the responsibility of potential and actual users to be aware of such constraints and to abide by them. By making use of material from a digitised thesis, you accept these copyright and disclaimer provisions. Where it is brought to the attention of Trinity College Library that there may be a breach of copyright or other restraint, it is the policy to withdraw or take down access to a thesis while the issue is being resolved.

Access Agreement

By using a Digitised Thesis from Trinity College Library you are bound by the following Terms & Conditions. Please read them carefully.

I have read and I understand the following statement: All material supplied via a Digitised Thesis from Trinity College Library is protected by copyright and other intellectual property rights, and duplication or sale of all or part of any of a thesis is not permitted, except that material may be duplicated by you for your research use or for educational purposes in electronic or print form providing the copyright owners are acknowledged using the normal conventions. You must obtain permission for any other use. Electronic or print copies may not be offered, whether for sale or otherwise to anyone. This copy has been supplied on the understanding that it is copyright material and that no quotation from the thesis may be published without proper acknowledgement.

**Preventing protein-dependent biofilm formation in
Staphylococcus aureus by targeting the serine aspartate
repeat protein C and fibronectin binding proteins.**

A thesis submitted for the degree of Doctor in Philosophy

by

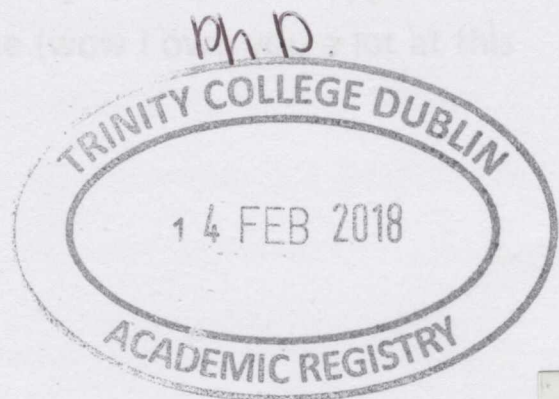
Leanne Hays

Moyne Institute of Preventive Medicine

Department of Microbiology

School of Genetics and Microbiology

Trinity College Dublin



SCHOOL OF GENETICS
AND MICROBIOLOGY

50763114



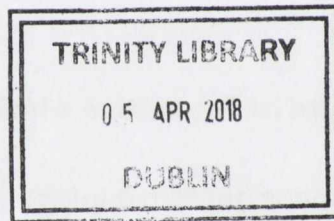
THESIS

11544

Declaration

I declare that this thesis has not been submitted as an exercise for a degree at this or any other university and it is entirely my own work, except where it is duly acknowledged in the text.

I agree to deposit this thesis in the University's open access institutional repository or allow the library to do so on my behalf, subject to Irish Copyright Legislation and Trinity College Library conditions of use and acknowledgement.



11544

Acknowledgements

I would like to thank the Irish Research Council for supporting my PhD through a Government of Ireland Postgraduate Scholarship. I would also like to thank the Microbiology Society for their generosity in supporting early stage researchers like myself to attend both national and international conferences. I would like to thank all the staff and students in the Moyne, both past and present, for their support throughout my PhD and for inspiring my interest in microbiology during my undergraduate degree. I would like to thank my thesis committee; Prof. Tim Foster and Dr. Kim Roberts. I'd also like to mention all participants in Moyne and MicroSoc events for providing many fun and memorable nights out and for fostering my love of wine and cheese.

I would like to thank Dr. Marian Brennan in RCSI who was an essential collaborator and hugely helpful to me during my PhD.

I would like to sincerely thank my PhD supervisor Dr. Joan Geoghegan for giving me this opportunity, supporting my work and teaching me how to become an independent researcher. Joan is always available for her students to discuss and help them with their projects. I always enjoy discussing science and ideas with her and members of the lab.

I'd like to thank all the members of the Geoghegan lab past and present; Dee, Dara, Orla, Joana, Aisling, Marta and Keenan for their constant support and friendship over the last 4 years. We've had many laughs and I've made some lasting friendships! I'd like to send a big thank you to Dee and Fiona Burke for their numerous protein purifications which were an unbelievable help to my work. I've also made a best friend; Joana, during the PhD which I am truly grateful for. Thank you Moyne. Beijinhos!

A huge thank you to my family; my parents Deirdre and Greg and my brother Paul. They have always encouraged and supported me without any pressure. I am so lucky to be a part of the Hays family.

And finally, to my partner Michael Prunty who has been my number one support and companion throughout my PhD. Thank you again Moyne (wow I owe you a lot at this stage). Ti amo Michele!

Summary

Staphylococcus aureus is a leading cause of biofilm infections on indwelling medical devices. *S. aureus* biofilm infections are intrinsically difficult to treat. They are recalcitrant to conventional antibiotics and resistant to host immune phagocytosis. Thus, treatment often involves removal of the device and new preventive and treatment strategies are greatly required. *S. aureus* biofilm formation is multifactorial and considered to occur through three distinct phases; primary attachment, accumulation and maturation and biofilm dispersal. Several cell wall-anchored proteins of *S. aureus* mediate biofilm accumulation. Proteins on adjacent cells form homophilic interactions causing cells to aggregate and biofilm to accumulate. These include the serine aspartate repeat protein C (SdrC) and the fibronectin binding proteins (FnBP) A and B. FnBPs also mediate *S. aureus* adherence to the host plasma protein fibrinogen (Fg) which is important for primary attachment of *S. aureus* to biotic surfaces. However, FnBP-mediated biofilm accumulation and adherence to Fg are mediated by two distinct mechanisms. This study investigated SdrC and FnBPs as novel targets for anti-biofilm agents in order to prevent *S. aureus* biofilm formation.

Molecular modelling and *in silico* docking techniques were used to identify putative inhibitors targeting SdrC and FnBP homophilic interactions in biofilm. Using this approach several small molecule inhibitors were identified which bound recombinant SdrC and inhibited SdrC-mediated biofilm *in vitro* without affecting bacterial growth. A peptide inhibitor of SdrC-mediated biofilm was also identified. In targeting FnBPs, four small molecule inhibitors were identified which inhibited FnBP-dependent biofilm of HA-MRSA strains *in vitro* without affecting bacterial growth and three, of the four small molecules, inhibited recombinant FnBPA-FnBPA homophilic interactions. Furthermore, the FnBP biofilm inhibitors did not inhibit FnBP-mediated adherence of *S. aureus* to Fg highlighting their specificity as biofilm accumulation inhibitors. This highlighted the potential for proteins which mediate biofilm accumulation to be targets for preventive agents.

This study also identified three inhibitors of FnBP-mediated adherence of *S. aureus* to Fg using *in silico* docking methods. Two of the three inhibitors were demonstrated to

inhibit both FnBPA- and FnBPB-Fg binding. These small molecules may serve as anti-adhesion inhibitors in the prevention of *S. aureus* primary attachment to biotic surfaces. Thus, inhibitors of two steps in *S. aureus* biofilm formation; primary attachment and biofilm accumulation, were identified in this study. The agents identified here may serve as scaffolds for further drug design.

This study also further characterised SdrC and FnBP interactions in biofilm at the molecular level. SdrC was found to promote biofilm formation in a clinically relevant HA-MRSA strain, MRSA252. FnBPA homophilic interactions were localised to subdomain N2 with five isotypes of FnBPA shown to mediate biofilm. FnBPB homophilic N2N3 interactions were demonstrated and heterophilic FnBPA and FnBPB interactions identified *in vitro*. Further characterisation of the molecular mechanisms underlying biofilm formation will also aid in the generation of novel preventive and treatment strategies against *S. aureus* biofilm infections.

Publications

Feuillie C*, Formosa-Dague C*, Hays LMC*, Vervaeck O, Derclaye S, Brennan MP, Foster TJ, Geoghegan JA, Dufrêne YF. 2017. Biofilm accumulation by the staphylococcal protein SdrC: molecular mechanism and inhibition. *Proceedings of the National Academy of Sciences of the United States of America*. 114(14):3738-3743.

*Joint first authors

Hays LMC, Zapotoczna M, Pietrocola G, Speziale P, Geoghegan JA. Preventing biofilm formation in methicillin resistant *Staphylococcus aureus* using molecules that inhibit the N2 subdomain of fibronectin binding protein A. In review.

Table of contents

| | |
|---|-------|
| Declaration | ii |
| Acknowledgements | iii |
| Summary | iv |
| Publications | vi |
| List of tables | xiv |
| List of figures | xv |
| Key to abbreviations | xviii |
| | |
| Chapter 1 Introduction | |
| 1.1 Characteristics of staphylococci..... | 2 |
| 1.2 <i>S. aureus</i> host interactions..... | 3 |
| 1.2.1 Colonisation..... | 3 |
| 1.2.1.1 Human nasopharynx..... | 3 |
| 1.2.1.2 Human skin..... | 4 |
| 1.2.2 Infection..... | 5 |
| 1.3 The <i>S. aureus</i> cell envelope..... | 6 |
| 1.4 <i>S. aureus</i> cell wall-anchored protein families..... | 7 |
| 1.4.1 MSCRAMM family..... | 9 |
| 1.4.1.1 'Dock, Lock and Latch'..... | 10 |
| 1.4.2 NEAT motif family..... | 12 |
| 1.4.3 Three-helical bundle family..... | 13 |

| | |
|---|----|
| 1.4.4 G5-E repeat family..... | 13 |
| 1.4.5 Legume-lectin family..... | 14 |
| 1.4.6 Major functions of the CWA proteins..... | 14 |
| 1.4.6.1 Adhesion to host proteins..... | 14 |
| 1.4.6.2 Invasion of host cells..... | 15 |
| 1.4.6.3 Immune evasion..... | 20 |
| 1.5. Biofilm formation by <i>S. aureus</i> | 20 |
| 1.5.1 Primary Attachment..... | 22 |
| 1.5.1.1 Abiotic attachment..... | 22 |
| 1.5.1.2 Biotic attachment..... | 23 |
| 1.5.2 Biofilm Accumulation and Maturation..... | 24 |
| 1.5.2.1 Polysaccharide Intercellular Adhesin..... | 26 |
| 1.5.2.2 Cell wall-anchored proteins..... | 27 |
| 1.5.2.2.1 Fibronectin binding protein-mediated biofilm accumulation..... | 27 |
| 1.5.2.2.2 Serine aspartate repeat protein C..... | 29 |
| 1.5.2.2.3 Clumping factor B..... | 29 |
| 1.5.2.2.4 <i>S. aureus</i> surface protein G..... | 29 |
| 1.5.2.2.5 Protein A..... | 30 |
| 1.5.2.2.6 <i>S. aureus</i> surface protein C..... | 31 |
| 1.5.2.2.7 Serine rich adhesin for platelets..... | 31 |
| 1.5.2.2.8 Biofilm-associated protein..... | 31 |

| | |
|--|----|
| 1.5.2.2.9 <i>S. aureus</i> surface protein X..... | 32 |
| 1.5.2.3 Fibrin-dependent biofilm accumulation..... | 32 |
| 1.5.2.4 Extracellular DNA and cytosolic proteins..... | 33 |
| 1.5.3 Biofilm Dispersal..... | 34 |
| 1.6 Similarities of biofilm formation by <i>S. epidermidis</i> | 36 |
| 1.7 Difficulties in the treatment of biofilm infections..... | 37 |
| 1.7.1 Resistance to host immune phagocytosis..... | 37 |
| 1.7.2 Recalcitrance to conventional antibiotics..... | 38 |
| 1.7.3 Antibiotic resistance..... | 39 |
| 1.7.3.1 Methicillin resistant <i>S. aureus</i> | 40 |
| 1.8 Treatment and prevention of <i>S. aureus</i> biofilm infections..... | 41 |
| 1.8.1 Anti-biofilm agents..... | 42 |
| 1.8.1.1 Preventing <i>S. aureus</i> primary attachment..... | 42 |
| 1.8.1.2 Chelation of metals..... | 43 |
| 1.8.1.3 Degradation of the extracellular matrix..... | 44 |
| 1.8.1.4 Promoting biofilm dispersal..... | 44 |
| 1.8.2 Vaccines against <i>S. aureus</i> | 45 |
| 1.8.2.1 <i>S. aureus</i> vaccine development..... | 45 |
| 1.8.2.2 Active and passive immunization against biofilm infections..... | 47 |
| 1.9 Aims and Objectives..... | 49 |
| Chapter 2 Materials and Methods | |
| 2.1. Bacterial strains and growth conditions..... | 51 |

| | |
|--|----|
| 2.2. DNA cloning and strain construction..... | 51 |
| 2.2.1 Cloning of DNA for recombinant protein expression in <i>E. coli</i> | 51 |
| 2.2.2 Generation of chimeric pQE30:: <i>fnbA</i> _{N2N3} plasmids with residues of the N2 subdomain replaced with ClfA sequence..... | 52 |
| 2.2.3 Generation of an <i>sdrC</i> deletion mutant of <i>S. aureus</i> strain MRSA252..... | 53 |
| 2.2.4 Generation of chimeric FnBPA plasmids carrying the N1N2N3 subdomains of different FnBPA isotypes..... | 53 |
| 2.3 <i>In silico</i> generation of homology models of SdrC and FnBPB..... | 54 |
| 2.4 <i>In silico</i> docking of small molecule libraries and selection of putative inhibitors.... | 54 |
| 2.5 Synthetic peptide..... | 55 |
| 2.6 <i>In silico</i> modelling of the SdrC- β -neurexin derived peptide complex..... | 55 |
| 2.7 Expression and purification of recombinant proteins..... | 55 |
| 2.7.1 Nickel Affinity Chromatography..... | 55 |
| 2.7.2 Glutathione Affinity Chromatography..... | 56 |
| 2.8 Western immunoblot..... | 56 |
| 2.9 Differential Scanning Fluorimetry..... | 57 |
| 2.10 Biofilm microtitre plate assays..... | 57 |
| 2.10.1 Biofilm assays with <i>L. lactis</i> | 57 |
| 2.10.2 Biofilm assays with <i>S. aureus</i> | 57 |
| 2.10.3 Biofilm inhibition assays..... | 57 |
| 2.10.4 Biofilm dispersal assay..... | 58 |

| | |
|--|----|
| 2.11 IC ₅₀ analysis of the β -neurexin derived peptide..... | 58 |
| 2.12 Growth curves..... | 58 |
| 2.13 Single cell spectroscopy..... | 59 |
| 2.14 Site directed mutagenesis..... | 59 |
| 2.15 Ligand affinity dot blot..... | 59 |
| 2.16 Enzyme-Linked Immunosorbent Assays (ELISA)..... | 59 |
| 2.16.1 SdrC-SdrC ELISA..... | 59 |
| 2.16.2 FnBP-FnBP ELISA..... | 60 |
| 2.17 Fibronectin binding assays..... | 60 |
| 2.18 Fibrinogen binding assays..... | 61 |
| 2.19 Amino acid alignments..... | 61 |
| 2.20 Statistical analyses..... | 62 |
| Chapter 3 <i>In silico</i> identification of novel inhibitors of serine aspartate repeat protein C-mediated biofilm formation of <i>Staphylococcus aureus</i> | |
| 3.1 Introduction..... | 70 |
| 3.2 Results..... | 75 |
| 3.2.1 <i>In silico</i> molecular modelling of the structure of SdrC N2N3 subdomains..... | 75 |
| 3.2.2 <i>In silico</i> analysis of RPGSV and VDQYT motifs..... | 79 |
| 3.2.3 <i>In silico</i> docking of two small molecule libraries targeting SdrC..... | 81 |
| 3.2.4 Assessment of the ability of putative SdrC inhibitors to bind recombinant SdrC by Differential Scanning Fluorimetry..... | 92 |

| | |
|--|-----|
| 3.2.5 <i>In silico</i> docking of a peptide ligand of SdrCN2N3..... | 96 |
| 3.2.6 Binding of the β -neurexin derived peptide to SdrC is not detected by Differential Scanning Fluorimetry..... | 96 |
| 3.2.7 Assessment of small molecules and the β -neurexin derived peptide for inhibition of SdrC-mediated biofilm using the surrogate host <i>L. lactis</i> expressing SdrC..... | 98 |
| 3.2.8 The β -neurexin derived peptide inhibits SdrC-mediated biofilm with an IC ₅₀ of ~0.9 μ M..... | 100 |
| 3.2.9 The peptide biofilm inhibitor does not disperse a mature biofilm..... | 100 |
| 3.2.10 The SdrC peptide inhibitor does not inhibit biofilm mediated by FnBPs but inhibits biofilm formed by the HA-MRSA isolate MRSA252..... | 104 |
| 3.2.11 Generation of an <i>sdrC</i> deficient mutant of MRSA252 (MRSA252 Δ <i>sdrC</i>) by allelic exchange..... | 106 |
| 3.2.12 SdrC promotes biofilm formation in the HA-MRSA strain MRSA252.... | 106 |
| 3.2.13 SdrC forms specific homophilic interactions between MRSA252 cells.. | 109 |
| 3.2.14 Assessment of SdrC inhibitors for inhibition of MRSA252 biofilm..... | 111 |
| 3.2.15 Residue R ₂₄₇ of the RPGSV motif is important for SdrC-SdrC interactions..... | 114 |
| 3.3 Discussion..... | 116 |
| Chapter 4 Characterisation of fibronectin binding protein interactions in biofilm and identification of anti-biofilm molecules which target fibronectin binding proteins | |
| 4.1 Introduction..... | 123 |
| 4.2 Results..... | 127 |
| 4.2.1 FnBPA homophilic interactions are mediated by subdomain N2..... | 127 |

| | |
|---|-----|
| 4.2.2 Sequence variation in subdomain N2 does not affect the ability of FnBPA to promote biofilm formation..... | 130 |
| 4.2.3 Recombinant FnBPA and FnBPB can form heterophilic interactions <i>in vitro</i> | 132 |
| 4.2.4 Localisation of FnBPA dimerization sites in subdomain N2..... | 134 |
| 4.2.5 Recombinant FnBPB forms homophilic interactions <i>in vitro</i> and both subdomains N2 and N3 participate..... | 138 |
| 4.2.6 Identification of putative small molecule inhibitors of FnBP-mediated biofilm using <i>in silico</i> approaches..... | 140 |
| 4.2.7 Assessment of small molecules for inhibition of FnBP-mediated biofilm of HA-MRSA strains..... | 142 |
| 4.2.8 Assessment of small molecules for inhibition of recombinant FnBPA-FnBPA interactions <i>in vitro</i> | 145 |
| 4.2.9 FnBP biofilm inhibitors do not inhibit FnBP-mediated adherence to fibrinogen..... | 145 |
| 4.2.10 Assessment of the ability of FnBP biofilm inhibitors to bind recombinant FnBPA _{N2N3} protein by Differential Scanning Fluorimetry..... | 148 |
| 4.2.11 Identification of inhibitors of FnBP-mediated adherence to fibrinogen..... | 150 |
| 4.2.12 Small molecules LH6 and LH7 inhibit both FnBPA- and FnBPB- mediated bacterial adherence to fibrinogen..... | 154 |
| 4.2.13 <i>In silico</i> docking of LH6, LH7 and LH10 onto a homology model of FnBPB _{N2N3} | 154 |
| 4.2.14 Assessment of the ability of small molecules LH6, LH7 and LH10 to bind recombinant FnBPA _{N2N3} and FnBPB _{N2N3} by Differential Scanning Fluorimetry..... | 158 |

| | |
|---------------------|-----|
| 4.3 Discussion..... | 162 |
|---------------------|-----|

Chapter 5 Discussion

| | |
|---------------------|-----|
| 5.1 Discussion..... | 169 |
|---------------------|-----|

References

| | |
|-----------------|-----|
| References..... | 179 |
|-----------------|-----|

List of Tables

| | |
|--|-----|
| Table 1.1 Functions of the <i>S. aureus</i> cell wall-anchored proteins..... | 16 |
| Table 2.1 Bacterial strains and plasmids used in this study..... | 63 |
| Table 2.2 Primers..... | 67 |
| Table 3.1 SdrCN2N3 homology models generated by Phyre ² | 77 |
| Table 3.2 Chemical structures of compounds from the Zinc library screen selected for <i>in vitro</i> screening..... | 83 |
| Table 3.3 <i>In silico</i> docking results of compounds from the Zinc library screen..... | 84 |
| Table 3.4 Chemical structures of compounds from the 'Malaria Box'..... | 87 |
| Table 3.5 <i>In silico</i> docking results of compounds from 'The Malaria box' screen..... | 90 |
| Table 3.6 ΔT_m of recombinant SdrC in the presence of small molecules..... | 95 |
| Table 4.1 Doubling times of BH1CC with DMSO or small molecules LH1-5..... | 144 |
| Table 4.2 ΔT_m of recombinant FnBPA _{N2N3} in the presence of small molecule FnBP biofilm inhibitors..... | 149 |
| Table 4.3 Predicted contacts of compounds LH6, LH7 and LH10 to FnBPA..... | 152 |
| Table 4.4 ΔT_m of recombinant FnBP proteins in the presence of small molecule inhibitors of FnBP-Fg binding..... | 159 |

List of Figures

| | |
|---|-----|
| Fig 1.1 Structural organization of <i>S. aureus</i> cell wall-anchored proteins..... | 8 |
| Fig 1.2 'Dock, Lock and Latch' mechanism of MSCRAMM-ligand binding..... | 11 |
| Fig 1.3 Biofilm formation by <i>S. aureus</i> occurs over three distinct phases..... | 21 |
| Fig 1.4 Scanning electron micrographs of PIA-dependent and protein-dependent biofilms..... | 25 |
| Fig 3.1 Schematic of the MSCRAMM domain organization..... | 72 |
| Fig 3.2 Principles of Differential Scanning Fluorimetry (DSF)..... | 74 |
| Fig 3.3 Homology models of SdrCN2N3..... | 76 |
| Fig 3.4 Position of the RPGSV and VDQYT motifs..... | 80 |
| Fig 3.5 Recombinant SdrC N2N3..... | 93 |
| Fig 3.6 Differential scanning fluorimetry of recombinant SdrC N2N3 in the presence of small molecules..... | 94 |
| Fig 3.7 Model of the β -neurexin derived peptide in complex with SdrC..... | 97 |
| Fig 3.8 DSF of recombinant SdrC in the presence of the β -neurexin derived peptide... | 97 |
| Fig 3.9 Assessment of small molecules and peptide for inhibition of SdrC-mediated biofilm..... | 99 |
| Fig 3.10 Representative growth curves of <i>L. lactis</i> with SdrC inhibitors..... | 101 |
| Fig 3.11 The β -neurexin derived peptide inhibits SdrC mediated biofilm with an IC_{50} of $\sim 0.9 \mu M$ | 102 |
| Fig 3.12 The peptide biofilm inhibitor does not disperse a mature biofilm..... | 103 |
| Fig 3.13 The SdrC peptide inhibitor does not inhibit FnBP-mediated biofilm but inhibits MRSA252 biofilm..... | 105 |

| | |
|--|-----|
| Fig 3.14 Generation of an <i>sdrC</i> deficient mutant of MRSA252..... | 107 |
| Fig 3.15 SdrC promotes biofilm in MRSA252..... | 108 |
| Fig 3.16 SdrC homophilic interactions between MRSA252 cells..... | 110 |
| Fig 3.17 Assessment of inhibition of MRSA252 biofilm..... | 112 |
| Fig 3.18 Assessment of LH4 and LH10 for inhibition of MRSA252 growth and biofilm..... | 113 |
| Fig 3.19 Residue R ₂₄₇ is important for SdrC homophilic interactions..... | 115 |
| Fig 4.1 Domain organization of FnBPs..... | 124 |
| Fig 4.2 ELISA to assess FnBPA-FnBPA interactions <i>in vitro</i> | 128 |
| Fig 4.3 FnBPA homophilic interactions are mediated by subdomain N2..... | 129 |
| Fig 4.4 Assessment of the ability of BH1CCΔ <i>fnbAfnbB</i> (pFnBA4) isotype I, III, IV, V and VI strains to adhere to fibronectin and mediate biofilm accumulation..... | 131 |
| Fig 4.5 Recombinant FnBPA and FnBPB form heterophilic interactions <i>in vitro</i> | 133 |
| Fig 4.6 <i>In silico</i> analyses of conserved amino acids in FnBPA and FnBPB N2..... | 135 |
| Fig 4.7 Assessment of FnBPA variants for the ability to form FnBPA-FnBPA interactions..... | 137 |
| Fig 4.8 FnBPB homophilic interactions are mediated by subdomains N2 and N3..... | 139 |
| Fig 4.9 Predicted docking sites of small molecules on FnBPA..... | 141 |
| Fig 4.10 Inhibition of FnBP-dependent biofilm by small molecules..... | 143 |
| Fig 4.11 FnBP biofilm inhibitors have no effect on <i>S. aureus</i> growth..... | 144 |
| Fig 4.12 Small molecules inhibit recombinant FnBPA-FnBPA interactions <i>in vitro</i> | 146 |
| Fig 4.13 FnBP biofilm inhibitors do not inhibit FnBP-mediated adherence to fibrinogen..... | 147 |

| | |
|---|-----|
| Fig 4.14 Predicted docking sites of LH6, LH7 and LH10 on FnBPA..... | 151 |
| Fig 4.15 Inhibition of FnBP-mediated adherence to fibrinogen by LH6, LH7 and LH10..... | 153 |
| Fig 4.16 LH6 and LH7 inhibit FnBPA- and FnBPB-mediated adherence to fibrinogen.. | 156 |
| Fig 4.17 Predicted docking sites of LH6, LH7 and LH10 on FnBPB..... | 157 |
| Fig 4.18 LH7 significantly increases the melting temperature of FnBPB _{N2N3} | 160 |
| Fig 5.1 Shared small molecule substructures..... | 176 |
| Fig 5.2 Summary model of biofilm inhibitors identified in this study..... | 178 |

Key to abbreviations

| | |
|---------|--|
| Sdr | serine aspartate repeat protein |
| FnBP | fibronectin binding protein |
| CWA | Cell wall-anchored |
| WTA | Wall teichoic acid |
| LTA | Lipoteichoic acid |
| CP | Capsular polysaccharide |
| MSCRAMM | Microbial surface components recognizing adhesive matrix molecules |
| DLL | Dock, Lock and Latch |
| Clf | Clumping factor |
| Cna | Collagen adhesin |
| NEAT | Near iron transporter |
| Isd | Iron-regulated surface determinant |
| Sas | <i>S. aureus</i> surface protein |
| SraP | Serine rich adhesin for platelets |
| IgG | Immunoglobulin |
| Fg | Fibrinogen |
| Fn | Fibronectin |
| FnBR | Fibronectin binding repeat |
| ECM | Extracellular matrix |
| Atl | Autolysin |
| PIA | Polysaccharide Intercellular Adhesin |
| PNAG | Poly- β -1,6- <i>N</i> -acetylglucosamine |
| Bap | Biofilm-associated protein |
| eDNA | Extracellular DNA |
| PSM | Phenol soluble modulins |
| Agr | Accessory gene regulator |
| AIP | Autoinducing peptide |
| Ses | <i>S. epidermidis</i> surface protein |
| Aap | Accumulation-associated protein |
| HA-MRSA | Hospital associated methicillin resistant <i>S. aureus</i> |

| | |
|---------------------|---|
| CA-MRSA | Community associated methicillin resistant <i>S. aureus</i> |
| MntC | Manganese transporter protein C |
| TSB | Tryptic soy broth |
| BHI | Brain heart infusion |
| w/v | Weight per volume |
| v/v | Volume per volume |
| DNA | Deoxyribonucleic acid |
| PCR | Polymerase chain reaction |
| kb | kilobases |
| kDa | Kilodalton |
| SLIC | Sequence and ligation-independent cloning |
| His | Hexahistidine |
| GST | Glutathione S-transferase |
| SDS-PAGE | Sodium dodecyl sulphate polyacrylamide gel electrophoresis |
| PVDF | Polyvinylidene fluoride |
| DSF | Differential Scanning Fluorimetry |
| T _m | Melting temperature |
| OD _{600nm} | Optical density measured at 600 nm |
| A _{570nm} | Absorbance measured at 570 nm |
| A _{450nm} | Absorbance measured at 450 nm |
| IC ₅₀ | Concentration where 50 % inhibition is observed |
| DMSO | Dimethyl sulfoxide |
| AFM | Atomic force microscopy |
| ELISA | Enzyme-linked immunosorbent assay |
| Amp ^r | Ampicillin resistance |
| Cm ^r | Chloramphenicol resistance |
| Erm ^r | Erythromycin resistance |
| MLST | Multilocus sequence type |
| CC | Clonal complex |
| SEM | Standard error of the mean |

Chapter 1

Introduction

1.1 Characteristics of staphylococci.

Staphylococci are a Gram-positive genus of bacteria originally observed by Ogston in 1882 (Baird-Parker, 1965). Staphylococci are a member of the phylum *Firmicutes*, within the class *Bacilli* and of the order *Bacillales* (Becker & von Eiff, 2011). More specifically, within the order *Bacillales*, the genus belongs to the family *Staphylococcaceae* (Becker & von Eiff, 2011). They are typically golden, cream or white in colour and under a microscope are visualized as cocci in grape-like clusters. These clusters are a result of staphylococcal cell division which occurs across more than one plane (Tzagoloff & Novick, 1977). This is phenotypically different to the genus *Streptococcus* which divide on a single plane forming strings of cells. Staphylococci are catalase positive, oxidase-negative, facultative anaerobes. They are non-motile and do not form spores (Corrigan *et al.*, 2007). They are resistant to heat and tolerant to high salt concentrations (Parfentjev & Catelli, 1964). Staphylococcal genomes contain a low G+C content of 30-40 % (Ludwig *et al.*, 1985, Stackebrandt & Teuber, 1988).

Two groups within the genus *Staphylococcus* have been described based on their ability to produce coagulase: coagulase-positive staphylococci including *Staphylococcus aureus* and the *S. intermedius* group, and coagulase-negative staphylococci which include the important human pathogens *S. epidermidis*, *S. haemolyticus* and *S. lugdunensis* (Becker *et al.*, 2014a). Historically coagulase-negative staphylococci have been considered the least pathogenic or non-pathogenic of the *Staphylococcus* genus (Becker *et al.*, 2014a). However, this view has changed and coagulase-negative staphylococci are now considered major nosocomial pathogens with *S. epidermidis* identified as a leading cause of indwelling-device related infections. *Staphylococcus aureus* and *S. epidermidis* have been the most extensively studied of the staphylococci. *S. aureus* and *S. epidermidis* are members of the human commensal microflora. *S. aureus* colonises the human nasopharynx while *S. epidermidis* colonises the human nose and skin. *S. aureus* is the most important human pathogen of the *Staphylococcus* genus which causes a wide spectrum of disease. The species name *aureus* refers to the golden colour commonly observed for *S. aureus* colonies due to the production of the carotenoid pigment staphyloxanthin (Pelz *et al.*, 2005).

1.2 *S. aureus* host interactions.

1.2.1 Colonisation.

1.2.1.1 Human nasopharynx

The primary site of *S. aureus* colonisation is the human nasal cavity (Weidenmaier *et al.*, 2012). 20 % of the human population persistently carry *S. aureus* in the nares while the remaining population are considered transient carriers (van Belkum *et al.*, 2009). Nasal colonisation has been identified as a major risk factor for infection with *S. aureus* (Wertheim *et al.*, 2004, von Eiff *et al.*, 2001, Munoz *et al.*, 2008). Within the human nasal cavity *S. aureus* colonises the anterior nares and the posterior nares with different cell surface factors mediating colonisation at each site (Weidenmaier *et al.*, 2008). The ability to colonise both sites aids the persistence of *S. aureus* in the nasal cavity (Weidenmaier *et al.*, 2012).

Colonisation of the anterior nares is mediated by interactions of *S. aureus* cell wall-anchored proteins with ligands on the surface of squames; dead keratinized cells on the surface of the squamous epithelium. The cell wall-anchored protein clumping factor B (ClfB) mediates adherence of *S. aureus* to the host proteins loricrin and cytokeratin (Mulcahy *et al.*, 2012, Walsh *et al.*, 2004, O'Brien *et al.*, 2002b) and promotes colonisation of human nares (Wertheim *et al.*, 2008). ClfB binding loricrin has been identified as the primary interaction in *S. aureus* nasal colonisation *in vivo* (Mulcahy *et al.*, 2012). Other cell wall-anchored proteins have also been implicated in nasal colonisation. The iron-regulated surface determinant (Isd) protein A promotes adherence of *S. aureus* to squames *in vitro* (Clarke *et al.*, 2009) and was found to promote colonisation of the nares of cotton rats *in vivo* (Clarke *et al.*, 2006). Furthermore, immunization with ClfB or IsdA reduced nasal colonisation in mice and cotton rats, respectively (Clarke *et al.*, 2006, Schaffer *et al.*, 2006). The *S. aureus* surface protein G (SasG) and the serine aspartate repeat (Sdr) proteins C and D were also found to promote *S. aureus* adherence to squames *in vitro* (Corrigan *et al.*, 2009). SdrD binds the host protein desmoglein 1 (Askarian *et al.*, 2016) while the ligands of SasG and SdrC remain unknown.

S. aureus attachment to the posterior nares is mediated by the cell wall-anchored anionic polymer wall teichoic acid (WTA). WTA interacts with a type F scavenger receptor SREC-1 expressed on ciliated nasal epithelial cells (Baur *et al.*, 2014) and promotes nasal colonisation of cotton rats *in vivo* (Weidenmaier *et al.*, 2004, Weidenmaier *et al.*, 2008).

S. aureus also colonises the human pharynx (Mertz *et al.*, 2007). Interestingly, pharyngeal colonisation can occur independently of nasal colonisation. A study of ~3,000 individuals reported that 37.1 % were nasal carriers while a significant portion; 12.8 % of individuals solely carried *S. aureus* in their pharynx (Mertz *et al.*, 2007). The bacterial factors mediating *S. aureus* pharyngeal colonisation remain unclear. Interactions with mucus may play a role in both nasal and pharyngeal colonisation (Sanford *et al.*, 1989).

1.2.1.2 Human skin

The community associated (CA)-methicillin resistant *S. aureus* (MRSA) USA300 lineage have been the most successful of the CA-MRSA strains in North America although the virulence of CA-MRSA strains is relatively comparable (DeLeo *et al.*, 2010). Thus, its success, at least in part, may be attributed to its enhanced ability to colonise human skin increasing its transmissibility. USA300 strains have acquired a mobile genetic element carrying a type IV staphylococcal chromosomal cassette (SCC) and the arginine catabolic mobile element (ACME) (Diep *et al.*, 2008, Diep *et al.*, 2006). The SCC carries the *mecA* gene which confers resistance to methicillin (Section 1.7.3.1) (Diep *et al.*, 2008). The ACME element encodes an arginine deiminase, an oligopeptide permease system (Diep *et al.*, 2006) and a spermine/spermidine N-acetyltransferase (*speG*) (Joshi *et al.*, 2011). The arginine deiminase and the spermine/spermidine N-acetyltransferase promote survival of USA300 strains on skin. The arginine deiminase activity results in the production of ammonia increasing the pH of skin and the spermine/spermidine N-acetyltransferase confers resistance of USA300 strains to polyamines produced by skin (Joshi *et al.*, 2011). The ACME element is prevalent among *S. epidermidis* strains suggesting it originated in *S. epidermidis*; a member of the commensal microflora of human skin. *S. aureus* also colonises the skin of the

majority of individuals with atopic dermatitis (AD) (Park *et al.*, 2013). Corneocytes located on the outer layer of skin have an altered morphology in AD skin (Riethmuller *et al.*, 2015). The cell wall-anchored protein ClfB promotes adhesion of *S. aureus* to these AD corneocytes (Fleury *et al.*, 2017). Furthermore, increased ClfB binding activity was associated with *S. aureus* strains isolated from AD skin in comparison to nasal isolates (Fleury *et al.*, 2017).

1.2.2 Infection.

Although *S. aureus* is a commensal in the nasopharynx of humans, it is a very important opportunistic human pathogen which causes a wide spectrum of disease. *S. aureus* is a cause of superficial skin infections such as styes, boils and impetigo. *S. aureus* also causes serious, life threatening infections. These include but are not limited to endocarditis, septicaemia, toxic shock syndrome, pneumonia and osteomyelitis. The centers for disease control and prevention (CDC) reported 80,461 severe methicillin resistant *S. aureus* (MRSA) infections and 11,285 deaths from MRSA in North America in 2011 (Dantes *et al.*, 2013) while in Ireland, in 2016, the health protection surveillance centre (HSPC) reported 1,168 *S. aureus* positive blood cultures, 14.7 % of which were MRSA strains (HSPC, 2016). In industrialised countries worldwide *S. aureus* is considered a leading cause of infective endocarditis, causing 16-34 % of cases, and bacteraemia with the incidence of *S. aureus* bacteraemia in these countries considered to be 10-30 per 100,000 person-years (Tong *et al.*, 2015). With advances in modern healthcare, a new infection opportunity has emerged with *S. aureus* causing infections on indwelling medical devices. Examples of these include prosthetic joints, heart valves and intravenous catheters. These infections involve formation of a multicellular biofilm community. Thus, *S. aureus* has the ability to cause both acute infections in a planktonic state and chronic, biofilm-associated infections.

The success and versatility of *S. aureus* as a pathogen is undoubtedly as a result of its vast array of virulence factors (Powers & Wardenburg, 2014, Alonzo & Torres, 2014) and immune evasion tactics (Spaan *et al.*, 2013, Thammavongsa *et al.*, 2015). *S. aureus* has evolved strategies to evade and manipulate all steps in the host immune response from recruitment of phagocytic cells through secretion of factors such as the

chemotaxis inhibitory protein of *Staphylococcus* (CHIPS) (Spaan *et al.*, 2013) and evasion of phagocyte killing to lysis of white blood cells by secreted bi-component pore-forming leucocidins (Alonzo & Torres, 2014) and nonspecific activation of host T cells (Stach *et al.*, 2014) and B cells (Falugi *et al.*, 2013). Furthermore, the widespread emergence of antibiotic resistant *S. aureus* strains (Foster, 2017) and the lack of success in studies to develop an *S. aureus* vaccine (Giersing *et al.*, 2016, Jansen *et al.*, 2013) complicates prevention and treatment of this major pathogen.

1.3 The *S. aureus* cell envelope.

S. aureus cells are enclosed in a cytoplasmic membrane surrounded by a thick cell wall which predominantly consists of peptidoglycan. The backbone of peptidoglycan is made up of alternating β -1,4-*N*-acetylglucosamine and *N*-acetylmuramic acid units (Giesbrecht *et al.*, 1998). A tetrapeptide of the amino acids L-alanine, D-glutamine, L-lysine and D-alanine extend from the *N*-acetylmuramic acid units of the disaccharide backbone (Giesbrecht *et al.*, 1998). These tetrapeptides are linked by a pentaglycine cross-bridge. The penicillin binding proteins (PBP) 2 and 4 mediate this cross-linking of *S. aureus* peptidoglycan. The other major components of the *S. aureus* cell envelope are teichoic acids; wall teichoic acid (WTA) and lipoteichoic acid (LTA). WTA and LTA are anionic polymers expressed on the surface of *S. aureus* which contribute to the overall negative charge of the cell surface. WTA is covalently attached to the *N*-acetylmuramic acid within peptidoglycan. WTA is abundant in the *S. aureus* cell wall with an estimate that every ninth *N*-acetylmuramic acid unit is linked to a WTA (Brown *et al.*, 2013). In the majority of *S. aureus* strains WTA consists of a disaccharide linkage unit followed by one to two subunits of glycerol 3-phosphate and a polymer of repeating subunits of ribitol 5-phosphate (Brown *et al.*, 2013). WTA polymers are decorated with D-alanine residues and *N*-acetylglucosamine moieties (Brown *et al.*, 2013). LTA consists of a poly glycerol phosphate backbone and a glycolipid anchor which attaches it to the cytoplasmic membrane (Xia *et al.*, 2010).

S. aureus strains may also be encapsulated. *S. aureus* capsular polysaccharide serotypes 5 and 8 are predominant in clinical isolates (O'Riordan & Lee, 2004). Other components of the *S. aureus* cell envelope include non-covalently associated and

covalently bound proteins. *S. aureus* can express many cell wall-anchored proteins on its cell surface which are covalently bound to peptidoglycan (Foster *et al.*, 2014). Expression of these cell wall-anchored proteins varies among strains, growth conditions and stages of growth. For example, the iron-regulated surface determinant (Isd) proteins are exclusively expressed in iron-limited conditions, clumping factor B (ClfB) expression is typically expressed *in vitro* in early exponential phase growth and the *S. aureus* surface protein G (SasG) is not expressed in all strains.

1.4 *S. aureus* cell wall-anchored protein families.

S. aureus cell wall-anchored (CWA) proteins all contain a Sec-dependent signal sequence at their amino-termini (Foster *et al.*, 2014) and a sorting signal at their C-termini containing the amino acid motif LPXTG, a membrane-spanning hydrophobic domain and a tail of positively charged residues (Schneewind *et al.*, 1993) (Fig 1.1). Following translation, the signal sequence directs the proteins to the Sec apparatus which secretes the proteins across the cytoplasmic membrane. The signal sequence is cleaved during secretion. The presence or absence of a YSIRK/GS motif in the Sec signal sequence determines the localisation of the protein (DeDent *et al.*, 2008). Signal sequences containing YSIRK/GS motifs direct proteins to the cross wall which contains newly synthesized peptidoglycan and becomes the cell envelope upon cell division leading to distribution of these proteins around the cell (DeDent *et al.*, 2008). In contrast, signal sequences without YSIRK/GS motifs direct proteins to the poles of the cells leading to their localisation at the secretion sites (DeDent *et al.*, 2008). An additional 'secretion motif' within the N1 subdomain of ClfA, FnBPB and most likely, FnBPA, is essential for the export of these proteins across the cell membrane (McCormack *et al.*, 2014, Geoghegan *et al.*, 2013). This secretion motif in ClfA has been localised to ten residues located at the junction of N1 with the N2 subdomain (Fig 1.1) (McCormack *et al.*, 2014). ClfA lacking its unstructured repeat region was exported in the absence of this N1 secretion motif implicating the importance of this motif in the secretion of the repeat regions of these proteins (McCormack *et al.*, 2014). Following secretion across the cell membrane, the proteins are subsequently covalently anchored to the cell wall peptidoglycan by the enzyme sortase A. Sortase A cleaves between the threonine and glycine of the LPXTG motif. An amide bond is

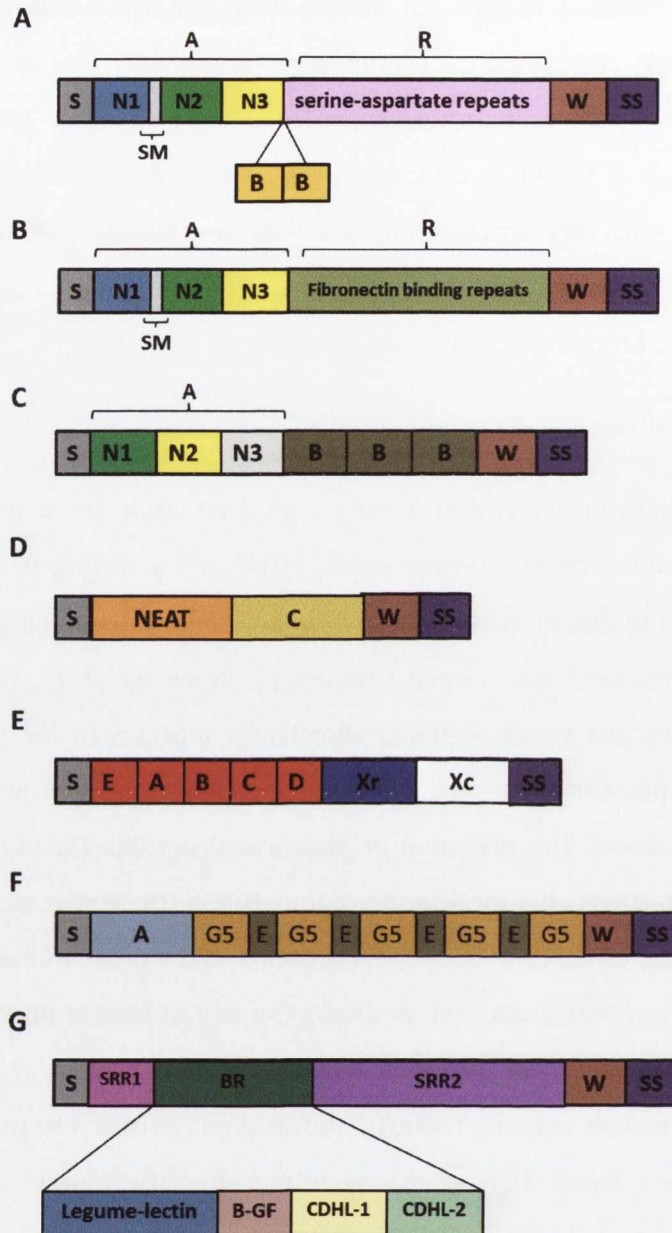


FIG 1.1 Structural organization of *S. aureus* cell wall-anchored proteins. All *S. aureus* cell wall-anchored proteins contain a signal sequence (S) at their N-terminus and a cell wall spanning domain (W) or Xc domain and a sorting signal (SS) at their C-terminus. The structural organization of the Clf-Sdr subfamily (A), fibronectin binding proteins (B) and the collagen adhesin (C) which are members of the MSCRAMM family are shown along with the NEAT motif family (D), the three-helical bundle family (E), the G5-E repeat family (F) and the legume-lectin like family (G) of *S. aureus* cell wall-anchored proteins. The Clf-Sdr subfamily (A) and fibronectin binding proteins (B) have an additional secretion motif (SM) in the N1 subdomain.

formed between the threonine and the pentaglycine cross-bridge of peptidoglycan anchoring the proteins to the cell wall (Mazmanian *et al.*, 2001).

Five families of *S. aureus* cell wall-anchored proteins have been described based on structural and functional studies (Geoghegan & Foster, 2015). These are the microbial surface components recognizing adhesive matrix molecules (MSCRAMMs), the near iron transporter (NEAT) motif proteins, the three-helical bundle family, the G5-E repeat family and the legume-lectin like family (Fig 1.1).

1.4.1 MSCRAMM family.

The MSCRAMMs are the largest family of *S. aureus* cell wall-anchored proteins. Members of the MSCRAMM family have a very similar overall domain structure and are characterised by tandem IgG-like folded subdomains termed N2 and N3 followed by a long, unstructured repeat region (Foster *et al.*, 2014) (Fig 1.1). The archetypal MSCRAMM structure consists of a signal sequence at the amino-terminus, followed by an A domain consisting of three independently followed subdomains N1, N2 and N3. The N1 subdomains of ClfA, FnBPA and FnBPB contain a 'secretion motif' which is essential for transport of these MSCRAMMs across the cell membrane (McCormack *et al.*, 2014). No function for the remainder of N1 has been identified. The N2N3 subdomains are the major ligand binding region of MSCRAMMs. The N2N3 subdomains adopt IgG-like folds. The A domain is followed by an unstructured repeat region R. This region acts as a flexible stalk projecting the ligand binding A domain from the cell surface. The R region is followed by a wall-spanning domain and the sorting signal. The crystal structures of the N2N3 subdomains of seven of the nine *S. aureus* MSCRAMMs have been solved and they all adopt the characteristic IgG-like folds with a hydrophobic trench separating the subdomains N2 and N3 (Ganesh *et al.*, 2008, Stemberk *et al.*, 2014, Wang *et al.*, 2013, Luo *et al.*, 2017, Xiang *et al.*, 2012, Zhang *et al.*, 2015, Zong *et al.*, 2005). The MSCRAMM family can be classified into three subfamilies; the clumping factor-serine aspartate repeat (Clf-Sdr) subfamily, the fibronectin binding proteins and the collagen adhesin.

The Clf-Sdr subfamily comprises ClfA, ClfB, SdrC, SdrD, SdrE and the bone sialoprotein-binding protein (Bbp) which is considered an isoform of SdrE (Foster *et al.*, 2014). The

A domain of Clf-Sdr proteins consists of N1N2N3 subdomains with the N2N3 subdomains considered the major ligand binding region. The repeat region of the Clf-Sdr subfamily consists of tandem serine-aspartate (SD) repeats (Fig 1.1A). The SD repeats are post translationally modified with N-acetylglucosamine moieties. This glycosylation protects the SD repeats from proteolytic degradation by the neutrophil protease cathepsin G (Hazenbos *et al.*, 2013). The Sdr and Bbp proteins contain between two and four additional B repeats between the N2N3 subdomains and the repeat region (Fig 1.1A). No ligands for the B repeats have been identified to date. Fibronectin binding proteins (FnBP) A and B contain an A region of N1N2N3 subdomains followed by a repeat region of tandem fibronectin binding repeats (FnBRs; Fig 1.1B). Like the Clf-Sdr subfamily the major ligand binding region of FnBPs are the N2N3 subdomains. FnBPA and FnBPB contain a large amount of sequence variation in their N2N3 subdomains with seven isotypes of both FnBPA (Loughman *et al.*, 2008) and FnBPB (Burke *et al.*, 2010) identified to date. Despite this sequence variation, the ability of FnBPA and FnBPB to bind their host ligands is conserved across isotypes (Burke *et al.*, 2010, Loughman *et al.*, 2008, Pietrocola *et al.*, 2016).

The collagen adhesin (Cna) is also a member of the MSCRAMM family of cell wall-anchored proteins and contains an A domain with three subdomains N1, N2, N3 (Foster *et al.*, 2014). However, its structure differs from the archetypal MSCRAMM structure (Fig 1.1C). The N1 and N2 subdomains of Cna, rather than its N2N3 subdomains, form tandem IgG-like folds and mediate ligand binding. Cna, like Sdr proteins, contains tandem B repeats which vary in number. However, their sequence differs to that of the Sdr B repeats. Furthermore, Cna does not contain an unstructured repeat region.

1.4.1.1 'Dock, Lock and Latch'

The major ligand binding region of MSCRAMMs is their N2N3 subdomains which mediate adherence to a wide variety of host ligands. A common, multistep ligand binding mechanism termed 'Dock, Lock and Latch' (DLL) has been identified among MSCRAMMs (Fig 1.2). The DLL mechanism of binding was originally described for the *S. epidermidis* MSCRAMM SdrG and the β -chain of human fibrinogen (Fg) through

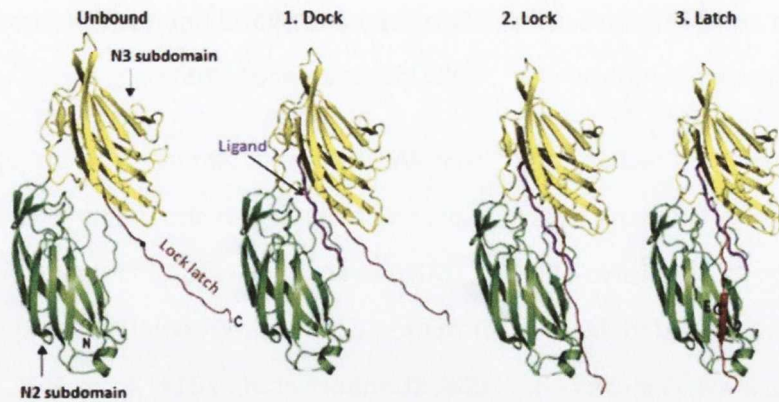


FIG 1.2 'Dock, Lock and Latch' mechanism of MSCRAMM-ligand binding. The archetypal MSCRAMM-ligand binding mechanism of 'Dock, Lock and Latch' involves three steps. The ligand (purple) 'docks' in the hydrophobic trench between the N2 and N3 subdomains (green and yellow, respectively) (1). The C-terminal extension of the N3 subdomain termed the 'Lock latch' (red) redirects and covers the ligand in the trench and the N2 and N3 subdomains form a number of contacts with the ligand 'locking' it in place (2). The latch then extends into the N2 subdomain forming a β -strand complementation with the D and E strands of the N2 subdomain 'latching' the ligand in place (3). The unbound IgG-like folded N2 N3 subdomain structure of SdrG is also shown. Adapted from Bowden *et al*, 2008.

crystallization and comparison of the SdrG apo and ligand bound structures along with biochemical studies (Ponnuraj *et al.*, 2003, Bowden *et al.*, 2008).

The archetypal DLL mechanism of MSCRAMM-ligand binding consists of the initial docking of the ligand in the hydrophobic trench between subdomains N2 and N3 (Fig 1.2). In the crystal structures of MSCRAMMs in complex with their ligand peptides, the ligands lie in an extended linear conformation within the trench (Ponnuraj *et al.*, 2003, Bowden *et al.*, 2008, Ganesh *et al.*, 2008, Stemberk *et al.*, 2014, Xiang *et al.*, 2012). The N3 subdomain contains a C-terminal extension termed the 'lock-latch region' (Fig 1.2). Upon ligand docking, the lock-latch region redirects covering the docked ligand and the N2N3 subdomains form a number of contacts with the ligand 'locking' it in place (Fig 1.2). In the case of SdrG, it's N2 and N3 subdomains form 62 contacts, including several hydrogen bonds, with the β -chain peptide of Fg locking the peptide in the trench (Ponnuraj *et al.*, 2003). Finally, the latch region extends into a cleft between two β -strands (labelled D and E) of the N2 subdomain forming an intramolecular β -strand complementation (Fig 1.2). This forms a closed N2N3 conformation and stabilizes the ligand bound structure. Variants of the DLL mechanism of MSCRAMM-ligand binding have been described. For example, in the case of FnBPA binding the Fg γ -chain the importance of the latch is unclear. The crystal structure of FnBPA in complex with the Fg γ -chain peptide was solved and FnBPA in this structure lacks the majority of the putative latch (Stemberk *et al.*, 2014). This indicated that the latch is not essential for FnBPA binding Fg (Stemberk *et al.*, 2014).

1.4.2 NEAT motif family

The near iron transporter (NEAT) motif family members are characterised by at least one NEAT domain within their structure which facilitates binding to haem or haemoglobin (Fig 1.1D) (Foster *et al.*, 2014). This ability to bind and acquire haem or haemoglobin is the major function of members of the NEAT motif family aiding *S. aureus* survival in iron-limited conditions within the host where iron is sequestered. The members of the NEAT motif family are the iron-regulated surface determinant (Isd) proteins A, IsdB, IsdH and IsdC which are exclusively expressed in iron-limited conditions. IsdA and IsdC proteins contain one NEAT domain, IsdB contains two NEAT

domains and IsdH three NEAT domains (Hammer & Skaar, 2011). Each NEAT domain can bind a single haem molecule, IsdH can also bind haptoglobin-haemoglobin and IsdB haemoglobin (Hammer & Skaar, 2011). Thus, these proteins are the initial step in acquiring iron for *S. aureus*. Following haem binding the haem is transferred from the cell wall-anchored Isd proteins to a transporter which facilitates haem transport across the cell membrane and into the cytoplasm where it is digested to release iron.

1.4.3 Three-helical bundle family

The three-helical bundle family member protein A of *S. aureus* is characterised by its five N-terminal three-helical bundle domains; EABCD (Fig 1.1E) (Foster *et al.*, 2014). Each three-helical bundle domain is separately folded. The three-helical bundle domains are the major ligand binding region of protein A. The three-helical bundles are followed by the variable Xr region which consists of a variable number of octapeptide repeats. Due to the variability of the Xr region, sequencing of this region, known as *spa* typing is often used in the typing of *S. aureus* strains (Foster *et al.*, 2014). The Xr region is followed by the constant, non-repetitive Xc region at the C-terminus of protein A. Protein A is also present in the supernatant of *S. aureus* in a released form through inefficient sorting (O'Halloran *et al.*, 2015) and the activity of the LytM endopeptidase (Becker *et al.*, 2014b).

1.4.4 G5-E repeat family

S. aureus surface protein G (SasG) is the only G5-E repeat protein expressed by *S. aureus* (Fig 1.1F). *S. epidermidis* also expresses a G5-E repeat protein; the accumulation associated protein (Aap). SasG contains an N-terminal A domain containing a legume-lectin like domain followed by variable numbers of alternating G5 and E domains (Gruszka *et al.*, 2012). The alternation of separately folded G5 and E domains is thought to prevent misfolding of the protein which otherwise may occur due to the repetitiveness of this region (Gruszka *et al.*, 2012, Gruszka *et al.*, 2015). The structure of the G5-E repeats consists of triple-stranded β -sheets arranged head-to-tail with structural similarity between the G5 and E domains (Gruszka *et al.*, 2012). SasG proteins form long extended fibrils on the surface of *S. aureus* due to the rod-like structure of these G5-E repeats (Gruszka *et al.*, 2015, Gruszka *et al.*, 2012).

1.4.5 Legume-lectin family

The serine-rich adhesin for platelets (SraP) is a glycosylated, serine rich repeat protein which contains a characteristic legume-lectin like region in its BR domain (Fig 1.1G) (Yang *et al.*, 2014, Sanchez *et al.*, 2010). SraP contains a large signal sequence at its N-terminus. Due to this and its glycosylation, SraP is secreted across the cell membrane by the accessory Sec system unlike other CWA proteins of *S. aureus* (Siboo *et al.*, 2008). Following the secretion signal, SraP consists of a short serine rich region at its N-terminus (SRR1). This is followed by the BR domain. The BR domain consists of four subdomains; the legume-lectin like subdomain, a β -grasp folded subdomain (B-GF) and two tandem cadherin-like domains (CDHL-1 and CDHL-2) (Yang *et al.*, 2014). The BR region is followed by a longer serine rich repeat region (SRR2) at the C-terminus.

1.4.6 Major functions of the cell wall-anchored proteins

S. aureus cell wall-anchored (CWA) proteins are essential factors in nasal colonisation and in local and systemic infections. *S. aureus* CWA proteins are often multifunctional and there is a large amount of functional redundancy among them. Functions of the CWA proteins include mediating adhesion to host proteins, invasion of host cells, immune evasion, iron scavenging (Section 1.4.2), and biofilm formation (Table 1.1, biofilm formation is extensively discussed in section 1.5.2.2) (Foster *et al.*, 2014).

1.4.6.1 Adhesion to host proteins

An important function of the MSCRAMM family of CWA proteins is their ability to bind to host plasma proteins (Table 1.1). ClfA is an important *S. aureus* virulence factor largely due to its ability to bind to fibrinogen (Fg) and fibrin. Its role in virulence has been demonstrated in a wide spectrum of *S. aureus* infections; endocarditis (Moreillon *et al.*, 1995, Que *et al.*, 2005), septicaemia (Josefsson *et al.*, 2001, Cheng *et al.*, 2009, Flick *et al.*, 2013), kidney abscesses (Cheng *et al.*, 2009) and septic arthritis (Josefsson *et al.*, 2001). ClfB, FnBPA, FnBPB and Bbp also mediate adherence of *S. aureus* to Fg. FnBPA and FnBPB N2N3 subdomains also mediate adherence of *S. aureus* to host proteins elastin (Keane *et al.*, 2007, Roche *et al.*, 2004) and plasminogen (Pietrocola *et al.*, 2016). The fibronectin binding repeats of FnBPA and FnBPB mediate adherence of

S. aureus to the N-terminal type-1 modules of fibronectin (Fn) (Greene *et al.*, 1995) promoting adherence to the host extracellular matrix. The Fg binding site and first Fn binding repeat of FnBPA and FnBPB are in close proximity and, in the case of FnBPA, binding of Fn sterically prevented Fg binding (Stemberk *et al.*, 2014). FnBPB also contains another Fn binding site in its N2N3 subdomains (Burke *et al.*, 2011). As previously described, interactions of CWA proteins with host proteins in the human nares and skin are essential in promoting *S. aureus* colonisation (Section 1.2.1, Table 1.1). Other interactions of *S. aureus* CWA proteins with host ligands are detailed in Table 1.1.

1.4.6.2 Invasion of host cells

The CWA proteins FnBPA, FnBPB, IsdB and SraP promote invasion of *S. aureus* into non-professional phagocytic host cells (Table 1.1). The fibronectin binding repeats (FnBRs) of FnBPA and FnBPB facilitate invasion into a variety of mammalian host cells (Edwards *et al.*, 2010, Edwards *et al.*, 2011, Liang *et al.*, 2016, Agerer *et al.*, 2005, Sinha *et al.*, 2000). Fn acts as a bridge between *S. aureus* and the host cell with FnBPs and $\alpha 5\beta 1$ integrins binding the same Fn molecules. FnBPs binding to multiple Fn proteins causes integrin clustering which results in intracellular signalling causing the host cell to endocytose *S. aureus* (Agerer *et al.*, 2005). Interestingly, both the affinity and number of FnBRs affect the efficiency of FnBP-mediated host cell invasion (Edwards *et al.*, 2010, Edwards *et al.*, 2011).

IsdB promotes adhesion to and invasion of host cells through binding of $\beta 3$ integrins (Zapotoczna *et al.*, 2013) and the legume-lectin like subdomain of SraP binds to N-acetylneuraminic acid mediating adherence and invasion of *S. aureus* into lung epithelial cells (Yang *et al.*, 2014). Host cell invasion allows *S. aureus* to evade detection by the host immune system, protects the bacteria from antibiotics, allows *S. aureus* access to deeper tissue and intracellular *S. aureus* may serve as reservoirs for chronic infections (Edwards *et al.*, 2011).

Table 1.1 Functions of the *S. aureus* cell wall-anchored proteins

| Cell wall anchored protein | Ligand(s) | Function | Reference |
|----------------------------|---|--|---|
| <u>MSCRAMM family</u> | | | |
| Clumping factor (Clf)A | Fg ^a γ-chain | Adhesion to immobilised Fg, immune evasion | (Ganesh <i>et al.</i> , 2008) |
| | Complement factor I | Enhances cleavage of C3b, evasion of opsonophagocytosis | (Hair <i>et al.</i> , 2010) |
| ClfB | Fg α-chain, loricrin, cytokeratin 10 | Adhesion to immobilised Fg, nasal colonisation, colonisation of atopic dermatitis skin | (Fleury <i>et al.</i> , 2017, Walsh <i>et al.</i> , 2004, Xiang <i>et al.</i> , 2012, Mulcahy <i>et al.</i> , 2012) |
| | Unknown | Biofilm formation | (Abraham & Jefferson, 2012) |
| | Serine aspartate repeat protein (Sdr) C | Unknown | Adherence to human desquamated nasal epithelial cells |
| | β-neurexin | Unknown | (Barbu <i>et al.</i> , 2010) |
| | SdrC | Homophilic interactions which mediate biofilm accumulation. | (Barbu <i>et al.</i> , 2014, Feuillie <i>et al.</i> , 2017) |
| | Hydrophobic surfaces | Attachment to abiotic surfaces | (Barbu <i>et al.</i> , 2014, Feuillie <i>et al.</i> , 2017) |

| | | | |
|--|---|---|---|
| SdrD | Desmoglein 1 | Adherence to human desquamated nasal epithelial cells | (Corrigan <i>et al.</i> , 2009, Askarian <i>et al.</i> , 2016) |
| SdrE | Complement factor H C4b binding protein | Evasion of complement | (Hair <i>et al.</i> , 2013, Zhang <i>et al.</i> , 2017, Sharp <i>et al.</i> , 2012) |
| Bone sialoprotein-binding protein (Bbp; isoform of SdrE) | Fg α -chain | Adhesion to immobilised Fg | (Zhang <i>et al.</i> , 2015) |
| | C4b binding protein | Evasion of complement | (Hair <i>et al.</i> , 2013) |
| Fibronectin binding proteins (FnBP) A and FnBPB | N2N3 subdomains bind Fg γ -chain, elastin, and plasminogen | Adherence to ECM ^c | (Keane <i>et al.</i> , 2007, Burke <i>et al.</i> , 2010, Pietrocola <i>et al.</i> , 2016, Roche <i>et al.</i> , 2004) |
| | FnBPB N2N3 also binds Fn ^b | Adherence to ECM | (Burke <i>et al.</i> , 2011) |
| | Fn binding repeats bind Fn | Adherence to ECM, invasion of host cells | (Greene <i>et al.</i> , 1995) |
| | FnBPA | FnBPA-FnBPA homophilic interactions mediate biofilm accumulation, FnBPB also mediates biofilm formation | (O'Neill <i>et al.</i> , 2008, Geoghegan <i>et al.</i> , 2013, Herman-Bausier <i>et al.</i> , 2015) |
| Collagen adhesin (Cna) | Collagen | Host tissue adhesion | (Zong <i>et al.</i> , 2005) |
| | Complement protein C1q | Prevents activation of classical pathway of complement | (Kang <i>et al.</i> , 2013) |

NEAT motif family

| | | | |
|--|---------------------------------------|---|--|
| Iron-regulated surface determinant (Isd) protein A | Haem | Iron scavenging | (Hammer & Skaar, 2011) |
| | Unknown | Resistance to H ₂ O ₂ , survival within neutrophils | (Palazzolo-Ballance <i>et al.</i> , 2008) |
| | Unknown | Resistance to fatty acids and peptides on human skin | (Clarke <i>et al.</i> , 2007) |
| | Unclear | Adherence to desquamated nasal epithelial cells; nasal colonisation | (Clarke <i>et al.</i> , 2006, Clarke <i>et al.</i> , 2009) |
| | lactoferrin | Resistance to lactoferrin | (Clarke & Foster, 2008) |
| IsdB | Haem, haemoglobin | Iron scavenging | (Hammer & Skaar, 2011) |
| | β 3 integrins | Invasion of host cells | (Zapotoczna <i>et al.</i> , 2013) |
| IsdC | Haem | Iron scavenging | (Hammer & Skaar, 2011) |
| IsdH | Haem, haptoglobin-haemoglobin complex | Iron scavenging | (Hammer & Skaar, 2011) |
| | Unknown | Accelerated degradation of C3b, reduce neutrophil phagocytosis | (Visai <i>et al.</i> , 2009) |

Three-helical bundle family

| | | | |
|-----------|-------------------|--|---|
| Protein A | Fc region of IgG | Evasion of opsonophagocytosis | (Cedergren <i>et al.</i> , 1993) |
| | Fab region of IgM | Nonspecific B cell expansion (B cell superantigen) | (Graille <i>et al.</i> , 2000, Falugi <i>et al.</i> , 2013) |
| | TNFR-1 | Pro-inflammatory | (Gomez <i>et al.</i> , 2006, Gomez <i>et al.</i> , 2004) |

G5-E repeat family

| | | | |
|--|---------|--|---|
| <i>S. aureus</i> surface protein (Sas) G | Unknown | Adherence to desquamated nasal epithelial cells | (Corrigan <i>et al.</i> , 2007) |
| | SasG | G5-E repeats form homophilic interactions mediating biofilm accumulation | (Geoghegan <i>et al.</i> , 2010, Corrigan <i>et al.</i> , 2007) |

Legume-lectin like family

| | | | |
|--|-------------------------|---|--------------------------------|
| Serine rich adhesin for platelets (SraP) | N-acetylneuraminic acid | Adherence to and invasion into lung epithelial cells | (Yang <i>et al.</i> , 2014) |
| | BR domain | BR domain forms homophilic interactions; biofilm accumulation | (Sanchez <i>et al.</i> , 2010) |

^a Fg = fibrinogen

^b Fn = fibronectin

^c ECM = extracellular matrix

1.4.6.3 Immune evasion

An important function of CWA proteins is in evasion of the host immune system (Table 1.1). Protein A forms multiple interactions with the host immune system which promote *S. aureus* immune evasion and infection. Protein A binds the Fc region of IgG preventing opsonophagocytosis of *S. aureus* (Deisenhofer, 1981, Cedergren *et al.*, 1993). This is because the IgG becomes bound by protein A in the incorrect orientation on the cell surface and is not recognised as an opsonin. Protein A is considered to be a B cell superantigen as it binds the Fab region of IgM mediating nonspecific B cell clonal expansion (Graille *et al.*, 2000, Kim *et al.*, 2015, Falugi *et al.*, 2013). Protein A is also pro-inflammatory through its binding and activation of TNFR-1 (Gomez *et al.*, 2006, Gomez *et al.*, 2004).

The CWA proteins ClfA (Hair *et al.*, 2010), SdrE (Hair *et al.*, 2013, Zhang *et al.*, 2017, Sharp *et al.*, 2012), Bbp (Hair *et al.*, 2013) and IsdH (Visai *et al.*, 2009) interfere with the host complement system which is an important component of the host immune response to *S. aureus* (Table 1.1). The complement system results in the production and deposition of the opsonin C3b, thus, promoting phagocytosis of *S. aureus*, and the production of the chemotactic molecule C5a which recruits phagocytes to the site of infection (Spaan *et al.*, 2013). Furthermore, IsdA confers resistance of *S. aureus* to hydrogen peroxide promoting bacterial survival within neutrophils following phagocytosis (Palazzolo-Ballance *et al.*, 2008). IsdA also mediates *S. aureus* evasion of innate immune defences on human skin (Clarke *et al.*, 2007) and in the nares (Clarke & Foster, 2008) (Table 1.1).

1.5 Biofilm formation by *S. aureus*

S. aureus is a leading cause of indwelling device related infections which typically involve formation of a biofilm. A biofilm is a multicellular community formed under specific conditions. Biofilm-associated infections also occur directly on host tissue, independent of devices, such as in osteomyelitis and native valve endocarditis. *S. aureus* biofilm formation is a multifactorial process and is traditionally considered to occur through three distinct phases; primary attachment, accumulation and maturation and biofilm dispersal (Fig 1.3). However, bacterial aggregation and the

1. Primary Attachment 2. Accumulation and maturation 3. Dispersal

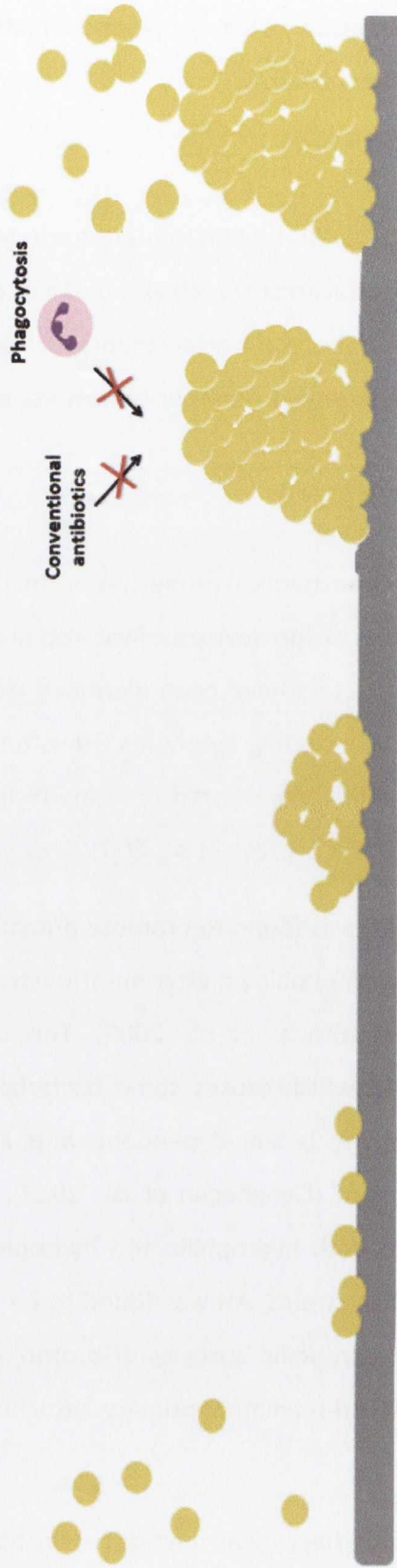


FIG 1.3 Biofilm formation by *S. aureus* occurs over three distinct phases. The first phase is primary attachment whereby *S. aureus* cells adhere to the indwelling device or host tissue. This is followed by biofilm accumulation and maturation where *S. aureus* cells aggregate and proliferate to form a mature biofilm. Biofilm maturation may involve the formation of a self-synthesized matrix in which the cells are embedded. The mature biofilm is refractive to conventional antibiotics and resistant to host immune defences. The final phase is biofilm dispersal whereby bacterial cells detach from the biofilm and can disseminate to other sites of the body.

formation of biofilms that are not surface attached have been described and associated with several types of infection including chronic wound infections and joint infections (Crosby *et al.*, 2016, Dastgheyb *et al.*, 2015).

1.5.1 Primary Attachment

Primary attachment is the first phase in *S. aureus* biofilm formation whereby bacterial cells adhere to an abiotic surface (abiotic attachment) such as a metal or plastic indwelling medical device or to a biotic surface (biotic attachment) such as a medical device that has become coated with host plasma proteins or to host tissue itself (Fig 1.3) (Speziale *et al.*, 2014).

1.5.1.1 Abiotic attachment

Abiotic attachment is governed by the physiochemical properties of the device surface and the bacteria itself. Thus, the properties of the device surface also play a large part in abiotic attachment. To date, several factors have been identified which promote adherence of *S. aureus* to abiotic surfaces including autolysins (Houston *et al.*, 2011), teichoic acids (Gross *et al.*, 2001) and cell wall-anchored proteins (Schroeder *et al.*, 2009, Barbu *et al.*, 2014, Feuillie *et al.*, 2017, Cucarella *et al.*, 2001, Li *et al.*, 2012).

The cell wall-anchored major autolysin Atl was found to promote primary attachment of *S. aureus* strains to hydrophilic and hydrophobic polystyrene (Houston *et al.*, 2011, Biswas *et al.*, 2006) and glass surfaces (Biswas *et al.*, 2006). This attachment is mediated by the autolytic activity of Atl which causes some bacterial cells to lyse releasing their DNA. This autolytic activity is zinc-dependent with Zn²⁺ chelation inhibiting Atl-mediated primary attachment (Geoghegan *et al.*, 2013). Atl mediates primary attachment of MRSA strains to both hydrophilic and hydrophobic surfaces (Houston *et al.*, 2011). However, for MSSA strains, Atl was found to be important for attachment to hydrophobic and not hydrophilic surfaces (Houston *et al.*, 2011). Furthermore, the *in vivo* relevance of Atl-mediated primary attachment remains unclear.

Wall teichoic acids and lipoteichoic acids have been implicated in abiotic primary attachment of *S. aureus* (Gross *et al.*, 2001). Specifically, deletion of *dltA*, which

incorporates D-alanine residues into teichoic acids, reduced the ability of *S. aureus* to adhere to polystyrene or glass surfaces (Gross *et al.*, 2001). A reduction in D-alanine esters in teichoic acids causes an increase in the overall negative charge of *S. aureus*. It is hypothesized that this increased negative charge may increase repulsive forces between the bacteria and the surface, decreasing attachment. However, deletion of *dltA* in *S. aureus* is known to also affect surface proteins, exoproteins and autolysins (Gross *et al.*, 2001) and thus, there is likely be indirect effects of this mutation on attachment. However, overexpression of *dltA* increased primary attachment indicating that the level of D-alanylation of teichoic acids likely plays a role in *S. aureus* attachment to abiotic surfaces (Gross *et al.*, 2001).

The cell wall-anchored *S. aureus* proteins SdrC (Barbu *et al.*, 2014, Feuillie *et al.*, 2017), SasC (Schroeder *et al.*, 2009), SasX (Li *et al.*, 2012) and the biofilm-associated protein (Bap) (Cucarella *et al.*, 2001) also promote bacterial adherence to abiotic surfaces *in vitro*. The ability of SdrC to promote bacterial attachment to abiotic surfaces was further explored by measuring the binding forces between SdrC and either hydrophobic or hydrophilic surfaces (Feuillie *et al.*, 2017). SdrC interactions with hydrophobic surfaces were much stronger than those to hydrophilic surfaces (Feuillie *et al.*, 2017). Thus, SdrC-mediated abiotic attachment to surfaces is likely due to hydrophobic interactions. In general, the *in vivo* importance of mechanisms of *S. aureus* abiotic attachment identified and, abiotic attachment itself, remain unclear.

1.5.1.2 Biotic Attachment

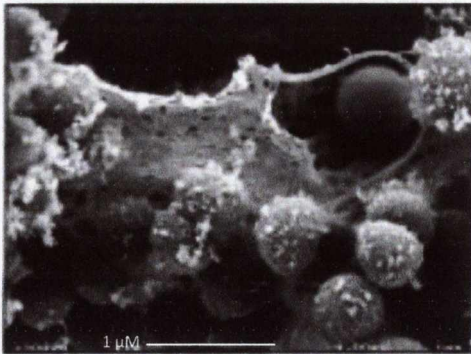
Biotic surfaces include indwelling devices coated with host plasma proteins fibrinogen, fibronectin and vitronectin and host tissues such as heart valves, bone and skin. Primary attachment of *S. aureus* to biotic surfaces is likely to be more relevant *in vivo* as once a medical device is inserted it becomes coated with host plasma proteins (Otto, 2008). Biotic attachment is mediated by the *S. aureus* cell wall-anchored MSCRAMM proteins ClfA, ClfB, FnBPA and FnBPB (Vaudaux *et al.*, 1995, Otto, 2008, Que *et al.*, 2005). ClfA, ClfB, FnBPA and FnBPB all bind the host plasma protein fibrinogen via their N2N3 subdomains (Ganesh *et al.*, 2008, Ganesh *et al.*, 2011, Walsh *et al.*, 2008, Wann *et al.*, 2000, Burke *et al.*, 2010). FnBPA and FnBPB also mediate

adherence of *S. aureus* to fibronectin through their fibronectin binding repeats and this interaction was shown to promote attachment to biomaterials *in vivo* (Greene *et al.*, 1995). FnBPA and FnBPB have also recently been shown to bind plasminogen which may be relevant to device related infections (Pietrocola *et al.*, 2016). MSCRAMM-mediated biotic attachment of *S. aureus* under shear has been demonstrated. ClfA promoted attachment through binding fibrinogen on a shunt surface under shear (Vaudaux *et al.*, 1995) and binding of *S. aureus* to the endothelium under shear was mediated by complexes of ClfA, von Willebrand factor binding protein and host von Willebrand factor (Claes *et al.*, 2017). Thus, *S. aureus* has several cell wall-anchored proteins which can mediate biotic attachment and there are a number of host ligands these proteins can bind to.

1.5.2 Biofilm Accumulation and Maturation

Following primary attachment to a device or host tissue, bacteria accumulate and proliferate forming a mature biofilm (Fig 1.3). Biofilm accumulation involves aggregation of *S. aureus* cells with two main mechanisms described; polysaccharide intercellular adhesin (PIA)-dependent biofilm (Arciola *et al.*, 2015) and protein-dependent biofilm where accumulation is mediated by cell wall-anchored proteins (O'Neill *et al.*, 2007). *In vivo* studies have demonstrated fibrin-dependent biofilm accumulation which involves both *S. aureus* and host factors (Zapotoczna *et al.*, 2015, Dastgheyb *et al.*, 2015, Vanassche *et al.*, 2013). Biofilm accumulation and maturation can also involve the formation of a self-synthesized matrix composed of extracellular DNA (Montanaro *et al.*, 2011) and cytoplasmic proteins (Foulston *et al.*, 2014). *In vitro*, PIA-dependent biofilm formation was found to be more prevalent among methicillin sensitive *S. aureus* (MSSA) strains and was stimulated by supplementation of media with salt inferring osmotic stress (O'Neill *et al.*, 2007). In contrast, protein-dependent biofilm was more prevalent among methicillin resistant *S. aureus* (MRSA) strains *in vitro* cultured in media supplemented with glucose leading to a low pH environment (O'Neill *et al.*, 2007). *S. aureus* grow and utilise the glucose as a nutrient source releasing acetic acid which reduces the pH of the medium (O'Neill *et al.*, 2007). Scanning electron microscopy of PIA- and protein-dependent biofilms *in vitro* revealed striking differences in the biofilm structures (Fig 1.4) (Vergara-Irigaray *et al.*, 2009).

PIA-dependent biofilm



Protein-dependent biofilm

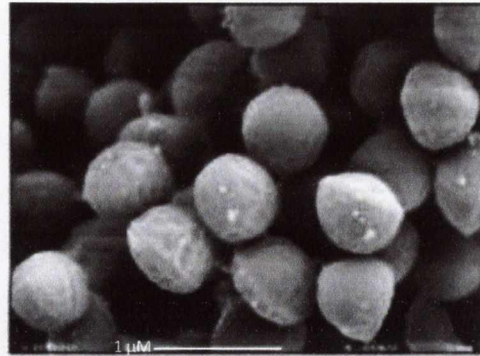


FIG 1.4. Scanning electron micrographs of PIA-dependent and protein-dependent biofilms. PIA-dependent and protein-dependent biofilms of *S. aureus* formed *in vitro* under continuous flow in TSB supplemented with NaCl or glucose, respectively, were visualised by scanning electron microscopy. In the PIA-dependent biofilm *S. aureus* cells are embedded in an extracellular matrix whereas in the protein-dependent biofilm *S. aureus* cells are in close contact and no surrounding matrix is observed. Taken from Vergara-Irigaray *et al.*, 2009.

Bacteria in the PIA-dependent biofilm were embedded in a polysaccharide matrix whereas bacteria in the protein-dependent biofilm were closely associated to each other but no matrix was observed (Fig 1.4) (Vergara-Irigaray *et al.*, 2009). Another important feature of a mature biofilm is channels within the biofilm structure which are generated to allow delivery of essential nutrients to cells in the lower levels of the biofilm (Le *et al.*, 2014).

1.5.2.1 Polysaccharide Intercellular Adhesin.

One of the main mechanisms of biofilm accumulation is mediated by the positively charged, exopolysaccharide polysaccharide intercellular adhesin (PIA). This type of biofilm is often termed 'PIA-dependent' biofilm formation. PIA is a poly- β -(1-6)-*N*-acetylglucosamine (PNAG). PIA is partially deacetylated leading to its positive charge and ~10 % of the *N*-acetylglucosamine units are modified with *O*-succinyl groups (Atkin *et al.*, 2014). The synthesis of PIA is mediated by genes of the *ica* locus, *icaADBC* (Heilmann *et al.*, 1996, Cramton *et al.*, 1999). The *ica* locus is not part of the core genome of *S. aureus* but is found in the majority of *S. aureus* clinical isolates. Each gene in the locus has an important role in the production and surface display of PIA. PNAG polymers are synthesized from UDP-*N*-acetylglucosamine by the enzyme IcaA in conjunction with IcaD (Arciola *et al.*, 2015). IcaC is an integral membrane protein considered to translocate PIA to the surface of *S. aureus* (Arciola *et al.*, 2015). However, the absence of the *icaC* gene in *ica* operons in other Gram-positive species suggest it is unlikely to function as the translocase and may have a function specific to certain staphylococcal species including *S. aureus* and *S. epidermidis* (Atkin *et al.*, 2014). It is likely that IcaA and IcaD synthesize and also translocate PIA. Analysis of the IcaC sequence indicated it may function as an *O*-succinyltransferase modifying the polymer as it is translocated (Atkin *et al.*, 2014). Following translocation, IcaB mediates the partial deacetylation of the exopolysaccharide (Arciola *et al.*, 2015).

Positively charged PIA interacts electrostatically with negatively charged teichoic acids on the surface of adjacent *S. aureus* cells mediating cell-cell interactions and biofilm accumulation (Formosa-Dague *et al.*, 2016a). During this PIA-dependent biofilm accumulation and maturation the bacterial cells become embedded in a polymeric matrix where PIA is an important structural component (Fig 1.4) (Formosa-Dague *et*

al., 2016a, Vergara-Irigaray *et al.*, 2009). It has also been reported that PIA promotes *S. epidermidis* attachment to orthopaedic biomaterials (Olson *et al.*, 2006). Thus, PIA may have a second role in biofilm formation.

1.5.2.2 Cell wall-anchored proteins

The other main mechanism of biofilm accumulation is mediated by *S. aureus* cell wall-anchored proteins. This has been termed 'protein-dependent' or '*ica*-independent' biofilm formation. A role for proteins in biofilm accumulation was initially discovered when strains lacking the *ica* locus or where the *ica* locus had been deleted were found to still form biofilm (O'Neill *et al.*, 2007). This initial observation was followed by many in depth studies identifying specific cell wall anchored-proteins which mediate biofilm accumulation. To date, several *S. aureus* cell wall-anchored proteins have been implicated in protein-dependent biofilm, namely fibronectin binding proteins (FnBP) A and B (Geoghegan *et al.*, 2013, O'Neill *et al.*, 2008, McCourt *et al.*, 2014, Vergara-Irigaray *et al.*, 2009), serine aspartate repeat protein (Sdr) C (Barbu *et al.*, 2014), serine rich adhesion for platelets (SraP) (Sanchez *et al.*, 2010), clumping factor B (ClfB) (Abraham & Jefferson, 2012), protein A (Merino *et al.*, 2009), biofilm-associated protein (Bap) (Cucarella *et al.*, 2001), *S. aureus* surface proteins (Sas) C (Schroeder *et al.*, 2009) SasG (Corrigan *et al.*, 2007, Geoghegan *et al.*, 2010) and SasX (Li *et al.*, 2012). The protein mediating biofilm accumulation varies between strains and is not necessarily limited to a single protein for each strain (Barbu *et al.*, 2014, O'Neill *et al.*, 2008). Until recently the mechanism of protein-dependent biofilm accumulation was unclear but growing evidence strongly implicates homophilic interactions of the cell wall-anchored proteins on adjacent bacteria leading to biofilm accumulation (Barbu *et al.*, 2014, Geoghegan *et al.*, 2010, Sanchez *et al.*, 2010, Yang *et al.*, 2014, Herman-Bausier *et al.*, 2015).

1.5.2.2.1 Fibronectin binding protein-mediated biofilm accumulation

Fibronectin binding protein (FnBP) A and B are members of the MSCRAMM family of *S. aureus* cell wall-anchored proteins. FnBPA and FnBPB promote biofilm formation in clinically relevant lineages; clonal complex (CC) 8 and CC22, of *S. aureus* including both hospital associated (HA-) and community associated (CA-) MRSA strains (O'Neill *et al.*,

2008, McCourt *et al.*, 2014, Planet *et al.*, 2013, Mashruwala *et al.*, 2017). Disruption of both *fnbA* and *fnbB* genes reduced the ability of HA-MRSA strain BH1CC and CA-MRSA strain LAC to form biofilm (O'Neill *et al.*, 2008, Geoghegan *et al.*, 2013, McCourt *et al.*, 2014). However, mutation of either *fnbA* or *fnbB* alone in BH1CC did not reduce biofilm (O'Neill *et al.*, 2008) indicating that FnBPA and FnBPB may compensate for each other in biofilm formation. Furthermore, biofilm formation of double *fnbAfnbB* mutants could be complemented by expression of either FnBPA or FnBPB on a multicopy plasmid (O'Neill *et al.*, 2008, McCourt *et al.*, 2014). *In vivo* FnBPs have been shown to promote catheter colonisation by *S. aureus* strain 132 in a mouse model of infection (Vergara-Irigaray *et al.*, 2009). Mutation of *fnbA* or *fnbB* alone in *S. aureus* strain 132 reduced the level of biofilm formed *in vitro* although a larger reduction in biofilm was associated with mutation of *fnbB*. This indicated that both FnBPA and FnBPB contribute to biofilm formed by *S. aureus* strain 132 but that FnBPB is likely to have a more prominent role (Vergara-Irigaray *et al.*, 2009). FnBPs are also required for biofilm formation induced by the polyamine spermidine in CA-MRSA USA300 strains which may be important for colonisation of the skin (Planet *et al.*, 2013). Under fermentative conditions, FnBPA promotes biofilm formed by the CA-MRSA strain LAC (Mashruwala *et al.*, 2017). This may be important for biofilm infections of host tissues, wounds and orthopedic implanted devices where hypoxic and anoxic conditions are encountered (Mashruwala *et al.*, 2017). Thus, the contribution of FnBPA and/or FnBPB to *S. aureus* biofilm is strain- and condition-dependent. Notably, although the majority of *S. aureus* strains carry both *fnbA* and *fnbB* genes, some strains carry only *fnbA* (Peacock *et al.*, 2000).

Studies into the molecular mechanism underlying FnBPA-mediated biofilm accumulation found that FnBPA proteins on adjacent cells form homophilic interactions allowing bacteria to aggregate and biofilm to accumulate (Herman-Bausier *et al.*, 2015). These interactions have been localised to FnBPA N2N3 subdomains (Geoghegan *et al.*, 2013) and were shown to consist of multiple weak interactions between FnBPA proteins on adjacent cells (Herman-Bausier *et al.*, 2015). The exact residues involved in FnBPA homophilic interactions remain unknown. Furthermore, FnBP-mediated biofilm of *S. aureus* is dependent upon the metal zinc

(Geoghegan *et al.*, 2013) whereby chelation of Zn^{2+} abolishes the ability of *S. aureus* to form an FnBP-dependent biofilm. The ability to form biofilm can subsequently be restored through addition of exogenous Zn^{2+} (Geoghegan *et al.*, 2013).

1.5.2.2.2 Serine aspartate repeat protein C

The *S. aureus* serine aspartate repeat protein C (SdrC) is also a member of the MSCRAMM family of *S. aureus* cell wall-anchored proteins. SdrC has been shown to mediate biofilm accumulation in the *S. aureus* lab strain Newman (Barbu *et al.*, 2014). SdrC mediates biofilm accumulation through homophilic interactions of its N2 subdomain (Barbu *et al.*, 2014) which, like FnBPA, are weak in binding force (Feuillie *et al.*, 2017). Two pentamer amino acid motifs within the N2 subdomain of SdrC; 'RPGSV' and 'VDQYT', have been implicated as dimerization sites of SdrC through phage display experiments (Barbu *et al.*, 2014). Phage expressing each motif was bound by recombinant SdrC N2N3 protein. Furthermore, addition of phage expressing each motif individually reduced SdrC N2 dimerization *in vitro* by approximately 50 %, while phage expressing both motifs abolished this dimerization. In the case of SdrC, biofilm is inhibited in the presence of manganese ions (Barbu *et al.*, 2014).

1.5.2.2.3 Clumping factor B

Another MSCRAMM clumping factor B (ClfB) was found to mediate biofilm accumulation in conditions where calcium is depleted (Abraham & Jefferson, 2012). ClfB-mediated biofilm was partially dependent upon the lack of expression of aureolysin, a protease which cleaves ClfB, in the *S. aureus* strain 10833 (Abraham & Jefferson, 2012). Furthermore, chelation of calcium was found to have strain-dependent effects on *S. aureus* biofilm formation; in some cases inhibiting biofilm formation and in other cases enhancing ClfB-dependent biofilm formation (Abraham *et al.*, 2012). The molecular mechanism underlying ClfB-mediated biofilm has not been characterised.

1.5.2.2.4 *S. aureus* surface protein G

The *S. aureus* surface protein G (SasG) is a member of the G5-E repeat family of *S. aureus* cell wall-anchored proteins. SasG is not expressed by typical *S. aureus* lab

strains grown *in vitro* but the SasG protein is produced by clinical isolates of *S. aureus* (Corrigan *et al.*, 2007). Furthermore, a previous study found SasG associated with disease isolates whereby presence of the *sasG* gene was more common among *S. aureus* invasive isolates than carriage isolates (Roche *et al.*, 2004). However, SasG-mediated biofilm accumulation has only been studied by expression of SasG on plasmids in lab strains and has not been demonstrated in clinical isolates to date.

During *S. aureus* growth, limited cleavage within the C-terminal G5-E repeat region of SasG occurs causing the N-terminal A domain to be released and exposing the SasG G5-E domains (Geoghegan *et al.*, 2013). These exposed G5-E repeats on neighbouring bacteria interact in a homophilic manner (Geoghegan *et al.*, 2010, Formosa-Dague *et al.*, 2016b) and mediate biofilm accumulation. At least five G5-E repeats are required for SasG to mediate biofilm accumulation (Corrigan *et al.*, 2007). Like FnBP-mediated biofilm accumulation, SasG-mediated biofilm is dependent upon Zn²⁺ (Geoghegan *et al.*, 2010, Formosa-Dague *et al.*, 2016b).

1.5.2.2.5 Protein A

The *S. aureus* IgG-binding protein, protein A was previously found to promote bacterial aggregation and biofilm formation (Merino *et al.*, 2009). However, this protein A-mediated biofilm phenotype was observed only when protein A was overexpressed from a plasmid in the *S. aureus* lab strain Newman and in *L. lactis* or in *S. aureus* mutants with inactive two-component systems *agr* or *arlRS* (Merino *et al.*, 2009). These two component systems negatively regulate biofilm formation in *S. aureus*. Thus, the biological relevance of protein A-mediated biofilm in a wild-type *S. aureus* strain is unclear. Interestingly, a role for protein A in biofilm was not limited to cell wall-anchored protein A with exogenous protein A or protein A present in *S. aureus* culture supernatants increasing biofilm formation (Merino *et al.*, 2009). The molecular mechanisms underlying biofilm mediated by both cell wall-anchored and extracellular released protein A are yet to be identified.

1.5.2.2.6 *S. aureus* surface protein C

The *S. aureus* surface protein C (SasC) mediates bacterial aggregation and biofilm accumulation (Schroeder *et al.*, 2009). A transposon mutant of SasC in the *S. aureus* lab strain SH1000 had a reduced ability to form biofilm (Schroeder *et al.*, 2009). Furthermore, expression of SasC in the surrogate host *S. carnosus* or overexpression of SasC in SH1000 on a plasmid promoted bacterial aggregation and biofilm formation. SasC-mediated biofilm was localised to its N-terminal domain (Schroeder *et al.*, 2009) although the molecular mechanism is yet to be determined. The *sasC* gene was found to be present in 66 of 68 clinical isolates by polymerase chain reaction (PCR) (Schroeder *et al.*, 2009). However, whether SasC is expressed on the surface of these clinical isolates and mediates biofilm in these strains has not been assessed. In the case of *S. aureus* strains COL, SH1000 and 4074, only a low level of surface displayed SasC was detected *in vitro* (Schroeder *et al.*, 2009). However, expression of SasC *in vivo* has been reported (Clarke *et al.*, 2006).

1.5.2.2.7 Serine rich adhesin for platelets

The serine rich adhesin for platelets (SraP) was found to promote biofilm formation of the *S. aureus* lab strain ISP479C (Sanchez *et al.*, 2010). The BR domain of SraP is likely to be involved in mediating biofilm accumulation. Recombinant SraP BR domain protein adhered to immobilised lysates of wild-type *S. aureus* but not lysates of *S. aureus* Δ *sraP* bacteria (Sanchez *et al.*, 2010). The BR domain of SraP contains two cadherin-like subdomains (CDHL-1 and CDHL-2) which dimerise *in vitro* (Yang *et al.*, 2014). In the solved crystal structure of the CDHL subdomain dimer, the SraP proteins lie parallel with the CDHL-2 of one protein interacting at the junction of the CDHL-1 and CDHL-2 of the adjacent protein (Yang *et al.*, 2014). This dimerization of the CDHL subdomains supports the likelihood that SraP mediates biofilm through homophilic BR domain interactions.

1.5.2.2.8 Biofilm-associated protein

The biofilm-associated protein (Bap) was the first cell wall-anchored protein found to mediate biofilm accumulation of *S. aureus* (Speziale *et al.*, 2014). Bap promotes biofilm

formation in chronic mastitis clinical isolates but the *bap* gene is not carried by human isolates of *S. aureus* (Arrizubieta *et al.*, 2004, Cucarella *et al.*, 2001). A role for Bap in biofilm formation was identified through the generation of a transposon mutant library in the biofilm-forming mastitis *S. aureus* isolate V329 where insertions in the *bap* gene abolished the ability of strain V329 to form a biofilm (Cucarella *et al.*, 2001). Biofilm mediated by Bap is also affected by the presence of metals. In contrast to ClfB, Bap-mediated biofilm formation is inhibited by calcium (Arrizubieta *et al.*, 2004). Similar to SdrC, biofilm formed by Bap is also inhibited by manganese (Arrizubieta *et al.*, 2004). Furthermore, Bap was found to promote catheter colonisation in the later stages of infection *in vivo* in a mouse foreign body model of infection (Cucarella *et al.*, 2001).

1.5.2.2.9 *S. aureus* surface protein X

The *S. aureus* surface protein X (SasX) promotes bacterial aggregation and biofilm formation (Li *et al.*, 2012). The molecular mechanisms underlying SasX-mediated biofilm remain unknown. SasX is a particularly interesting biofilm accumulation factor as, unlike the other chromosomally encoded factors described here, SasX is encoded on a mobile genetic element; a prophage. SasX carriage has mainly been associated with strains of the ST239 clone; the major MRSA clone in Asia (Li *et al.*, 2012). However, the frequency of SasX carriage among other *S. aureus* sequence types and, in general, in invasive isolates and MRSA isolates was found to be increasing over time (Li *et al.*, 2012). Notably, SasX carriage is predominantly associated with hospital settings. This presents the possibility of biofilm accumulation factors being spread among *S. aureus* strains by horizontal gene transfer.

1.5.2.3 Fibrin-dependent biofilm accumulation.

Fibrin-dependent biofilm accumulation by *S. aureus* utilises host proteins to build the biofilm scaffold (Zapotoczna *et al.*, 2015, Dastgheyb *et al.*, 2015, Vanassche *et al.*, 2013). Staphylothrombin complexes are formed through the binding of *S. aureus* coagulases; staphylocoagulase or von Willebrand factor-binding protein, to host prothrombin (Vanassche *et al.*, 2013). Staphylothrombin mediates the conversion of monomeric fibrinogen to polymerized fibrin. This insoluble fibrin is bound by cell wall-

anchored MSCRAMM proteins and forms the biofilm scaffold. In this regard, ClfA, ClfB, FnBPA and FnBPB have been implicated in fibrin-dependent biofilm accumulation (Dastgheyb *et al.*, 2015). Fibrin-dependent biofilm accumulation has been associated with indwelling device related infections (Zapotoczna *et al.*, 2015, Dastgheyb *et al.*, 2015, Vanassche *et al.*, 2013) and joint infections (Dastgheyb *et al.*, 2015). Fibrin-dependent biofilms may be surface attached or free floating (Crosby *et al.*, 2016, Dastgheyb *et al.*, 2015).

1.5.2.4 Extracellular DNA and cytoplasmic proteins

During biofilm accumulation and maturation, *S. aureus* cells may become embedded in a self-synthesized matrix. Extracellular DNA (eDNA) is a major component of these matrices where it acts as a 'glue' linking cells together allowing biofilm to accumulate (DeFrancesco *et al.*, 2017, Montanaro *et al.*, 2011). The negative charge of DNA is important in biofilm accumulation and may link positively charged polymers including the exopolysaccharide PIA (Otto, 2008). The release of eDNA is likely to be a result of autolysis of a small number of cells within the biofilm (Otto, 2008), although other mechanisms of eDNA release have been reported (DeFrancesco *et al.*, 2017). Several enzymes have been implicated in this autolysis of cells and eDNA release. One, example is CidA which regulates murein hydrolase activity (Rice *et al.*, 2007). Mutation of *cidA* in the MSSA clinical isolate UAMS-1 reduced levels of eDNA within the biofilm and overall biofilm formation (Rice *et al.*, 2007).

Along with eDNA and PIA, cytoplasmic proteins have been reported as components of biofilm matrices through mass spectrometric analysis (Foulston *et al.*, 2014). Biofilm-associated cytoplasmic proteins are considered to be 'moonlighting' or being recycled as components of the extracellular matrix. The cytoplasmic proteins aggregate at the surface of *S. aureus* cells in a low pH-dependent manner and this aggregation is thought to form a matrix surrounding cells and linking them together (Foulston *et al.*, 2014). It is worth noting that the study by Foulston *et al.* (2014), exclusively assessed MSSA strains and not MRSA strains, where cell wall-anchored protein-dependent biofilm formation was found to be more prevalent (O'Neill *et al.*, 2007). Furthermore, such cell wall-anchored protein-dependent biofilms were not embedded in a self-

synthesized matrix when viewed by scanning electron microscopy unlike PIA-dependent biofilms (Fig 1.4; Vergara-Irigaray *et al.*, 2009). Thus, the importance of biofilm matrices and each accumulation factor varies among *S. aureus* strains and infection sites.

1.5.3 Biofilm Dispersal

The final phase of *S. aureus* biofilm formation is dispersal whereby bacterial cells detach from the biofilm and can disseminate to other sites (Fig 1.3). Thus, biofilms serve as foci for secondary infections, where bacteria originally associated with a biofilm infection can cause secondary infections at other body sites. A large proportion of *S. aureus* bloodstream infections are due to initial catheter-associated infections (Hogan *et al.*, 2015). *S. aureus* biofilm dispersal is mediated by secreted surfactants and enzymes which destabilize the mature biofilm structure.

Phenol soluble modulins (PSMs) have been shown to mediate *S. aureus* biofilm dispersal *in vitro* and *in vivo* (Periasamy *et al.*, 2012). PSMs are small, amphipathic peptides with α -helical secondary structures. *S. aureus* expresses seven PSMs; four PSM α peptides, two PSM β peptides and δ -toxin (Le *et al.*, 2014). The PSM α peptides are smaller; ~20 amino acids in length while the PSM β peptides are ~44 amino acids in length (Le *et al.*, 2014). All three types of PSMs were found to mediate biofilm dispersal through their nonspecific surfactant activity (Periasamy *et al.*, 2012). An isogenic deletion mutant of the three types of PSMs had reduced dissemination in comparison to the parental CA-MRSA USA300 strain LAC in a mouse catheter model of infection (Periasamy *et al.*, 2012).

Other mechanisms of biofilm dispersal have been identified which are dependent upon the type of mature biofilm formed unlike the nonspecific activity of PSMs which can mediate dispersal of most biofilms (Lister & Horswill, 2014). These include protease-mediated biofilm dispersal. *S. aureus* can secrete up to ten different proteases which can degrade proteins in the mature biofilm (Lister & Horswill, 2014). This destabilises the biofilm structure and facilitates dispersal. Of course protease-mediated biofilm dispersal is only relevant to mature biofilms where proteins are a component such as in protein-dependent biofilms or extracellular matrices containing

cytosolic proteins. Interestingly, the protease Esp secreted by *S. epidermidis* can disperse *S. aureus* biofilms and is important in competition between these strains for colonisation of the nares (Lister & Horswill, 2014). Upregulation of protease production through activation of the accessory gene regulator (Agr) system has been reported to mediate biofilm dispersal (Boles & Horswill, 2008). Agr is a quorum sensing system which is stimulated by autoinducing peptides (AIP) and is a master regulator of *S. aureus* virulence factors and adhesins. Activated Agr upregulates virulence factor expression such as toxins and downregulates expression of PSMs and microbial surface components such as cell wall-anchored proteins (Le & Otto, 2015). Interestingly, low Agr activity and *agr* defective mutants are thus, known to enhance *S. aureus* biofilm formation (Le & Otto, 2015, Boles & Horswill, 2008) while, activation of Agr by AIP causes biofilm dispersal through the upregulation of proteases (Boles & Horswill, 2008). This is an interesting observation which implicates the Agr system at the interface between planktonic and biofilm-associated *S. aureus* (Boles & Horswill, 2008) whereby low Agr activity promotes biofilm formation and maintenance whereas activation of Agr through AIP leads to biofilm dispersal and reversion to a planktonic lifestyle. This Agr activation would also upregulate virulence factors in the dispersed, planktonic *S. aureus* which would be advantageous in subsequent acute infections in other body sites.

S. aureus nucleases, in particular the main nuclease (Nuc) and to a lesser extent the second nuclease of *S. aureus*, Nuc2, also mediate biofilm dispersal (Lister & Horswill, 2014). The expression of nucleases causes degradation of eDNA within the biofilm matrix mediating biofilm dispersal. Deletion of *nuc* resulted in enhanced eDNA levels and overall biofilm formation whereas addition of Nuc caused a reduction in *S. aureus* biofilm formation (Mann *et al.*, 2009, Kiedrowski *et al.*, 2011). The production of D-amino acids during stationary phase *S. aureus* growth has also been implicated in biofilm dispersal (Kolodkin-Gal *et al.*, 2010) although the mechanism underlying D-amino acid-mediated dispersal is unclear. Apart from PSM-mediated biofilm dispersal, the other mechanisms of biofilm dispersal described here have been limited to *in vitro* studies with their *in vivo* relevance yet to be assessed.

1.6 Similarities of biofilm formation by *S. epidermidis*

The coagulase-negative staphylococcal species *S. epidermidis* is also a leading cause of indwelling device related infections that involve formation of a biofilm (Buttner *et al.*, 2015). *S. epidermidis* is traditionally considered a commensal bacterium which colonises the skin and nares of healthy individuals. However, with advances in modern medicine and the use of indwelling devices *S. epidermidis* has become an opportunistic pathogen (Becker *et al.*, 2014a). *S. epidermidis* biofilm is also considered to occur over the same three distinct phases; primary attachment, accumulation and maturation and dispersal. There are many similarities between *S. epidermidis* and *S. aureus* factors which mediate primary attachment and biofilm accumulation.

Similarly to *S. aureus* abiotic attachment, the major autolysin AtlE of *S. epidermidis* has been shown to promote bacterial attachment to polystyrene surfaces (Heilmann *et al.*, 1997). AtlE was also shown to promote adherence of *S. epidermidis* to biotic surfaces through binding of vitronectin (Heilmann *et al.*, 1997). *S. epidermidis* also expresses a number of cell wall-anchored MSCRAMMs which mediate *S. epidermidis* attachment to biotic surfaces. These MSCRAMMs are the Sdr proteins SdrG, SdrF and SdrH. SdrG binds the β -chain of fibrinogen through its N2N3 subdomains by DLL (Ponnuraj *et al.*, 2003, Bowden *et al.*, 2008) while SdrF binds type I collagen via its B repeats (Arrecubieta *et al.*, 2007).

Several factors mediating biofilm accumulation of *S. epidermidis* are similar to those in *S. aureus*. PIA also mediates biofilm accumulation in many *S. epidermidis* strains and eDNA has also been associated with *S. epidermidis* biofilm matrices; linking cells and promoting biofilm accumulation (Buttner *et al.*, 2015). Like protein-dependent biofilm formation in *S. aureus*, several cell wall anchored-proteins of *S. epidermidis* promote biofilm accumulation. The accumulation-associated protein (Aap) of *S. epidermidis* is a G5-E repeat protein which is orthologous to SasG of *S. aureus*. Aap, like SasG, mediates biofilm accumulation which is zinc-dependent through homophilic interactions of its G5-E domains (Rohde *et al.*, 2005, Conrady *et al.*, 2008, Conrady *et al.*, 2013). However, unlike SasG, the A domain of Aap has been associated with promoting primary attachment to abiotic surfaces (Conlon *et al.*, 2014, Schaeffer *et al.*, 2015).

Thus, Aap has a dual function in promoting *S. epidermidis* biofilm formation. The *in vivo* relevance of Aap-mediated biofilm was demonstrated in a rat catheter model of infection (Schaeffer *et al.*, 2015). The *S. epidermidis* surface protein (Ses) C is a cell wall-anchored protein which is distantly related to ClfA of *S. aureus* (Buttner *et al.*, 2015). SesC promotes biofilm formation although the underlying mechanism remains unclear (Buttner *et al.*, 2015). Furthermore, Bap-mediated biofilm has also been observed in *S. epidermidis* (Tormo *et al.*, 2005).

1.7 Difficulties in the treatment of biofilm infections

1.7.1 Resistance to host immune phagocytosis

S. aureus biofilms are resistant to host immune phagocytosis and often cause chronic infections. In many ways, formation of a biofilm could be considered an immune evasion strategy employed by *S. aureus*. The polymorphonuclear leucocytes (PMNs); neutrophils and macrophages, are the main host response which clear *S. aureus* planktonic bacteria. However, the situation in a biofilm is quite different. In terms of the biofilm structure, bacteria in a biofilm are surrounded in a bacterial community or embedded in a matrix. Penetration of a biofilm is very difficult and thus, immune cells have limited access to bacteria for clearance. The semi-dormant state of bacteria in a biofilm likely leads to less detection than actively growing, toxin-producing bacteria. Furthermore, bacteria may be shielded from immune detection by matrix components. *S. epidermidis* PIA (Vuong *et al.*, 2004) and host fibrin utilised by *S. aureus* in its biofilm scaffold (Zapotoczna *et al.*, 2016) have been shown to protect bacteria from phagocytosis. Bacterial biofilms have also been shown to have increased resistance to antimicrobial peptides (AMPs) which is likely a result of electrostatic repulsion of such AMPs by components of the biofilm (Otto, 2008). In *S. epidermidis*, PIA was shown to confer resistance to both cationic and anionic AMPs (Vuong *et al.*, 2004).

In studies of human patients with orthopaedic device-associated infections, PMNs were found to be prevalent at the biofilm site (Paharik & Horswill, 2016). However, their efficacy against bacteria in a biofilm appears to be much lower than against planktonic bacteria. Studies involving *in vitro* co-culture of macrophages with *S. aureus* biofilms observed very little phagocytosis by the macrophages (Scherr *et al.*, 2013,

Thurlow *et al.*, 2011). Interestingly, studies assessing macrophage responses to *S. aureus* biofilms have found that *S. aureus* biofilms actively alter the immune response of macrophages to an M2 macrophage response which is anti-inflammatory and pro-fibrotic (Paharik & Horswill, 2016, Scherr *et al.*, 2014). In contrast, the M1 macrophage response which is pro-inflammatory is favoured in response to *S. aureus* acute infections involving planktonic bacteria (Paharik & Horswill, 2016, Scherr *et al.*, 2014). It has also been found that *S. aureus* biofilms attenuate the levels of pro-inflammatory mediators at the local site of infection (Scherr *et al.*, 2014).

Differences in gene expression between *S. aureus* cells in a biofilm and planktonic cells may also reflect differences in the capability of the host to clear bacteria in a biofilm (Scherr *et al.*, 2014). Co-culture of macrophages with an *S. aureus* biofilm resulted in a large downregulation of genes within the bacteria indicating they may alter their gene expression to avoid macrophage detection and clearance (Scherr *et al.*, 2014). Interestingly, such major gene expression alterations in bacterial cells in a biofilm were not observed in response to neutrophils which may hint at M1 macrophages as a more significant threat to biofilms than neutrophils. When added exogenously, M1 macrophages were able to clear established biofilms whereas exogenous addition of neutrophils did not have much effect on *S. aureus* biofilms *in vitro* (Scherr *et al.*, 2014).

1.7.2 Recalcitrance to conventional antibiotics

Once a mature *S. aureus* biofilm is formed, it is extremely difficult to treat as it is recalcitrant to conventional antibiotics. Thus, treatment often involves removal of the indwelling device (Hogan *et al.*, 2015). This recalcitrance is another major reason that biofilm infections can be chronic. Astoundingly, increases in minimum inhibitory concentrations (MIC) of antibiotics of 1000-fold have been reported for bacteria in a biofilm in comparison to a planktonic state (Olson *et al.*, 2002). The main reasons for the biofilm recalcitrance to antibiotics are the semi-dormant nature of bacteria themselves within a biofilm (Otto, 2008), the presence of persister cells (Conlon, 2014) (Singh *et al.*, 2009) and the overall structure of the biofilm (Otto, 2008).

Bacteria in a biofilm lie in a low-energy, semi-dormant state. Although the bacteria themselves may not have acquired resistance to the antibiotic, they are largely

unaffected. This is because conventional antibiotics target essential processes in growing cells such as protein synthesis and peptidoglycan synthesis among others. Bacteria in a mature biofilm are not actively growing and thus, remain unaffected by these antibiotics. Persister cells also play a pivotal role. Persister cells are a sub-population of bacterial phenotypic variants that are unresponsive to antibiotics (Conlon, 2014). There is an increased abundance of these persister cells in *S. aureus* biofilms (Singh *et al.*, 2009). A model for the role of persister cells in relapsing biofilm infections has been proposed (Conlon, 2014) where bacterial cells are protected from host immune clearance by matrix components. Upon antibiotic treatment the majority of the cells in the biofilm are killed but a sub-population of persister cells survive. When the antibiotic pressure is removed these persister cells then revert to an actively growing state and repopulate the biofilm (Conlon, 2014).

The biofilm structure also limits the effectiveness of antibiotic intervention. This is because the antibiotic must penetrate and diffuse through the biofilm structure to reach its target. Components of the mature biofilm may also be electrostatically repulsive to some antibiotics. For example, PIA has been shown to repel antimicrobial peptides in this manner (Vuong *et al.*, 2004). Furthermore, it is also possible that components of the mature biofilm may sequester antimicrobial compounds preventing them reaching their target site (Otto, 2008).

1.7.3 Antibiotic resistance

Along with the refractive nature of biofilms to antibiotics, many *S. aureus* biofilm infections are caused by antibiotic resistant strains, in particular, MRSA strains. This further complicates treatment options. The main targets of antibiotics against *S. aureus* are the cell envelope, protein synthesis and nucleic acid synthesis. *S. aureus* strains have been able to develop resistance to most, if not all, antibiotics used clinically (Foster, 2017). The development of antibiotic resistance in *S. aureus* may be acquired by horizontal gene transfer of mobile genetic elements or through mutation of chromosomal genes leading to alteration of the drug target or the upregulation of efflux pumps already present on the *S. aureus* chromosome (Foster, 2017). For conventional antibiotics which are natural products resistance mechanisms typically exist in nature either in the antibiotic producing species itself for protection or among

competitors in their natural environment and these may be horizontally transferred (Foster, 2017).

In particular, MRSA strains (Section 1.7.3.1) are widespread and may be hospital associated (HA) or community associated (CA) (Chambers & Deleo, 2009). A 2014 report from the World Health Organization (WHO) found that in five of six WHO regions surveyed MRSA rates of 50 % or more were recorded (WHO, 2014). Both an increased risk of mortality and increased hospital expenses were associated with MRSA versus MSSA infections (WHO, 2014). However, the overall incidence of MRSA infections in North America and Ireland has considerably decreased by 31 % from 2005-2011 (Dantes *et al.*, 2013) and 27.1 % from 2004-2016 (HSPC, 2016), respectively. However, despite this reduction a considerable number of cases of invasive MRSA infections; ~80,000 in North America, were recorded in 2011 (Dantes *et al.*, 2013).

The glycopeptide antibiotic vancomycin is the most commonly used treatment for invasive MRSA infections (NCEC, 2013). Vancomycin resistance has been widely reported in enterococci. However, vancomycin resistant *S. aureus* strains have only been reported on a few occasions and there is a significant fitness cost to high level vancomycin resistance in these strains (Foster, 2017). As a result, widespread resistance has not emerged. However, *S. aureus* strains with an increased MIC to vancomycin, but not high level resistance, described as vancomycin-intermediate *S. aureus* strains, exist and can cause vancomycin treatment failure (Foster, 2017). This intermediate resistance to vancomycin typically involves the accumulation of up to six mutations in different genes which lead to overall alterations and increased thickness of the *S. aureus* cell envelope rendering the bacteria less susceptible to vancomycin (Foster, 2017).

1.7.3.1. Methicillin resistant *S. aureus*

Methicillin is a β -lactam antibiotic which targets the transpeptidase domain of penicillin binding protein (PBP) 2 by binding at its active site serine (Foster, 2017). PBP2 has two important functions in the formation of the bacterial cell wall peptidoglycan. PBP2 is a transglycosylase which removes the disaccharide

pentapeptide of peptidoglycan from lipid II and attaches it to the growing peptidoglycan chains. PBP2 is also a transpeptidase mediating the pentaglycine cross-bridge formation. Methicillin resistance was gained by *S. aureus* through the acquisition of staphylococcal chromosomal cassettes (SCC) which contain the *mecA* gene (SCC*mec*) (Peacock & Paterson, 2015). The *mecA* gene encodes an alternative PBP2 known as PBP2a or PBP2' whose transpeptidase active site serine is buried and thus, is not accessible for β -lactam binding (Peacock & Paterson, 2015).

Initially, HA-MRSA strains were observed in the 1960s (Chambers & Deleo, 2009). HA-MRSA strains typically cause bacteraemia, wound and indwelling device-related infections in patients. HA-MRSA strains are associated with lower virulence, high β -lactam resistance, carry large SCC*mec* elements and are also typically resistant to multiple drugs (Rudkin *et al.*, 2012). In contrast, CA-MRSA strains emerged in the 1990s and were unusual, in that they were infecting otherwise healthy individuals (Chambers & Deleo, 2009, DeLeo *et al.*, 2010). CA-MRSA strains are associated with severe skin and soft tissue infections (DeLeo *et al.*, 2010). They are hypervirulent, carry smaller SCC*mec* elements and have lower levels of β -lactam resistance in comparison to HA-MRSA strains (Rudkin *et al.*, 2012). CA-MRSA strains are typically not resistant to multiple antibiotics (DeLeo *et al.*, 2010). Studies have found that HA-MRSA strains sacrifice their virulence for high level antibiotic resistance which is more important in a hospital setting (Rudkin *et al.*, 2012). In comparison, in the community, among healthy individuals where antibiotic pressure is much lower, it is more advantageous for CA-MRSA strains to be highly virulent.

1.8 Treatment and prevention of *S. aureus* biofilm infections

Treatment of bacteria within a biofilm is very different from treatment of planktonic bacteria. As described previously, *S. aureus* biofilms are recalcitrant to conventional antibiotics and resistant to host immune phagocytosis. Thus, treatment strategies that are effective against infections of planktonic *S. aureus* are not effective against biofilm infections. There has been a considerable amount of research into strategies for treating and preventing biofilm infections including the development of anti-biofilm agents and vaccines. As *S. aureus* biofilm formation is clearly a multifactorial process it is very difficult to identify a single factor that could be targeted.

1.8.1 Anti-biofilm agents

Anti-biofilm strategies have been investigated, which, instead of killing the bacteria interfere with processes involved in biofilm formation. Anti-biofilm agents have been investigated targeting each stage of biofilm development and several will be discussed here.

1.8.1.1 Preventing *S. aureus* primary attachment

Prevention of *S. aureus* primary attachment may be achieved by altering the device/site of primary attachment or by inhibiting the bacterial factors such as MSCRAMMs which promote *S. aureus* primary attachment. A lot of research has explored the former i.e. altering the medical device surface to prevent bacterial attachment. These have included altering the physiochemical properties of the device such as its charge, hydrophilicity and roughness, coating the device with antibiotics, metals such as silver and platinum, which have antibacterial properties, or antiseptics (Hogan *et al.*, 2015). In general, negatively charged, hydrophilic surfaces with low surface energy show reduced bacterial attachment. These strategies have also been assessed in combination with antimicrobials whereby planktonic cells are prevented from attaching to the device and, in their planktonic state, are killed by the antimicrobial. However, such broad use of antibiotics or antiseptics has a major drawback as it will increase the selective pressure for bacterial resistance. Certain polysaccharide coatings of devices have been found to prevent bacterial attachment. These coatings may be anti-adhesive due to the hydrophilic nature of the polysaccharides used or antibacterial (Junter *et al.*, 2016). An example of an anti-adhesive polysaccharide coating is hyaluronic acid which has been found in several studies to reduce *S. aureus* attachment to devices (Harris & Richards, 2004, Hu *et al.*, 2010, Palumbo *et al.*, 2015). Hyaluronic acid infers a hydrophilic surface (Junter *et al.*, 2016) but also has bacteriostatic activity (Pirnazar *et al.*, 1999). Of course such preventive strategies are not relevant to biofilm infections formed directly on host tissue and may also, depending on cytotoxicity, not be applicable to devices fully inserted into the host such as orthopaedic prosthetic devices where bone regeneration is important (Junter *et al.*, 2016).

Another preventive strategy is targeting the bacterial factors which promote *S. aureus* primary attachment. Medical devices become coated with host plasma proteins upon insertion and thus, it is more likely that biotic attachment is the main mechanism of primary attachment *in vivo*. Thus, the cell-wall anchored MSCRAMM proteins are attractive targets for inhibition. These MSCRAMM proteins are anchored to the cell wall by the enzyme sortase A. Thus, inhibition of sortase A would prevent the surface display of these proteins and inhibit adhesion of *S. aureus* to biotic surfaces. A rational design study identified a small molecule inhibitor of sortase A which was effective *in vivo* in increasing mouse survival in an *S. aureus* bacteraemia model (Zhang *et al.*, 2014). As expected, the small molecule inhibitor reduced the ability of *S. aureus* to adhere to fibrinogen *in vitro* (Zhang *et al.*, 2014). Although this inhibitor has not been assessed in a catheter model of infection, such an inhibitor could be used as a catheter coating to prevent MSCRAMM-mediated primary attachment.

1.8.1.2 Chelation of metals

Metals are essential cofactors for many bacterial enzymes and have also been implicated in mechanisms of *S. aureus* biofilm formation. Thus, chelation of metals may represent an attractive method for preventing and also treating *S. aureus* biofilm infections. Several chelators have shown efficacy in inhibiting biofilm formation (Hogan *et al.*, 2015). Ethylenediaminetetraacetic acid (EDTA) was found to inhibit *S. aureus* biofilm formation and showed promise as a potential catheter lock solution in combination with antibiotics both *in vitro* and *in vivo* (Bookstaver *et al.*, 2009, Chauhan *et al.*, 2012). *In vivo* the EDTA based lock solutions were found to be effective in treating established biofilms (Chauhan *et al.*, 2012). EDTA is known to have bacteriostatic activity but metal chelators may also inhibit bacterial factors mediating biofilm accumulation. For example, zinc is essential for both FnBP- and SasG-mediated biofilm accumulation and *in vitro* the zinc chelator diethylenetriaminepentaacetic acid (DTPA) prevented both FnBP- and SasG- mediated biofilm accumulation of *S. aureus* (Geoghegan *et al.*, 2010, Geoghegan *et al.*, 2013).

1.8.1.3 Degradation of the extracellular matrix

Another attractive strategy for anti-biofilm agents is disrupting components of the biofilm extracellular matrix (ECM). Several enzymes have been identified which degrade components of the ECM and have potential as anti-biofilm agents. A limitation to this strategy is the variation that exists among *S. aureus* biofilms with some strains forming matrices of PIA and eDNA and other strains forming protein-dependent biofilms where cell wall-anchored proteins link cells together (Fig 1.4). However, these agents could be used in combination to enhance their success.

The enzyme Dispersin B cleaves the glycosidic linkages of PIA, degrading PIA and removing biofilm (Kaplan *et al.*, 2004). This enzyme is not produced by staphylococci but by other bacterial species and was originally identified in the periodontal gram-negative pathogen *Actinobacillus actinomycetemcomitans* (Kaplan *et al.*, 2004). Another component of *S. aureus* biofilm ECMs is eDNA and the enzyme DNase I, which degrades eDNA, has been shown to degrade *S. aureus* biofilm matrices (Lauderdale *et al.*, 2010, Mann *et al.*, 2009). Cell wall-anchored proteins are important factors linking cells together in protein-dependent biofilms and cytosolic proteins have been found in some ECMs. Degradation of these protein components using proteinase K or trypsin has also been found to treat mature biofilms (Lauderdale *et al.*, 2010). The most promising agent assessed to date is lysostaphin which cleaves the pentaglycine bridges of the cell wall peptidoglycan of *S. aureus*. Lysostaphin has been shown to be effective in both preventing and treating *S. aureus* biofilms *in vivo* (Aguinaga *et al.*, 2011, Kokai-Kun *et al.*, 2009). Furthermore, its target; the cell wall, is conserved across *S. aureus* biofilms and lysostaphin is also effective against *S. epidermidis* biofilms (Wu *et al.*, 2003).

1.8.1.4 Promoting biofilm dispersal

Biofilm infections could potentially be treated through the promotion of dispersal followed by antibiotic treatment of the dispersed, planktonic cells which are no longer refractive to conventional antibiotics. Analogues of autoinducing peptides (AIP) (Boles & Horswill, 2008) and phenol soluble modulins (PSMs) (Periasamy *et al.*, 2012) could be exploited for such use. However, AIP-mediated activation of the Agr system may cause the planktonic bacteria which are dispersed to have increased expression levels

of virulence factors such as toxins. The PSM β peptides, and not the PSM α peptides, would be more suitable as PSM dispersal agents as they are not cytotoxic (Le *et al.*, 2014). D-amino acids have also been implicated in *S. aureus* biofilm dispersal (Kolodkin-Gal *et al.*, 2010). D-amino acids were found to both disperse and prevent *S. aureus* biofilm formation *in vitro* and *in vivo* (Hochbaum *et al.*, 2011, Sanchez *et al.*, 2013). In prevention of biofilm formation, the D-amino acids did not inhibit primary attachment but inhibited biofilm accumulation and maturation and were found to be effective against protein-dependent but not PIA-dependent biofilms (Hochbaum *et al.*, 2011). However, the mechanism underlying this inhibition remains unclear. A medium chain fatty acid messenger produced by *Pseudomonas aeruginosa*; cis-2-decenoic acid (CD2A) has also shown promise as a dispersal agent of *S. aureus* biofilms (Jennings *et al.*, 2012). CD2A has also been shown to have *S. aureus* bactericidal activity and may have a dual capability in treating biofilms (Desbois & Smith, 2010).

1.8.2 Vaccines against *S. aureus*

1.8.2.1 *S. aureus* vaccine development

With the widespread resistance to antibiotics among *S. aureus* strains, the development of a vaccine to protect against or treat *S. aureus* infections is warranted. However, to date no *S. aureus* vaccine has been successful in clinical trials. Like many early bacterial vaccines, initially dead whole *S. aureus* cells were assessed as a vaccine with no protective effect observed (Missiakas & Schneewind, 2016). A similar lack of protective immunity is observed in individuals colonised with *S. aureus* or those who have previously been infected (Missiakas & Schneewind, 2016). This complicates development of a vaccine as correlates of protective immunity have remained unclear. However, reduced disease severity is observed in those colonised with *S. aureus* indicating some level of immune memory and subsequent protection (Giersing *et al.*, 2016).

Past *S. aureus* vaccines assessed in clinical trials included a vaccine comprised of the *S. aureus* capsular polysaccharide (CP) type 5 and type 8 conjugated to exotoxin A of *Pseudomonas aeruginosa*, called StaphVax, and the cell wall-anchored protein IsdB vaccine; V710 (Missiakas & Schneewind, 2016). StaphVax generated high levels of

antibodies against CP but was not effective in clinical trials (Missiakas & Schneewind, 2016). V710 generated function neutralising antibodies against IsdB and some protection against bacteraemia in animal models but V710 was not protective in clinical trials and actually enhanced patient mortality (Missiakas & Schneewind, 2016). Several other single factors; staphylococcal enterotoxin B, ClfA, LTA and the ABC transporter component GrfA have also been assessed as vaccines in clinical trials with no successful outcome to date (Fowler & Proctor, 2014).

Several reasons for the failure of these vaccines have been suggested (Jansen *et al.*, 2013, Missiakas & Schneewind, 2016, Fowler & Proctor, 2014). These include the lack of knowledge of correlates of protective immunity. Previous vaccines have focused on antibody responses alone whereas recent research has identified the importance of T cell responses, in particular Th1 (Brown *et al.*, 2015) and Th17 (Fowler & Proctor, 2014) responses, in host protection to *S. aureus*. Interestingly, a nasal vaccine which stimulated T cell responses; Th1 and Th17, but not antibody responses, protected mice against systemic *S. aureus* infection further highlighting the importance of cellular immunity in protection (Misstear *et al.*, 2014). The CWA protein ClfA elicits T cell responses in mice (Brown *et al.*, 2015, Misstear *et al.*, 2014) and humans (Brown *et al.*, 2015) and as a vaccine afforded protection to systemic infection in mice (Brown *et al.*, 2015, Misstear *et al.*, 2014). There has also been a lack of correlation between preclinical results in animal models and trials in humans. Furthermore, the clinical trial patient groups have consisted of individuals who are very vulnerable to infection whereas most successful vaccines are administered to healthy individuals. It has been suggested that nasal colonisation or skin and soft tissue infections may be more appropriate endpoints for vaccine efficacy tests (Missiakas & Schneewind, 2016). StaphVax was assessed with decolonisation as an endpoint with no reduction in nasal colonisation recorded (Fowler & Proctor, 2014). However, the capsular polysaccharides have not been implicated as an essential factor in nasal colonisation and not all *S. aureus* clinical isolates are encapsulated. Past vaccines have been monovalent whereas a combined vaccine may be more effective considering the wide spectrum of disease caused by *S. aureus*, the numerous virulence and immune evasion factors it employs and the functional redundancy among these factors.

Most of the vaccines in ongoing clinical trials are multivalent. Pfizer currently have a multivalent vaccine in phase IIb trials; SA4Ag, which consists of CP5 and CP8 conjugated to inactivated diphtheria toxin, recombinant CWA protein ClfA and recombinant manganese transporter protein C (MntC) (Missiakas & Schneewind, 2016, Begier *et al.*, 2017, Frenck *et al.*, 2017). In the SA4Ag phase I trial, its safety and efficacy to elicit antibody responses were demonstrated although T cell responses were not reported (Begier *et al.*, 2017, Frenck *et al.*, 2017). Another vaccine currently in phase II clinical trials is NDV3 which consists of recombinant Als3p protein; a homologue of ClfA expressed on the surface of *Candida albicans* (Lacey *et al.*, 2016). NDV3 generated both antibody and T cell responses against *C. albicans* and *S. aureus* in its phase I trial along with meeting safety requirements (Schmidt *et al.*, 2012). There are also other vaccines in preclinical development, some of which include inactivated toxins and toxoids as potential vaccine antigens (Giersing *et al.*, 2016).

1.8.2.2 Active and passive immunization against biofilm infections

Most *S. aureus* vaccines to date have focused on protection of acute infections caused by planktonic *S. aureus*. Due to the differences in antigen expression and host immune responses in acute infections versus biofilm infections an ideal vaccine would include antigens relevant to both infection types and elicit immune responses that clear either an acute or biofilm *S. aureus* infection. However, there has been huge difficulty in generating a vaccine to prevent acute *S. aureus* infections alone without also considering protection against biofilm infections (Bhattacharya *et al.*, 2015). However, several studies have investigated both active and passive immunization strategies to prevent biofilm infections.

A study by Brady *et al.*, (2006), began to look at antigens associated with biofilms. The study identified several proteins in an *S. aureus* biofilm infection which generated an antibody response *in vivo*. The proteins identified were a β -lactamase, lipoprotein, lipase, autolysin and an ABC transporter lipoprotein (Brady *et al.*, 2006). Several of these antigens were later assessed in a vaccination study using a rabbit biofilm model of chronic osteomyelitis (Brady *et al.*, 2011). Notably, the vaccination was combined with vancomycin treatment in order to clear planktonic bacteria. The vaccine antibiotic

combination was successful *in vivo* with both components required for high efficacy (Brady *et al.*, 2011). SesC, a cell wall-anchored protein which mediates biofilm formation in *S. epidermidis*, showed promise as a vaccine candidate *in vivo* in animal biofilm models (Shahrooei *et al.*, 2012). Active immunization of rats with recombinant SesC reduced *S. epidermidis* biofilm formation on catheters inserted post vaccination (Shahrooei *et al.*, 2012). Passive immunization with anti-SesC antibodies also inhibited *S. epidermidis* biofilm formation in a rat catheter model (Shahrooei *et al.*, 2012). Cell wall-anchored proteins also represent attractive antigens for an *S. aureus* vaccine as they are displayed on the surface of *S. aureus*, generate a potent immune response and play important roles in primary attachment and biofilm accumulation (Speziale *et al.*, 2014). PIA has also been assessed as a vaccine candidate alone, and in a conjugate vaccine with ClfA, and was found to generate a strong humoral response (Maira-Litran *et al.*, 2012). Theoretically, PIA as an antigen could provide protection against both *S. aureus* and *S. epidermidis* biofilm infections. As *S. aureus* can also form PIA-independent biofilms, combining PIA with cell wall-anchored proteins in a vaccine would provide a more broadly, efficacious vaccine. However, PIA was assessed as a monovalent *S. aureus* vaccine in clinical trials but was terminated in phase II. This may be due to the reasons suggested for the failure of *S. aureus* vaccines to date (Section 1.8.2.1).

Several studies have shown promise for the use of specific antibodies in preventing *S. aureus* biofilm infections. *In vitro*, Fab fragments generated specifically against the A domain of FnBPA inhibited FnBP-mediated biofilm (O'Neill *et al.*, 2008). Similarly, inhibition of Aap-dependent biofilms of *S. epidermidis* was observed with polyclonal and monoclonal Aap antibodies (Rohde *et al.*, 2005, Hu *et al.*, 2011). There is also some potential for passive immunization with antibodies against mediators of biofilm dispersal in order to prevent dissemination of bacteria. For example, antibodies generated against PSMs were found to reduce bacterial dissemination (Wang *et al.*, 2011).

1.9 Aims and objectives

S. aureus biofilm infections are a significant cause of morbidity and mortality. *S. aureus* biofilm infections are extremely difficult to treat and novel treatment and preventive strategies are required to overcome these infections. Cell wall-anchored proteins of *S. aureus* mediate biofilm accumulation through specific homophilic interactions although more studies are required to further characterise these interactions. These cell wall-anchored proteins have not been assessed as targets for anti-biofilm agents previously. The major aims and objectives of this project were:

- To characterise SdrC- and FnBP- mediated biofilm accumulation at the molecular level.
- To identify novel inhibitors of SdrC- and FnBP- mediated biofilm formation of *S. aureus* using a rational drug design approach targeting their homophilic interactions. This allowed assessment of SdrC and FnBP homophilic interactions as anti-biofilm targets in the prevention of *S. aureus* biofilm formation.

Chapter 2

Materials and Methods

2.1. Bacterial strains and growth conditions. *Escherichia coli* strains were grown in Lennox broth (LB; 10 g/L Tryptone, 5 g/L Yeast Extract, 5 g/L NaCl, pH 6.8-7.2) at 37 °C. *Lactococcus lactis* strains were grown in M17 (0.5 g/L ascorbic acid, 5 g/L lactose, 0.25 g/L magnesium sulfate, 5 g/L meat extract, 2.5 g/L meat peptone, 19 g/L sodium glycerophosphate, 5 g/L soya peptone, 2.5 g/L tryptone, 2.5 g/L yeast extract, pH 7.4 ± 0.2) or brain heart infusion (BHI; 12.5 g/L brain infusion solids, 5 g/L beef heart infusion solids, 10 g/L proteose peptone, 2 g/L glucose, 5 g/L NaCl, 2.5 g/L disodium phosphate, pH 7.4 ± 0.2) broth statically at 28 °C. *Staphylococcus aureus* strains were grown in tryptic soy broth (TSB; 17 g/L Bacto™ tryptone, 3 g/L Bacto Soytone, 2.5 g/L glucose, 5 g/L NaCl, 2.5 g/L dipotassium hydrogen phosphate, pH 7.3 ± 0.2) or BHI broth at 37 °C. Media were supplemented with D-glucose (10 g/L; Sigma Aldrich), ampicillin (100 µg/ml), erythromycin (10 µg/ml), chloramphenicol (10 µg/ml) or nisin (32 ng/ml) where appropriate. Stationary phase cultures were typically grown for 16-18 h. For growth to exponential phase, cultures were washed in TSB, diluted to a starting OD_{600nm} of ~0.05 and grown to an OD_{600nm} of 0.5. Strains used in this study are listed in Table 2.1.

2.2. DNA cloning and strain construction. Plasmids used in this study are listed in Table 2.1. Primer sequences are listed in Table 2.2.

2.2.1 Cloning of DNA for recombinant protein expression in *E. coli*. DNA encoding the N2 and N3 subdomains of SdrC (0.947 kb) was amplified by polymerase chain reaction (PCR) with primers SdrCN2N3F and SdrCN2N3R (Table 2.2) using genomic DNA from *S. aureus* strain Newman as template and cloned into the IPTG-inducible vector pQE30 using sequence-and ligation-independent cloning (SLIC) as previously described by Li and Elledge (Li & Elledge, 2012). The plasmid pQE30::*sdrC* was transformed into chemically competent XL-1 Blue *E. coli*. The plasmid was isolated from XL-1 Blue and confirmed by DNA sequencing (Eurofins MWG). The plasmid was transformed into chemically competent Topp3 *E. coli* cells for protein expression.

DNA encoding the N2 and N3 subdomains of SdrC from *S. aureus* strain Newman was cloned into the IPTG-inducible vector pGEX-KG to generate the plasmid pGEX::*sdrC*. Plasmids pGEX-KG and pQE30::*sdrC* were digested in separate reactions with

restriction enzymes BamHI and KpnI at 37 °C. The plasmid pQE30 and its *sdrC* insert were separated by agarose gel electrophoresis and the *sdrC* insert was purified by gel extraction. The plasmid pGEX-KG and the *sdrC* insert were joined by cohesive-end ligation with T4 DNA ligase at 22 °C (LigaFast™ Rapid DNA Ligation System, Promega). The ligation reaction was transformed into chemically competent XL-1 Blue *E.coli*. The plasmid was isolated from XL-1 Blue and confirmed by DNA sequencing (GATC biotech).

DNA encoding the N2 subdomain of FnBPA from *S. aureus* strain 8325 was cloned into the IPTG-inducible vector pGEX-4T2 to generate the plasmid pGEX::*fnbA*_{N2}. Plasmids pGEX-4T2 and pQE30::*fnbA*_{N2} were digested with restriction enzymes BamHI and Sall at 37 °C. The plasmid pQE30 and the *fnbA*_{N2} insert were separated by agarose gel electrophoresis and the *fnbA*_{N2} insert was purified by gel extraction. The plasmid pGEX-4T2 and the *fnbA*_{N2} insert were joined by cohesive-end ligation with T4 DNA ligase at 22 °C (LigaFast™ Rapid DNA Ligation System, Promega). The ligation reaction was transformed into chemically competent XL-1 Blue *E. coli*. The pGEX::*fnbA*_{N2} plasmid was extracted from XL-1 Blue and verified by DNA sequencing (GATC biotech).

2.2.2 Generation of chimeric pQE30::*fnbA*_{N2N3} plasmids with residues of the N2 subdomain replaced with ClfA sequence.

Three variants of pQE30::*fnbA*_{N2N3} where regions of *fnbA* sequence were replaced with the corresponding *clfA* sequence were constructed using blunt-end ligation. To do this primers were designed upstream; Site1F, Site4F and Site6F (Table 2.2), and downstream; Site1R, Site4R and Site6R (Table 2.2) of the *fnbA* sequence to be deleted. These primers contained 5' extensions carrying the *clfA*-derived sequence to be added. The plasmid pQE30::*fnbA*_{N2N3} (~4.4 kb) was amplified by inverse PCR with primers Site1F and Site1R, Site4F and Site4R and Site6F and Site6R in separate reactions. The reactions were incubated with 1 U of the restriction enzyme DpnI for 2 h at 37 °C to digest methylated template DNA. The products were each joined by blunt-end ligation at 22 °C (LigaFast™ Rapid DNA Ligation System, Promega) and transformed into chemically competent XL-1 Blue *E. coli*. Plasmids pQE30::*fnbA*_{Site1}, pQE30::*fnbA*_{Site4} and

pQE30::*fnbA*_{Site6} were extracted from XL-1 Blue and confirmed by DNA sequencing (GATC biotech).

2.2.3 Generation of an *sdrC* deletion mutant of *S. aureus* strain MRSA252.

Deletion of the *sdrC* gene in the HA-MRSA strain MRSA252 to generate MRSA252Δ*sdrC* was achieved by allelic exchange using plasmid pIMAY (Monk *et al.*, 2012). DNA encoding 486 nucleotides of sequence upstream of the *sdrC* gene was amplified using MRSA252 genomic DNA as template with primers SdrCA and SdrCB (Table 2.2). DNA encoding 72 nucleotides of the 3' sequence of *sdrC* and 359 nucleotides of sequence downstream was amplified using primers SdrCC and SdrCD (Table 2.2). The upstream and downstream fragments were joined using splicing by overlap extension PCR and cloned into pIMAY using SLIC (Li & Elledge, 2012). The resulting plasmid was transformed into *E.coli* DC10B and verified by DNA sequencing (GATC biotech). The plasmid was transformed into electrocompetent MRSA252 cells and deletion of the *sdrC* gene was achieved by allelic replacement as previously described (Monk *et al.*, 2012). Deletion of *sdrC* was confirmed by extraction of genomic DNA from MRSA252Δ*sdrC* and amplification of the region of the *sdrC* gene with primers upstream; SdrCOUTF, and downstream; SdrCOUTR (Table 2.2), of the deleted region. Deletion of *sdrC* was confirmed by DNA sequencing of this PCR product (GATC biotech).

2.2.4 Generation of chimeric FnBPA plasmids carrying the N1N2N3 subdomains of different FnBPA isotypes.

Cloning of subdomains N123 of different isotypes of *fnbA* in the plasmid pFnBA4 was carried out using SLIC (Li & Elledge, 2012). Primers for amplifying insert sequences contained 5' extensions with homology to the target vector. The N123 subdomains and part of the first fibronectin binding repeat of *fnbA* isotypes III, IV, V and VI (~1.68 kb) were amplified by PCR with primers FnBPAinsertF and FnBPAinsertR (Table 2.2) using genomic DNA from *S. aureus* strains N315, P1, 3110 and 19, respectively, as templates. The plasmid pFnBA4 (~10.6 kb) was used as template for inverse PCR with primers pFnBA4SLICF and pFnBA4SLICR (Table 2.2) yielding PCR products of ~8.9 kb. Amplimers of *fnbA* isotypes III, IV, V and VI were joined individually to the pFnBA4

amplimer by SLIC to generate plasmids pFnBA4_{isoIII}, pFnBA4_{isoIV}, pFnBA4_{isoV} and pFnBA4_{isoVI}, respectively. Each plasmid was transformed into chemically competent *E. coli* IM08B and confirmed by DNA sequencing (GATC biotech). Each plasmid was then transformed into electrocompetent *S. aureus* BH1CCΔ*fnbAfnbB* cells.

2.3 *In silico* generation of homology models of SdrC and FnBPB. The amino acid sequences of the N2 and N3 subdomains of SdrC (residues 178-335) and FnBPB (residues 163-480) from *S. aureus* strains Newman and 8325, respectively, were submitted to Phyre² version 2.0 (Kelley *et al.*, 2015) to generate homology models of SdrCN2N3 and FnBPBN2N3. The N2N3 sequence of SdrC was also submitted to a second modelling program; I-TASSER (Zhang, 2008). Homology models were visualised using the molecular modelling software Chimera version 1.9 (Pettersen *et al.*, 2004).

2.4 *In silico* docking of small molecule libraries and selection of putative inhibitors.

The clean lead subset of the Zinc library (Irwin *et al.*, 2012) was screened for docking at either the 'RPGSV' or 'VDQYT' site of SdrC using the docking program DOCK Blaster (Irwin *et al.*, 2009). The SdrC homology model structure from either I-TASSER or Phyre² was uploaded and the target site of interest, 'RPGSV' or 'VDQYT' indicated. The top 20-30 molecules identified to dock at the selected site on the SdrC model were assessed, with those smaller than 250 Daltons in molecular mass excluded. The remaining small molecules were examined in complex with SdrC using Chimera version 1.9 software (Pettersen *et al.*, 2004) to visualise the predicted site of docking and interactions between the small molecule and SdrC, in particular, predicted interactions to the targeted motif. Molecules were selected based on these analyses and their commercial availability. A second library of small molecules; 'The Malaria Box' provided by the Medicines for Malaria Venture (MMV) (Spangenberg *et al.*, 2013), was screened. Docking was carried out using Autodock vina (Trott & Olson, 2010) with the 'RPGSV' or 'VDQYT' sites of both the I-TASSER and Phyre² models selected as targets. The docking sites and predicted interactions with the target site were assessed using Chimera version 1.9 (Pettersen *et al.*, 2004) for compounds with predicted high affinity across both models.

Small molecules LH1-5 from the clean lead subset of the Zinc library and LH6, LH7 and LH10 from the 'Malaria Box' library were docked onto the crystal structure of FnBPAN2N3 (PDB ID=4B5Z) using Autodock vina (Trott & Olson, 2010). LH6, LH7 and LH10 were also docked onto the homology model of FnBPBN2N3 using Autodock vina. Docking sites and predicted interactions of the small molecules with FnBPAN2N3 and FnBPBN2N3 were examined using Chimera version 1.9 (Pettersen *et al.*, 2004).

2.5 Synthetic peptide. A synthetic peptide of the SdrC binding site within β -neurexin (Barbu *et al.*, 2010) (SLGAHHIHHFHGSSKHHS) was synthesized by Genscript (Piscataway, NJ).

2.6 *In silico* modelling of the SdrC- β -neurexin derived peptide complex. The β -neurexin derived peptide was constructed *in silico* using the Molecular Operating Environment (MOE) (Chemical Computing Group Inc., 2015.). Docking of the β -neurexin derived peptide on the Phyre² SdrC model was carried out using Autodock vina (Trott & Olson, 2010). The predicted SdrC-peptide complex was analysed using Chimera version 1.9 (Pettersen *et al.*, 2004).

2.7 Expression and purification of recombinant proteins. *E. coli* XL-1 Blue or Topp3 cells carrying IPTG-inducible pQE30 or pGEX plasmids for expression and purification of recombinant proteins with an N-terminal hexahistidine tag or glutathione-S-transferase (GST) fusion proteins, respectively, were grown to late exponential phase ($OD_{600nm} = \sim 0.6$) and induced with isopropyl β -D-1-thiogalactopyranoside (IPTG, 1 mM) for 3 h at 37 °C. Cells were mechanically lysed using a French pressure cell (1,000 psi) in the presence of EDTA-free protease inhibitors (Roche).

2.7.1 Nickel Affinity Chromatography. Recombinant proteins with an N-terminal hexahistidine tag (His-tagged) were purified by nickel (Ni^{2+}) affinity chromatography. A Ni^{2+} packed column (5ml HisTrapTM HP column; GE Healthcare) was equilibrated with binding buffer (0.5 M NaCl, 20 mM Tris-HCl, pH 7.9). Following column preparation, the bacterial cell lysate was added to the column. The column was washed with binding buffer containing a low concentration of imidazole (5-8 mM). Bound protein was eluted from the column over a gradient of increasing concentration of imidazole (5-100 mM) in binding buffer with fractions (~ 10 ml) collected. Fractions were

separated by sodium dodecyl sulphate polyacrylamide gel electrophoresis (SDS-PAGE, 4.5 % w/v stacking and 10 % w/v separating acrylamide gels) and analysed by protein staining (Coomassie blue or InstantBlue; Sigma Aldrich). Fractions containing the recombinant His-tagged protein were pooled and dialysed against phosphate buffered saline (PBS) for 16 h at 4 °C. Protein purity and integrity was confirmed following dialysis by SDS-PAGE and protein staining. Protein concentrations were determined by $A_{280\text{nm}}$ measurement or through a bicinchoninic acid (BCA) assay (Pierce™ BCA Protein Assay Kit; Thermo Fisher Scientific).

2.7.2 Glutathione Affinity Chromatography. Recombinant GST fusion (GST-tagged) proteins were purified by glutathione affinity chromatography. A GST affinity column (5 ml GSTrap™ FF column; GE Healthcare) was equilibrated with PBS. Following column preparation, the bacterial cell lysate was added to the column. The column was washed with PBS. Bound protein was eluted from the column with reduced glutathione elution buffer (50mM Tris-HCl, 10 mM glutathione, pH 8.0) and fractions (~2 ml) were collected. Fractions were separated by SDS-PAGE (4.5 % w/v stacking and 10 % w/v separating acrylamide gels) and analysed by protein staining (Coomassie blue or InstantBlue; Sigma Aldrich). Fractions containing the recombinant GST-tagged proteins were then pooled and dialysed against PBS for 16 h at 4 °C. Protein purity and integrity were confirmed following dialysis by SDS-PAGE and protein staining. Protein concentrations were determined by $A_{280\text{nm}}$ measurement.

2.8 Western immunoblot. Recombinant His-tagged SdrC protein was separated by SDS-PAGE (4.5 % stacking and 10 % w/v separating acrylamide gel) and subsequently electroblotted onto a PVDF membrane (Roche). The membrane was blocked with skimmed milk powder (10 % w/v; Marvel) in TS buffer (10 mM Tris-HCl, 0.9 % w/v NaCl, pH 7.4) for 2 h at room temperature. Monoclonal mouse anti-His IgG was added for 1 h at room temperature. The membrane was then washed three times with TS buffer. Rabbit anti-mouse horseradish peroxidase (HRP)-conjugated IgG (Dako) was added to the membrane for 1 h at room temperature. The membrane was then washed three times with TS buffer. Bound antibody was visualised with the LumiGLO reagent and peroxidase detection system (Cell Signalling Technology) and the membrane visualised using ImageQuant TL software (GE).

2.9 Differential Scanning Fluorimetry (DSF). Recombinant SdrC, FnBPA_{N2N3} and FnBPB_{N2N3} proteins (0.5 mg/ml) were gradually heated (ramp rate 0.3 °C) in Tris-buffered saline (TBS) in the presence of individual compounds (25 µM) and the reporter dye SYPRO orange in a Real-Time PCR machine. Solvent controls were included (2.5% v/v dimethyl sulfoxide; DMSO). Fluorescence values were normalised with the lowest and highest value set as 0 and 100 fluorescence units, respectively. Melt curves of fluorescence units vs temperature (°C) were analysed using Prism GraphPad software version 5.01 and the melting temperature (T_m) calculated.

2.10 Biofilm microtitre plate assays.

2.10.1 Biofilm assays with *L. lactis*. *L. lactis* strains were grown for 16-18 h in BHI broth supplemented with erythromycin (10 µg/ml) and diluted 1:200 into M17 broth supplemented with D-glucose (5 g/L; Sigma Aldrich). Diluted bacteria (275 µl) were added to wells of sterile tissue culture-treated polystyrene plates (Nunclon Delta) and incubated statically at 28 °C for 24 h. After 24 h incubation, wells were washed three times with PBS and inverted for 30 min to dry. Wells were stained with crystal violet (0.5 % w/v) and A_{570nm} was measured.

2.10.2 Biofilm assays with *S. aureus*. *S. aureus* strains were grown for 16-18 h in TSB, supplemented with chloramphenicol (10 µg/ml) where appropriate. Bacteria were subsequently diluted 1:200 in TSB (strains used in SdrC biofilm analyses) or BHI broth (strains used in FnBP-mediated biofilm analyses) supplemented with D-glucose (10 g/L; Sigma Aldrich). The diluted bacteria (200 µl) were added in triplicate to sterile tissue culture-treated polystyrene plates (Nunclon Delta). Plates were incubated statically at 37 °C for 24 h. Wells were washed three times with PBS and dried for 30 min by inversion. Biofilm was stained with crystal violet (0.5 % w/v) and A_{570nm} was measured.

2.10.3 Biofilm inhibition assays. *L. lactis* and *S. aureus* biofilm assays were performed as described above with the following changes. Small molecules or peptide were added to the diluted bacteria prior to addition to the microtitre plate. DMSO (0.5 or 1 % v/v) was added to the diluted bacteria as a solvent control prior to addition to the plate. A_{570nm} values were normalised as % biofilm formation relative to the DMSO control set as 100 % biofilm formation.

2.10.4 Biofilm dispersal assay. *L. lactis* strains were allowed to form biofilm for 24 h at 28 °C. Wells were washed twice with PBS. The β -neurexin derived peptide (12.5 μ M) or proteinase K (100 μ g/ml) in PBS were added in triplicate to wells with established biofilms and the plates incubated for 2 h at 28 °C. PBS was also added to triplicate wells as an untreated control. Following the 2 h incubation, wells were washed three times with PBS and dried by inversion for 30 min. Biofilm was stained with crystal violet (0.5 % w/v) and A_{570nm} values measured.

2.11 IC₅₀ analysis of the β -neurexin derived peptide. Inhibition of SdrC biofilm formation using the surrogate host *L. lactis* was carried out as described above with the following change. Varying concentrations of the β -neurexin derived peptide (0.195 μ M to 12.5 μ M) were added to the diluted bacteria prior to addition to the microtitre plate. An IC₅₀ curve of Log [peptide concentration] vs % biofilm formation was generated and the IC₅₀ determined using Prism GraphPad software version 5.01.

2.12 Growth curves. For *L. lactis* growth curves, *L. lactis* strains were grown for 16-18 h in BHI broth supplemented with erythromycin (10 μ g/ml) and subsequently diluted 1:200 in M17 broth supplemented with D-glucose (5 g/L; Sigma Aldrich). Diluted bacteria (200 μ l) were added in triplicate to sterile round-bottomed 96 well plates (Starstedt). Plates were incubated statically at 30 °C in a Synergy H1 plate reader (Biotek) for 16 h with OD_{600nm} values measured at 30 min intervals.

For *S. aureus* growth curves, *S. aureus* strains were grown for 16-18 h in TSB and subsequently diluted 1:200 in TSB or BHI broth. Bacteria were added (200 μ l) in triplicate to sterile round-bottomed 96 well plates (Starstedt). Plates were incubated at 37 °C with continuous shaking in a Synergy H1 plate reader (Biotek) for 16 h with OD_{600nm} values measured at 30 min intervals.

For assays assessing growth inhibition of small molecules and the peptide, media was supplemented with D-glucose (5 g/L for *L. lactis* and 10 g/L for *S. aureus*; Sigma Aldrich). The small molecules or DMSO as a solvent control and the peptide were added to diluted bacteria prior to addition to the plate.

2.13 Single cell spectroscopy. Single cell spectroscopy experiments were carried out by Cécile Feuille and Cécile Formosa-Dague at the Université Catholique de Louvain.

2.14 Site directed mutagenesis. Residue R247 of SdrC was substituted to an alanine in the plasmid pQE30::*sdrC* by site-directed mutagenesis. Overlapping complementary primers R247AF and R247AR (Table 2.2) containing the desired nucleotide changes were used to amplify the plasmid (~4.4 kb). The reaction was incubated with 1 U of the restriction enzyme DpnI for 2 h at 37 °C to digest methylated template DNA and transformed into chemically competent XL-1 Blue *E. coli*. The plasmid pQE30::*sdrC*_{R247A} was extracted from XL-1 Blue and the mutation was confirmed by DNA sequencing (GATC biotech).

2.15 Ligand affinity dot blot. Recombinant His-tagged SdrC native and R27A proteins were immobilised in doubling dilutions (1.25 µM -20 µM) onto a nitrocellulose membrane. The membrane was blocked with skimmed milk powder (10 % w/v; Marvel) for 2 h at room temperature. Recombinant GST-tagged SdrC was added to the membrane for 1 h at room temperature. Monoclonal mouse anti-GST IgG was added to the membrane for 1 h at room temperature. The membrane was washed three times with PBS and tween (0.05 % v/v). Rabbit anti-mouse HRP-conjugated IgG (Dako) was added to the membrane for 1 h at room temperature. The membrane was washed three times with PBS and tween (0.05 % v/v). Bound antibody was visualised with the LumiGLO reagent and peroxidase detection system (Cell Signalling Technology) and the membrane visualised using ImageQuant TL software (GE Healthcare).

2.16 Enzyme-Linked Immunosorbent Assays (ELISA).

2.16.1 SdrC-SdrC ELISA. Recombinant GST-tagged SdrC (1 µM) was coated onto microtitre plates (Nunclon maxisorp) in sodium carbonate buffer (pH 9.6) at 4 °C overnight. Plates were blocked with skimmed milk powder (5 % w/v; Marvel) in PBS for 2 h at 37 °C. Recombinant His-tagged SdrC and R247A proteins were added to the plate (5 µM) and the plate incubated at room temperature, shaking for 2 h. Wells were washed three times with PBS. Monoclonal mouse anti-His IgG (100 µl) was added to the wells and the plate incubated at room temperature, shaking for 1 h. Wells were

washed three times with PBS and rabbit anti-mouse HRP-conjugated IgG (100 μ l; Dako) was added to the wells and the plate incubated at room temperature, shaking for 1 h. Wells were washed three times with PBS. To detect bound rabbit anti-mouse HRP-conjugated IgG 3, 3', 5, 5'-tetramethylbenzidine (TMB, 0.1 mg/ml; Sigma Aldrich) prepared in phosphate citrate buffer (0.05 M) with hydrogen peroxide (0.006 % v/v) was added (100 μ l) to the wells. To stop the reaction, H₂SO₄ (50 μ l; 2M) was subsequently added to the wells and A_{450nm} values measured. Values were normalised relative to His-tagged SdrC binding GST-tagged SdrC as 1.0.

2.16.2 FnBP-FnBP ELISA. Recombinant GST-tagged FnBPA_{N2N3} (1 μ M), FnBPA_{N2} (6 μ M) or FnBPB_{N2N3} (1 μ M) proteins were coated onto microtitre plates (Nunclon maxisorp) in sodium carbonate buffer (pH 9.6) at 4 °C overnight. Plates were blocked with skimmed milk powder (5% w/v; Marvel) in PBS for 2 h at 37 °C. Recombinant His-tagged FnBPA and FnBPB proteins were added to the plate in doubling dilutions (0.156 μ M -2.5 μ M) and the plates incubated at 37 °C, shaking for 2 h. Bound His-tagged proteins were detected as described above (Section 2.16.1).

For recombinant FnBPA_{N2N3}-FnBPA_{N2N3} inhibition assays, ELISAs were carried out as described above with the following changes. His-tagged FnBPA_{N2N3} protein (0.25 μ M) was incubated with small molecules (1.25 μ M) or DMSO (0.125 % v/v) for 30 min, 200 rpm at 37 °C prior to addition to the plate. Protein and small molecules/DMSO (100 μ l) were then added to the plate in triplicate and the plate incubated for 1 h 30 min at 37 °C.

2.17 Fibronectin binding assays. Flat-bottomed microtitre plates (Sarstedt) were coated with doubling dilutions of human fibronectin (0.156 μ g/ml -10 μ g/ml; Calbiochem) in PBS at 4 °C overnight. Plates were blocked with bovine serum albumin (BSA; 5% w/v) for 2 h at 37 °C. *S. aureus* strains were grown to exponential phase in TSB, supplemented with chloramphenicol (10 μ g/ml) where appropriate, at 37 °C. Cells were subsequently washed with PBS and adjusted to an OD_{600nm}=1.0 in PBS. Bacteria (200 μ l) were added in triplicate to wells of the microtitre plate and incubated statically at 37 °C for 2 h. Wells were washed three times with PBS and adherent

bacteria fixed with formaldehyde (25 % v/v) for 15 min. Adherent bacteria were stained with crystal violet and $A_{570\text{nm}}$ measured.

2.18 Fibrinogen binding assays. Flat-bottomed microtitre plates (Starstedt) were coated with human fibrinogen (5 $\mu\text{g}/\text{ml}$; Calbiochem) in PBS at 4 °C overnight. Plates were blocked with BSA (5 % w/v) for 2 h at 37 °C. *S. aureus* strains were grown to exponential phase in TSB at 37 °C. Cells were washed with PBS and adjusted to an $\text{OD}_{600\text{nm}}=1.0$ in PBS. Small molecules or DMSO were added to the adjusted bacteria and incubated for 30 min, 200 rpm at 37 °C. Bacteria with small molecules/DMSO (200 μl) were then added in triplicate to wells of the microtitre plate and incubated statically at 37 °C for 2 h. Wells were washed three times with PBS and adherent bacteria fixed with formaldehyde (25 % v/v) for 15 min. Adherent bacteria were stained with crystal violet and $A_{570\text{nm}}$ measured. $A_{570\text{nm}}$ values were normalised to % fibrinogen binding with SH1000 *clfA clfB* with DMSO as 100 %.

Fibrinogen binding assays with *L. lactis* pNZ8037::*fnbA* and *L. lactis* pNZ8037::*fnbB* strains were carried out as described above with the following changes. *L. lactis* strains were grown for 16-18 h in BHI broth supplemented with chloramphenicol (10 $\mu\text{g}/\text{ml}$) statically at 28 °C. Strains were subsequently diluted 1:100 in BHI broth supplemented with chloramphenicol (10 $\mu\text{g}/\text{ml}$) and grown to exponential phase statically at 28 °C. Strains were then induced with nisin (32 ng/ml) for 16 h statically at 28 °C. Following induction, strains were washed in PBS and adjusted to an $\text{OD}_{600\text{nm}}=1.0$ in PBS. Fibrinogen binding and inhibition were then assessed as described above. $A_{570\text{nm}}$ values were normalised to % fibrinogen binding with *L. lactis* pNZ8037::*fnbA* or *L. lactis* pNZ8037::*fnbB* with DMSO as 100 %.

2.19 Amino acid alignments. Amino acid alignments were carried out using the web based multiple sequence alignment program Clustal Omega (Sievers *et al.*, 2011). The N2 subdomains (residues 194-336) of FnBPA isotypes I, III, IV, V and VI and the N2 subdomain (residues 163-307) of FnBPB isotype I were aligned. The N2 subdomain (residues 194-336) of FnBPA isotype I from *S. aureus* strain 8325 was aligned with the N2 subdomain (residues 221-368) of ClfA from *S. aureus* strain Newman.

2.20 Statistical analyses. Statistical analyses were performed using Prism Graphpad software version 5.01 using unpaired two-tailed Student's t-tests, one-way ANOVA or two-way ANOVA with Bonferroni post-test analyses where *, ** and *** represent *p*-values of ≤ 0.05 , ≤ 0.01 and ≤ 0.001 . *P*-values > 0.05 are considered not significant.

TABLE 2.1. Bacterial strains and plasmids used in this study.

| Strain or plasmid | Description | Reference or Source |
|-----------------------------------|---|---|
| <i>E. coli</i> strains | | |
| XL-1 Blue | <i>recA1 endA1 gyrA96 thi-1 hsdR17 supE44 relA1 lac</i> | Stratagene |
| Topp3 | Rif ^r , [F' proAB ⁺ lacI ^q ZΔM15 Tn10 (Tet ^r) (Kan ^r)] | Stratagene |
| DC10B | <i>dam⁺ Δdcm ΔhsdRMS endA1 recA1</i> | (Monk <i>et al.</i> , 2012) |
| IM08B | <i>dam⁺ Δdcm hsdRMS^{CC8}</i> | (Monk <i>et al.</i> , 2015) |
| <i>L. lactis</i> MG1363 | Derivative of strain NCD0712 which is plasmid free | (Gasson, 1983) |
| <i>S. aureus</i> strains | | |
| MRSA252 | HA-MRSA, SCCmec type II, MLST ^a type 36, CC ^b 30 | (Holden <i>et al.</i> , 2004) |
| MRSA252Δ <i>sdrC</i> | <i>sdrC</i> deficient mutant of MRSA252 | This study |
| BH1CC | HA-MRSA, SCCmec type II, MLST type 8, CC8 | (O'Neill <i>et al.</i> , 2008) |
| BH1CCΔ <i>fnbAfnbB</i> | <i>fnbA</i> and <i>fnbB</i> deficient mutant of BH1CC | (Geoghegan <i>et al.</i> , 2013) |
| DAR70 | HA-MRSA, SCCmec type II, MLST type 45, CC45 | (O'Neill <i>et al.</i> , 2008) |
| DAR70Δ <i>fnbAfnbB</i> | <i>fnbA</i> and <i>fnbB</i> deficient mutant of DAR70 | Zapotoczna M and Geoghegan JA (Unpublished) |
| SH1000 | Derivative of laboratory strain 8325-4 with repaired defect in <i>rsbU</i> | (Horsburgh <i>et al.</i> , 2002) |
| SH1000 <i>clfA clfB</i> | <i>clfA clfB::Erm^r</i> | Foster TJ (Unpublished) |
| SH1000 <i>clfA clfB fnbA fnbB</i> | <i>clfA clfB::Erm^r fnbA::Erm^r fnbB::Tet^r</i> | (O'Neill <i>et al.</i> , 2008) |
| N315 | HA-MRSA, SCCmec type II, MLST type 5, CC5 | (Kuroda <i>et al.</i> , 2001) |
| P1 | Rabbit MSSA isolate, MLST type 973 | (Loughman <i>et al.</i> , 2008) |
| 3110 | MSSA clinical isolate, MLST type 12 | (Feil <i>et al.</i> , 2003) |

| | | |
|--------------------------------------|--|---|
| 19 | MSSA clinical isolate, MLST type 10 | (Feil <i>et al.</i> , 2003) |
| Plasmids | | |
| pQE30 | <i>E. coli</i> plasmid for expression of proteins with N-terminal hexahistidine tags, Amp ^r | Qiagen |
| pQE30:: <i>sdrC</i> | pQE30 plasmid containing DNA encoding the N2 and N3 subdomains of SdrC from <i>S. aureus</i> strain Newman, Amp ^r | This study |
| pQE30:: <i>sdrC</i> _{R247A} | pQE30:: <i>sdrC</i> with amino acid substitution R247A, Amp ^r | This study |
| pQE30:: <i>fnbA</i> _{N2N3} | pQE30 plasmid containing DNA encoding the N2 and N3 subdomains of FnBPA from <i>S. aureus</i> strain 8325, Amp ^r | (Geoghegan <i>et al.</i> , 2013) |
| pQE30:: <i>fnbA</i> _{N2} | pQE30 plasmid containing DNA encoding the N2 subdomain of FnBPA from <i>S. aureus</i> strain 8325, Amp ^r | Pietrocola G and Speziale P (Unpublished) |
| pQE30:: <i>fnbA</i> _{N3} | pQE30 plasmid containing DNA encoding the N3 subdomain of FnBPA from <i>S. aureus</i> strain 8325, Amp ^r | Pietrocola G and Speziale P (Unpublished) |
| pQE30:: <i>fnbB</i> _{N2N3} | pQE30 plasmid containing DNA encoding the N2 and N3 subdomains of FnBPB from <i>S. aureus</i> strain 8325, Amp ^r | (Burke <i>et al.</i> , 2011) |
| pQE30:: <i>fnbB</i> _{N2} | pQE30 plasmid containing DNA encoding the N2 subdomain of FnBPB from <i>S. aureus</i> strain 8325, Amp ^r | (Pietrocola <i>et al.</i> , 2016) |
| pQE30:: <i>fnbB</i> _{N3} | pQE30 plasmid containing DNA encoding the N3 subdomain of FnBPB from <i>S. aureus</i> strain 8325, Amp ^r | (Pietrocola <i>et al.</i> , 2016) |
| pQE30:: <i>fnbA</i> _{Site1} | pQE30:: <i>fnbA</i> _{N2N3} with residues 166-173 exchanged for residues 224-231 of <i>clfA</i> , Amp ^r | This study |
| pQE30:: <i>fnbA</i> _{Site4} | pQE30:: <i>fnbA</i> _{N2N3} with residues 220-230 exchanged for residues 274-284 of <i>clfA</i> , Amp ^r | This study |

| | | |
|--------------------------------------|--|---|
| pQE30:: <i>fnbA</i> _{Site6} | pQE30:: <i>fnbA</i> _{N2N3} with residues 268-281 exchanged for residues 322-335 of <i>clfA</i> , Amp ^r | This study |
| pGEX-KG | <i>E. coli</i> plasmid for expression of GST fusion proteins, Amp ^r | GE Lifesciences |
| pGEX:: <i>sdrC</i> | pGEX-KG plasmid containing DNA encoding the N2 and N3 subdomains of SdrC from <i>S. aureus</i> strain Newman, Amp ^r | This study |
| pGEX-4T2 | <i>E. coli</i> plasmid for expression of GST fusion proteins, Amp ^r | GE Lifesciences |
| pGEX:: <i>fnbA</i> _{N2N3} | pGEX-4T2 plasmid containing DNA encoding the N2 and N3 subdomains of FnBPA from <i>S. aureus</i> strain 8325, Amp ^r | Burke FM and Geoghegan JA (Unpublished) |
| pGEX:: <i>fnbA</i> _{N2} | pGEX-4T2 plasmid containing DNA encoding the N2 subdomain of FnBPA from <i>S. aureus</i> strain 8325, Amp ^r | This study |
| pGEX:: <i>fnbB</i> _{N2N3} | pGEX-4T2 plasmid containing DNA encoding the N2 and N3 subdomains of FnBPB from <i>S. aureus</i> strain 8325, Amp ^r | Burke FM and Foster TJ (Unpublished) |
| pKS80 | Constitutive expression plasmid for heterologous gene expression in <i>L. lactis</i> , Erm ^r | (Wells <i>et al.</i> , 1996) |
| pKS80:: <i>sdrC</i> | pKS80 plasmid carrying DNA encoding the full length <i>sdrC</i> gene, Erm ^r | (O'Brien <i>et al.</i> , 2002a) |
| pIMAY | Temperature-sensitive vector for allelic exchange in Staphylococci, Cm ^r | (Monk <i>et al.</i> , 2012) |
| pIMAYΔ <i>sdrC</i> | pIMAY for deletion of <i>sdrC</i> in MRSA252 by allelic exchange | This study |
| pFnBA4 | Multicopy plasmid expressing entire <i>fnbA</i> gene from <i>S. aureus</i> strain 8325, Cm ^r | (Greene <i>et al.</i> , 1995) |
| pFnBA4 _{isoIII} | pFnBA4 with DNA encoding the N1N2N3 subdomains of <i>S. aureus</i> strain N315, Cm ^r | This study |
| pFnBA4 _{isoIV} | pFnBA4 with DNA encoding the N1N2N3 | This study |

| | | |
|-------------------------|--|------------------------------------|
| | subdomains of <i>S. aureus</i> strain P1, Cm ^r | |
| pFnBA4 _{isoV} | pFnBA4 with DNA encoding the N1N2N3 subdomains of <i>S. aureus</i> strain 3110, Cm ^r | This study |
| pFnBA4 _{isoVI} | pFnBA4 with DNA encoding the N1N2N3 subdomains of <i>S. aureus</i> strain 19, Cm ^r | This study |
| pNZ8037:: <i>fnbA</i> | Nisin-inducible plasmid carrying the full length <i>fnbA</i> gene from <i>S. aureus</i> strain 8325, Cm ^r | (Arrecubieta <i>et al.</i> , 2006) |
| pNZ8037:: <i>fnbB</i> | Nisin-inducible plasmid carrying the full length <i>fnbB</i> gene from <i>S. aureus</i> strain 8325, Cm ^r | (Arrecubieta <i>et al.</i> , 2006) |

^aMLST: Multilocus sequence type

^bCC: Clonal Complex

^c Resistance is denoted ^r

TABLE 2.2 Primers

| Primer Name | Sequence (5'-3') |
|--------------------|--|
| pQE30F | aagcttaattagctgagcttg |
| pQE30R | ggatccgtgatggtgatg |
| SdrCN2N3F | ggatcgcatcaccatcaccatcacggatccggaacaaatgtaataagataag |
| SdrCN2N3R | acaggagtccaagctcagctaattaagcttttatttctttggtcgccattag |
| pIMAYF | ggtaccagcttttgttccttagtgagg |
| pIMAYR | gagctccaattcgccctatagtgagtcg |
| SdrCA | cctcactaaaggaacaaaagctgggtacctcgatcaaattgtatctttgtg- |
| SdrCB | cattaataatactccttaaaatc |
| SdrCC | tatttaaaggagtattattaaatgacgttattggcggattattc |
| SdrCD | cgactcactatagggcgaattggagctctattttacatataaaaaattgtattc |
| SdrCOUTF | ttctgatttgctaaaaatgaag |
| SdrCOUTR | tttgttattgcctttttgtatc |
| R247AF | gtcaatatttcgctccaggatcagtaa |
| R247AR | cttactgatcctggagcgaaatattgac |
| FnBPAinsertF | caatcttaggtacggcattagaaaac |
| FnBPAinsertR | catctatagctgtgtgtaataatcaatg |
| pFnBA4SLICF | cattgattaccacacagctatagatg |
| pFnBA4SLICR | gttttctaagccgtacctaaagattg |
| Site1F | ttgacgaatgtgattggttctattgaggggcataac |

| | |
|--------|--|
| Site1R | ctgattcgtaatatctgtaccggatccgtgatg |
| Site4F | ggtgtaacttcaactgctaaagtaccagaaattaaaaatg |
| Site4R | attaagtttaattcgtagtcaccttgatgtaaac |
| Site6F | gcttatattgacctgaaaatgtacaaaactaatggaaatcaaac |
| Site6R | gggcatggtaaagttgcttttacatcaaccttatcttcaatc |

Chapter 3

In silico* identification of novel inhibitors of serine aspartate repeat protein C-mediated biofilm formation of *Staphylococcus aureus

3.1 Introduction

S. aureus biofilm formation is multifactorial occurring through three distinct phases; primary attachment, biofilm accumulation and maturation and biofilm dispersal (Section 1.5). The main mechanisms of biofilm accumulation are mediated by the exopolysaccharide polysaccharide intercellular adhesin (PIA-dependent biofilm) or by *S. aureus* cell wall-anchored proteins (protein-dependent biofilm) (Section 1.5.2). To date, several cell wall-anchored proteins have been shown to mediate biofilm accumulation, namely the fibronectin binding proteins (FnBPs) A and B, the serine aspartate repeat protein (Sdr) C, serine rich adhesion for platelets (SraP), clumping factor B (ClfB), protein A, biofilm-associated protein (Bap) and *S. aureus* surface proteins (Sas) C, SasX and SasG (Speziale *et al.*, 2014). There is growing evidence that the mechanism for protein-dependent biofilm accumulation involves the same proteins on adjacent bacterial cells forming homophilic interactions allowing bacteria to aggregate and biofilm to accumulate (Speziale *et al.*, 2014).

The *S. aureus* cell wall-anchored protein SdrC mediates biofilm accumulation in the *S. aureus* laboratory strain Newman (Barbu *et al.*, 2014). An SdrC-deficient mutant of Newman had a reduced ability to form biofilm compared to the parental strain. Expression of SdrC in the surrogate host *Lactococcus lactis* (*L. lactis* pKS80::*sdrC*) produced a similar level of biofilm as *L. lactis* expressing other *S. aureus* cell wall-anchored proteins known to mediate biofilm accumulation (Barbu *et al.*, 2014). However, the clinical relevance of SdrC-mediated biofilm remains unknown.

L. lactis has been widely used in functional studies of cell wall-anchored proteins of *S. aureus* (Foster *et al.*, 2014). This is due to the high level of functional redundancy among *S. aureus* proteins and the multifactorial nature of *S. aureus* biofilm formation which complicates the study of a single factor *in vitro*. *L. lactis* is a non-pathogenic Gram-positive bacterium which does not form biofilm. Thus, expression of SdrC in this surrogate host allows the study of biofilm which is mediated solely by SdrC without any interference from other *S. aureus* factors.

SdrC is a member of the microbial surface components recognizing adhesive matrix molecules (MSCRAMM) family of *S. aureus* cell wall-anchored proteins (Section 1.4.1)

(Foster *et al.*, 2014). The MSCRAMM family share a conserved domain structure and are characterised by the presence of two tandem IgG-like folded subdomains termed N2 and N3 followed by a long, unstructured repeat region (Foster *et al.*, 2014) (Fig 3.1).

The N2 subdomain of SdrC forms homophilic interactions (Barbu *et al.*, 2014). These homophilic interactions lead to cell-cell aggregation and biofilm accumulation. Through the use of phage display, two amino acid pentamer motifs of the N2 subdomain were identified; RPGSV and VDQYT, which specifically bound recombinant SdrCN2N3 and not SdrGN2N3, a closely-related MSCRAMM from *S. epidermidis* (Barbu *et al.*, 2014). Specific purified phage clones expressing either motif alone caused ~50% reduction in recombinant SdrC N2 dimerization while phage expressing both the consensus motifs; RPGSV and VDQYT, completely inhibited this homophilic dimerization (Barbu *et al.*, 2014). Thus, both motifs were implicated as dimerization sites in SdrC homophilic interactions. It was also shown that SdrC is capable of mediating primary attachment to abiotic surfaces using the surrogate host *L. lactis* (Barbu *et al.*, 2014, Feuillie *et al.*, 2017). This suggests SdrC has two functions in biofilm formation; firstly in mediating primary attachment and then in biofilm accumulation.

Aside from its role in biofilm formation, previous studies identified a role for SdrC in promoting adherence of *S. aureus* strain Newman to human desquamated nasal epithelial cells (Corrigan *et al.*, 2009) suggesting it could have a role in nasal colonisation. However, the ligand for SdrC on desquamated nasal epithelial cells has not been identified. The N2N3 subdomains of SdrC bind to human β -neurexin (Barbu *et al.*, 2010). SdrC recognises the sequence 'SLGAHHIHHFHGSSKHHS' in β -neurexin (Barbu *et al.*, 2010). However, the biological relevance of this interaction is unclear.

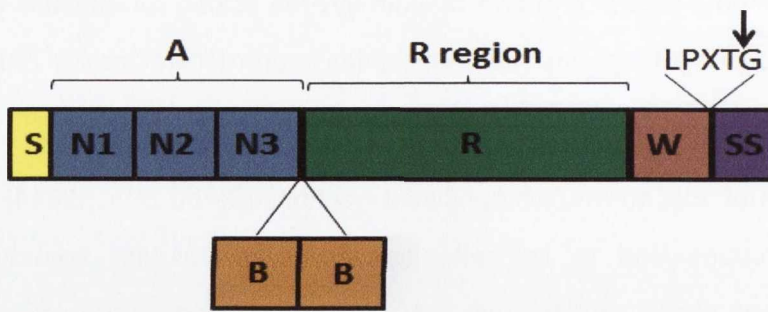


FIG 3.1 Schematic of the MSCRAMM domain organization. The N-terminal signal sequence (S) is followed by the A domain which consists of three independently folded subdomains; N1, N2 and N3. This is followed by a long unstructured repeat (R) region. For SdrC, this R region consists of serine-aspartate (SD) dipeptide repeats. SdrC contains two tandem B domains between the A domain and R region. Following the R region is a proline rich region predicted to span the call wall (W) and a sorting signal (SS) which contains the 'LPXTG' motif. The arrow indicates the cleavage site for the enzyme sortase A.

In this chapter the molecular mechanism of SdrC-mediated biofilm is explored and novel inhibitors of SdrC biofilm are identified. Differential Scanning Fluorimetry (DSF) is used to screen putative inhibitors for binding to a recombinant polypeptide comprising SdrC subdomains N2 and N3. DSF is a spectroscopy based technique which measures the unfolding of protein structures over an increasing temperature gradient (Mashalidis *et al.*, 2013) (Fig 3.2). With increasing temperature proteins begin to unfold and their inner hydrophobic residues become exposed. DSF measures the increase in fluorescence of a dye which preferentially binds these inner hydrophobic residues. When the protein is completely unfolded, it begins to aggregate and the dye no longer has access to these hydrophobic residues. Thus, the dye dissociates and fluorescence does not increase further. The point at which 50 % of the protein is unfolded is termed its melting temperature (T_m). This temperature differs among proteins due to differences in their sequence and structure and is dependent upon the stability of these structures as temperature increases. If an inhibitor or ligand binds the protein and stabilises its structure, the melting temperature of the protein will increase. DSF is widely used as an initial screening tool for rational inhibitor identification studies (Mashalidis *et al.*, 2013). DSF is an ideal screening tool due to the relatively low amount of purified protein required and its semi-high throughput nature (Mashalidis *et al.*, 2013).

The specific aims of this study were to identify novel small molecules which bind to motifs RPGSV and/or VDQYT in order to prevent SdrC-dependent biofilm formation through the inhibition of SdrC homophilic interactions. Along with inhibitor identification, this study aimed to further characterise SdrC homophilic interactions and assess the clinical relevance of SdrC-mediated biofilm. This study successfully utilised a rational inhibitor design approach and identified several novel inhibitors of SdrC-mediated biofilm. These inhibitors may serve as scaffolds for further drug design. This study also identified a role for SdrC in biofilm accumulation in a hospital associated (HA)- methicillin resistant *S. aureus* (MRSA) isolate and defined an important residue involved in SdrC homophilic interactions.

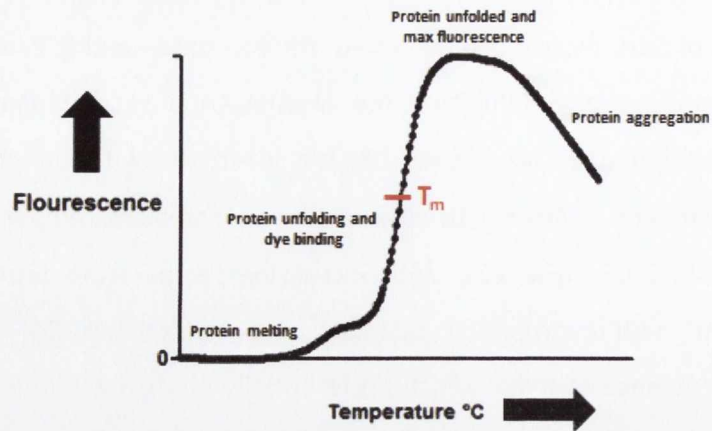


FIG 3.2 Principles of Differential Scanning Fluorimetry (DSF). The protein is gradually heated in the presence of a dye which fluoresces upon binding hydrophobic residues. As the protein is heated, it begins to unfold and its inner hydrophobic residues become exposed. The dye binds these residues and fluoresces. Dye binding and fluorescence increases as the protein unfolds to a maximum point where the protein is fully unfolded. The unfolded protein then aggregates and the dye dissociates causing a decrease in fluorescence. The point at which 50 % of the protein is unfolded is termed its melting temperature (T_m).

3.2 Results

3.2.1 *In silico* molecular modelling of the structure of SdrC N2N3 subdomains.

SdrC mediates biofilm accumulation through homophilic interactions of its N2 subdomain (Barbu *et al.*, 2014). The structure of SdrC N2N3 subdomains has not been solved to date. In order to identify putative inhibitors by *in silico* methods, it was necessary to construct a homology model of SdrC subdomains N2 and N3 (SdrCN2N3). Homology models were constructed *in silico* using two programs; I-TASSER (Zhang, 2008) and Phyre² (Kelley & Sternberg, 2009). Homology models are generated based on proteins with known crystal structures. I-TASSER produced one homology model of SdrCN2N3 which was based on the crystal structure of SdrG, an MSCRAMM of *S. epidermidis* in complex with its ligand (Fig 3.3A). Phyre² generated several homology models for SdrCN2N3 based on different MSCRAMMs namely; ClfA, ClfB, FnBPA and SdrD of *S. aureus* and SdrG of *S. epidermidis* (Table 3.1). The models generated by Phyre² are ranked by confidence scores from 0 to 100 based on the probability that there is true homology between the sequence submitted and the template utilised for the homology model generation (Kelley & Sternberg, 2009). The SdrCN2N3 model with the highest confidence score was based on ClfA in its apo form (Fig 3.3B). Both homology models of SdrCN2N3 show tandem IgG-like folds with a hydrophobic trench located between the subdomains (Fig 3.3). The root mean square deviation (RMSD) between the models generated by ITASSER and Phyre² was 1.038 Å highlighting the overall similarity of the models generated from the two different programs. All MSCRAMM N2N3 subdomain proteins crystallised to date; ClfA (Ganesh *et al.*, 2008), ClfB (Ganesh *et al.*, 2011), FnBPA (Stemberk *et al.*, 2014), SdrD (Wang *et al.*, 2013) and SdrE (Zhang *et al.*, 2017) of *S. aureus* and SdrG (Ponnuraj *et al.*, 2003, Bowden *et al.*, 2008) of *S. epidermidis* have this overall domain structure. Thus, it is most likely SdrCN2N3 also adopts this structure.

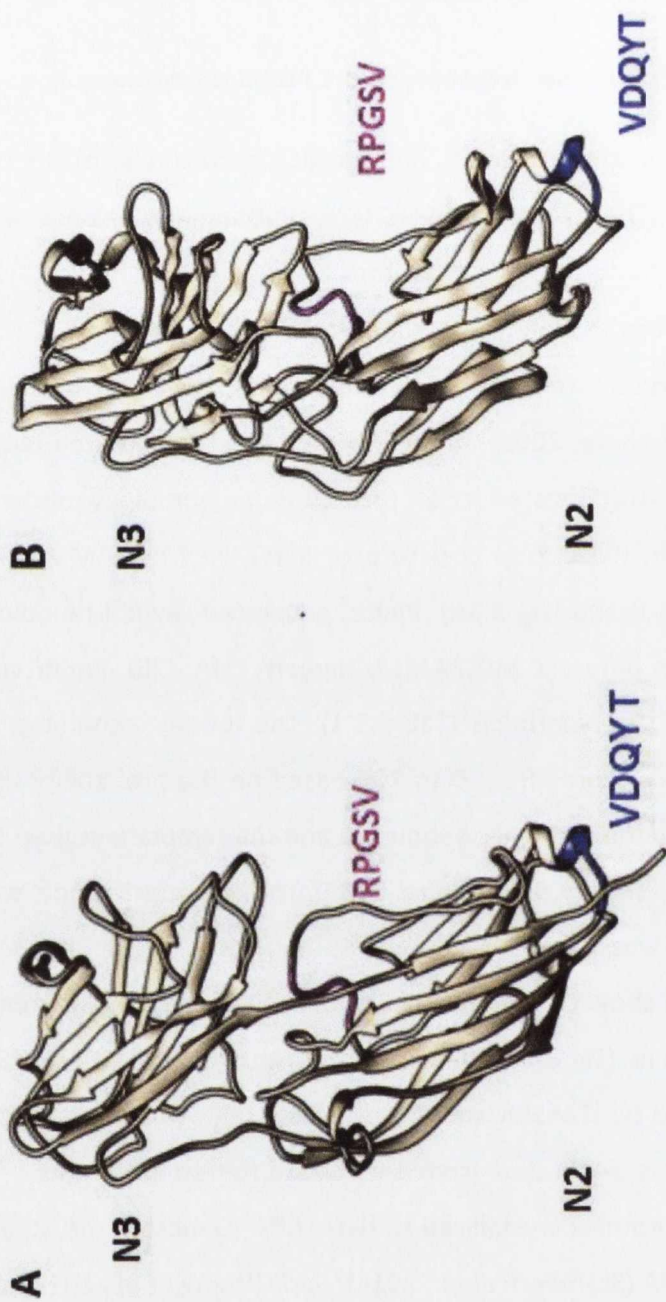
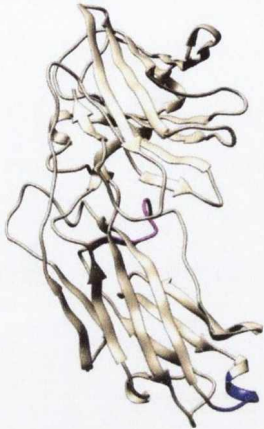
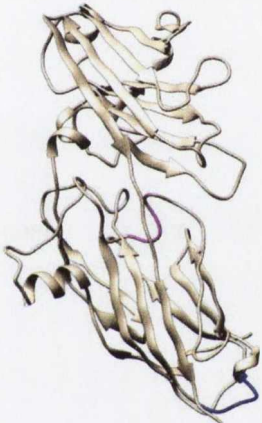

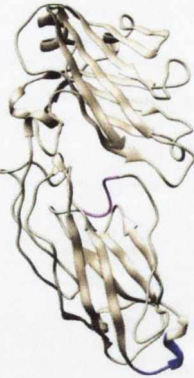
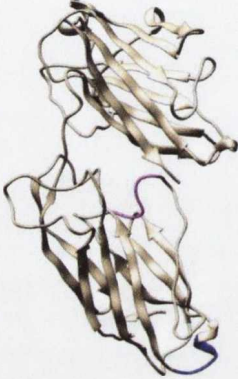




FIG 3.3. Homology models of SdrCN2N3. A) Homology model of SdrCN2N3 generated by I-TASSER based on SdrG of *S. epidermidis* in its ligand bound form. B) Homology model of SdrCN2N3 generated by Phyre² based on ClfA of *S. aureus* in its apo form. Both models are shown in ribbon structure with the backbone of the RPGSV motif coloured magenta and the backbone of the VDQYT motif in blue with subdomains N2 and N3 labelled.

Table 3.1 SdrCN2N3 homology models generated by Phyre²

| Model ^a | Crystal structure source | Model Rank | Confidence (%) | Sequence identity (%) | Sequence Coverage (%) | PDB ID |
|---|---|------------|----------------|-----------------------|-----------------------|--------|
|  | C1fA | 1 | 100 | 21 | 99 | 1N67 |
|  | C1fB | 2 | 100 | 27 | 98 | 4F24 |
|  | C1fA in complex with the fibrinogen γ -chain peptide | 4 | 100 | 21 | 98 | 2VR3 |

| | | | | | | |
|---|--|----|-----|----|----|------|
|  | ClfB | 5 | 100 | 28 | 94 | 3AU0 |
|  | SdrG | 6 | 100 | 21 | 94 | 1R17 |
|  | FnBPA in complex with the fibrinogen γ - chain peptide | 8 | 100 | 19 | 95 | 4B60 |
|  | SdrD | 12 | 100 | 25 | 98 | 4JE0 |

^a SdrC models are shown in ribbon structure with the backbone of the RPGSV motif coloured magenta and the backbone of the VDQYT motif in blue.

3.2.2 *In silico* analysis of RPGSV and VDQYT motifs

Two pentamer motifs involved in SdrC homodimer formation were previously identified by phage display; RPGSV and VDQYT (Barbu *et al.*, 2014). The RPGSV and VDQYT motifs of the homology models were analysed *in silico* in order to make predictions of the type of homophilic interactions occurring and to assess the feasibility of small molecule inhibitor docking. The RPGSV and VDQYT motifs are located in the same region on all homology models generated based on other MSCRAMMs (Fig 3.3, Table 3.1). The RPGSV motif is located in the trench between subdomains N2 and N3 (Fig 3.4A and B) and the VDQYT motif is located at the base of subdomain N2 (Fig 3.4D and E). The RPGSV residues are located on a flexible linker region between two β -strands of subdomain N2 although P₂₄₈ may add some rigidity to the region and all residues are predicted to be surface accessible. R₂₄₇ is predicted to contribute to a positively charged pocket (Fig 3.4C). All residues except V₂₈₈ of the VDQYT motif are predicted to be surface exposed projecting from the protein (Fig 3.4F). V₂₈₈ is located in a turn of a short α -helix but the remaining residues are located in a flexible linker region. The VDQYT residues form a pocket at the base of subdomain N2 where D₂₈₉ contributes to the negative charge of this pocket (Fig 3.4E). Both the RPGSV and VDQYT sites are predicted to be surface exposed and thus available to form homophilic interactions and are accessible sites for an inhibitor to bind. Notably, the RPGSV motif is predicted to form part of a positively charged pocket and the VDQYT motif part of a negatively charged pocket. Based on the charges at each site and the *in silico* prediction of their surface accessibility, there is the possibility that the homophilic interaction may be based on charge attraction. Furthermore, these sites are suitable for *in silico* docking of small molecules as they form part of a pocket into which an inhibitor could dock.

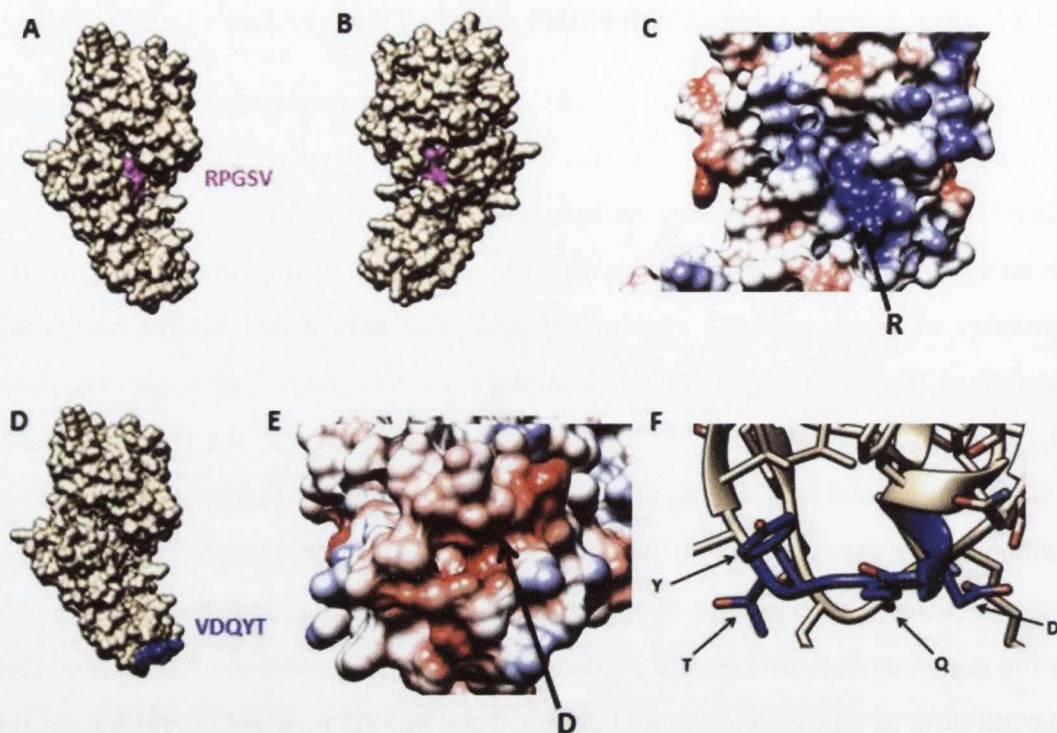


FIG 3.4. Position of the RPGSV and VDQYT motifs. A and B) The location of RPGSV on SdrC. SdrC is shown in space filled with the RPGSV motif coloured magenta. Two sides of SdrC are shown. C) R_{247} contributes to a positively charged pocket. SdrC is shown in space filled with amino acid residues coloured by charge (red=negative, blue=positive, white=no charge). The location of R_{247} (R) is indicated. D) The location of VDQYT on SdrC. SdrC is shown in space filled with the VDQYT motif coloured blue. E) VDQYT forms part of a negatively charged pocket. SdrC is shown in space filled from the base of subdomain N2 and coloured by charge. The location of D_{289} (D) is indicated. F) The side chains of residues D_{289} - T_{292} are projected from the surface of SdrC. SdrC is shown in ribbon format with amino acid residues shown as sticks and D_{289} - T_{292} shown in blue and indicated (D, Q, Y, T). The SdrC model used here was generated by Phyre² based on ClfA.

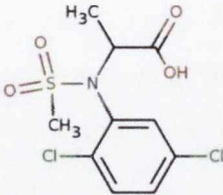
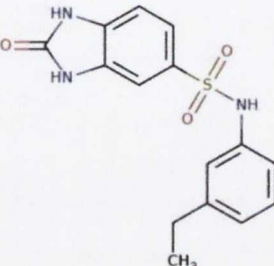
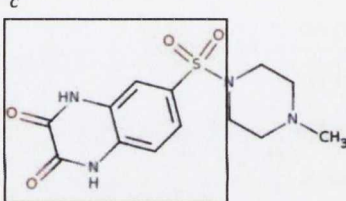
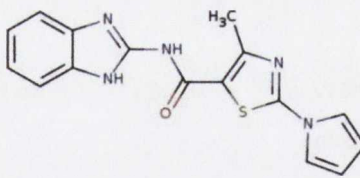
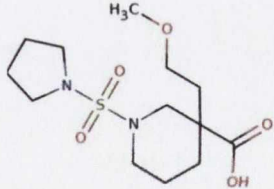
3.2.3 *In silico* docking of two small molecule libraries targeting SdrC

Two small molecule libraries were screened to identify putative inhibitors of SdrC-mediated biofilm; the Zinc database (Irwin *et al.*, 2012), specifically the clean lead subset, and 'The Malaria box' of compounds provided by the Medicines for Malaria Venture (MMV) (Spangenberg *et al.*, 2013). The Zinc database contains commercially available compounds (Irwin *et al.*, 2012) and was screened for putative inhibitors that would dock at either the RPGSV or VDQYT motifs of the SdrC models using the online docking program DOCK Blaster (Irwin *et al.*, 2009). DOCK Blaster ranks the molecules in order of predicted binding affinity to the specified target site (kcal/mol) (Irwin *et al.*, 2009). Identified small molecules were further studied in their docked position at SdrC with Chimera (Pettersen *et al.*, 2004) used for visualisation of these complexes. The predicted docking sites of the small molecules were examined and putative interactions to SdrC and more specifically, the RPGSV or VDQYT residues, were predicted allowing an informed identification of putative inhibitors and selection for *in vitro* analysis (Tables 3.2 and 3.3).

Nine small molecules from the Zinc library screen which docked at the RPGSV motif were analysed *in silico*. All nine molecules docked in the positively charged pocket of RPGSV. They also all contained a negatively charged carboxylate group (COO⁻) which allows interactions to the positively charged pocket. Thus, due to these initial overall similarities among the small molecules, the small molecules were selected based on their putative hydrogen bonds and contacts to the RPGSV motif. From these analyses two small molecules; termed LH1 and LH5, were selected which were both predicted to form salt bridges to the positively charged side chain of residue R₂₄₇ through their carboxylate group (Tables 3.2 and 3.3). Seventeen small molecules from the Zinc library screen that docked at the VDQYT motif were further examined *in silico*. All seventeen of these small molecules docked at the negatively charged pocket partially formed by residues VDQYT. Twelve of the seventeen small molecules contained a similar substructure (Table 3.2). On comparison of these molecules the common substructure docked in the pocket at the VDQYT residues and interacted with the protein but the variable region of each molecule projected out from the protein and was not predicted to interact with residues VDQYT. Thus, this structural similarity was

highlighted in the screen as a potential chemical structure for interaction to the VDQYT motif. A representative compound; termed LH3, containing this substructure was selected for *in vitro* analysis (Tables 3.2 and 3.3). Two other small molecules of structural diversity which dock at the VDQYT motif; termed LH2 and LH4, were also selected for further analysis *in vitro* (Tables 3.2 and 3.3). Only one of the three compounds, LH4, is predicted to form a hydrogen bond to the VDQYT motif. Interestingly, LH2 and LH4 are also predicted to dock at the RPGSV motif (Table 3.3). However, this docking is not at the positively charged pocket but at the opening of the trench between subdomains N2 and N3.

TABLE 3.2. Chemical structures of compounds from the Zinc library screen selected for *in vitro* screening

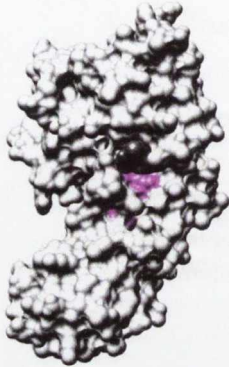
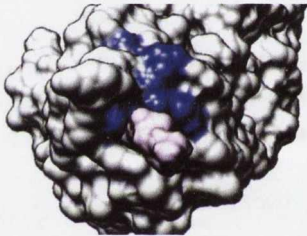
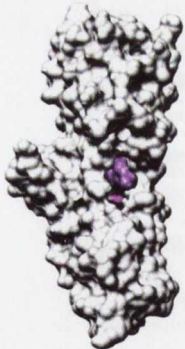
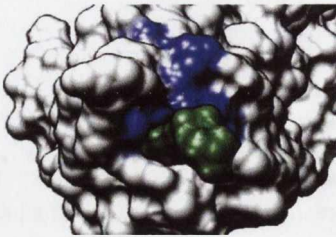
| Chemical Name | Abbreviation | Zinc ID ^a | Chemical structure ^b | Molecular weight |
|--|--------------|----------------------|--|------------------|
| 2-[N-(2,5-dichlorophenyl) methanesulfonamido] propanoic acid | LH1 | ZINC 04777325 |  | 311.17 |
| N-(3-ethylphenyl)-2-oxo-2,3-dihydro-1H-1,3-benzodiazole-5-sulfonamide | LH2 | ZINC 07486132 |  | 317.37 |
| 6-[(4-methylpiperazin-1-yl)sulfonyl]-1,2,3,4-tetrahydroquinoxaline-2,3-dione hydrochloride | LH3 | ZINC 13582133 |  | 324.36 |
| N-(1H-1,3-benzodiazol-2-yl)-4-methyl-2-(1H-pyrrol-1-yl)-1,3-thiazole-5-carboxamide | LH4 | ZINC 12323863 |  | 323.38 |
| 3-(2-methoxyethyl)-1-(pyrrolidine-1-sulfonyl)piperidine-3-carboxylic acid | LH5 | ZINC92065 187 |  | 319.4 |

^aZinc ID = Identification code in the Zinc library.

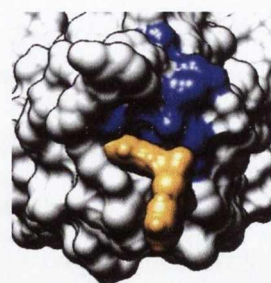
^b Atoms are coloured by element with oxygens in red, nitrogens in blue, sulphurs in brown, chlorines in green and carbons and hydrogens in black.

^c Substructure found in twelve of the seventeen inhibitors examined docked at the VDQYT motif.

TABLE 3.3. *In silico* docking results of compounds from the Zinc library screen

| Name | Site of docking | <i>In silico</i> binding affinity (kcal/mol) | Hydrogen (H-) bonds and contacts to RPGSV and/or VDQYT motif | Docking at SdrC ^a |
|------|----------------------------------|--|---|---|
| LH1 | RPGSV; positively charged pocket | -78.25 | 3 H-bonds: -2 x COO ⁻ group to R247 -S=O to R306 ^b 7 contacts to R247 and V251 |  |
| LH2 | VDQYT; negatively charged pocket | -112 | 1 H-bond -to D289 33 contacts to residues V288, D289, Y291 and T292 |  |
| | RPGSV; opening of trench | -88.65 | No H-bonds to RPGSV 18 contacts to residues P248, S250 and V251 |  |
| LH3 | VDQYT; negatively charged pocket | -104.9 | 1 H-bond: -None to VDQYT - 1 to V232 ^c 47 contacts to V288, D289, Y291 and T292 |  |

LH4 VDQYT; -99.18 1 H-bond
 negatively charged pocket
 -None to VDQYT
 - 1 to V232
 30 contacts to residues V288,D289, Y291 and T292



RPGSV; -97.16 No H-bonds to RPGSV
 opening of trench
 11 contacts to V251



LH5 RPGSV; -73.57 3 H-bonds:
 positively charged pocket
 -COO⁻ group to R247
 -S=O to R247
 -COO⁻ group to R306
 11 contacts to R247 and V251



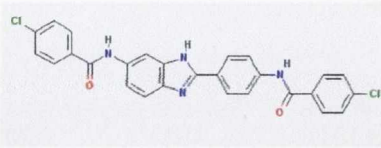
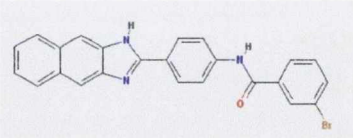
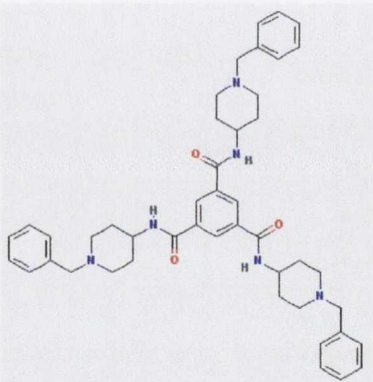
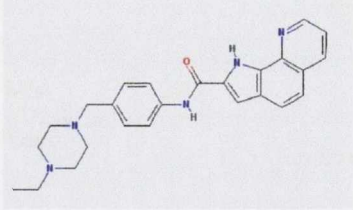
^a SdrC is shown in space filled with the RPGSV motif in magenta or the VDQYT motif in blue. The small molecules are shown in space filled with LH1, LH2, LH3, LH4 and LH5 coloured grey, purple, green, orange and black, respectively. For small molecules docked at the VDQYT motif SdrC is viewed from the base of subdomain N2.

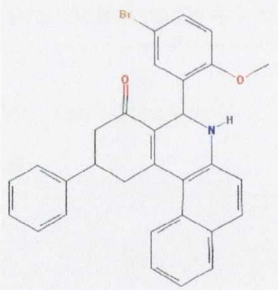
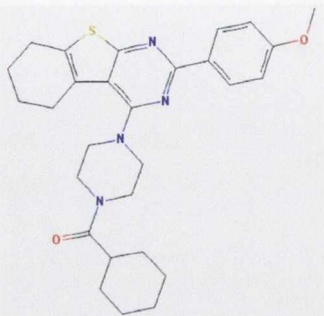
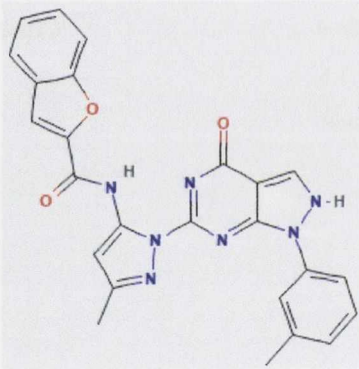
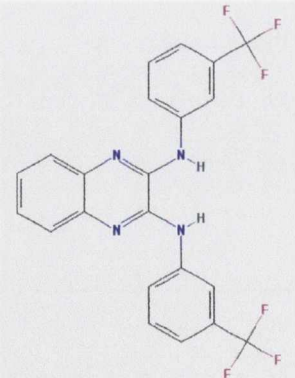
^b R306 is a neighbouring residue of the RPGSV motif which also contributes to the same positively charged pocket as R247.

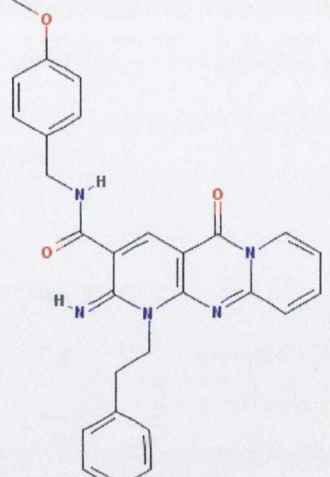
^c V232 is a neighbouring residue of the VDQYT motif which forms part of the same pocket at the base of subdomain N2.

'The Malaria box' library was screened for compounds docking at the RPGSV or VDQYT motifs on the I-TASSER generated SdrC homology model and, separately, on the Phyre² generated SdrC model using Autodock vina (Trott & Olson, 2010). 'The Malaria box' consists of 400 freely available compounds originally identified for their antiparasitic properties against *Plasmodium* species, the causative agent of malaria (Spangenberg *et al.*, 2013). Although this library is relatively small in comparison to the Zinc database it allows access to many diverse chemical scaffolds. The 400 compounds include 200 probe-like and 200 drug-like molecules which were selected from 20,000 hits in order to provide a high level of structural diversity (Spangenberg *et al.*, 2013). The compounds were also selected based on an acceptable level of cytotoxicity for initial drug discovery programmes with compounds included having a 10-fold reduction in toxicity against human embryonic kidney cells in comparison to *Plasmodium falciparum*. In the case of drug-like molecules, they were also selected based on properties favourable for oral absorption and any compounds with known toxicophores were not included (Spangenberg *et al.*, 2013). This database is known to also contain compounds with bacterial targets. Similar to DOCK Blaster, Autodock vina (Trott & Olson, 2010) also provides predicted binding affinities of each small molecule for the site and model specified (kcal/mol) (Trott & Olson, 2010). From this screen, compounds with high affinity scores across both models were visualised docking with SdrC using Chimera. Again, analysis of the docking location of compounds and their predicted interactions to SdrC and specifically, the RPGSV and VDQYT motifs, were assessed. Nine compounds were selected for further *in vitro* analysis (Tables 3.4 and 3.5). All nine compounds dock at the RPGSV motif. In contrast to the selected small molecules from the Zinc library, these compounds are larger in size (>400 Daltons in comparison to ~300 Daltons) and do not make a large number of hydrogen bonds or contacts to the RPGSV motif. However, they do have high affinity for the site and all docked at the opening of the trench. In all cases, except for LH10, when visualised using Chimera, the selected compounds are predicted to almost fully block the opening of the trench (Table 3.5). LH10 only partially blocks this opening. Thus, along with having high affinity for the target site, based on the predicted docking sites, these compounds may also sterically restrict access to the RPGSV motif preventing the necessary homophilic interactions in SdrC-mediated biofilm accumulation.

TABLE 3.4. Chemical structures of compounds from the 'Malaria Box'

| Chemical Name | Abbreviation | 'Malaria Box' ID ^a | Chemical structure ^b | Molecular weight |
|--|--------------|-------------------------------|--|------------------|
| 4-chloro-N-[4-[6-[(4-chlorobenzoyl)amino]-1H-benzimidazol-2-yl]phenyl]benzamide | LH6 | MMV 006962 |  | 501.4 |
| 3-bromo-N-[4-(1H-naphtho[2,3-d]imidazol-2-yl)phenyl]benzamide | LH7 | MMV 019241 |  | 442.3 |
| 1-N,3-N,5-N-tris(1-benzylpiperidin-4-yl)benzene-1,3,5-tricarboxamide | LH8 | MMV 019881 |  | 723 |
| N-[4-[(4-ethylpiperazin-1-yl)methyl]phenyl]-1H-pyrrolo[3,2-h]quinoline-2-carboxamide | LH9 | MMV 020548 |  | 413.5 |

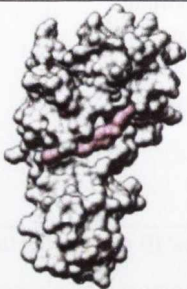

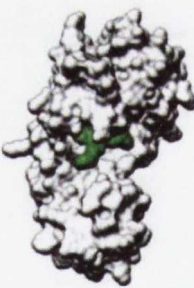
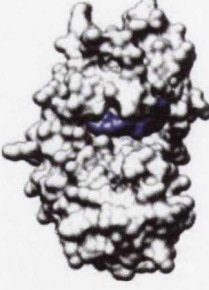
| | | | | |
|---|------|---------------|--|-------|
| 5-(5-bromo-2-methoxyphenyl)-2-phenyl-2,3,5,6-tetrahydro-1H-benzo[a]phenanthridin-4-one | LH10 | MMV 020885 |  | 510.4 |
| cyclohexyl-[4-[2-(4-methoxyphenyl)-5,6,7,8-tetrahydro-[1]benzothio[2,3-d]pyrimidin-4-yl]piperazin-1-yl]methanone | LH11 | MMV 396594 |  | 490.7 |
| N-(3-methyl-1-(4-oxo-1-(m-tolyl)-4,5-dihydro-1H-pyrazolo[3,4-d]pyrimidin-6-yl)-1H-pyrazol-5-yl)benzofuran-2-carboxamide | LH12 | MMV 403679 |  | 465.5 |
| 2,3-Quinoxalinediamine, N,N'-bis[3-(trifluoromethyl)phenyl] | LH13 | MMV 665794 |  | 448.4 |


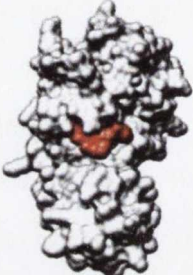
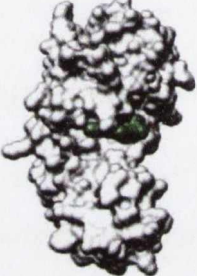
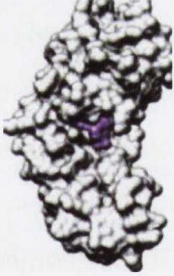
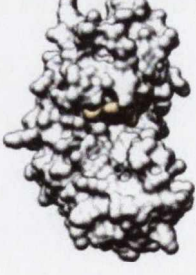
| | | | | |
|--|------|---------------|--|-------|
| <p>[2-imino-5-oxo-1-(2-phenylethyl)(1,6-dihydropyridino[1,2-a]pyridino[2,3-d]pyrimidin-3-yl)]-N-[(4-methoxyphenyl)methyl]carboxamide</p> | LH14 | MMV 665881 |  | 479.5 |
|--|------|---------------|--|-------|

^a 'Malaria Box' ID = Identification code for compounds in the 'Malaria Box'.

^b Atoms are coloured by element with oxygens in red, nitrogens in blue, sulphurs in yellow, chlorines in green, bromines in orange, fluorines in purple, hydrogens in grey and carbons in black.

TABLE 3.5. *In silico* docking results of compounds from 'The Malaria box' screen

| Abbreviation | Docking site | Binding affinity (kcal/mol) | Hydrogen (H-) bonds and contacts to RPGSV motif | Image of small molecule docked at SdrC ^a |
|--------------|---|-----------------------------|---|--|
| LH6 | RPGSV motif, across the opening of the trench | -9.2 | 4 contacts to G249 and S250 |  |
| LH7 | RPGSV motif, inside the trench | -9.6 | 2 contacts to G249 and S250 |  |
| LH8 | RPGSV motif, across the opening of the trench | -9.1 | 9 contacts to G249 and S250 |  |
| LH9 | RPGSV motif, across the opening of the trench | -9 | 1 contact to S250 |  |

| | | | | |
|------|---|------|---|--|
| LH10 | RPGSV motif, in the trench | -8.9 | 4 contacts to S250 |  |
| LH11 | RPGSV motif, across the opening of the trench | -8.8 | 3 contacts to G249 and S250 |  |
| LH12 | RPGSV motif, across the opening of the trench | -8.8 | -1 H-bond to G249 -4 contacts to G249 and S250 |  |
| LH13 | RPGSV motif, at the opening of the trench | -9.4 | 4 contacts to G249 and S250 |  |
| LH14 | RPGSV motif, across the opening of the trench | -8.8 | 5 contacts to G249 and S250 |  |

^aThe SdrC homology model generated by Phyre² based on ClfA is shown in space filled. Each small molecule is shown docked in space filled and coloured.

3.2.4 Assessment of the ability of putative SdrC inhibitors to bind recombinant SdrC by Differential Scanning Fluorimetry

In order to assess if putative inhibitors can bind recombinant SdrC protein, DNA encoding subdomains N2 and N3 of *sdrC* was cloned into the IPTG-inducible vector pQE30 and recombinant SdrC N2N3 (rSdrC) was purified with an N-terminal hexahistidine tag. The purity and integrity of rSdrC was assessed by SDS-PAGE and coomassie blue protein staining (Fig 3.5A) or Western immunoblot with an antibody detecting the hexahistidine tag (Fig. 3.5B). Purified rSdrC migrates according to size (~37 kDa) (Fig 3.5A and B). A faint band of higher molecular weight (~70 kDa) is visible on the Coomassie stained gel (Fig 3.5A). This likely corresponds to a dimer of SdrC. In the Western immunoblot, several other faint bands of higher molecular weight can also be observed. These may correspond to dimer formation (~70 kDa) and breakdown products of this dimer (Fig 3.5B).

Binding of the fourteen selected compounds (25 μ M) to rSdrC protein (0.5 mg/ml) was then tested by differential scanning fluorimetry (DSF) as the first step in screening the potential inhibitors. Five compounds significantly increased the melting temperature of rSdrC by ≥ 2 $^{\circ}$ C; LH4 by 2.4 ± 0.6 $^{\circ}$ C (Fig 3.6A), LH6 by 4.4 ± 0.9 $^{\circ}$ C (Fig 3.6B), LH7 by 6.5 ± 1.7 $^{\circ}$ C (Fig 3.6C), LH10 by 1.9 ± 0.04 $^{\circ}$ C (Fig 3.6D) and LH13 by 6.9 ± 1.6 $^{\circ}$ C (Fig 3.6E). The change in melting temperature of rSdrC in the presence of the remaining nine compounds was < 2 $^{\circ}$ C (Table 3.6) and these are not considered to bind rSdrC in this assay. Thus, 5 compounds; LH4, LH6, LH7, LH10 and LH13 predicted to target SdrC by *in silico* docking were found to bind rSdrC increasing its melting temperature by ≥ 2 $^{\circ}$ C. All of these inhibitors are predicted to dock at the RPGSV motif with LH4 also docking at the VDQYT motif of SdrC.

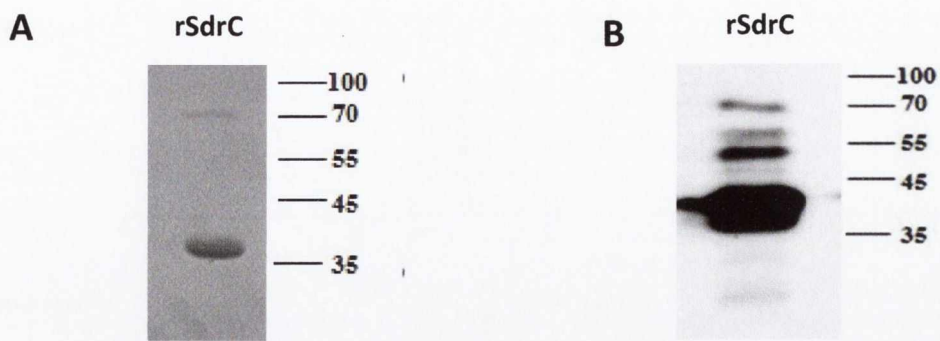


FIG 3.5 Recombinant SdrC N2N3. A) Coomassie stained gel of recombinant SdrCN2N3 (rSdrC). Purified rSdrC protein was separated on a 12.5% SDS gel and stained with coomassie blue protein stain. B) Western Immunoblot of rSdrC. Purified rSdrC protein was analysed by western immunoblot probing with anti-His IgG followed by protein A peroxidase. Size markers (kDa) are shown.

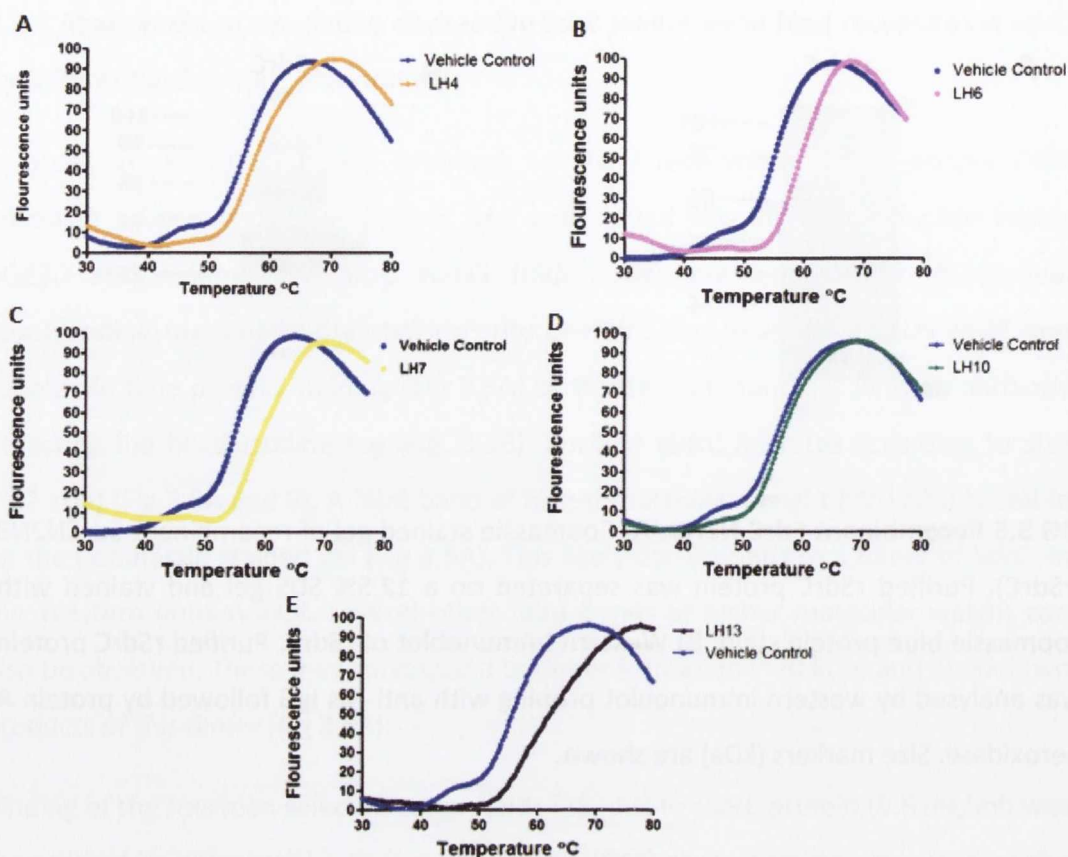


FIG 3.6 Differential scanning fluorimetry of recombinant SdrC N2N3 in the presence of small molecules. Differential scanning fluorimetry was carried out with recombinant SdrC N2N3 (0.5 mg/ml) and the reporter dye SYPRO orange in the presence of compounds (25 μ M) (A) LH4 (p -value=0.004), (B) LH6 (p -value=0.003), (C) LH7 (p -value=0.055), (D) LH10 (p -value=0.04) and (E) LH13 (p -value=0.012). A DMSO solvent control was carried out (labelled Vehicle control). Thermal melt curves were generated using Prism Graphpad software version 5.01 and are the mean of three independent experiments for all curves except for LH4 (A) which is the mean of five independent experiments. Fluorescence values were normalised relative to the minimum and maximum fluorescence values as 0 and 100 fluorescence units, respectively. Thermal melt curves of fluorescence units vs temperature ($^{\circ}$ C) were assessed. The melting temperature was identified as the temperature corresponding to a fluorescence units value of 50. P -values were calculated using an unpaired two-tailed Student's t -test where p -values ≤ 0.05 are considered significant.

TABLE 3.6. ΔT_m of recombinant SdrC in the presence of small molecules

| Small molecule | ΔT_m ($^{\circ}\text{C}$) ^a | SEM ($^{\circ}\text{C}$) ^b |
|----------------|--|---|
| LH1 | 0.3 | ± 0.1 |
| LH2 | 0.2 | ± 0.6 |
| LH3 | 0.3 | ± 0.1 |
| LH5 | 0.4 | ± 0.1 |
| LH8 | 1.0 | ± 0.3 |
| LH9 | 0.8 | ± 0.5 |
| LH11 | 0.8 | ± 0.6 |
| LH12 | 0.8 | ± 0.5 |
| LH14 | 0.7 | ± 0.4 |

^aThe ΔT_m is the mean of three independent experiments.

^b SEM=standard error of the mean.

3.2.5 *In silico* docking of a peptide ligand of SdrCN2N3

A peptide derived from the β -neurexin protein was previously shown to bind recombinant SdrCN2N3 (Barbu *et al.*, 2010). The peptide binding site on SdrC and mechanism of binding remains unknown. *In silico* docking of the β -neurexin derived peptide to SdrC was carried out using Autodock vina to predict its binding site. Surprisingly, the β -neurexin derived peptide was not predicted to dock in a linear conformation along the trench which would be consistent to MSCRAMM-ligand binding by dock, lock and latch (Section 1.4.1.1, Foster *et al.*, 2014). In contrast, the β -neurexin derived peptide was predicted to dock in a semi-circle conformation at the opening of the trench and extending into the positively charged pocket (Fig 3.7). Interestingly, the β -neurexin derived peptide docking occurs along the RPGSV motif (Fig 3.7). The β -neurexin derived peptide is predicted to form 11 H-bonds to SdrC, one of which is to residue G₂₄₉ of the RPGSV motif. The β -neurexin derived peptide was also predicted to form a H-bond to R₃₀₆, a neighbouring residue of the RPGSV motif, which contributes to the same positively charged pocket as R₂₄₇. The β -neurexin derived peptide forms a further 11 contacts to the RPGSV motif to all residues except P₂₄₈. Thus, we hypothesised that this peptide could potentially inhibit SdrC-mediated biofilm.

3.2.6 Binding of the β -neurexin derived peptide to SdrC is not detected by Differential Scanning Fluorimetry

The β -neurexin derived peptide was screened for binding to recombinant SdrC N2N3 (rSdrC) by DSF (Fig 3.8). The peptide did not significantly increase the melting temperature of rSdrC (Fig 3.8). This indicates that, at least by DSF, binding of the peptide to rSdrC is not detected. This is likely due to the crude nature of DSF as the peptide had previously been shown to bind rSdrC in a more sensitive, fluorescence polarization assay (Barbu *et al.*, 2010).

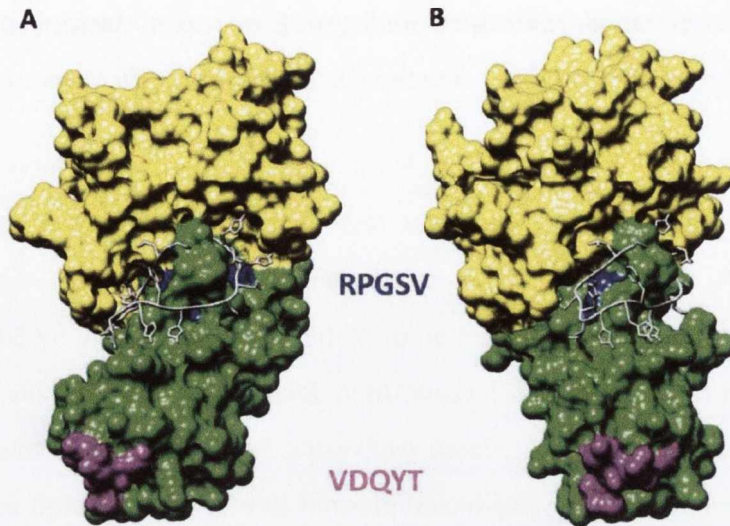


FIG 3.7. Model of the β -neurexin derived peptide in complex with SdrC. SdrC N2 and N3 subdomains are shown in space filled coloured green and yellow, respectively. The RPGSV and VDQYT motifs are coloured in blue and pink, respectively. The peptide is shown in white in stick format. The image shown in panel B is rotated 42° right compared to the view in panel A.

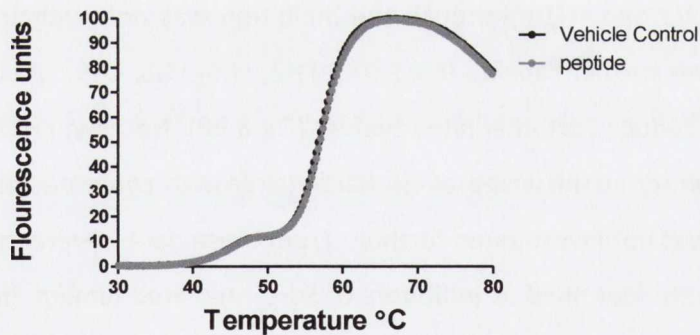


FIG 3.8 DSF of recombinant SdrC in the presence of the β -neurexin derived peptide. DSF was carried out with recombinant SdrC (rSdrC; 0.5 mg/ml) and the reporter dye SYPRO orange in the presence of the β -neurexin derived peptide (peptide; 25 μ M). Thermal melt curves were generated using Prism Graphpad software version 5.01 and are the mean of three independent experiments. Fluorescence values were normalised relative to the minimum and maximum fluorescence values as 0 and 100 fluorescence units, respectively. Thermal melt curves of fluorescence units vs temperature ($^{\circ}$ C) were assessed and the melting temperature was identified as the temperature corresponding to a fluorescence units value of 50.

3.2.7 Assessment of small molecules and the β -neurexin derived peptide for inhibition of SdrC-mediated biofilm using the surrogate host *L. lactis* expressing SdrC

The ability of the fourteen small molecules and the β -neurexin derived peptide to inhibit SdrC-mediated biofilm *in vitro* was tested using the surrogate host *L. lactis* expressing SdrC. As *S. aureus* biofilm formation is multifactorial the use of a surrogate host allowed the assessment of inhibition of biofilm mediated solely by SdrC with no interference from other *S. aureus* factors. As *L. lactis* does not naturally produce a biofilm, biofilm accumulation by *L. lactis* expressing SdrC is mediated solely by SdrC (SdrC⁺). *L. lactis* carrying the empty pKS80 plasmid (SdrC⁻) was included to show the level of biofilm produced that is not mediated by SdrC.

LH1-5 (50 μ M), LH6-14 (25 μ M) and the β -neurexin derived peptide (12.5 μ M) were assessed for their ability to inhibit SdrC-mediated biofilm formation (Fig 3.9A and B). LH3, LH4, LH6, LH7, and LH12 significantly reduced SdrC-mediated biofilm formation (Fig 3.9A). The peptide abolished SdrC-mediated biofilm reducing the biofilm formed to a level similar to the negative control (SdrC⁻) (Fig 3.9A). A reduction in biofilm was observed with LH1 and LH10 although the inhibition was not statistically significant and likely requires further repeats (Fig 3.9A). LH2, LH5, LH8, LH9, LH11 and LH14 did not significantly reduce SdrC-mediated biofilm (Fig 3.9B). Notably, LH13 was found to be growth inhibitory at this stage as no bacterial growth could be measured in this assay and thus was not investigated further. From these data, several small molecules and a peptide were identified as inhibitors of SdrC-mediated biofilm. Interestingly, all of the inhibitors found to bind rSdrC by DSF (Section 3.2.4) inhibited biofilm formation in this assay. LH3 was not found to bind rSdrC by DSF but does inhibit SdrC-mediated biofilm. However, of the biofilm inhibitors, LH3 is the only inhibitor which binds exclusively to the VDQYT motif. As this motif is located at an outer region of the protein, binding of the motif may not cause a stabilised structure increasing the protein melting temperature.

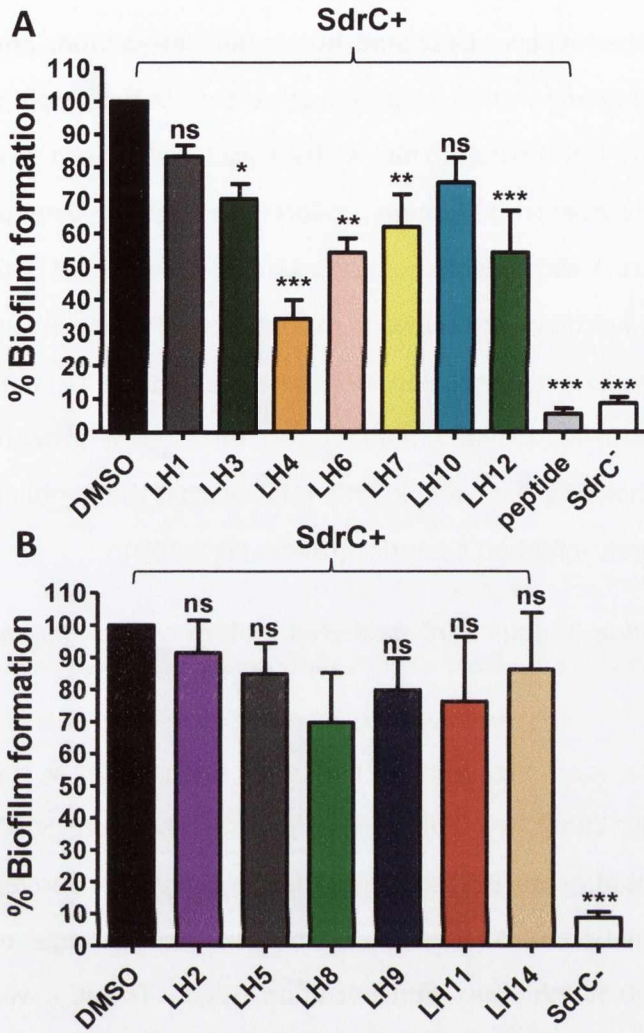


FIG 3.9. Assessment of small molecules and peptide for inhibition of SdrC-mediated biofilm. *L. lactis* pKS80::*sdrC* (labelled SdrC⁺) was allowed to develop biofilm for 24 h statically at 28 °C in the presence of LH1-5 (50 μM), LH6-14 (25 μM) and the β-neurexin derived peptide (12.5 μM) in tissue-culture treated microtiter plates (Nunclon delta). A solvent control (DMSO) was included for comparison to the small molecules. *L. lactis* pKS80 (SdrC⁻) was included as a biofilm negative control. LH1, LH3, LH4, LH6, LH7, LH10, LH12 and the peptide inhibited SdrC-mediated biofilm (A). LH2, LH5, LH8, LH9, LH11 and LH14 did not inhibit SdrC-mediated biofilm (B). Biofilm was stained with crystal violet and A_{570nm} measured. A_{570nm} values were normalised as % biofilm formation relative to the *L. lactis* pKS80::*sdrC* solvent control as 100% (DMSO). All values are the mean of at least three independent experiments except for assessment of LH8 which is the mean of two independent assays. Error bars present SEM. *P*-values were calculated using a one-way ANOVA where *, ** and *** represent *p*-values of ≤0.05, ≤0.01 and ≤0.001, respectively and values were compared to the DMSO control. *P*-values >0.05 are considered not significant (ns).

This study aimed to identify inhibitors which target SdrC homophilic interactions and prevent biofilm formation. Since inhibition of bacterial growth would reduce biofilm formation, it was essential to assess if the SdrC inhibitors affect bacterial growth or if the inhibition observed was solely due to disruption of SdrC interactions. Growth curves of *L. lactis* pKS80::*sdrC* (SdrC⁺) with inhibitors LH1, LH3, LH4, LH6, LH7, LH10, LH12 and the β -neurexin derived peptide or the relevant solvent control were carried out (Fig 3.10). LH3 and the β -neurexin derived peptide had no effect on *L. lactis* growth (Fig 3.10A, B). LH6, LH7 and LH10 had a minor effect on *L. lactis* growth, increasing the length of the log phase of growth (Fig 3.10C). LH4 reduced the doubling time of *L. lactis* while LH12 completely inhibited bacterial growth (Fig 3.10D).

3.2.8 The β -neurexin derived peptide inhibits SdrC-mediated biofilm with an IC₅₀ of ~0.9 μ M

The β -neurexin derived peptide was identified in initial biofilm inhibition tests as the most potent inhibitor in this study. The β -neurexin derived peptide abolished SdrC-mediated biofilm (12.5 μ M) without affecting bacterial growth. The β -neurexin derived peptide was then tested for inhibition of SdrC-mediated biofilm over a range of concentrations to determine its 50 % Inhibitory Concentration (IC₅₀). The IC₅₀ was determined to be ~0.9 μ M (Fig 3.11).

3.2.9 The peptide biofilm inhibitor does not disperse a mature biofilm

It was of interest to further assess the specificity of the β -neurexin derived peptide as an inhibitor of SdrC homophilic interactions in biofilm. Thus, the peptide was assessed for the ability to disperse a mature biofilm (Fig 3.12). Proteinase K was included as a positive control as it disperses established protein-dependent biofilms (O'Neill *et al.*, 2008). The peptide did not have any effect on an already formed mature biofilm (Fig 3.12). This result indicates that the peptide is not able to disperse a mature biofilm.

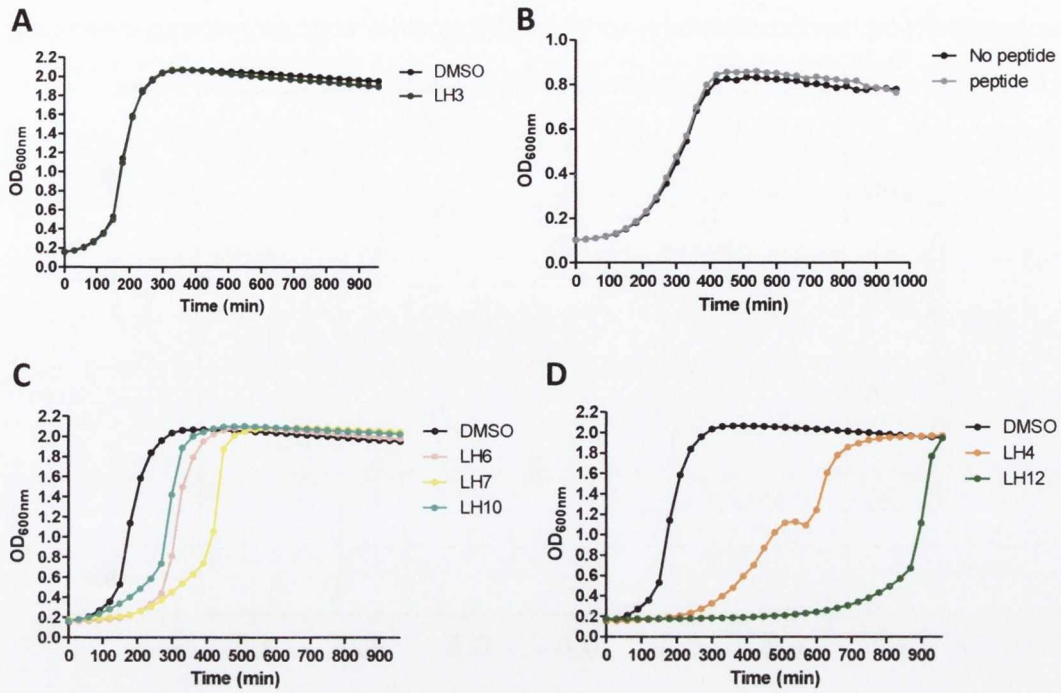


FIG 3.10. Representative growth curves of *L. lactis* with SdrC inhibitors. *L. lactis* SdrC⁺ was grown for 16 h statically with OD_{600nm} values measured at 30 min intervals in the presence of small molecules LH3 (50 μM, A), the β-neurexin derived peptide (peptide; 12.5 μM, B), LH6, LH7 and LH10 (25 μM, C), LH4 (50 μM, D) and LH12 (25 μM, D). Growth curves of *L. lactis* SdrC⁺ with DMSO (A, C, D) or no peptide (B) were measured as controls for the inhibitors.

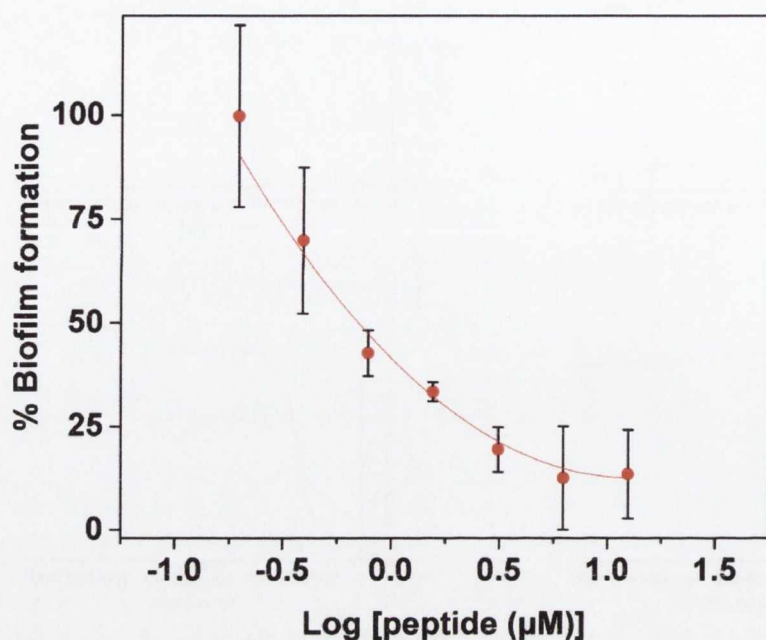


FIG 3.11. The β -neurexin derived peptide inhibits SdrC-mediated biofilm with an IC_{50} of $\sim 0.9 \mu M$. *L. lactis* pKS80::*sdrC* biofilm was allowed to develop for 24 h statically at 28 °C in the presence of varying concentrations of the peptide (0.195 μM to 12.5 μM) in tissue-culture treated microtiter plates (Nunclon delta). Biofilm was stained with crystal violet and A_{570nm} measured. A_{570nm} values were normalised as % biofilm formation relative to the *L. lactis* pKS80::*sdrC* no peptide control as 100 %. Values are the mean of three independent experiments. Error bars represent SEM. The IC_{50} was calculated from this curve.

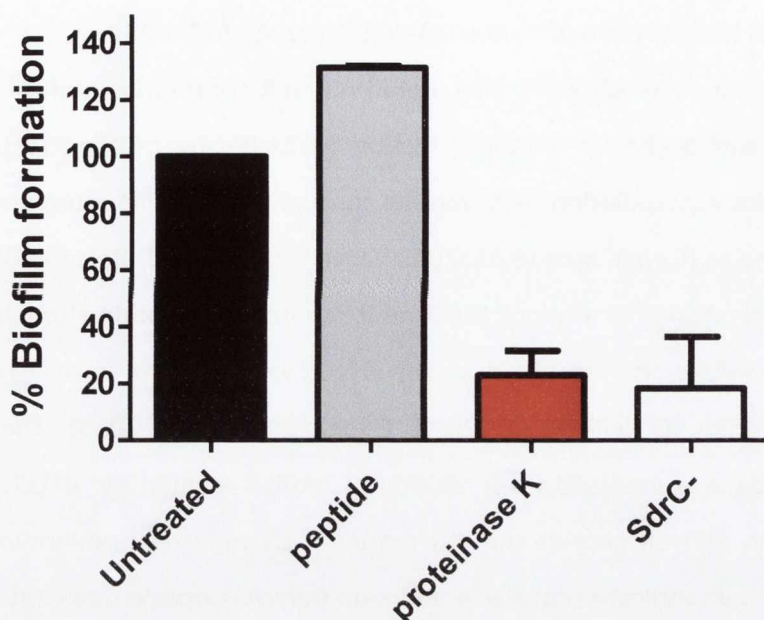


FIG 3.12. The peptide biofilm inhibitor does not disperse a mature biofilm. *L. lactis* pKS80::*sdrC* biofilm was allowed to develop for 24 h statically at 28 °C. *L. lactis* pKS80 (SdrC⁻) was included as a control to show the level of biofilm formed in the absence of SdrC. Established biofilms were then incubated with the peptide inhibitor (12.5 μM), proteinase K (100 μg/ml) or diluent only (untreated) for 2 h at 28 °C. Biofilm was then stained with crystal violet and A_{570nm} values measured. A_{570nm} values were normalised as % biofilm formation relative to the untreated control as 100 %. All values are the mean of two independent experiments. Error bars present SEM.

3.2.10 The SdrC peptide inhibitor does not inhibit biofilm mediated by FnBPs but inhibits biofilm formed by the HA-MRSA isolate MRSA252.

Like SdrC, fibronectin binding proteins (FnBP) A and B are members of the MSCRAMM family of cell wall-anchored proteins (Section 1.4.1) (Foster *et al.*, 2014). FnBPs also mediate biofilm accumulation in *S. aureus* through homophilic interactions of their N2N3 subdomains (Geoghegan *et al.*, 2013, O'Neill *et al.*, 2008, Herman-Bausier *et al.*, 2015). It was of interest to assess if the β -neurexin derived peptide also inhibits biofilm mediated by FnBPs. The HA-MRSA strain BH1CC is known to form a robust FnBP-dependent biofilm (O'Neill *et al.*, 2008, Geoghegan *et al.*, 2013). The β -neurexin derived peptide was assessed for inhibition of biofilm formed by BH1CC (Fig 3.13A). The β -neurexin derived peptide did not reduce FnBP-mediated biofilm in BH1CC (Fig 3.13A). These data indicate that the β -neurexin derived peptide does not affect FnBP-mediated biofilm and further indicates its specificity for SdrC.

To date, SdrC has been shown to promote biofilm in the *S. aureus* lab strain Newman (Barbu *et al.*, 2014). However, whether SdrC promotes biofilm in a clinical isolate remains unknown. Generation of an *sdrC* deletion mutant of a clinical isolate is the ideal way to assess this. Biofilm formed by the HA-MRSA clinical isolate MRSA252 was inhibited by recombinant SdrC N2 subdomain protein *in vitro* (Barbu *et al.*, 2014). This indirectly suggested that MRSA252 biofilm may be mediated by SdrC. As shown here, the SdrC peptide inhibitor appears to be specific to SdrC biofilm with no effect on biofilm mediated by FnBPs. In order to further assess if SdrC may have a role in biofilm formed by MRSA252, MRSA252 biofilm was screened *in vitro* for inhibition with the peptide (Fig 3.13B). Biofilm formation by MRSA252 was significantly inhibited by the peptide further indicating that MRSA252 may form an SdrC-mediated biofilm (Fig 3.13B). Inhibition of MRSA252 biofilm with the SdrC peptide inhibitor here and recombinant SdrC N2 protein previously (Barbu *et al.*, 2014) provided a strong rationale for the generation of an *sdrC* deletion mutant of MRSA252.

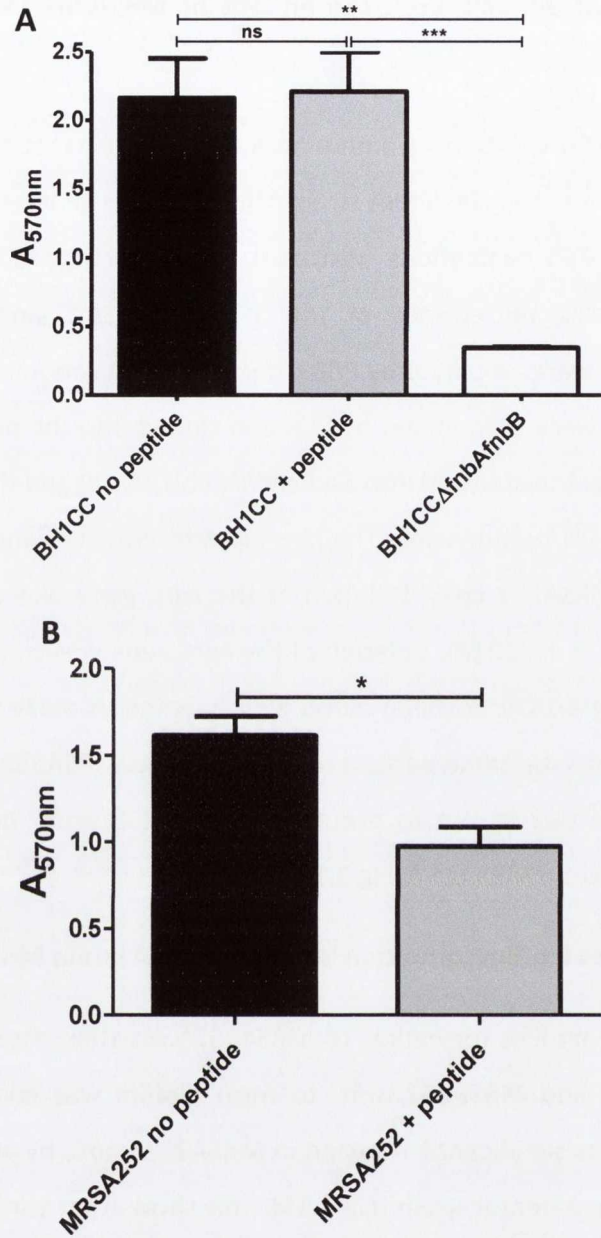


FIG 3.13. The SdrC peptide inhibitor does not inhibit FnBP-mediated biofilm but inhibits MRSA252 biofilm. HA-MRSA strains BH1CC (A) or MRSA252 (B) were allowed to form biofilm at 37 °C for 24 h in the presence or absence of the β -neurexin derived peptide (12.5 μ M). Biofilms were stained with crystal violet and A_{570nm} values measured. Values are the mean of three independent experiments. Error bars represent SEM. Statistical analysis was carried out using a one-way ANOVA with all values compared (A) and an unpaired Student's t- test (B) where * and *** represent *p*-values of ≤ 0.05 and ≤ 0.001 and a *p*-value > 0.05 is considered not significant (ns).

3.2.11 Generation of an *sdrC* deficient mutant of MRSA252 (MRSA252 Δ *sdrC*) by allelic exchange

In order to assess if SdrC mediates biofilm in a clinically relevant *S. aureus* strain, an *sdrC*-deficient mutant in the HA-MRSA strain MRSA252 was generated. In brief, a DNA fragment encoding 486 nucleotides upstream of the *sdrC* gene and another DNA fragment encoding 72 nucleotides of the 3' end of *sdrC* and 359 nucleotides downstream of *sdrC* were amplified by PCR using MRSA252 genomic DNA as template. The DNA fragments were then joined by PCR and cloned into the plasmid pIMAY. The resulting plasmid was transformed into *Escherichia coli* DC10B and the sequence of the insert confirmed by DNA sequencing. The plasmid was extracted and transformed into electrocompetent MRSA252 cells. Deletion of the *sdrC* gene was achieved by allelic replacement (Monk *et al.*, 2012). Deletion of the *sdrC* gene was confirmed by PCR and DNA sequencing (Fig 3.14A). A sheep blood agar haemolysis assay was carried out to ensure the mutant has the same pattern of haemolysis as MRSA252 (data not shown). Growth curves were carried out to ensure the MRSA252 Δ *sdrC* (Δ *sdrC*) strain had a similar growth pattern to MRSA252 (Fig 3.14B).

3.2.12 SdrC promotes biofilm formation in the HA-MRSA strain MRSA252

The role of SdrC in biofilm formation of MRSA252 was then assessed *in vitro*. The ability of MRSA252 and MRSA252 Δ *sdrC* to form biofilm was compared (Fig 3.15). Biofilm formation was significantly reduced in MRSA252 Δ *sdrC*, by approximately 40%, in comparison to the parental strain (Fig 3.15). This shows that SdrC promotes biofilm in MRSA252. However, the deletion of *sdrC* did not abolish the ability of MRSA252 to form biofilm with the MRSA252 Δ *sdrC* still forming biofilm albeit to a significantly reduced level (Fig 3.15). This indicates that MRSA252 biofilm involves other factors along with SdrC. This is not surprising as biofilm formation in *S. aureus* is a multifactorial process.

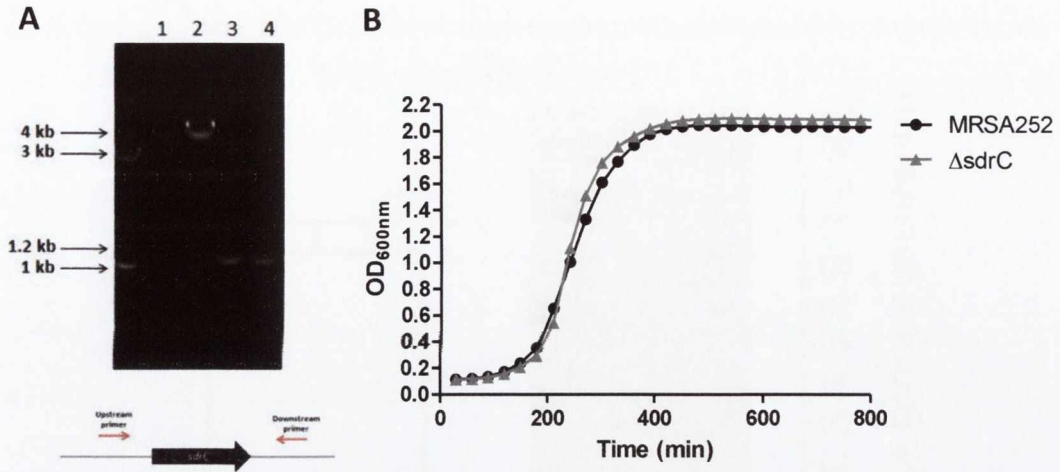


FIG 3.14 Generation of an *sdrC* deficient mutant of MRSA252. A) Confirmation of deletion of *sdrC* in MRSA252. The region of the *sdrC* gene on the chromosome was amplified by PCR using primers located upstream and downstream of *sdrC*. MRSA252 $\Delta sdrC$ yielded a product of approximately 1 kb (lanes 3 and 4) in comparison to a 4 kb product for the parental strain (lanes 1 and 2) confirming deletion of the gene. Size markers (kb) are shown. A schematic of the *sdrC* gene in MRSA252 and the primers used to confirm the deletion is shown below the gel image. B) MRSA252 $\Delta sdrC$ ($\Delta sdrC$) has a similar growth pattern to MRSA252. MRSA252 strains were grown in TSB for 18 h with shaking. OD_{600nm} values were measured at 30 min intervals. The growth curve is representative of three independent experiments.

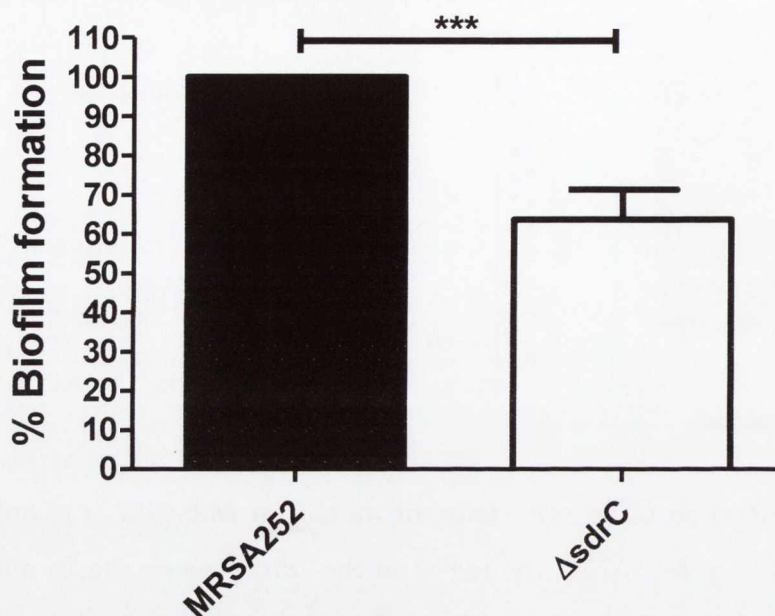


FIG 3.15. SdrC promotes biofilm in MRSA252. MRSA252 and MRSA252 $\Delta sdrC$ ($\Delta sdrC$) strains were allowed to form biofilm for 24 h at 37 °C. Biofilm was stained with crystal violet and A_{570nm} values measured. A_{570nm} values were normalised as % biofilm formation relative to MRSA252. Values are the mean of eight independent experiments. Error bars represent SEM. *P*-values were calculated using an unpaired Student's t-test where *** represents a *p*-value of ≤ 0.001 .

3.2.13 SdrC forms specific homophilic interactions between MRSA252 cells

SdrC-mediated biofilm in MRSA252 is likely to involve the formation of SdrC homophilic interactions between adjacent bacteria. To confirm that SdrC homophilic interactions are occurring between MRSA252 cells, the ability of MRSA252 and MRSA252 Δ *sdrC* single cells to interact was assessed using atomic force microscopy (AFM) by Cécile Feuillie and Cécile Formosa-Dague at the Institute of Life Sciences, Université Catholique de Louvain (Fig 3.16). More specifically, single cell force spectroscopy was used to assess the adhesion frequency and force between single cells. Single well-defined adhesion peaks were observed for MRSA252 cells (Fig 3.16A and B). The frequency of adhesion and the adhesion force between cells increased with increasing contact time (from 0.1 sec to 1 sec; Fig 3.16C and D) with an adhesion force of 42 ± 16 pN measured between cells. This force is consistent with a single SdrC-SdrC bond (Feuillie *et al.*, 2017). A large reduction in cell-cell adhesion was observed between MRSA252 Δ *sdrC* cells (Fig 3.16E and F). This indicates that the intercellular adhesion observed between MRSA252 cells is mediated by SdrC. Furthermore, cell adhesion between MRSA252 and MRSA252 Δ *sdrC* cells was also greatly reduced (Fig 3.16G and H). This confirms that the interactions between MRSA252 cells consist of SdrC homophilic interactions and that SdrC is not interacting with another surface component. These data show that adjacent MRSA252 cells adhere through SdrC homophilic interactions supporting a role for SdrC in promoting MRSA252 aggregation and biofilm formation.

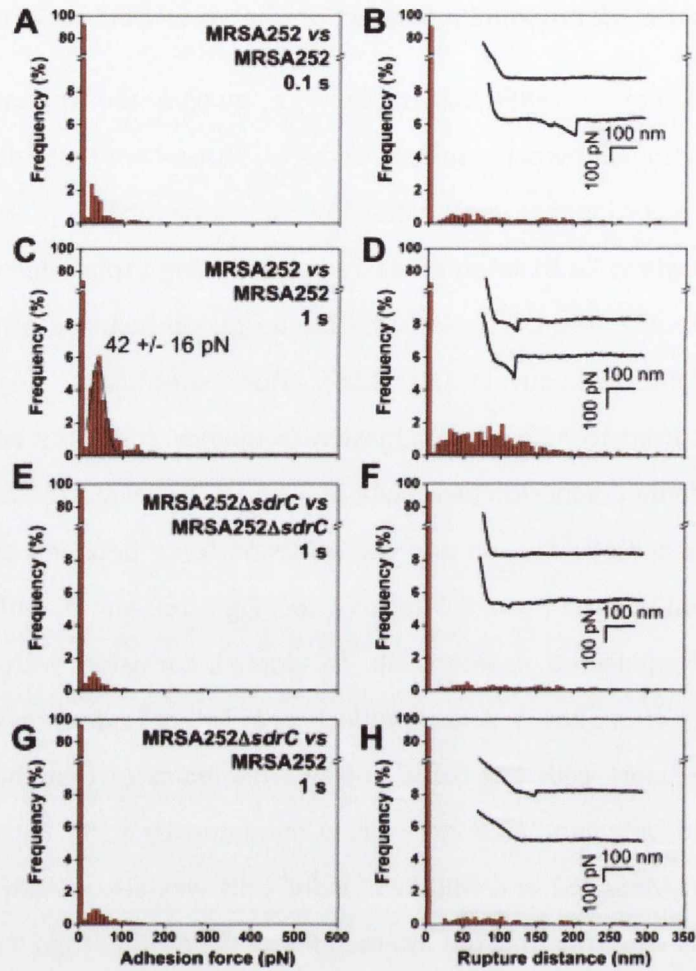


FIG 3.16. SdrC homophilic interactions between MRSA252 cells. (A and C) Adhesion force and (B and D) rupture distance histograms obtained at 100 ms (A and B) or 1 s (C and D) contact time in PBS buffer for six cell pairs of MRSA252. Results obtained at 1 s for six cell pairs of MRSA252Δ*sdrC* (E and F) and for six pairs of MRSA252 and MRSA252Δ*sdrC* cells (G and H). (Insets) Representative force signatures. All curves were obtained using an applied force of 250 pN and an approach and retraction speed of 1.0 μm/s. AFM experiments were carried out by Cécile Feuillie and Cécile Formosa-Dague at the Institute of Life Sciences, Université Catholique de Louvain.

3.2.14 Assessment of SdrC inhibitors for inhibition of MRSA252 biofilm

This study identified six small molecules and a peptide which inhibit SdrC-mediated biofilm using the surrogate host *L. lactis*. SdrC promotes biofilm formation in the HA-MRSA strain MRSA252. Thus, the small molecules and peptide were assessed for their ability to inhibit biofilm formed by MRSA252 (Fig 3.17). The small molecule LH4 and the peptide were found to significantly reduce MRSA252 biofilm (Fig 3.17). Small molecules LH1, LH3, LH6 and LH7 did not affect MRSA252 biofilm (Fig 3.17). LH10 had significant effects on growth at the concentration tested in this assay and thus, is not shown here. LH10 was further assessed for inhibition of MRSA252 biofilm at lower concentrations (Fig 3.18).

In order to assess if LH10 inhibited SdrC-mediated biofilm at sub growth inhibitory concentrations, growth curves and biofilm assays with MRSA252 in the presence of LH10 over a range of concentrations were carried out (Fig 3.18A and B). LH10 inhibited MRSA252 growth at 50 μ M but had only a minor effect on growth at 25 μ M and did not inhibit growth at concentrations lower than 25 μ M (Fig 3.18A). However, LH10 inhibited MRSA252 biofilm at all concentrations tested except 1.5 μ M (Fig 3.18B). These data indicate that LH10 inhibits MRSA252 biofilm and, only at higher concentrations, is also growth inhibitory.

LH4 inhibits MRSA252 biofilm formation (Fig 3.17). As LH4 caused some growth inhibition of *L. lactis* at 50 μ M, it was important to assess if LH4 inhibits MRSA252 growth in order to assess if it is an anti-biofilm inhibitor or affecting growth. Growth curves and biofilm assays of MRSA252 in the presence of LH4 over a range of concentrations were carried out (Fig 3.18C and D). LH4 had minor effects on growth of MRSA252 at concentrations of 50 μ M and 25 μ M with no growth inhibition occurring at concentrations lower than this (Fig 3.18C). However, LH4 inhibited MRSA252 biofilm at all concentrations tested except 1.5 μ M (Fig 3.18D). These data indicate that LH4 has little to no effect on MRSA252 growth but is a potent anti-biofilm inhibitor. From these data, three SdrC inhibitors, the two small molecules, LH4 and LH10, and the β -neurexin derived peptide significantly inhibited MRSA252 biofilm.

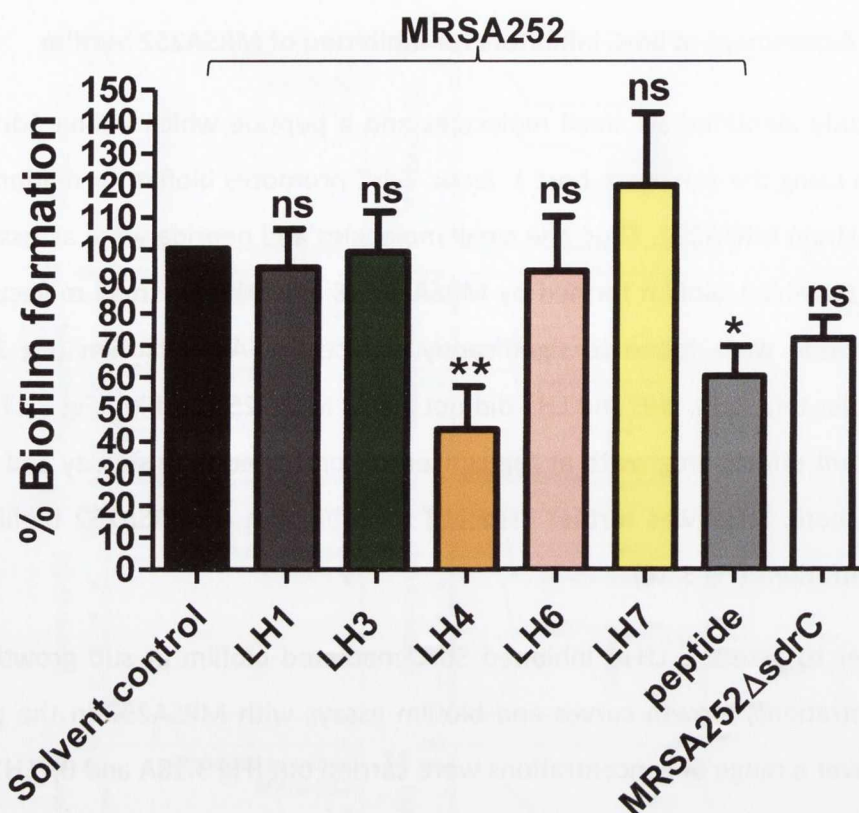


FIG 3.17. Assessment of inhibition of MRSA252 biofilm. MRSA252 biofilm was allowed to develop at 37 °C for 24 h in the presence of small molecules LH1, LH3, LH4, LH6 and LH7 (50 μM), the β-neurexin derived peptide (12.5 μM) or the relevant solvent (solvent control). MRSA252ΔsdrC was included to show the level of biofilm formed without SdrC expressed. Biofilm was stained with crystal violet and A_{570nm} values measured. Values were normalised as % biofilm formation relative to the MRSA252 solvent control as 100 %. Values are the mean of at least three independent experiments. Error bars represent SEM. *P*-values were calculated with values compared to the MRSA252 solvent control in each assay using a one-way ANOVA where * and ** represent *p*-values of ≤0.05 and ≤0.01, respectively and a *p*-value >0.05 is considered not significant (ns).

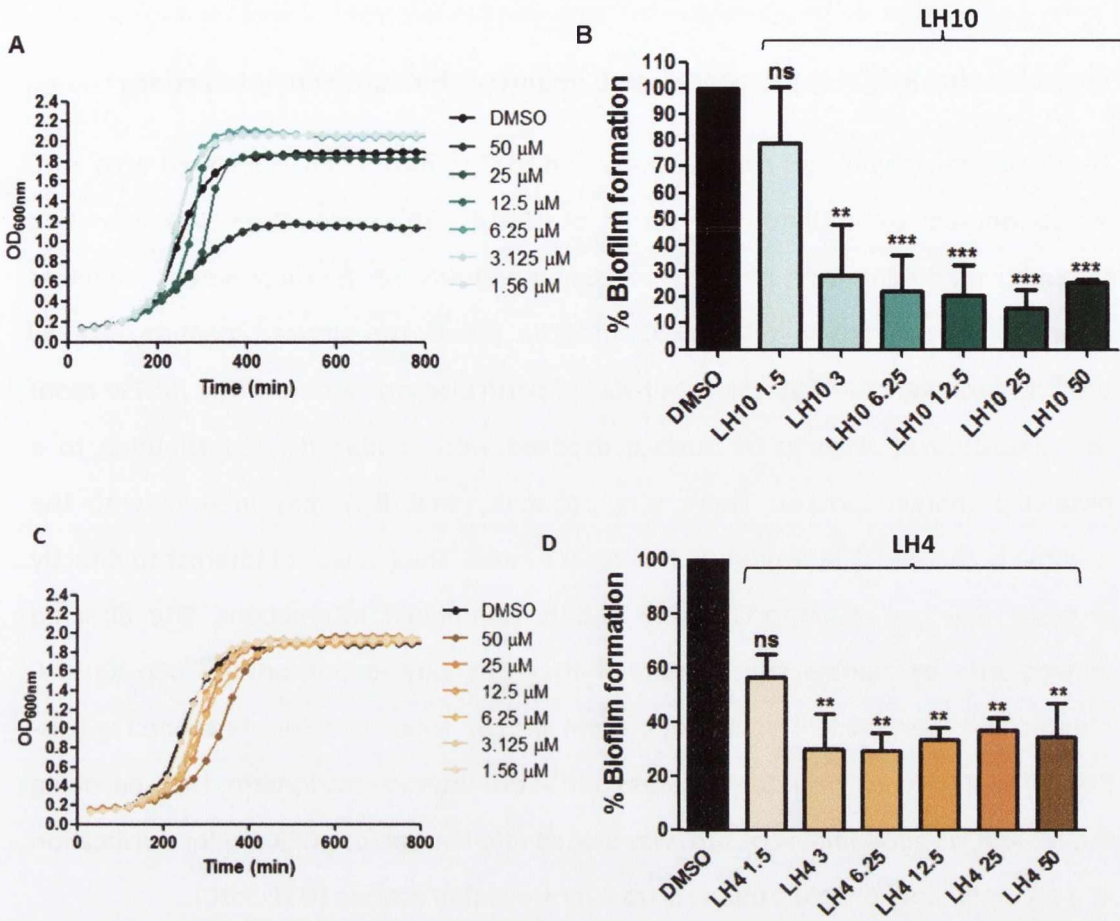


FIG 3.18. Assessment of LH4 and LH10 for inhibition of MRSA252 growth and biofilm.

A and C) MRSA252 was grown for 18 h at 37 °C shaking in the presence of varying concentrations of LH4 and LH10 (1.56 μM –50 μM) or DMSO. OD_{600nm} values were measured at 30 min intervals. Growth curves are representative of three independent experiments. B and D) MRSA252 biofilm was allowed to develop for 24 h at 37 °C statically in the presence of LH4 and LH10 at varying concentrations (1.56 μM – 50 μM) or DMSO. Biofilm was stained with crystal violet and A_{570nm} values measured. A_{570nm} values are normalised as % biofilm formation relative to MRSA252 with DMSO as 100 %. Values are the mean of three independent experiments. Error bars represent SEM. *P*-values were calculated using a one-way ANOVA where values were compared to the DMSO control and ** and *** represent *p*-values of ≤0.01 and ≤0.001, respectively.

3.2.15 Residue R₂₄₇ of the RPGSV motif is important for SdrC-SdrC interactions

The pentamer amino acid motifs RPGSV and VDQYT have been associated with SdrC N2 subdomain dimerization (Barbu *et al.*, 2014). This association was identified through experiments with phage expressing the motifs. As the most potent inhibitors identified in this study; LH4, LH10 and the β -neurexin derived peptide, are all predicted to bind at RPGSV this motif was of particular interest here. The RPGSV motif was predicted *in silico* to be surface exposed with residue R₂₄₇ contributing to a positively charged pocket. There is a possibility that R₂₄₇ may interact with the negatively charged D₂₈₉ residue of the VDQYT motif. Thus, it was of interest to directly assess if R₂₄₇ has an important role in SdrC homophilic interactions. Site directed mutagenesis by alanine substitution of R₂₄₇ was carried out on the pQE30::*sdrC* plasmid and the SdrC R247A variant protein with an N-terminal hexahistidine tag (His-R247A) was purified. In order to assess SdrC-SdrC interactions *in vitro*, DNA encoding the N2 and N3 subdomains of *sdrC* was cloned into the vector pGEX-KG for purification of a recombinant SdrC glutathione S-transferase fusion protein (GST-SdrC).

His-R247A protein was initially screened for the ability to form SdrC-SdrC homophilic interactions by a ligand affinity dot blot (Fig 3.19A) where recombinant His-tagged native SdrC (His-SdrC) and His-R247A proteins were immobilised onto a membrane and binding of GST-SdrC to each protein was compared. GST-SdrC bound His-SdrC in a dose-dependent manner (Fig 3.19A). There was a significant reduction in binding of GST-SdrC to His-R247A with only a very faint level of binding detected at the highest concentrations of His-R247A. This indicated that residue R₂₄₇ is involved in SdrC homophilic interactions. To confirm a similar concentration of each protein was being immobilised onto the membrane loading controls were carried out (Fig 3.19B).

The importance of residue R₂₄₇ in SdrC-SdrC interactions was further explored in a more sensitive manner by an enzyme linked immunosorbent assay (ELISA). Binding of His-SdrC and His-R247A proteins to immobilised GST-SdrC was compared (Fig 3.19C). There was a significant reduction in binding of GST-SdrC by His-R247A in comparison to His-SdrC (Fig 3.19C). These data confirmed that residue R₂₄₇ of the RPGSV motif is important in the formation of SdrC-SdrC interactions.

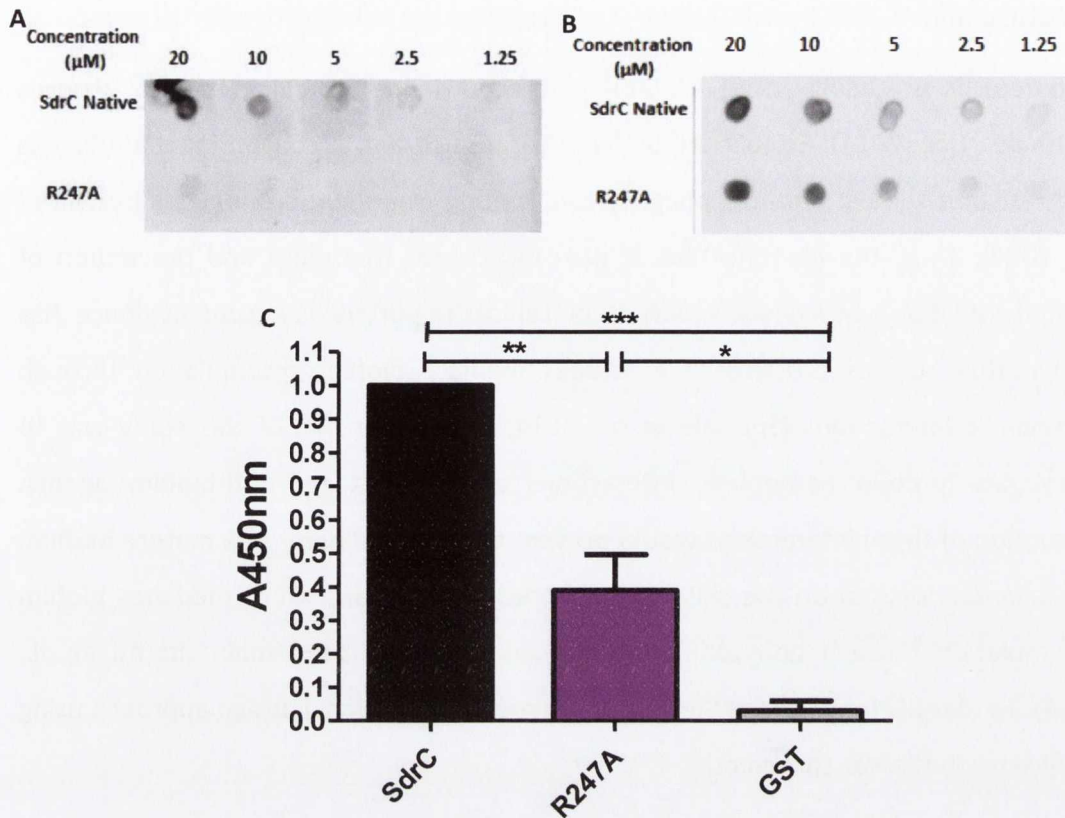


FIG 3.19. Residue R₂₄₇ is important for SdrC homophilic interactions. A) Binding of recombinant GST-SdrC to immobilised His-SdrC native and His-R247A proteins. Recombinant His-SdrC native and His-R247A proteins were immobilised in doubling dilutions onto a nitrocellulose membrane. GST-SdrC was added to the membranes for 1 h at room temperature with shaking. GST-SdrC binding to the immobilised proteins was detected with monoclonal mouse anti-GST IgG followed by HRP-conjugated rabbit anti-mouse IgG. B) Loading controls for His-SdrC and His-R247A proteins. Recombinant His-SdrC native and His-R247A proteins were immobilised in doubling dilutions onto a nitrocellulose membrane. The immobilised His-tagged proteins were detected with monoclonal mouse anti-His IgG followed by HRP-conjugated rabbit anti-mouse IgG. C) Assessment of His-SdrC and His-R247A binding GST-SdrC by ELISA. Wells of a microtitre plate were coated with recombinant GST-SdrC (1 μM). Recombinant His-SdrC and His-R247A proteins (5 μM) were added for 2 h at room temperature. Bound protein was detected with monoclonal mouse anti-His IgG followed by HRP-conjugated rabbit anti-mouse IgG. Binding of His-SdrC to GST (1 μM) only coated wells was included to measure background levels of binding (labelled 'GST' on graph). Values are expressed relative to the A_{450nm} reading for His-SdrC as 1.0. Values are the mean of three independent experiments. Error bars represent SEM. *P*-values were calculated using a one-way ANOVA where all values were compared and *, ** and *** represent *p*-values of ≤0.05, ≤0.01 and ≤0.001, respectively.

3.3 Discussion

S. aureus is a leading cause of biofilm infections on indwelling medical devices (Speziale *et al.*, 2014). Established biofilms are recalcitrant to conventional antibiotics and resistant to host immune phagocytosis limiting treatment strategies (Speziale *et al.*, 2014). Thus, the identification of new targets for treatment and prevention of biofilm infections and novel agents is of clinical importance. Recent evidence has shown that surface proteins of *S. aureus* mediate biofilm accumulation through homophilic interactions (Speziale *et al.*, 2014). The major aim of this study was to investigate protein homophilic interactions as a target for anti-biofilm agents. Disruption of these interactions would prevent the establishment of a mature biofilm. This chapter focused on the cell wall-anchored protein SdrC which mediates biofilm accumulation through homophilic interactions of its N2 subdomain (Barbu *et al.*, 2014). To identify inhibitors of SdrC-SdrC interactions, a rational design approach using *in silico* methods was carried out.

In order to screen small molecule libraries *in silico*, a structure for the target protein is required. As there is no crystal structure of SdrC, this study generated homology models of SdrC N2N3 subdomains (Fig 3.3). To increase the reliability of the models, homology models were generated using two separate programs; I-TASSER (Yang *et al.*, 2015) and Phyre² (Kelley *et al.*, 2015) using the SdrC N2N3 amino acid sequence as the input. The models generated by both programs were predominantly based on other members of the MSCRAMM family of cell wall-anchored proteins with the models consisting of two IgG-like folded N2 and N3 subdomains separated by a trench (Fig 3.3). These results gave confidence in the models. Crystal structures of the N2N3 subdomains of six members of the MSCRAMM family have been resolved to date and they all adopt this general structure (Ponnuraj *et al.*, 2003, Stemberk *et al.*, 2014, Wang *et al.*, 2013, Zhang *et al.*, 2017, Ganesh *et al.*, 2008, Ganesh *et al.*, 2011). Thus, it is likely that SdrC N2N3 subdomains would adopt the same folds.

More specifically, I-TASSER generated a model based on SdrG, an MSCRAMM in *S. epidermidis*, in its ligand bound form (Fig 3.3A) and the top hit in Phyre² was generated based on ClfA in its apo form (Fig 3.3B). To confirm the high level of structural

similarity between these two models generated by separate programs, an overlay of the two models was generated using the molecular structures visualization and analysis program, Chimera (Pettersen *et al.*, 2004). The root mean square deviation (RMSD) between the models was found to be 1.038 Å highlighting their similarity. The sequence identity between SdrC and both ClfA and SdrG is relatively low, ~20-30 % (Foster *et al.*, 2014). However, many sequences with a low identity can have very similar structures due to the limited number of protein folds found in nature. The MSCRAMM family are an example of this. MSCRAMMs do not share a high level of sequence identity within their N2N3 subdomains but their structure is well conserved (Foster *et al.*, 2014). Furthermore, it is common for Phyre² to generate accurate homology models where the sequence identity range is 15-25 % (Kelley *et al.*, 2015).

Two pentamer motifs of amino acid sequence RPGSV and VDQYT of subdomain N2 had previously been postulated to be the dimerization sites within SdrC based on recombinant SdrC binding bacteriophage expressing these motifs and the inhibition of SdrC-SdrC interactions through display of these sequences on bacteriophage (Barbu *et al.*, 2014). The RPGSV and VDQYT motifs are located in the same regions on all the SdrC homology models generated based on MSCRAMMs by both programs (Fig 3.3, Table 3.1). This gave confidence in their predicted location and allowed a rational screening approach with specified target sites. Two small molecule libraries were docked *in silico* at these motifs to screen for putative inhibitors of SdrC.

The *in silico* screening was followed by *in vitro* analyses of selected putative inhibitors. Several small molecules were identified which bound recombinant SdrC (rSdrC; Fig 3.6) and inhibited SdrC-mediated biofilm in the surrogate host *L. lactis* (Fig 3.9) with little or no effect on bacterial growth (Fig 3.10). This indicated success of the screening approach used here and small molecules LH3, LH4, LH6, LH7 and LH10 were identified as lead inhibitors. As DSF is a relatively crude technique, the measurement of the binding affinity of small molecules to SdrC could be measured by Isothermal Titration Calorimetry or ligand-observed nuclear magnetic resonance (Mashalidis *et al.*, 2013). It is possible that some small molecules binding rSdrC such as LH3 may have been overlooked due to inherent drawbacks of using DSF. If binding does not infer a stabilisation of the protein structure then no melting temperature change will occur.

The success of the screen gives confidence in the docking sites of the small molecules. However, to confirm the binding sites of the lead inhibitors, experimental validation would be required. The binding affinity of the lead inhibitors to rSdrC variant proteins with single amino acid changes in residues of the RPGSV and VDQYT motifs could be compared to that of the native protein. X-ray crystallography could also be used to accurately determine the binding site of small molecules in complex with SdrC through the resolution of crystal structures of the complexes.

Following the identification of SdrC biofilm inhibitors it was essential to assess if they could inhibit SdrC biofilm formed by a clinically relevant *S. aureus* strain. Here, for the first time, SdrC was found to mediate biofilm accumulation in a clinically relevant strain of *S. aureus*. SdrC promoted biofilm formation in the HA-MRSA clinical isolate MRSA252 (Fig 3.15), a representative of the highly successful and widely disseminated EMRSA-16 clone (Holden *et al.*, 2004). An MRSA252 *sdrC* deletion mutant (MRSA252 Δ *sdrC*) had a reduced ability to form biofilm (Fig 3.15). MRSA252 Δ *sdrC* still formed some biofilm, albeit at a lower level which is likely due to the fact that *S. aureus* biofilm is a multifactorial process (Speziale *et al.*, 2014). Furthermore, AFM experiments showed that adjacent MRSA252 cells adhere through specific SdrC homophilic interactions (Fig 3.16) supporting a role for SdrC in biofilm accumulation in this HA-MRSA strain.

Of the SdrC lead inhibitors initially identified, LH4 and LH10 significantly inhibited biofilm formed by the HA-MRSA strain MRSA252 (Fig 3.18). LH3, LH6 and LH7 did not reduce biofilm formed by MRSA252 (Fig 3.17). However, they inhibited biofilm mediated solely by SdrC using the surrogate host *L. lactis* although complete inhibition was not observed (Fig 3.9). It is possible that the effect of these inhibitors on SdrC may be masked in MRSA252 biofilm due to the multifactorial nature of this biofilm. Another factor may have compensated for the partial inhibition of SdrC inferred by these small molecules. In contrast, in the *L. lactis* system the biofilm is solely mediated by SdrC so partial inhibition is easily measured. It is also likely that considerably more SdrC protein is expressed on the surface of *L. lactis* cells than on *S. aureus* MRSA252 cells in this study. In the *L. lactis* system *sdrC* is constitutively expressed on the plasmid pKS80 whereas in *S. aureus* *sdrC* expression is likely to be dependent on the growth

phase of the bacteria and experimental conditions. For example, cell wall-anchored SdrC was previously found on the surface of MRSA252 cells during exponential growth but not on cells in stationary phase (Barbu *et al.*, 2010). Aside from MRSA252 in this study, in general, *sdrC* expression is likely to vary among *S. aureus* strains. Furthermore, in the *L. lactis* system the cell wall is largely available for SdrC expression whereas in *S. aureus* cells other factors will also be expressed on the cell wall and thus, there are spatial limitations to the expression levels of SdrC in *S. aureus*. Thus, the level of SdrC on the cell wall of *S. aureus* will be saturated with less protein molecules than on the *L. lactis* surface. These differences in SdrC expression were evident in AFM studies where forces of SdrC-SdrC interactions between *L. lactis* SdrC⁺ cells were considerably higher than those between MRSA252 cells (Feuillie *et al.*, 2017). These forces were indicative of multiple SdrC-SdrC interactions between *L. lactis* SdrC⁺ cells but only single SdrC-SdrC interactions between MRSA252 cells.

This study also demonstrated that a peptide derived from human β -neurexin protein could inhibit SdrC-mediated biofilm (Fig 3.9). β -neurexin protein was previously found to be a ligand for SdrC but the type of interaction or binding site on SdrC was unknown (Barbu *et al.*, 2010). It was of interest to predict the binding site of this peptide using *in silico* docking to SdrC. The peptide was predicted to dock at a site overlapping the RPGSV motif associated with SdrC-SdrC interactions (Fig 3.7). This raised the possibility that the peptide may inhibit SdrC homophilic interactions and biofilm accumulation. The peptide was found to be a potent inhibitor of SdrC-mediated biofilm abolishing SdrC biofilm in the surrogate host *L. lactis* (Fig 3.9) and reducing MRSA252 biofilm to a similar level of biofilm to MRSA252 Δ *sdrC* (Fig 3.13). This again demonstrated the ability to prevent biofilm through targeting and disrupting protein homophilic interactions.

Two small molecules LH12 and LH13 were found to inhibit the growth of *L. lactis* and, in the case of LH12, growth of the HA-MRSA strain BH1CC (data not shown). As this study was looking for anti-biofilm agents and not antibacterial agents these inhibitors were not pursued further here. It is worth noting, however, that neither inhibitor contains any well documented antibacterial chemical structures (McDonnell & Russell, 1999). A recent study by Van Voorhis *et al.*, (2016), also reported *S. aureus* growth

inhibition by both small molecules. In the aforementioned study, these small molecules were also assessed for inhibition of other Gram-positive and Gram-negative bacteria. They did not observe growth inhibition of *Streptococcus pneumoniae*, *Streptococcus suis* or Gram-negative bacteria *Escherichia coli*, *Klebsiella pneumoniae*, *Pseudomonas aeruginosa*, *Salmonella typhimurium* and *Acinetobacter baumannii*. However, LH13 was found to inhibit several mycobacterial species. The target of these small molecules is unknown. Perhaps the limited spectrum of bacteria they inhibit may indicate that the target is specific to *S. aureus* and *L. lactis* and is not conserved or accessible among all Gram-positive bacteria and is not present in Gram-negative bacteria.

The identification of several inhibitors of SdrC-mediated biofilm through targeting of the RPGSV and VDQYT motifs in this study further supports these motifs as dimerization sites of SdrC. In this study, we also directly confirmed that residue R₂₄₇ is important for SdrC-SdrC interactions (Fig 3.19). However, the type of interaction(s) occurring between the RPGSV and VDQYT binding sites remains unclear. There are several possibilities. The equivalent motifs on adjacent proteins could interact, or the RPGSV of SdrC on one cell may interact with VDQYT of SdrC on another cell or there could be more than two binding sites. It is worth noting that residue R₂₄₇ of RPGSV is positively charged and residue D₂₈₉ of VDQYT is negatively charged with each motif predicted to partially contribute to a charged pocket *in silico* (Fig 3.4). This allows for a hypothesis that the sites may interact based on charge. The abolishment of biofilm in the presence of the β -neurexin derived peptide (Fig 3.9), predicted to bind at the RPGSV motif, may indirectly suggest that blocking one site is sufficient for reducing SdrC biofilm. This would support the hypothesis of an interaction between RPGSV and VDQYT. However, that is based on the assumption that the predicted peptide binding site is at the RPGSV motif and that the peptide has a single binding site. Overall, experimental evidence would be required to validate the type of SdrC-SdrC binding interaction occurring. A crystal structure of the dimer would provide this information. Biochemical studies altering the charge at either site, from positive to negative and *vice versa*, may address whether charge is important in the interaction. However, such alterations would have a risk of affecting the overall protein structure.

In conclusion, this study further characterised SdrC-mediated biofilm and identified novel inhibitors of SdrC biofilm. The lead SdrC inhibitors identified here may serve as scaffolds for further drug design. As the leads are small molecules, other chemical moieties may be added to increase their size and potency. A detailed structure-activity relationships (SARs) analysis followed by *in vitro* testing would allow a thorough investigation of the substructures mediating the observed inhibition. This approach would allow the development of a larger, more potent drug-like molecule. This study also demonstrated, for the first time, that protein homophilic interactions are an attractive target for prevention of biofilm formation and the development of anti-biofilm agents.

Chapter 4

Characterisation of fibronectin binding protein interactions in biofilm and identification of anti-biofilm molecules which target fibronectin binding proteins

4.1 Introduction

The cell wall-anchored FnBPA and B proteins are likely to be of particular clinical importance as mediators of protein-dependent biofilm accumulation. FnBPs mediate biofilm in CC8 and CC22 lineages of hospital associated (HA)- and community associated (CA)-MRSA strains *in vitro* (O'Neill *et al.*, 2008, McCourt *et al.*, 2014, Planet *et al.*, 2013, Mashruwala *et al.*, 2017). FnBP-mediated biofilm may be important in colonisation of skin (Planet *et al.*, 2013) and in biofilm infections occurring under fermentative conditions (Mashruwala *et al.*, 2017). Furthermore, FnBPs were also shown to promote *S. aureus* infection of a mouse catheter *in vivo* (Vergara-Irigaray *et al.*, 2009). Thus, FnBPs represent an attractive target for anti-biofilm therapy but this approach has yet to be explored. To mediate biofilm FnBPA proteins on neighbouring bacteria form homophilic interactions through their N2N3 subdomains (Herman-Bausier *et al.*, 2015). FnBPB homophilic interactions have yet to be demonstrated. FnBPs are members of the MSCRAMM family of *S. aureus* cell wall-anchored proteins (Fig 4.1A) (Foster *et al.*, 2014) and a crystal structure of FnBPA subdomains N2 and N3 has been solved showing the characteristic IgG-like folded N2 and N3 with a hydrophobic trench separating the subdomains (Fig 4.1B) (Stemberk *et al.*, 2014). Many *S. aureus* biofilm-forming strains express both FnBPA and FnBPB (O'Neill *et al.*, 2008, McCourt *et al.*, 2014). These proteins share only 50 % amino acid identity in their N2N3 subdomains. Whether FnBPA and FnBPB can interact in a heterophilic manner has not been explored.

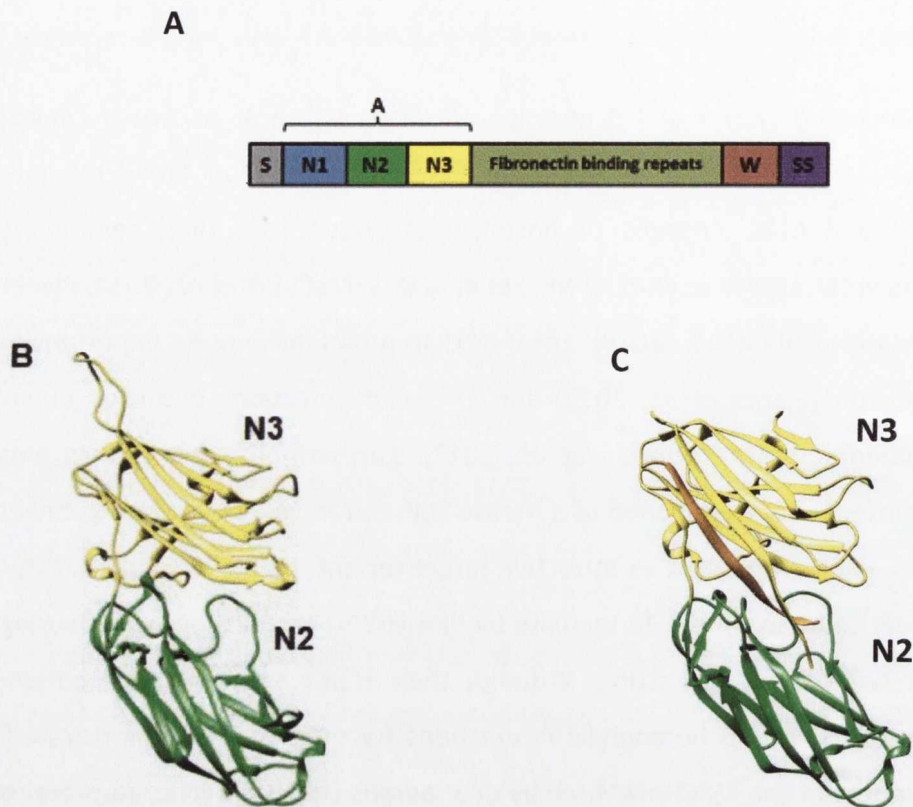


FIG 4.1 Domain organization of FnBPs. A) Schematic representation of FnBPA and FnBPB. The N-terminal signal sequence (S) is followed by the A domain which consists of three subdomains; N1, N2 and N3. This is followed by a long unstructured repeat region composed of fibronectin binding repeats, a cell wall spanning domain (W) and a sorting signal (SS). B) Crystal structure of FnBPA N2N3 in its apo form. The structure of FnBPAN2N3 was obtained from the Protein Data Bank (PDB ID=4B5Z) and visualised on Chimera. FnBPA N2N3 is shown in ribbon with subdomains N2 and N3 coloured green and yellow, respectively. C) Crystal structure of the FnBPA-fibrinogen peptide complex. The structure of the FnBPA-fibrinogen peptide complex was obtained from the Protein Data Bank (PDB ID=4B60) and visualised on Chimera. FnBPA N2N3 and the fibrinogen γ -chain peptide are shown in ribbon with FnBPA subdomains N2 and N3 coloured green and yellow, respectively and the peptide coloured orange.

The N2 and N3 subdomains of FnBPA and FnBPB also mediate *S. aureus* adherence to the host proteins fibrinogen (Keane *et al.*, 2007, Wann *et al.*, 2000, Burke *et al.*, 2010), elastin (Roche *et al.*, 2004, Keane *et al.*, 2007) and plasminogen (Pietrocola *et al.*, 2016). FnBPB N2N3 subdomains can also bind fibronectin although the mechanism of binding differs from that of the fibronectin binding repeats (Burke *et al.*, 2011). The crystal structure of FnBPA in complex with a peptide corresponding to its binding site on fibrinogen; the γ -chain, has been solved (Stemberk *et al.*, 2014) (Fig 4.1C). In the structure, the peptide is docked in the ligand binding trench between the N2 and N3 subdomains and is locked in place by interactions between FnBPA N2 and N3 subdomains (Stemberk *et al.*, 2014). Notably, indwelling devices can become coated with host plasma proteins including fibrinogen. Under these circumstances *S. aureus* adherence to fibrinogen can promote primary attachment of bacteria to the device (Speziale *et al.*, 2014, Otto, 2008). This attachment to a biotic surface is an initial step in biofilm formation. Binding of fibrinogen and fibrin by the cell-wall anchored proteins FnBPA, FnBPB, ClfA and ClfB also promotes fibrin-dependent biofilms which are associated with infections of indwelling catheters (Vanassche *et al.*, 2013, Zapotoczna *et al.*, 2015) and joints (Dastgheyb *et al.*, 2015).

Although FnBPA and FnBPB ligand binding and FnBPA-mediated biofilm accumulation have been localised to subdomains N2 and N3, FnBPA-mediated adherence to fibrinogen and biofilm formation occur through distinct mechanisms (Geoghegan *et al.*, 2013, O'Neill *et al.*, 2008). Several residues of FnBPA, including residue N304, are critical to fibrinogen binding (Keane *et al.*, 2007). Alanine substitution of N304 abolished the ability of FnBPA to bind fibrinogen (Keane *et al.*, 2007) but did not reduce the ability of FnBPA to mediate biofilm (O'Neill *et al.*, 2008). Deletion of the lock and latch region of FnBPA was also shown to abolish the ability of bacteria expressing FnBPA to adhere to fibrinogen but had no effect on its ability to mediate biofilm (Geoghegan *et al.*, 2013). Furthermore, addition of the fibrinogen γ -chain peptide which inhibits the ability of FnBPA to bind fibrinogen (Keane *et al.*, 2007) did not inhibit FnBPA-mediated biofilm and chelation of zinc, which inhibits FnBP-mediated biofilm, had no effect on fibrinogen binding by FnBPA (Geoghegan *et al.*, 2013).

Interestingly, the N2 and N3 subdomains of both FnBPA and FnBPB vary considerably in their amino acid sequence, with seven isotypes of each protein identified to date (Loughman *et al.*, 2008, Burke *et al.*, 2010). Despite this amino acid variation, all isotypes of FnBPA and FnBPB have been shown to bind their ligands fibrinogen and elastin with similar affinity (Loughman *et al.*, 2008, Burke *et al.*, 2010). All isotypes of FnBPB have also been shown to bind plasminogen with similar affinity but only isotype I of FnBPA binding plasminogen has been assessed to date (Pietrocola *et al.*, 2016). In contrast, only the ability of isotypes I of FnBPA and FnBPB to promote biofilm formation has been assessed (O'Neill *et al.*, 2008).

This study aimed to further our understanding of the mechanisms of FnBP-mediated biofilm accumulation and to evaluate FnBPs as a novel target for anti-biofilm inhibitors.

4.2 Results

4.2.1 FnBPA homophilic interactions are mediated by subdomain N2.

FnBPA mediates biofilm accumulation through homophilic interactions which have been localised to subdomains N2N3 but subdomain N1 and the fibronectin binding repeats are not involved (Geoghegan *et al.*, 2013). This study set out to further localise the region(s) of FnBPA involved in mediating FnBPA-FnBPA interactions and biofilm accumulation. An ELISA was established to study these FnBPA interactions *in vitro* (Fig 4.2). Binding of recombinant FnBPA_{N2N3} protein with an N-terminal hexahistidine tag (His-FnBPA_{N2N3}) to recombinant GST-tagged FnBPA_{N2N3} protein (GST-FnBPA_{N2N3}) and GST alone was initially assessed (Fig 4.2). His-FnBPA_{N2N3} bound GST-FnBPA_{N2N3} in a dose-dependent manner. His-FnBPA_{N2N3} did not bind GST indicating that the interaction observed between the FnBPA_{N2N3} proteins was specific.

In order to localise the sites involved in FnBPA homophilic interactions, the N2 and N3 subdomains were expressed individually with N-terminal hexahistidine tags (His-FnBPA_{N2} and His-FnBPA_{N3}). The ability of single subdomains to bind to recombinant GST-FnBPA_{N2N3} was compared to His-FnBPA_{N2N3} (Fig 4.3A). Subdomain N2 bound GST-FnBPA_{N2N3} in a dose-dependent manner with similar levels of binding to His-FnBPA_{N2N3}. His-FnBPA_{N3} did not bind GST-FnBPA_{N2N3} at any of the concentrations tested. These data indicate that the N2 subdomain of FnBPA and not the N3 subdomain is important in FnBPA homophilic interactions. To investigate if subdomain N2 binds to N2, His-FnBPA_{N2} and His-FnBPA_{N2N3} binding to GST-FnBPA_{N2} was assessed (Fig 4.3B). Both His-FnBPA_{N2} and His-FnBPA_{N2N3} bound to GST-FnBPA_{N2} in a dose-dependent manner and with a similar binding profile. These data indicate that only the N2 subdomain is required for the formation of FnBPA-FnBPA homophilic interactions, *in vitro*.

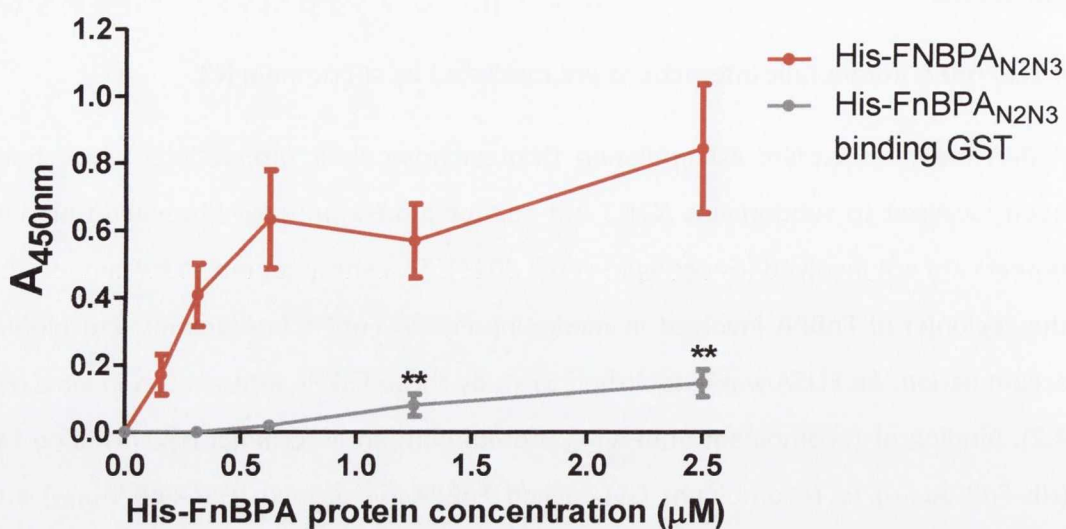


FIG 4.2 ELISA to assess FnBPA-FnBPA interactions *in vitro*. Microtitre wells were coated with GST-FnBPA_{N2N3} or GST (1 μM) and increasing concentrations of His-FnBPA_{N2N3} were added for 2 h at 37 °C. Bound protein was detected with monoclonal mouse anti-His IgG followed by HRP-conjugated rabbit anti-mouse IgG. Values are the mean of 7 independent assays. Error bars represent standard error of the mean (SEM). Binding of His-FnBPA_{N2N3} to GST was significantly reduced compared to His-FnBPA_{N2N3} binding to GST-FnBPA_{N2N3} (**, $P \leq 0.01$).

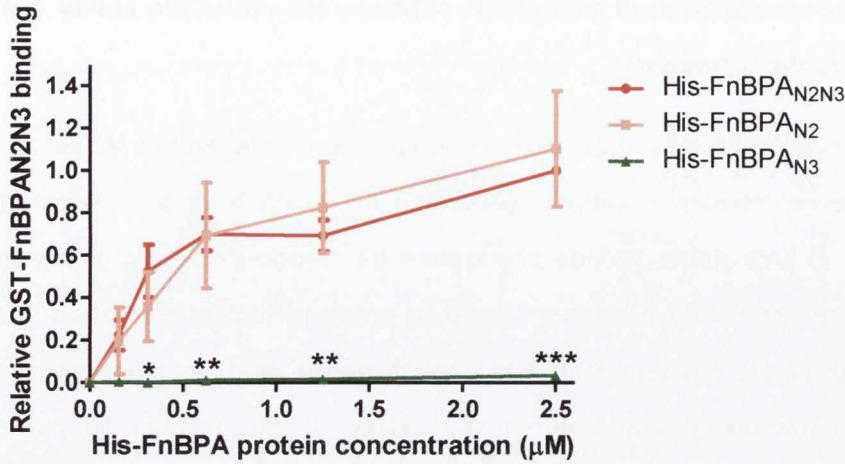
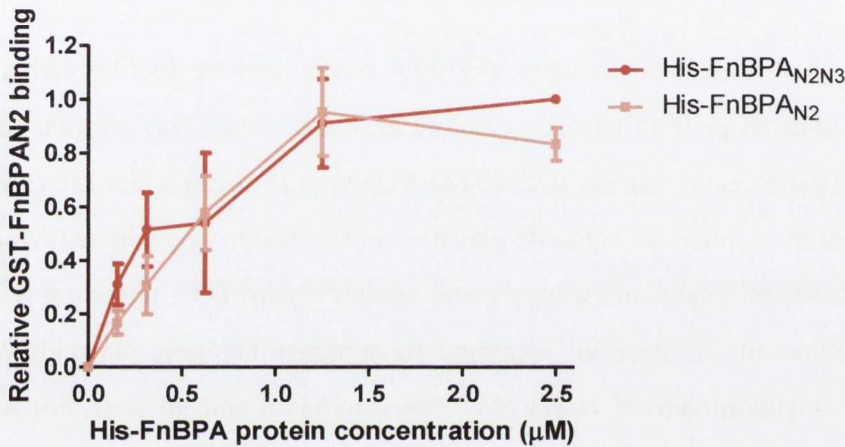
A**B**

FIG 4.3 FnBPA homophilic interactions are mediated by subdomain N2. Microtitre wells were coated with GST-FnBPA_{N2N3} (1 μM; A) or GST-FnBPA_{N2} (6 μM; B) and increasing concentrations of FnBPA subdomain proteins His-FnBPA_{N2N3}, His-FnBPA_{N2} and His-FnBPA_{N3} were added for 2 h at 37 °C. Bound protein was detected with monoclonal mouse anti-His IgG followed by HRP-conjugated rabbit anti-mouse IgG. Values are expressed relative to the A_{450nm} reading measured for the highest concentration of His-FnBPA_{N2N3} (2.5 μM = 1.0). Values are the mean of 4-5 independent assays (A) or 3 independent assays (B). Error bars represent SEM. *P*-values were calculated using a two-way ANOVA with Bonferroni post-test where *, ** and *** represent *p*-values of ≤0.05, ≤0.01 and ≤0.001 (A) and an unpaired Student's *t*-test (B). There was no significant difference between the values measured for His-FnBPA_{N2N3} and His-FnBPA_{N2} binding to GST-FnBPA_{N2N3} or GST-FnBPA_{N2}. Binding of His-FnBPA_{N3} to GST-FnBPA_{N2N3} was significantly reduced compared to His-FnBPA_{N2N3} at all concentrations tested except 0.156 μM.

4.2.2 Sequence variation in subdomain N2 does not affect the ability of FnBPA to promote biofilm formation.

There is considerable amino acid sequence variation in the FnBPA N2 subdomain and seven different sequence variants (isotypes) of FnBPA have been identified which share only 75-84% amino acid identity in their N2 subdomains (Loughman *et al.*, 2008). Only isotype I of FnBPA has been shown to promote biofilm formation in *S. aureus* (Geoghegan *et al.*, 2013, O'Neill *et al.*, 2008). Amino acid sequence variation in the FnBPA N2 subdomain could affect the ability of the protein to participate in homophilic interactions and mediate biofilm formation.

To investigate if sequence variants of FnBPA could mediate biofilm formation, the multicopy plasmid pFnBA4 (Greene *et al.*, 1995) was used. This plasmid carries the entire *fnbA* gene from *S. aureus* strain 8325-4 (isotype I FnBPA) under the control of its own promoter. A series of chimeric plasmids were constructed where DNA encoding the N1N2N3 subdomains of isotype I was replaced with DNA encoding N1N2N3 of FnBPA isotypes III, IV, V or VI. Attempts to generate chimeric plasmids with DNA encoding the subdomains N1N2N3 of FnBPA isotypes II and VII were not successful. While only the N2 subdomain is essential for homophilic FnBPA-FnBPA interactions *in vitro* (Fig 4.3), we included the flanking N1 and N3 subdomains to ensure proper folding and secretion of the chimeric FnBPA proteins. The chimeric plasmids were transformed into the biofilm forming HA-MRSA strain BH1CC. A double *fnbA fnbB* mutant of BH1CC (BH1CC Δ *fnbAfnbB*) does not form biofilm (Geoghegan *et al.*, 2013, O'Neill *et al.*, 2008). Biofilm formation can be restored by complementation of the mutant with pFnBA4 restoring expression of FnBPA isotype I (O'Neill *et al.*, 2008, Geoghegan *et al.*, 2013). To confirm that FnBPA was being expressed from each chimeric plasmid, bacterial adherence to fibronectin was assessed (Fig 4.4A). All strains showed a similar ability to adhere to fibronectin while the mutant did not adhere indicating that an FnBPA protein was expressed on the surface of *S. aureus* from each chimeric plasmid. The ability of the chimeric FnBPA proteins to promote biofilm formation *in vitro* was assessed (Fig 4.4B). All strains were capable of forming biofilm albeit different levels of biofilm were formed by strains expressing different chimeric plasmids. Thus, these data show that FnBPA proteins with isotype I, III, IV, V

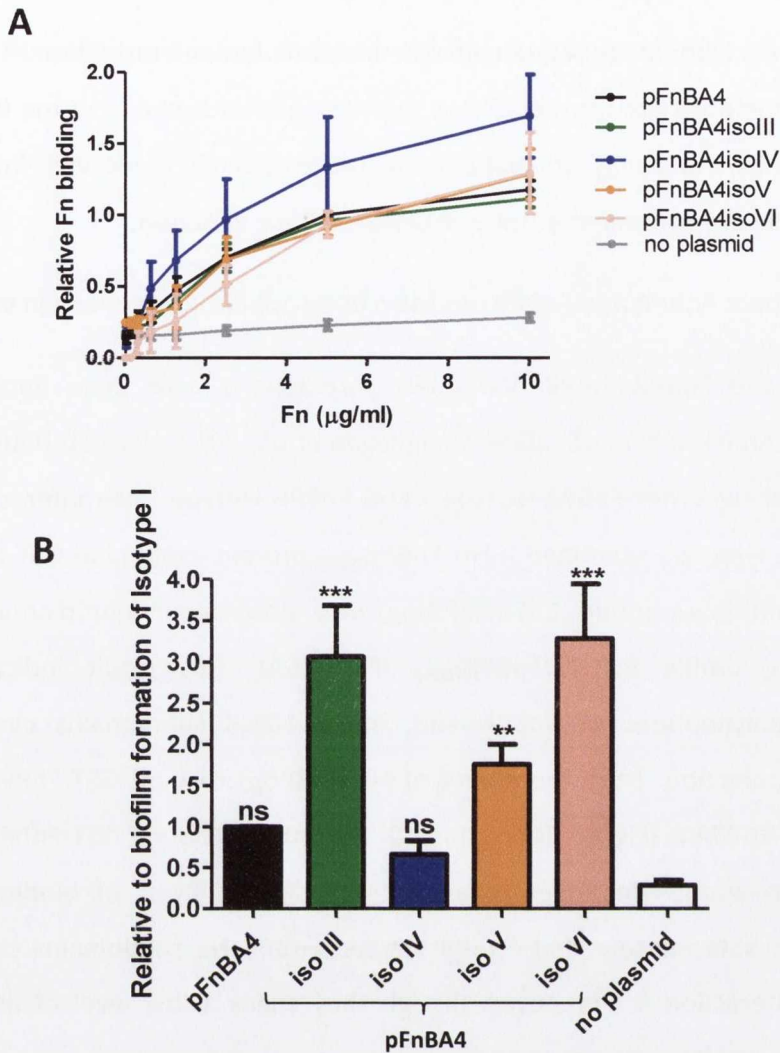


FIG 4.4. Assessment of the ability of BH1CCΔ*fnbAfnbB* (pFnBA4) isotype I, III, IV, V and VI strains to adhere to fibronectin and mediate biofilm accumulation. A) Strains were grown in TSB, supplemented with chloramphenicol (10 µg/ml) where necessary, to exponential phase and added to fibronectin (Fn) coated wells for 2 h at 37 °C. Adherent bacteria were stained with crystal violet and A_{570nm} values were measured. A_{570nm} values are expressed relative to BH1CCΔ*fnbAfnbB* pFnBA4 (isotype I) binding Fn (5 µg/ml value=1.0). Values are the mean of at least 3 independent experiments. Error bars represent SEM. There were no significant differences between any of the five plasmid bearing strains adhering to Fn. B) Overnight cultures were diluted (1:200) in BHI supplemented with D-glucose (10 g/L) and added to tissue-culture treated microtiter plates. Biofilm was allowed to develop for 24 h statically at 37 °C. Biofilm was stained with crystal violet and A_{570nm} values measured. A_{570nm} values are expressed relative to BH1CCΔ*fnbAfnbB* pFnBA4 (isotype I) as 1.0. All values are the mean of at least three independent experiments. Error bars represent SEM. *P*-values were calculated using a one-way ANOVA where ** and *** represent *p*-values ≤0.01 and ≤0.001, respectively.

and VI N1N2N3 subdomain sequences can mediate biofilm formation. This result indicates that the ability to form biofilm is a conserved function across the five FnBPA isotypes tested here and suggests that the residues involved in homophilic interactions in subdomain N2 are conserved despite FnBPA sequence variation.

4.2.3 Recombinant FnBPA and FnBPB can form heterophilic interactions *in vitro*.

FnBPA-FnBPA and FnBPB-FnBPB homophilic interactions have been implicated in biofilm formation (O'Neill *et al.*, 2008, Geoghegan *et al.*, 2013, Herman-Bausier *et al.*, 2015). However, whether FnBPA isotype I and FnBPB isotype I can interact has not been assessed. Here we examined if His-FnBPB_{N2N3} protein could bind GST-FnBPA_{N2N3} *in vitro*. His-FnBPB_{N2N3} bound GST-FnBPA_{N2N3} in a dose-dependent manner with a similar binding profile to His-FnBPA_{N2N3} (Fig 4.5A). This result indicates that recombinant polypeptides of FnBPA and FnBPB N2N3 subdomains can form a heterophilic interaction. Next the ability of His-FnBPB_{N2} to bind GST-FnBPA_{N2N3} (Fig 4.5B) and GST-FnBPA_{N2} (Fig 4.5C) was tested. His-FnBPB_{N2} bound GST-FnBPA_{N2N3} and GST-FnBPA_{N2} in a dose-dependent manner with similar levels of binding to His-FnBPA_{N2}. These data indicate that FnBPA N2 and FnBPB N2 subdomains can form a heterophilic interaction *in vitro* even though they share a low level of amino acid identity (45%).

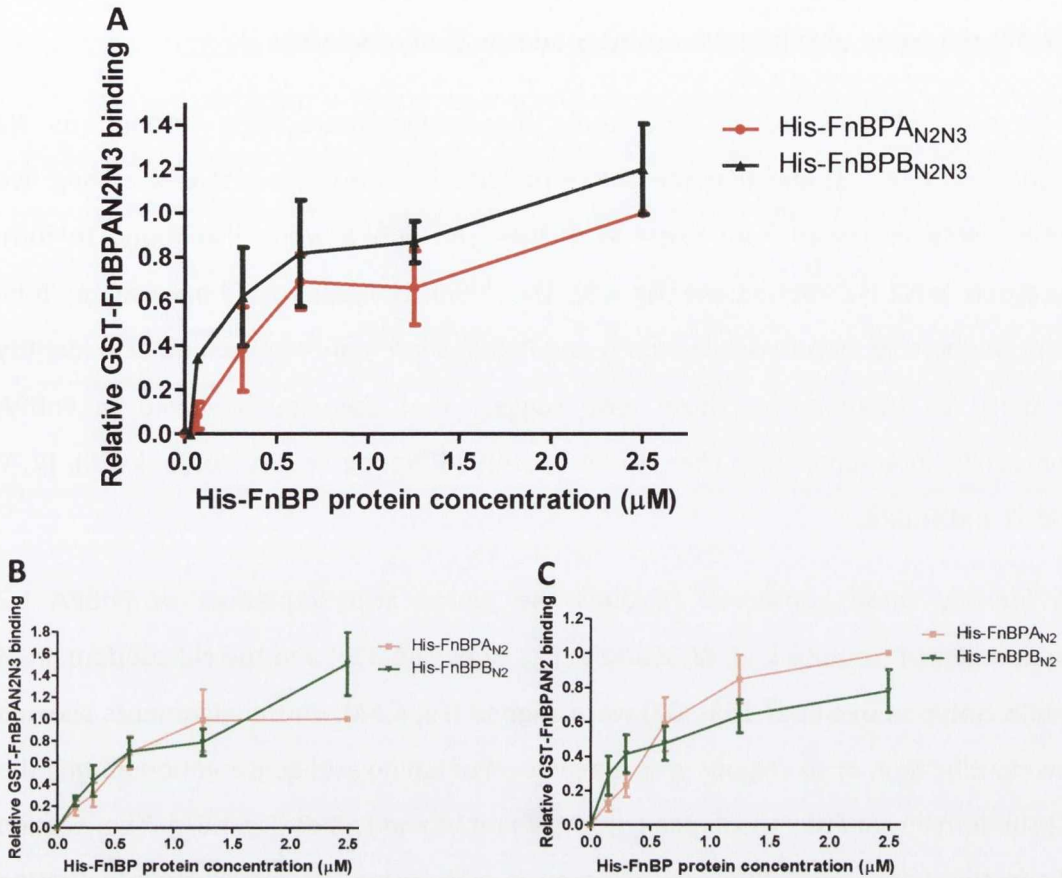


FIG 4.5 Recombinant FnBPA and FnBPB form heterophilic interactions *in vitro*.

Microtitre wells were coated with GST-FnBPA_{N2N3} (1 μM ; A, B) or GST-FnBPA_{N2} (6 μM ; C) and increasing concentrations of His-FnBPB_{N2N3} and His-FnBPA_{N2N3} (A) or His-FnBPB_{N2} and His-FnBPA_{N2} (B, C) were added for 2 h at 37 °C. Bound protein was detected with monoclonal mouse anti-His IgG followed by HRP-conjugated rabbit anti-mouse IgG. Values are the mean of 3 (A) and 4 (B, C) independent assays. Error bars represent SEM. *P*-values were calculated using an unpaired Student's *t*-test. There was no significant difference ($p > 0.05$) between the values measured for His-FnBPB_{N2N3} and His-FnBPA_{N2N3} binding to GST-FnBPA_{N2N3} (A) or between the values measured for His-FnBPB_{N2} and His-FnBPA_{N2} binding GST-FnBPA_{N2N3} (B) and GST-FnBPA_{N2} (C). Values are expressed relative to the $A_{450\text{nm}}$ reading measured for the highest concentration of His-FnBPA_{N2N3} (A) or His-FnBPA_{N2} (B, C) (2.5 μM = 1.0).

4.2.4 Localisation of FnBPA dimerization sites in subdomain N2

This study showed that FnBPA forms homophilic interactions through its N2 subdomain (Fig 4.3) and that the ability to form biofilm was conserved among five FnBPA isotypes tested here (Fig 4.4). FnBPA and FnBPB were also found to form heterophilic N2-N2 interactions (Fig 4.5). The FnBPA isotypes tested here share 75-84 % N2 amino acid identity while FnBPA and FnBPB share only 45 % amino acid identity in their N2 subdomains. These data suggest that the sites involved in FnBPA homophilic interactions are likely to be conserved among FnBPA isotypes I, III, IV, V and VI and FnBPB.

To identify these conserved residues the amino acid sequences of FnBPA N2 subdomains of isotypes I, III, IV, V and VI (residues 194-336) and the N2 subdomain of FnBPB isotype I (residues 163-307) were aligned (Fig 4.6A). These alignments allowed the identification of six regions with a high level of amino acid conservation among the N2 subdomains of FnBPA isotypes I, III, IV, V and VI and FnBPB (Fig 4.6A). The location of the six regions on FnBPA was assessed *in silico* using the molecular visualization software Chimera version 1.9 and the crystal structure of FnBPA N2N3 (Pettersen *et al.*, 2004, Stemberk *et al.*, 2014) (Fig 4.6B). From these *in silico* analyses, three regions; termed site 1, site 4 and site 6, were selected for further study as they were highly conserved across all six sequences and are surface exposed sites which could participate in N2-N2 homophilic interactions (Fig 4.6B). Site 4 was of particular interest as it contains the equivalent region to one of the dimerization sites of the MSCRAMM SdrC which also mediates biofilm through N2-N2 interactions (Barbu *et al.*, 2014). The amino acid sequence 'NTHGV' of FnBPA is at the equivalent position to the 'RPGSV' motif of SdrC (Section 3.1).

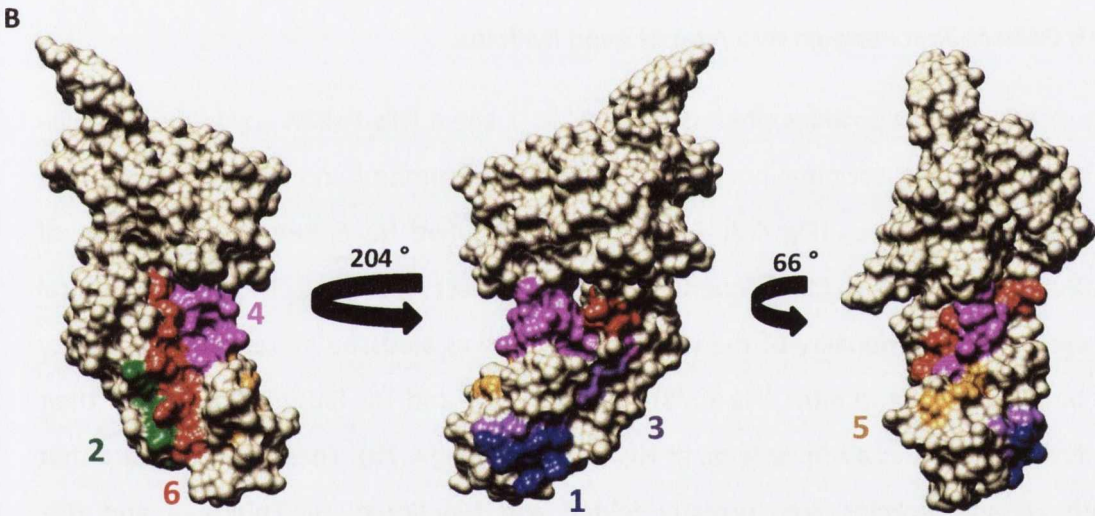


FIG 4.6 *In silico* analyses of conserved amino acids in FnBPA and FnBPB N2. A) Amino acid alignment of the N2 subdomains of FnBPA isotypes (iso) I, III, IV, V and VI and FnBPB isotype I. Amino acid sequences of N2 of FnBPA isotypes I, III, IV, V and VI (residues 194-336) and N2 of FnBPB isotype I (residues 163-307) were aligned using Clustal Omega (Sievers *et al.*, 2011). Conserved residues are highlighted in yellow. Six regions, numbered 1-6, which contain a high level of amino acid conservation were identified. B) The locations of these six regions were visualized on the crystal structure of FnBPAN2N3 (PDB ID=4B5Z) using Chimera version 1.9. FnBPAN2N3 is shown in space filled and each of the six regions coloured separately and labelled 1-6.

Amino acid substitutions were carried out to determine if residues at sites 1, 4 or 6 are important for FnBPA N2 homophilic interactions. DNA encoding sites 1, 4 and 6 of FnBPA N2 was replaced with DNA encoding the equivalent sequence of the N2 subdomain of clumping factor A (ClfA) (Fig 4.7A) on the plasmid pQE30::*fnbA*_{N2N3} resulting in four, six and five residue substitutions, respectively. ClfA was selected as it is also a member of the MSCRAMM family of *S. aureus* surface proteins and the N2N3 subdomains adopt similar folds (Section 1.4.1). ClfA binds the same site on fibrinogen (Fg) as FnBPs; the γ -chain (Ganesh *et al.*, 2008, Deivanayagam *et al.*, 2002). However, it does not mediate biofilm accumulation and recombinant ClfA N2N3 protein does not migrate as a dimer when separated by gel electrophoresis on native gels (Burke FM and Geoghegan JA, unpublished). Thus, residues involved in FnBPA homophilic interactions are unlikely to be conserved in ClfA N2 and replacing the FnBPA motifs with ClfA sequence should retain the N2 and N3 folds.

The FnBPA variant proteins site 1 (His-FnBPA_{Site1}), site 4 (His-FnBPA_{Site4}) and site 6 (His-FnBPA_{Site6}) with N-terminal hexahistidine tags were purified and their ability to bind GST-tagged FnBPA_{N2N3} (Fig 4.7C-E) compared to native His-FnBPA_{N2N3}. Alteration of FnBPA N2 sequence to ClfA sequence should not affect Fg binding. Thus, the structural integrity and functionality of the variant proteins was assessed by testing their ability to bind human Fg *in vitro* (Fig 4.7B). His-FnBPA_{Site1} and His-FnBPA_{Site6} retained their ability to bind Fg at a similar level as His-FnBPA_{N2N3} (Fig 4.7B). These data indicate that both variant proteins are correctly folded and functional. His-FnBPA_{Site1} and His-FnBPA_{Site6} bound GST-FnBPA_{N2N3} in a dose-dependent manner with a similar binding profile as His-FnBPA_{N2N3} (Fig 4.7C,E). These results suggest that the residues altered in these variant proteins are not involved in FnBPA homophilic interactions. His-FnBPA_{Site4} had a reduced ability to bind Fg in comparison to His-FnBPA_{N2N3} (Fig 4.7B). This may indicate that His-FnBPA_{Site4} is not correctly folded or that the Fg binding site has been disrupted. However, His-FnBPA_{Site4} bound GST-FnBPA_{N2N3} in a dose-dependent manner with a similar binding profile to His-FnBPA_{N2N3} (Fig 4.7D). In conclusion, the dimerization sites of FnBPA were not identified when the FnBPA sequence of sites 1 and 6 were replaced with ClfA sequence and it remains unclear if residues at site 4 are important in FnBPA-FnBPA interactions.

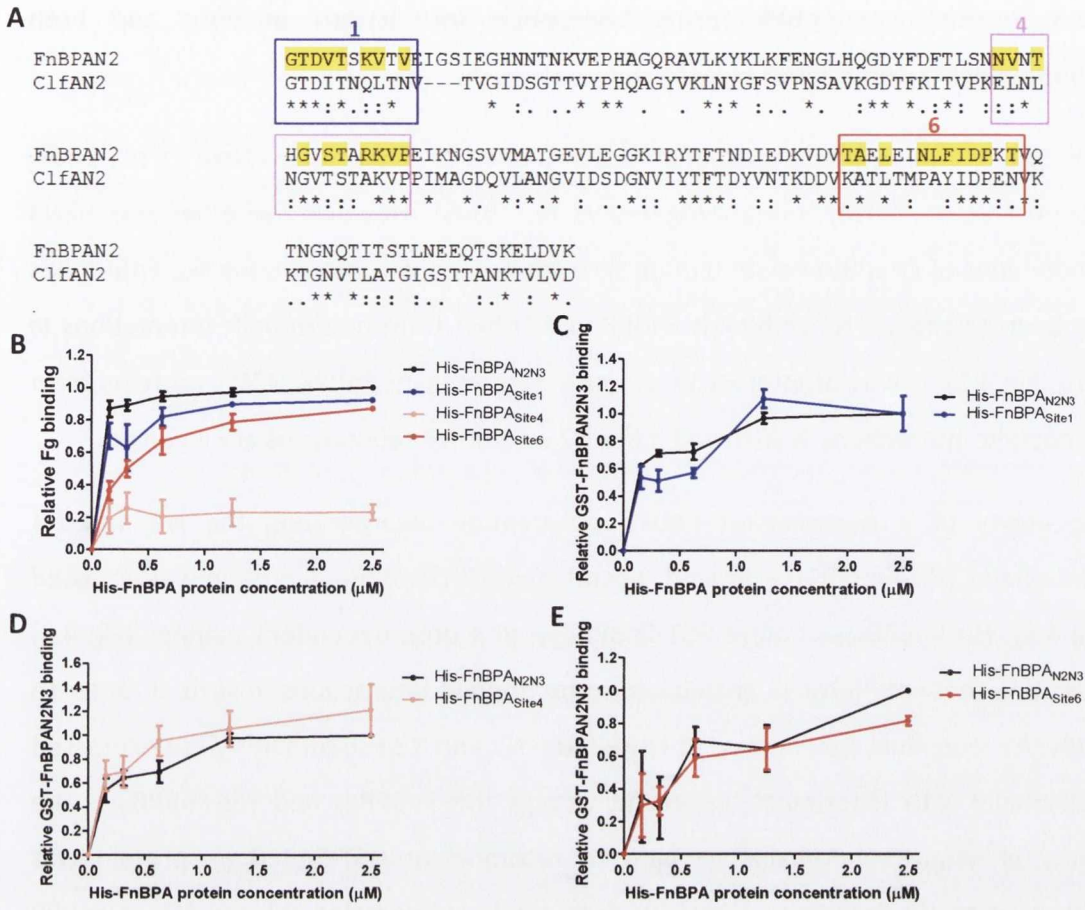


FIG 4.7. Assessment of FnBPA variants for the ability to form FnBPA-FnBPA interactions. A) Amino acid alignment of the N2 subdomains of FnBPA and ClfA. The amino acid sequences of N2 of FnBPA isotype I (residues 196-307) and N2 of ClfA (residues 221-368) were aligned using Clustal Omega (Sievers *et al.*, 2011). Residues of sites 1, 4 and 6 which are well conserved among FnBPA isotypes I, III, IV, V and VI and FnBPB are highlighted. B-E) Binding of recombinant FnBPA proteins to immobilised human Fg and GST-FnBPA_{N2N3} protein. Microtitre wells were coated with Fg (10 µg/ml; Calbiochem; B) or GST-FnBPA_{N2N3} (1 µM; C-E) and increasing concentrations of FnBPA proteins His-FnBPA_{N2N3}, His-FnBPA_{Site1}, His-FnBPA_{Site4} and His-FnBPA_{Site6} were added for 2 h at 37 °C. Bound protein was detected with monoclonal mouse anti-His IgG followed by HRP-conjugated rabbit anti-mouse IgG. Values are expressed relative to the A_{450nm} reading measured for the highest concentration of His-FnBPA_{N2N3} binding Fg (B) or GST-FnBPA_{N2N3} (C-E, 2.5 µM = 1.0). Values are the mean of 3 independent assays for ELISAs with His-FnBPA_{Site1} and His-FnBPA_{Site4} and 2 independent assays for ELISAs with His-FnBPA_{Site6}. Error bars represent SEM. *P*-values were calculated using an unpaired Student's *t*-test (C, D). There was no significant difference (*p*>0.05) between the values measured for His-FnBPA_{N2N3}, His-FnBPA_{Site1} and His-FnBPA_{Site4} binding to GST-FnBPA_{N2N3}.

4.2.5 Recombinant FnBPB forms homophilic interactions *in vitro* and both subdomains N2 and N3 participate

FnBPB, like FnBPA, mediates biofilm accumulation in *S. aureus* (O'Neill *et al.*, 2008, McCourt *et al.*, 2014, Vergara-Irigaray *et al.*, 2009). However, whether the N2N3 subdomains of FnBPB mediate biofilm through homophilic interactions like FnBPA has not been tested. As recombinant FnBPB and FnBPA form heterophilic interactions *in vitro* (Fig 4.5), it was of interest to assess if recombinant FnBPB N2N3 proteins form homophilic interactions *in vitro* and if the N2 and/or N3 subdomains are involved.

The ability of a recombinant FnBPB polypeptide incorporating the N2 and N3 subdomains (His-FnBPB_{N2N3}) to bind recombinant GST-FnBPB_{N2N3} protein was assessed (Fig 4.8). His-FnBPB_{N2N3} bound GST-FnBPB_{N2N3} in a dose-dependent manner (Fig 4.8) indicating that FnBPB N2N3 proteins form homophilic interactions *in vitro*. In order to study the individual subdomains of FnBPB, the N2 and N3 subdomains were expressed individually with N-terminal hexahistidine tags (His-FnBPB_{N2} and His-FnBPB_{N3}). The ability of single subdomains to bind to recombinant GST-FnBPB_{N2N3} protein was compared to His-FnBPB_{N2N3} (Fig 4.8). Both single subdomains N2 and N3 of FnBPB bound GST-FnBPB_{N2N3} in a dose-dependent manner. However, at the highest concentration tested in this assay (2.5 μ M) both His-FnBPB_{N2} and His-FnBPB_{N3} had a significantly lower level of binding to GST-FnBPB_{N2N3} in comparison to His-FnBPB_{N2N3} (Fig 4.8). These data indicate that FnBPB forms homophilic interactions and that FnBPB N2 and N3 subdomains are involved. This differs from data obtained for FnBPA where only the N2 subdomain of FnBPA was capable of binding GST-FnBPA_{N2N3} *in vitro* (Fig 4.3). Further analyses would be required to assess if FnBPB homophilic interactions consist of N2-N2 along with N3-N3 interactions or N2-N3 interactions.

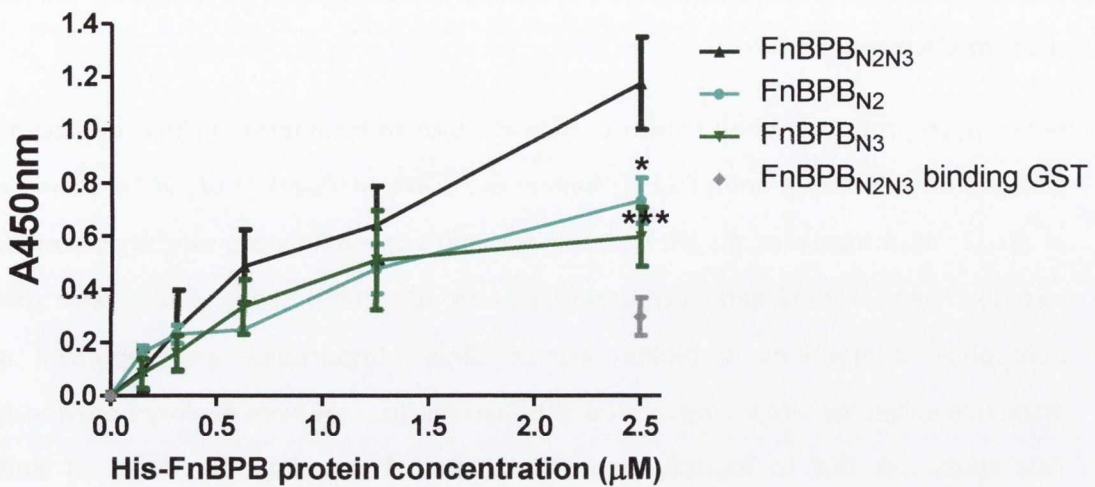


FIG 4.8. FnBPB homophilic interactions are mediated by subdomains N2 and N3. Binding of recombinant FnBPB subdomain proteins to immobilised GST-FnBPB_{N2N3} fusion protein. Microtitre wells were coated with GST-FnBPB_{N2N3} (1 µM) and increasing concentrations of FnBPB subdomain proteins His-FnBPB_{N2N3}, His-FnBPB_{N2} and His-FnBPB_{N3} were added for 2 h at 37 °C. Bound protein was detected with monoclonal mouse anti-His IgG followed by HRP-conjugated rabbit anti-mouse IgG. Binding of His-FnBPB_{N2N3} to GST (1 µM) only coated wells was included to detect background levels of binding. Absorbance values were measured at 450 nm. Values are the mean of 4-5 independent assays. Error bars represent SEM. *P*-values were calculated using a two-way ANOVA with Bonferroni post-test where * and *** represent a *p*-value of ≤0.05 and ≤0.001 and at all other points differences were not significant (*p*-value >0.05).

4.2.6 Identification of putative small molecule inhibitors of FnBP-mediated biofilm using *in silico* approaches

FnBPs have previously been shown to mediate biofilm formation in clinically relevant lineages of MRSA; CC8 and CC22 (O'Neill *et al.*, 2008, McCourt *et al.*, 2014, Planet *et al.*, 2013, Mashruwala *et al.*, 2017). A role for FnBPs *in vivo* in a mouse catheter model has also been established (Vergara-Irigaray *et al.*, 2009). Thus, FnBPs and their homophilic interactions in biofilm are of clinical importance and represent an attractive target for biofilm prevention although this has not been explored previously. This study set out to identify non-antibiotic small molecule inhibitors of FnBP homophilic interactions in order to prevent biofilm formation.

Small molecules LH1-5 (Table 3.2) were docked onto the crystal structure of FnBPA N2N3 subdomains (PDB ID = 4B5Z) (Stemberk *et al.*, 2014) using Autodock vina (Trott & Olson, 2010). LH1-5 were further assessed as putative FnBP biofilm inhibitors as they all dock at overlapping sites at amino acid residues equivalent to the 'RPGSV' motif of SdrC; residues 'NTHGV' (Fig 4.9). Their docking sites lie in one of the regions previously described in this study, termed site 4, which is well conserved among FnBPA isotypes I, III, IV, V and VI and FnBPB (Fig 4.6). Furthermore, LH1-5 are predicted to form the majority, if not all, of their contacts to the N2 subdomain of FnBPA; the subdomain involved in FnBPA homophilic interactions. Many of these predicted contacts are to residues G₂₅₅ and V₂₅₆ which are the equivalent residues to amino acids S₂₅₀ and V₂₅₁ of the 'RPGSV' motif of SdrC.

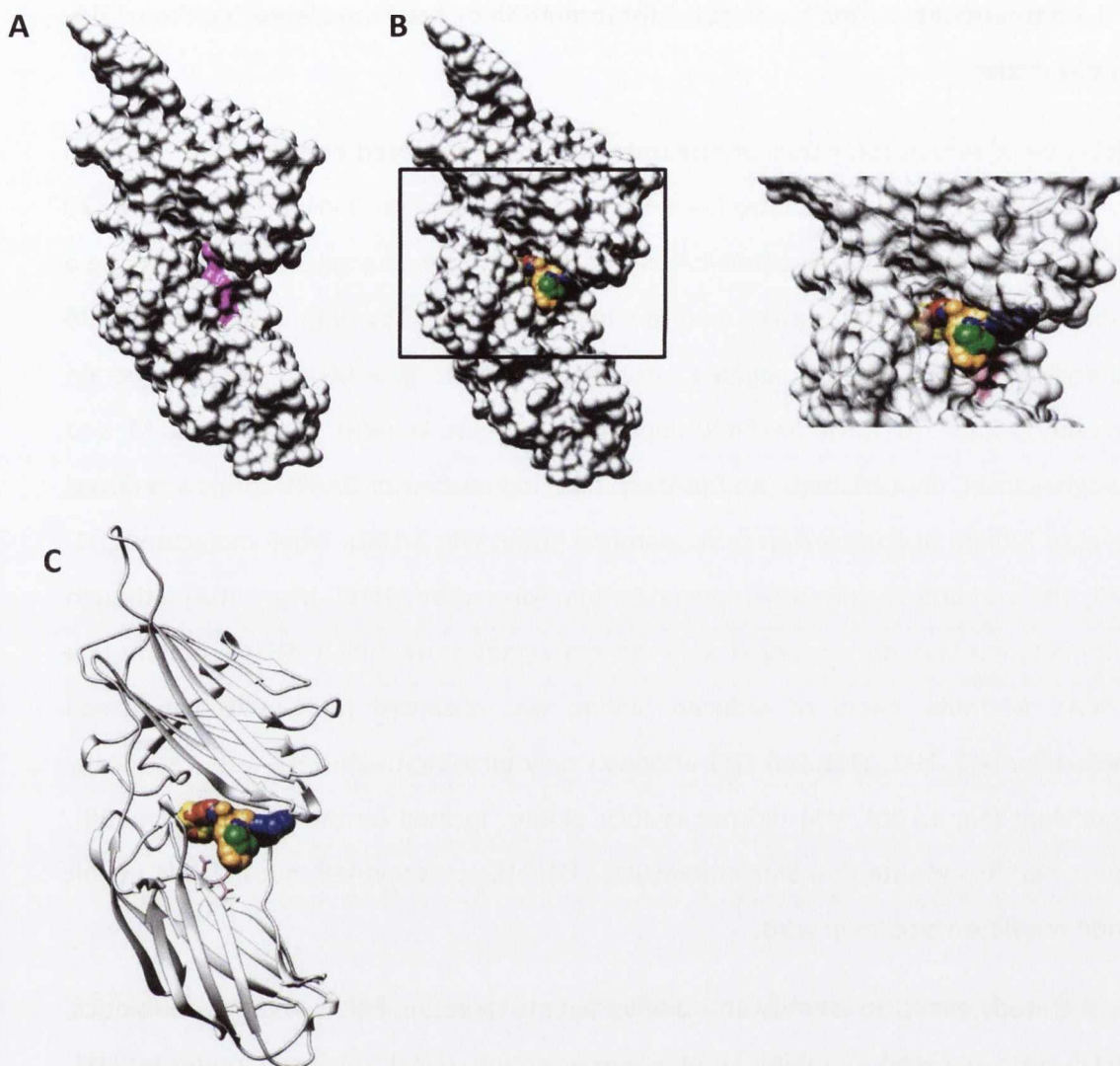


FIG 4.9. Predicted docking sites of small molecules on FnBPA. Small molecules from the Zinc library were docked onto the crystal structure of FnBPA (PDB ID=4B5Z) using Autodock vina (Trott & Olson, 2010). Small molecule docking sites were visualized using Chimera version 1.9 (Pettersen *et al.*, 2004). Small molecules LH1-5 docked at overlapping sites at the equivalent residues to 'RPGSV' of SdrC; 'NTHGV' in FnBPA. FnBPA is shown in space filled (A, B) and in ribbon format (C). Residues 'NTHGV' are coloured magenta. LH1, LH2, LH3, LH4 and LH5 are shown space filled coloured yellow, blue, green, orange and red, respectively (B, C).

4.2.7 Assessment of small molecules for inhibition of FnBP-mediated biofilm of HA-MRSA strains

LH1-5 were assessed for their ability to inhibit FnBP-mediated biofilm *in vitro* formed by two HA-MRSA clinical isolates from distinct genetic backgrounds; BH1CC and DAR70 (Fig 4.10). BH1CC is a CC8, HA-MRSA strain which is well characterised for forming a robust FnBP-dependent biofilm *in vitro* which is mediated by both *FnBPA* and *FnBPB* (O'Neill *et al.*, 2008, Geoghegan *et al.*, 2013). DAR70 is a CC45, HA-MRSA strain recently shown to form an FnBP-dependent biofilm *in vitro* (Zapotoczna M and Geoghegan JA, unpublished). An *fnbAfnbB* deletion mutant of DAR70 forms a reduced level of biofilm in comparison to its parental strain (Fig 4.10B). Small molecules LH1, LH2, LH3 and LH5 significantly reduced biofilm formed by BH1CC (Fig 4.10A) although full inhibition was not observed. LH4 did not significantly inhibit BH1CC biofilm (Fig 4.10A). A similar trend of reduced biofilm was observed for DAR70 with small molecules LH1, LH2, LH3 and LH5 although only inhibition with LH3 was statistically significant (Fig 4.10B). LH4 did not reduce biofilm formed by this strain (Fig 4.10B). These results indicate that small molecules LH1, LH2, LH3 and LH5 but not LH4 inhibit FnBP-mediated biofilm *in vitro*.

As this study aimed to identify anti-biofilm agents targeting FnBPs and not antibiotics, LH1-5 were assessed for inhibition of *S. aureus* growth (Fig 4.11). Small molecules LH1, LH2, LH3 and LH5 did not affect growth of *S. aureus* strain BH1CC *in vitro* (Fig 4.11, Table 4.1). LH4 reduced the doubling time of BH1CC *in vitro* (Table 4.1). However, LH4 did not inhibit BH1CC biofilm formation and thus, the reduction in doubling time of BH1CC in the presence of LH4 does not affect the ability of BH1CC to form biofilm. These results show that the reduction in biofilm caused by small molecules LH1, LH2, LH3 and LH5 is not due to reduced bacterial growth and that biofilm formation is inhibited.

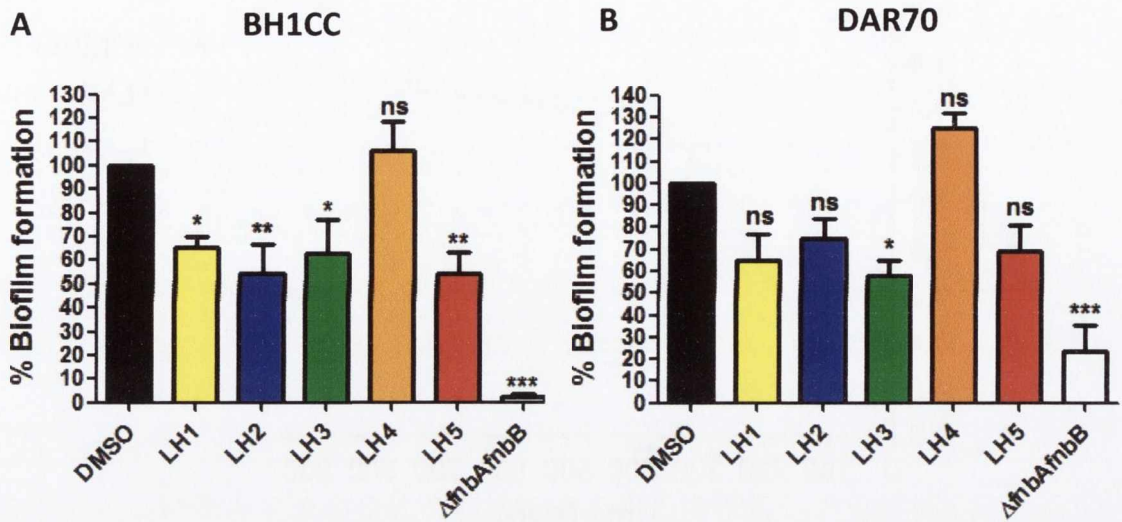


FIG 4.10. Inhibition of FnBP-dependent biofilm by small molecules. *S. aureus* strains BH1CC and BH1CC Δ fnbAfnbB (A) and DAR70 and DAR70 Δ fnbAfnbB (B) were allowed to form biofilm at 37 °C for 24 h in the presence of small molecules LH1, LH2, LH3, LH4 and LH5 (100 μ M) or the equivalent concentration of DMSO (1 % v/v). Biofilms were stained with crystal violet and absorbance values measured at 570 nm. Values are expressed as % biofilm formation relative to BH1CC (A) or DAR70 (B) with DMSO as 100 %. Results shown are the mean of at least 3 independent experiments. Error bars represent SEM. *P*-values were calculated using a one-way ANOVA where values were compared to the DMSO control and *, ** and *** represent *p*-values of ≤ 0.05 , ≤ 0.01 and ≤ 0.001 , respectively. *P*-values > 0.05 are considered not significant (ns).

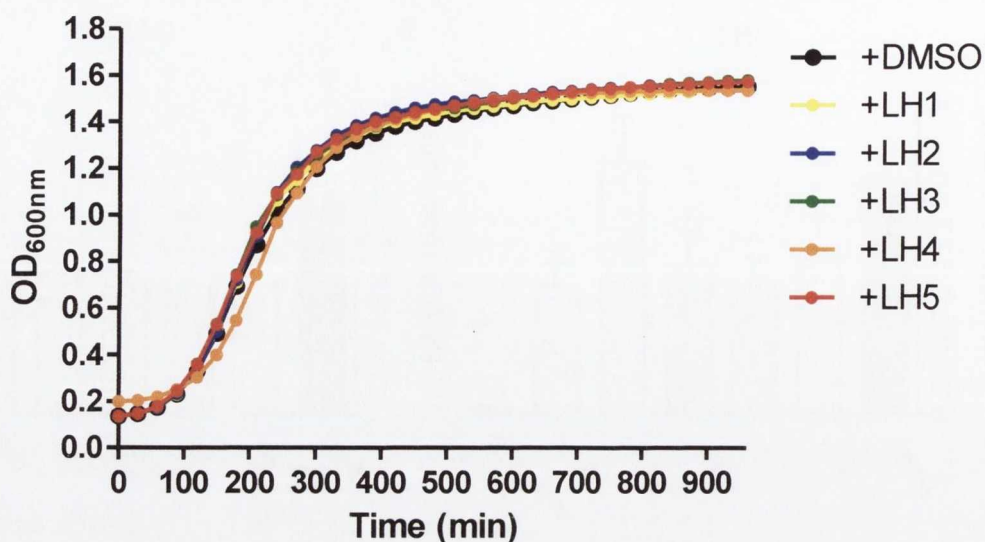


FIG 4.11. FnBP biofilm inhibitors have no effect on *S. aureus* growth. Overnight cultures of BH1CC were diluted 1/200 in BHI supplemented with D-glucose (10 g/L). Small molecules LH1, LH2, LH3, LH4 and LH5 (100 μ M) or DMSO (1 % v/v) were added to the diluted bacteria. Diluted bacteria (200 μ l) were added to round-bottomed wells of sterile microtitre plates. Plates were incubated with shaking at 37 °C for 16 h. OD_{600nm} values were measured at 30 min intervals. Each curve is representative of 3 independent experiments with different cultures of bacteria.

Table 4.1. Doubling times of BH1CC with DMSO or small molecules LH1-5

| DMSO/Small molecule | Doubling Time (min) ^a | SEM (min) ^b |
|---------------------|----------------------------------|------------------------|
| DMSO | 49.2 | ± 11.8 |
| LH1 | 42.7 | ± 13.6 |
| LH2 | 43.5 | ± 13.0 |
| LH3 | 59.7 | ± 11.2 |
| LH4 | 91.9 | ± 9.8 |
| LH5 | 46.0 | ± 14.2 |

^a Doubling times are the average of the doubling times obtained from three independent growth curves.

^bSEM = Standard error of the mean

4.2.8 Assessment of small molecules for inhibition of recombinant FnBPA-FnBPA interactions *in vitro*

To determine if biofilm inhibition (Fig 4.10) was due to prevention of FnBPA homophilic interactions, small molecules LH1-5 were assessed for their ability to prevent recombinant FnBPA_{N2N3}-FnBPA_{N2N3} protein interactions *in vitro* (Fig 4.12). LH1, LH3 and LH5 significantly reduced His-FnBPA_{N2N3} binding to GST-FnBPA_{N2N3} (Fig 4.12). LH2 and LH4 did not significantly reduce His-FnBPA_{N2N3} binding to GST-FnBPA_{N2N3} (Fig 4.12). These data indicate that LH1, LH3 and LH5 inhibit recombinant FnBPA_{N2N3}-FnBPA_{N2N3} interactions *in vitro*. Since LH2 inhibited FnBP-mediated biofilm (Fig 4.10) but did not inhibit recombinant FnBPA_{N2N3}-FnBPA_{N2N3} interactions *in vitro* it is possible LH2 is inhibiting FnBPB-FnBPB or FnBPA-FnBPB interactions.

4.2.9 FnBP biofilm inhibitors do not inhibit FnBP-mediated adherence to fibrinogen

FnBPA and FnBPB mediate *S. aureus* adherence to human fibrinogen (Fg) and biofilm accumulation through their N2 and N3 subdomains although the mechanisms underlying FnBPA-mediated biofilm accumulation and FnBPA Fg binding are distinct (Section 4.1) (Geoghegan *et al.*, 2013). Thus, it was of interest to assess if the small molecule FnBP biofilm inhibitors identified in this study have an effect on FnBP-mediated adherence to fibrinogen.

There is a high level of functional redundancy among *S. aureus* cell wall-anchored proteins with MSCRAMMs ClfA and ClfB also promoting *S. aureus* adherence to Fg (Xiang *et al.*, 2012, Ganesh *et al.*, 2008). In order to specifically assess inhibition of FnBP-mediated adherence to Fg without interference from ClfA and ClfB, a mutant of the *S. aureus* lab strain SH1000 was used (SH1000 *clfA clfB*). Small molecules LH1-5 were assessed for the ability to inhibit SH1000 *clfA clfB* adhering to human Fg *in vitro* (Fig 4.13). An SH1000 strain deficient for all four proteins; ClfA, ClfB, FnBPA and FnBPB, was included as a negative control. This strain did not adhere to human fibrinogen confirming that the adherence observed for SH1000 *clfA clfB* is solely mediated by FnBPA and FnBPB (Fig 4.13). Small molecules LH1-5 did not inhibit SH1000 *clfA clfB* adherence to fibrinogen (Fig 4.13). These data suggest specificity of small molecules LH1, LH2, LH3 and LH5 as inhibitors of FnBP-mediated biofilm formation. These data

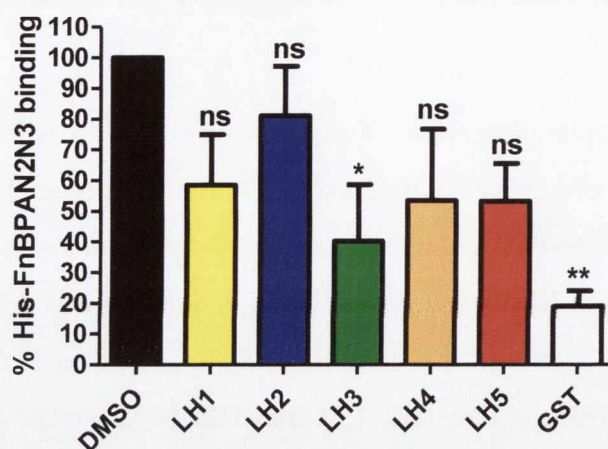


FIG 4.12. Small molecules inhibit recombinant FnBPA-FnBPA interactions *in vitro*.

Microtitre wells were coated with GST-FnBPA_{N2N3} (1 μ M). Small molecules LH1, LH2, LH3, LH4 and LH5 (1.25 μ M) or the equivalent concentration of DMSO (0.125 % v/v) were added to recombinant His-FnBPA_{N2N3} (0.25 μ M) and incubated at 37 $^{\circ}$ C, 200 rpm for 30 min. The His-FnBPA_{N2N3} small molecule or DMSO mixtures were subsequently added (100 μ l) in triplicate to the GST-FnBPA_{N2N3} coated wells at 37 $^{\circ}$ C for 1 h 30 min. Control wells were coated with GST (1 μ M) only and His-FnBPA_{N2N3} with DMSO added to control for background binding to GST. Bound protein was detected with monoclonal mouse anti-His IgG followed by HRP-conjugated rabbit anti-mouse IgG. Values are expressed as a percentage of the values for His-FnBPA_{N2N3} with DMSO binding GST-FnBPA_{N2N3}. Values are the mean of 4-5 independent experiments. Error bars represent SEM. *P*-values were calculated using a one-way ANOVA where values were compared to the DMSO control and * and ** represent *p*-values of ≤ 0.05 and ≤ 0.01 , respectively. *P*-values > 0.05 are considered not significant (ns).

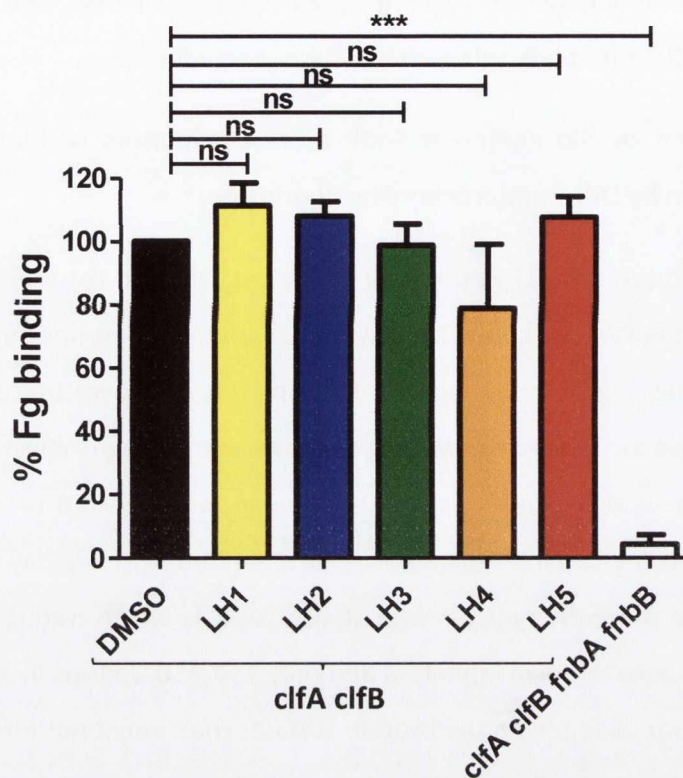


FIG 4.13. FnBP biofilm inhibitors do not inhibit FnBP-mediated adherence to fibrinogen. *S. aureus* strains SH1000 *clfA clfB* and SH1000 *clfA clfB fnbA fnbB* were grown to exponential phase in TSB and adjusted to an $OD_{600nm}=1.0$. Small molecules LH1, LH2, LH3, LH4 and LH5 (100 μ M) or DMSO (1 % v/v) were added to the bacterial suspension and incubated at 37 $^{\circ}$ C, 200 rpm for 30 min. Bacteria mixed with small molecules or DMSO (200 μ l) were subsequently added to Fg coated wells and incubated at 37 $^{\circ}$ C for 2 h. Adherent bacteria were stained with crystal violet and the absorbance was read at 570 nm. Values are expressed as percentage of the A_{570nm} values measured for SH1000 *clfA clfB* with DMSO. Values are the mean of 3-4 independent experiments. Error bars represent SEM. *P*-values were calculated using a one-way ANOVA where *** represents a *p*-value of ≤ 0.001 and *p*-values > 0.05 are considered not significant (ns).

suggest the binding site of these small molecules likely blocks one or more sites important for FnBP homophilic interactions but not Fg adherence.

4.2.10 Assessment of the ability of FnBP biofilm inhibitors to bind recombinant FnBPA_{N2N3} protein by Differential Scanning Fluorimetry

FnBP biofilm inhibitors LH1, LH2, LH3 and LH5 were assessed for their ability to bind recombinant His-FnBPA_{N2N3} protein by differential scanning fluorimetry (DSF). None of the small molecules significantly increased the melting temperature of recombinant FnBPA_{N2N3} (Table 4.2). These results may indicate one of two things; that the small molecules do not bind to FnBPA_{N2N3} under the conditions tested or that binding of these small molecules to FnBPA_{N2N3} cannot be detected in this assay as the binding does not stabilise the FnBPA_{N2N3} protein structure. It is worth noting that the small molecules tested here are lead inhibitors and only 250-350 Daltons in size and may be binding to a site, for example on the protein surface, that would not infer an increased stability to the protein structure.

TABLE 4.2. ΔT_m of recombinant FnBPA_{N2N3} in the presence of small molecule FnBP biofilm inhibitors

| Small molecule | ΔT_m (°C) ^a | SEM (°C) ^b |
|----------------|--------------------------------|-----------------------|
| LH1 | 0.25 | 0.1 |
| LH2 | 0.23 | 0.01 |
| LH3 | -0.14 | 0.29 |
| LH5 | 0.17 | 0.11 |

^a Values are the mean of three independent experiments.

^b SEM = Standard error of the mean

4.2.11 Identification of inhibitors of FnBP-mediated adherence to fibrinogen

Small molecules LH6, LH7 and LH10 of the 'Malaria Box' were also tested for inhibition of FnBP-mediated adherence of *S. aureus* to fibrinogen (Fg). These small molecules were assessed due to their docking poses on SdrC (Chapter 1). LH6, LH7 and LH10 were predicted to dock in the trench between subdomains N2 and N3 of SdrC blocking the opening to the trench. As Fg docks in the equivalent trench between N2 and N3 subdomains of FnBPA and FnBPB, a similar docking site on FnBPs should block ligand binding. Thus, LH6, LH7 and LH10 were docked onto the crystal structure of FnBPA N2N3 using Autodock Vina (Trott & Olson, 2010). LH6 was predicted to dock at the opening of the trench, extending into N2 (Fig 4.14A). LH7 and LH10 were also predicted to dock at the opening of the trench with LH10 extending across the opening (Fig 4.14B, C). These predicted docking sites overlap the binding site of the Fg γ -chain peptide in the crystal structure of FnBPA in complex with its ligand peptide (Fig 4.14D; PDB ID=4B60). *In silico*, LH6, LH7 and LH10 were predicted to form a large number of contacts to FnBPA including several residues important in FnBPA-Fg binding (Table 4.3). Thus, their predicted docking sites indicate they may inhibit FnBP-mediated adherence to Fg. The ability of LH6, LH7 and LH10 to inhibit SH1000 *clfA clfB* adherence to human Fg *in vitro* was assessed (Fig 4.15). Small molecules LH6, LH7 and LH10 all significantly reduced FnBP-mediated adherence to Fg. These data indicate that LH6, LH7 and LH10 inhibit the ability of FnBPs to bind Fg.

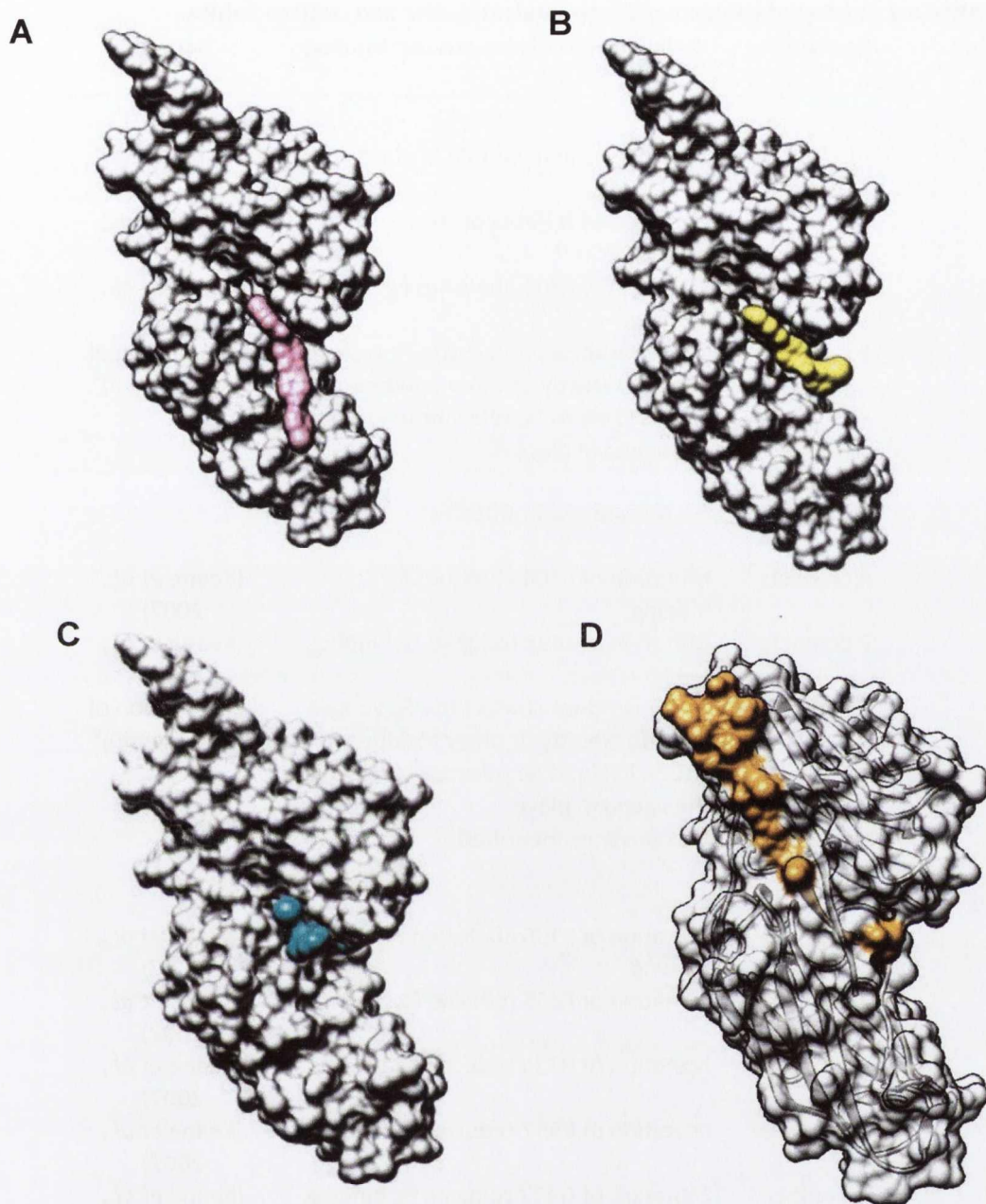


Fig 4.14. Predicted docking sites of LH6, LH7 and LH10 on FnBPA. Small molecules LH6, LH7 and LH10 were docked onto the crystal structure of FnBPA (PDB ID=4B5Z) using Autodock vina (Trott & Olson, 2010). The predicted docking sites were visualized using Chimera version 1.9 (Pettersen *et al.*, 2004). FnBPA is shown in space filled. LH6, LH7 and LH10 are shown in space filled in pink (A), yellow (B) and turquoise (C), respectively. D) The FnBPA-Fg γ -chain peptide complex. FnBPA and the peptide are shown in space filled in grey and orange, respectively. FnBPA is shown at 50 % transparency in order to clearly visualise the peptide docking site.

TABLE 4.3. Predicted contacts of compounds LH6, LH7 and LH10 to FnBPA

| Interacting residue | Contact(s) | Relevance to fibrinogen (Fg) binding | Source |
|---------------------|--------------------|---|---|
| 1. LH6 | | | |
| N304 | Hydrogen (H-) bond | Locks Fg γ -chain peptide in place. | (Stemberk <i>et al.</i> , 2014) |
| | | Mutation of N304 abolishes Fg binding. | (Keane <i>et al.</i> , 2007) |
| F306 | 7 contacts | Mutation of F306 abolishes Fg binding. | (Keane <i>et al.</i> , 2007) |
| P263 | 8 contacts | These residues contact the Fg γ -chain peptide directly or other residues of FnBPA likely to be relevant to locking the ligand in place. | (examination of PDB ID=4B60) ^a |
| V256 | 4 contacts | | |
| G255 | 1 contact | | |
| H254 | 1 contact | | |
| Q302 | 1 contact | | |
| | | No relevance identified | |
| 2. LH7 | | | |
| F306 | 4 contacts | Mutation of F306 abolishes Fg binding. | (Keane <i>et al.</i> , 2007) |
| L498 | 2 contacts | Mutation of L498 reduced Fg binding. | (Keane <i>et al.</i> , 2007) |
| V256 | 2 contacts | These residues contact the Fg γ -chain peptide directly or other residues of FnBPA likely to be relevant to locking the ligand in place. | (examination of PDB ID=4B60) ^a |
| G255 | 1 contact | | |
| S257 | 1 contact | | |
| V262 | 1 contact | | |
| K261 | 2 contacts | | |
| | | No relevance identified | |
| 3. LH10 | | | |
| F306 | 4 contacts | Mutation of F306 abolished Fg binding. | (Keane <i>et al.</i> , 2007) |
| F355 | 2 contacts | Mutation of F355 reduced Fg binding | (Keane <i>et al.</i> , 2007) |
| R224 | 2 contacts | Mutation of R224 reduced Fg binding | (Keane <i>et al.</i> , 2007) |
| K357 | 2 contacts | Mutation of K357 reduced Fg binding | (Keane <i>et al.</i> , 2007) |
| G497 | 1 contact | Mutation of G497 reduced Fg binding | (Keane <i>et al.</i> , 2007) |
| V499 | 5 contacts | These residues contact the Fg γ -chain peptide directly or other residues of FnBPA likely to be relevant to locking the ligand in place. | examination of PDB ID=4B60) ^a |
| V256 | 3 contacts | | |
| L500 | 2 contacts | | |
| G255 | 1 contact | | |
| G222 | 2 contacts | | |
| | | Mutation of G222 had no effect on Fg binding | (Keane <i>et al.</i> , 2007) |
| | | However, G222 involved in stabilisation of Fg peptide bound FnBPA | (Stemberk <i>et al.</i> , 2014) |

^a The relevance of these FnBPA residues to Fg binding was identified through analysis of the crystal structure of FnBPA in complex with the Fg γ -chain peptide (PDB ID=4B60) in Chimera.

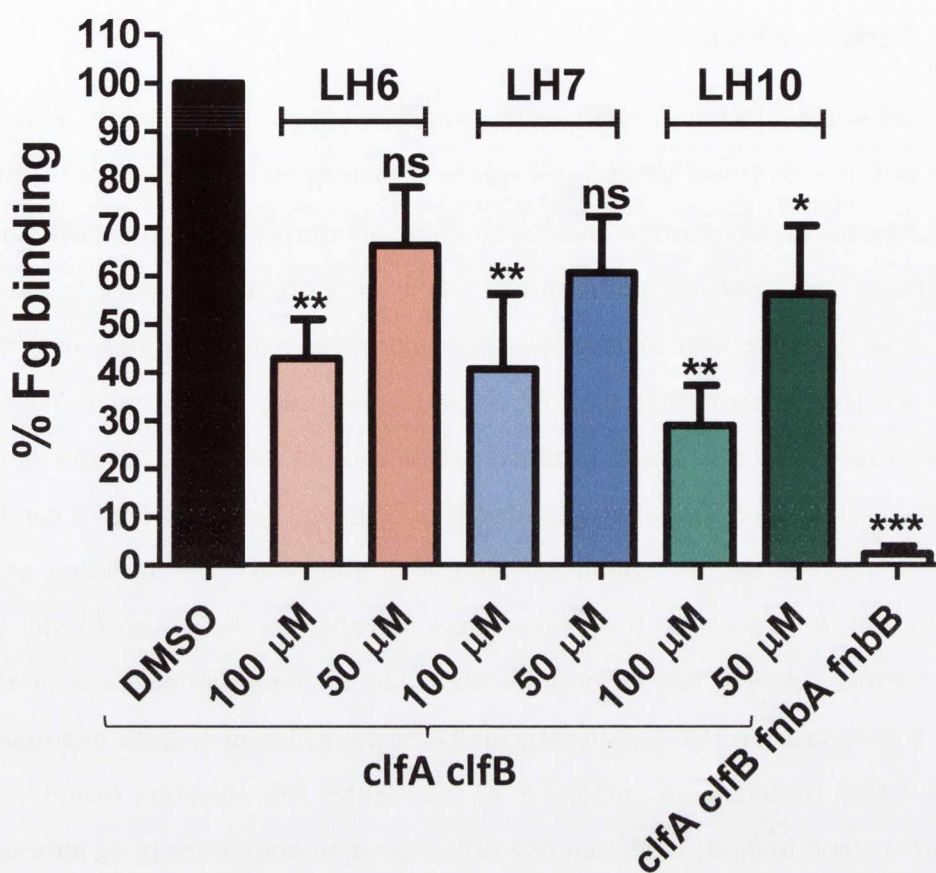


FIG 4.15 Inhibition of FnBP-mediated adherence to fibrinogen by LH6, LH7 and LH10. *S. aureus* strains SH1000 *clfA clfB* and SH1000 *clfA clfB fnbA fnbB* were grown to exponential phase in TSB and adjusted to an $OD_{600nm}=1.0$. Small molecules LH6, LH7, and LH10 (50 μ M, 100 μ M) or DMSO (0.5 %, 1% v/v) were added to the bacterial suspension and incubated at 37 °C, 200 rpm for 30 min. Bacteria mixed with small molecules or DMSO (200 μ l) were subsequently added to Fg coated wells and incubated at 37 °C for 2 h. Adherent bacteria were stained with crystal violet and the absorbance was read at 570 nm. Values are expressed as percentage of the A_{570nm} value measured for SH1000 *clfA clfB* with DMSO. Values are the mean of 3-4 independent experiments. Error bars represent SEM. *P*-values were calculated using a one-way ANOVA where *, ** and *** represent *p*-values of ≤ 0.05 , ≤ 0.01 and ≤ 0.001 , respectively. For all statistical analyses values were compared to SH1000 *clfA clfB* with DMSO.

4.2.12 Small molecules LH6 and LH7 inhibit both FnBPA- and FnBPB-mediated bacterial adherence to fibrinogen

Small molecules LH6, LH7 and LH10 were identified which inhibit FnBP-mediated adherence of *S. aureus* strain SH1000 *clfA clfB* to human Fg. In this assay, both FnBPA and FnBPB mediate *S. aureus* adherence to Fg. It was of interest to identify if the small molecules inhibit the ability of FnBPA and/or FnBPB to promote adherence to Fg. To assess this, the surrogate host *Lactococcus lactis* expressing full length *fnbA* and *fnbB* individually on the nisin-inducible plasmid pNZ8037 was used. The surrogate host *L. lactis* allows expression of a single *S. aureus* factor without interference from other factors. Thus, inhibition of Fg adherence mediated solely by FnBPA or FnBPB can be assessed. For each strain, an uninduced culture of the strain was included as a negative control. It is possible that a low level of FnBPA or FnBPB could still be expressed in this strain in the absence of nisin due to potential leakiness of the promoter. Small molecule LH6 significantly inhibited the ability of *L. lactis* expressing FnBPA (Fig 4.16A) to adhere to human Fg. At the highest concentration tested here LH7 showed a trend towards inhibition of FnBPA-mediated adherence to Fg although this was not statistically significant (Fig 4.16A). Both small molecules LH6 and LH7 inhibited the ability of *L. lactis* expressing FnBPB (Fig 4.16B) to adhere to human Fg. These data indicate that LH6 and potentially LH7 inhibit both FnBPA- and FnBPB-mediated bacterial adherence to Fg. Unfortunately, due to limited commercial availability LH10 was not included in these assays.

4.2.13 *In silico* docking of LH6, LH7 and LH10 onto a homology model of FnBPB_{N2N3}.

The inhibitors of FnBP-mediated adherence to Fg in this study were identified based on their predicted *in silico* docking sites on the crystal structure of FnBPA (Fig 4.14). Small molecules LH6, LH7 and LH10 were predicted to dock at sites on FnBPA that would block Fg binding (Fig 4.14). Initial docking was carried out on FnBPA, and not FnBPB, as the structure of FnBPA N₂N₃ subdomains has been solved (Stemberk *et al.*, 2014). Small molecules LH6, LH7 and LH10 inhibited FnBP-mediated adherence of *S. aureus* to Fg *in vitro* (Fig 4.15) and LH6 and LH7 were shown to inhibit both FnBPA- and FnBPB-mediated bacterial adherence to Fg (Fig 4.16). Thus, it was of interest to assess

if small molecules LH6, LH7 and LH10 are predicted to dock at sites overlapping the Fg binding site on FnBPB. A homology model of FnBPB N2N3 subdomains based on the crystal structure of FnBPA N2N3 in complex with the Fg γ -chain peptide (PDB ID=4B60) was generated using Phyre² (Kelley & Sternberg, 2009) (Fig 4.17A). In the homology model, FnBPB N2N3 subdomains form IgG-like folded N2 and N3 subdomains with a trench separating the subdomains (Fig 4.17A). Small molecules LH6, LH7 and LH10 were docked onto the homology model of FnBPB using Autodock vina (Trott & Olson, 2010). LH6 and LH7 were predicted to dock in the ligand binding trench of FnBPB where Fg would bind (Fig 4.17B, C). LH10 was predicted to dock near, but not in, the trench between subdomains N2N3 (Fig 4.17D). Notably, LH7 is predicted to contact residue F314 of FnBPB. F314 of FnBPB is in an equivalent position to residue F306 of FnBPA and similar to F306 of FnBPA, alanine substitution of F314 of FnBPB greatly reduces FnBPB's ability to bind Fg (Burke *et al.*, 2011).

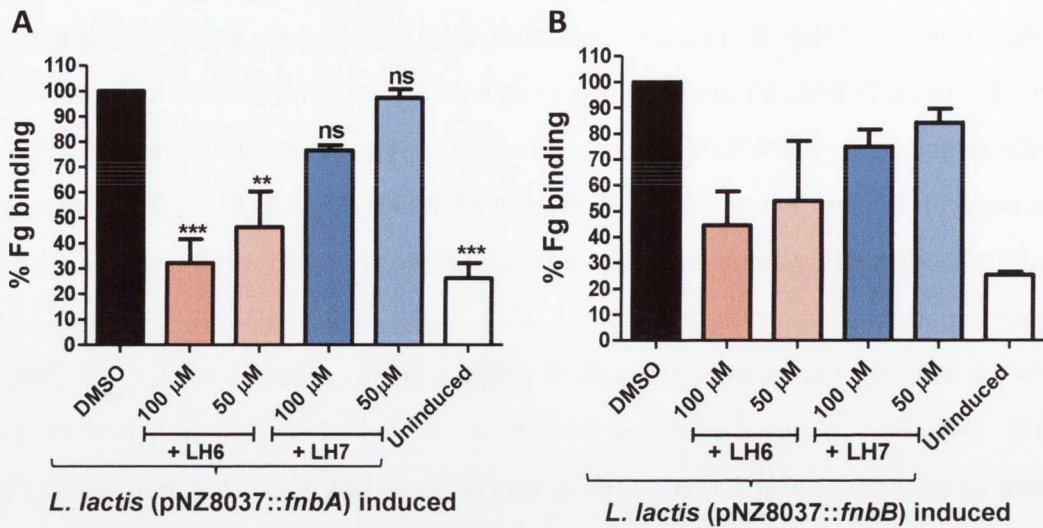


FIG 4.16. LH6 and LH7 inhibit FnBPA- and FnBPB-mediated adherence to fibrinogen.

L. lactis (pNZ8037::fnbA) (A) and *L. lactis* (pNZ8037::fnbB) (B) were grown to exponential phase and induced with nisin (32 ng/ml) for 16-18 h at 28 °C. A culture of each strain was not induced and included as a negative control for adherence to Fg (uninduced). Bacteria were adjusted to an $OD_{600nm} = 1.0$ in PBS. Small molecules LH6 and LH7 (50 μM or 100 μM) or the equivalent concentration of DMSO (0.5 % or 1% v/v) were added to adjusted bacteria and incubated at 37 °C, 200 rpm for 30 min. Bacteria small molecules or DMSO mixtures were subsequently added to Fg coated wells and incubated for 2 h. Adherent bacteria were stained with crystal violet and A_{570nm} values measured. Values are expressed as percentage of the A_{570nm} value measured for *L. lactis* (pNZ8037::fnbA) (A) or *L. lactis* (pNZ8037::fnbB) (B) with DMSO. Values are the mean of 3 (A) or 2 (B) independent assays. Error bars represent SEM. *P*-values were calculated using a one-way ANOVA where ** and *** represent *p*-values of ≤ 0.01 and ≤ 0.001 , respectively (A). A *p*-value > 0.05 is considered not significant (ns). For statistical analyses values were compared to induced *L. lactis* (pNZ8037::fnbA) with DMSO (A). Statistical analyses were not performed in B as the values are the mean of two, not three, independent assays.

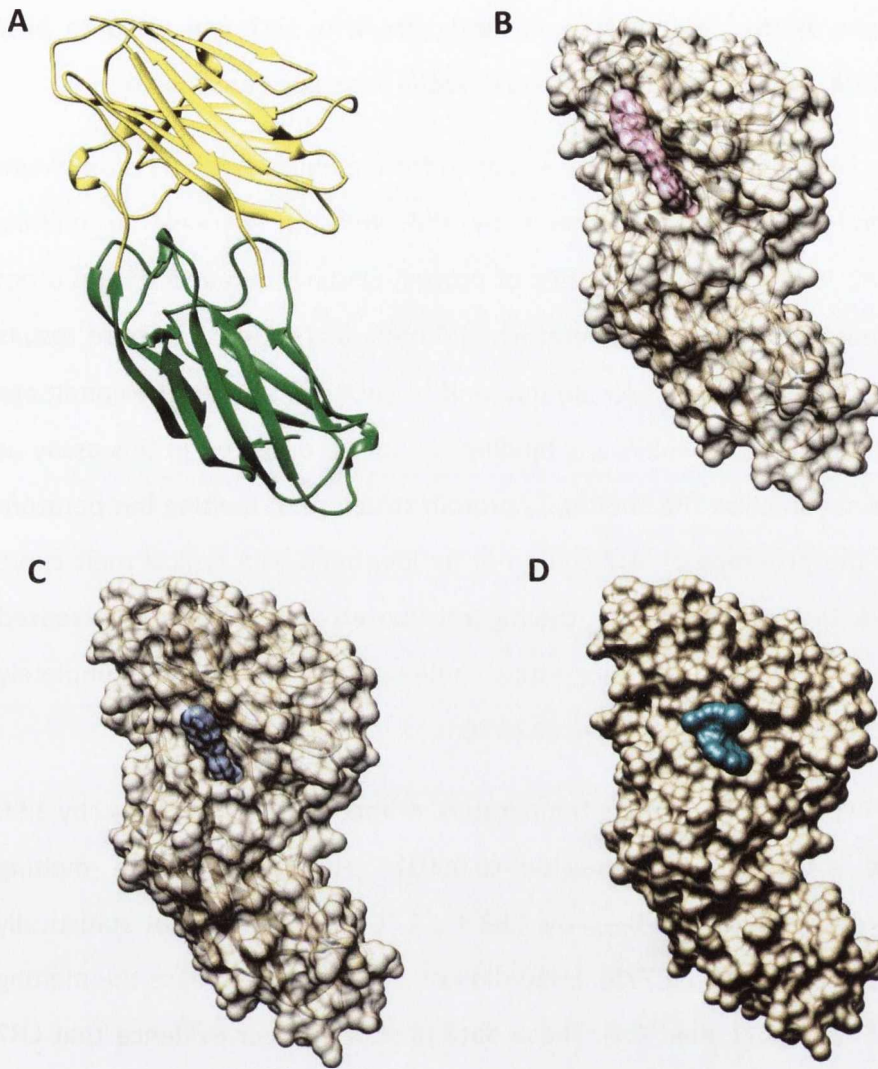


FIG 4.17 Predicted docking sites of LH6, LH7 and LH10 on FnBPB. A) Homology model of FnBPB. A homology model of FnBPB N2N3 subdomains was generated based on the crystal structure of FnBPA in complex with the Fg γ -chain peptide (PDB ID=4B60) using Phyre² (Kelley & Sternberg, 2009) and the model visualized using Chimera version 1.9 (Pettersen *et al.*, 2004). FnBPB is shown in ribbon with N2 and N3 subdomains coloured green and yellow, respectively. Small molecules LH6 (B), LH7 (C) and LH10 (D) were docked onto the FnBPB model using Autodock vina (Trott & Olson, 2010) and their docking sites visualized using Chimera version 1.9 (Pettersen *et al.*, 2004). FnBPB and the small molecules are shown in space filled (B-D). For docking sites of LH6 (B) and LH7 (C) FnBPB and the small molecules are shown partially transparent to visualise the full docking site.

4.2.14 Assessment of the ability of small molecules LH6, LH7 and LH10 to bind recombinant FnBPA_{N2N3} and FnBPB_{N2N3} by Differential Scanning Fluorimetry

Small molecules LH6, LH7 and LH10 were screened for the ability to bind recombinant His-FnBPA_{N2N3} and His-FnBPB_{N2N3} proteins by DSF with an increase in melting temperature of ≥ 2 °C considered indicative of protein binding. LH6 and LH10 did not significantly increase the melting temperature of FnBPA_{N2N3} (Table 4.4). These results may indicate that the small molecules do not bind to FnBPA_{N2N3} under the conditions tested or that small molecule FnBPA_{N2N3} binding cannot be detected in this assay as the binding does not stabilise the FnBPA_{N2N3} protein structure. A melting temperature for FnBPA_{N2N3} in the presence of LH7 could not be identified as a typical melt curve was not obtained. The curve started at the highest fluorescence value and decreased over time/increasing temperature suggesting FnBPA_{N2N3} with LH7 was completely unfolded when the measurements began at 25 °C.

LH7 significantly increased the melting temperature of recombinant FnBPB_{N2N3} by 3.56 ± 0.81 °C (Table 4.4, Fig 4.18A; p -value= <0.0001). LH6 increased the melting temperature of recombinant FnBPB_{N2N3} by 2.83 ± 1.2 °C but this was not statistically significant (Table 4.4; p -value=0.0775). LH10 did not significantly increase the melting temperature of FnBPB_{N2N3} (Table 4.4). These data provided direct evidence that LH7 binds FnBPB_{N2N3} when assessed by DSF.

As LH7 was shown to inhibit FnBPB-mediated adherence to Fg and binding of LH7 to FnBPB_{N2N3} could be detected by DSF, LH7 was further assessed for the ability to bind a recombinant non-Fg binding variant of FnBPB_{N2N3} (His-FnBPB_{N312AF314A}) by DSF. FnBPB_{N312AF314A} contains alanine substitutions of residues N312 and F314 which lie along the ligand binding trench. FnBPB_{N312AF314A} has previously been shown to have a significantly reduced ability to bind Fg in comparison to native FnBPB_{N2N3} protein (Burke *et al.*, 2011). Notably, LH7 was predicted to contact residue F314 when docked onto the homology model of FnBPB. LH7 did not increase the melting temperature of FnBPB_{N312AF314A} (Fig 4.18B). These data suggest that when residues N312 and F314 are substituted, LH7 no longer binds recombinant FnBPB *in vitro*. These data suggest that LH7 binds within the trench of FnBPB at residues N312 and/or F314. LH7 binding at

TABLE 4.4. ΔT_m of recombinant FnBP proteins in the presence of small molecule inhibitors of FnBP-Fg binding

| Small molecule | ΔT_m (°C) ^a | SEM (°C) ^b |
|-----------------------------|--------------------------------|-----------------------|
| FnBPA_{N2N3} | | |
| LH6 | 0.82 | 0.4 |
| LH7 | ND ^c | ND |
| LH10 | -0.11 | 0.36 |
| FnBPB_{N2N3} | | |
| LH6 | 2.83 | 1.2 |
| LH7 | 3.56 | 0.81 |
| LH10 | 0.99 | 0.44 |

^a Values are the mean of three independent experiments except for LH6 with FnBPA_{N2N3} which is the mean of two independent experiments

^b SEM=Standard error of the mean

^c ND=not determined

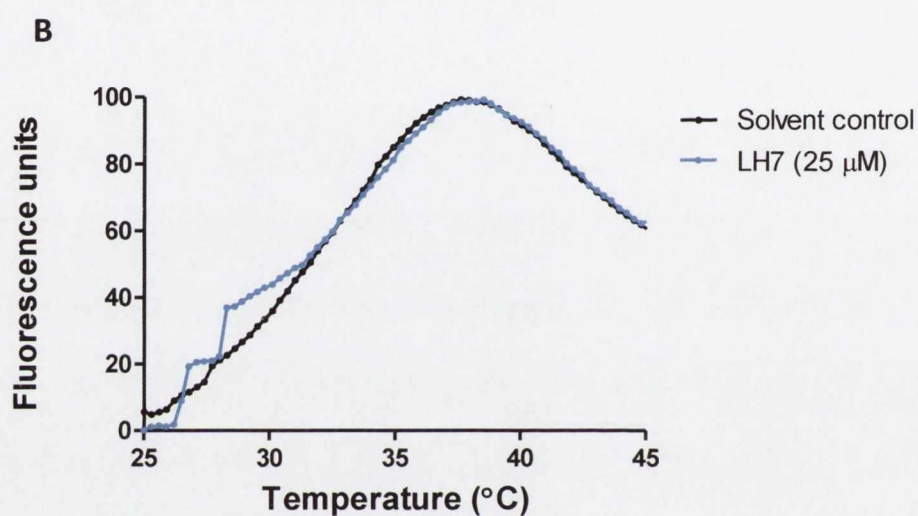
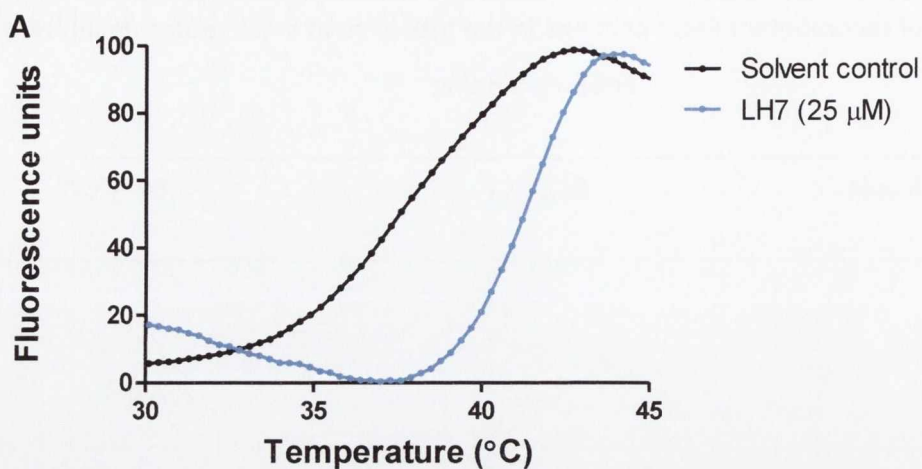


FIG 4.18 LH7 significantly increases the melting temperature of FnBPB_{N2N3}. Differential scanning fluorimetry was carried out with recombinant His-FnBPB_{N2N3} (A) and His-FnBPB_{N312AF314A} (B) proteins (0.5 mg/ml) and the reporter dye SYPRO orange in the presence of LH7 (25 μM). A DMSO (solvent) control was also carried out. Thermal melt curves were generated using Prism Graphpad software version 5.01 and are the mean of 3 (A) and 2 (B) independent experiments. Fluorescence values were normalised relative to the minimum and maximum fluorescence values as 0 and 100 fluorescence units, respectively. Thermal melt curves of fluorescence units vs temperature (°C) were assessed. The melting temperature was identified as the temperature corresponding to a fluorescence units value of 50.

this site would be consistent with inhibition of FnBPB-mediated bacterial adherence to fibrinogen in the presence of LH7 (Fig 4.16B) and the predicted docking site of LH7 on FnBPB (Fig 4.17C).

4.3 Discussion

There is a growing body of evidence highlighting the importance of the cell wall-anchored proteins FnBPA and FnBPB in mediating biofilm accumulation in clinically relevant lineages of *S. aureus*; namely CC8 and CC22 including HA- and CA-MRSA strains (O'Neill *et al.*, 2008, McCourt *et al.*, 2014, Planet *et al.*, 2013, Mashruwala *et al.*, 2017). It has recently emerged that, in the case of FnBPA, homophilic interactions between FnBPA proteins on neighbouring bacteria allow this biofilm accumulation to occur (Herman-Bausier *et al.*, 2015). FnBPA homophilic interactions have previously been localised to subdomains N2 and N3 although the binding sites involved remained unknown (Geoghegan *et al.*, 2013, Herman-Bausier *et al.*, 2015). Here, we further localise FnBPA-FnBPA interactions to the N2 subdomain (Fig 4.3). This is reminiscent of SdrC homophilic interactions in biofilm which also consist of N2-N2 interactions (Barbu *et al.*, 2014). FnBPA-mediated biofilm accumulation and adherence to fibrinogen (Fg) occur through two distinct mechanisms (Geoghegan *et al.*, 2013). This is further supported here, as the N3 subdomain, which is essential in FnBPA-mediated adherence to Fg, is not required for homophilic interactions. This study showed, for the first time, that FnBPB proteins also form homophilic interactions *in vitro* (Fig 4.8). These interactions differed from FnBPA *in vitro* as both recombinant N2 and N3 subdomains of FnBPB contributed to FnBPB-FnBPB homophilic interactions (Fig 4.8). Further experiments could explore whether recombinant FnBPB proteins form N2-N3 interactions or whether N2 binds N2 and N3 binds N3.

In an attempt to further localise the binding sites involved in FnBPA-FnBPA interactions, this study assessed whether isotypes of FnBPA which contain a large amount of natural amino acid sequence variation in their N2 subdomains (Loughman *et al.*, 2008) are capable of mediating biofilm. To date, only isotype I of FnBPA has been shown to mediate biofilm (O'Neill *et al.*, 2008, Geoghegan *et al.*, 2013). This study found that the five FnBPA isotypes tested here, namely isotypes III, IV, V and VI, can mediate biofilm along with isotype I despite the isotypes sharing only 75-84% amino acid identity in their N2 subdomains (Fig 4.4). This result suggests that the residues within the FnBPA-FnBPA binding sites are likely to be conserved across the isotypes tested here. In a wider context, these data highlight that the ability to form

biofilm is conserved across FnBPA isotypes. This is not unexpected as the ability to form biofilm allows bacteria to survive in many harsh environments. In the case of *S. aureus*, the ability to form biofilms on indwelling medical devices or host tissue allows them to evade host immune phagocytosis and conventional antibiotic treatment (Section 1.7). Other important functions of FnBPA N2N3 subdomains, namely binding of host proteins fibrinogen and elastin are also conserved across FnBPA isotypes despite sequence divergence (Loughman *et al.*, 2008, Burke *et al.*, 2010).

Along with FnBPA many *S. aureus* strains express a second fibronectin binding protein; FnBPB. FnBPB also mediates biofilm accumulation (O'Neill *et al.*, 2008) through homophilic interactions (Fig 4.8). When expressed alone, both FnBPA and FnBPB can mediate biofilm (Geoghegan *et al.*, 2013, O'Neill *et al.*, 2008). However, the possibility that FnBPA and FnBPB proteins expressed on neighbouring bacteria may interact in a heterophilic manner has not been explored. Here, we present data showing that recombinant FnBPA and FnBPB proteins are capable of interacting and that the N2 subdomains are involved in these interactions (Fig 4.5). These data suggest the possibility of FnBPA and FnBPB forming a heterophilic interaction in biofilm accumulation. However, the biological relevance of this interaction occurring when full length FnBPA and FnBPB proteins are expressed on the surface of *S. aureus* remains unknown. In order to appropriately assess this without interference from FnBPA-FnBPA and FnBPB-FnBPB homophilic interactions, single cell techniques could be used such as single cell spectroscopy. Single cell spectroscopy is an atomic force microscopy technique which allows interactions of proteins expressed on single cells to be assessed. In this case, single cells of *S. aureus* expressing FnBPA alone or FnBPB alone could be tested for heterophilic binding and the strength of interaction measured. This technique has been successfully used to measure homophilic interactions of FnBPA (Herman-Bausier *et al.*, 2015) and SdrC (Fig 3.16, Feuillie *et al.*, 2017) proteins expressed on the surface of *S. aureus*. Whether FnBPA-FnBPB heterophilic interactions do occur between *S. aureus* cells could be assessed visually using confocal microscopy. A biofilm consisting of FnBPA⁺ and FnBPB⁺ cells differentially tagged with mCherry and GFP, respectively, could be set up. These experiments would allow colocalisation of FnBPA⁺ and FnBPB⁺ cells to be visualised or, if heterophilic interactions do not occur,

FnBPA⁺ cells may aggregate separately to FnBPB⁺ cells in the biofilm. Previous studies would suggest that if this type of interaction does occur that it is not essential to *S. aureus* biofilm accumulation as expression of FnBPA or FnBPB alone can restore the ability of *S. aureus* deletion mutants of both *fnbA* and *fnbB* to form biofilm (Geoghegan *et al.*, 2013, O'Neill *et al.*, 2008). However, in these studies *fnbA* and *fnbB* are expressed on multicopy plasmids and therefore their expression may be higher than on the chromosome of the parental strain.

Amino acid alignments of the N2 subdomains of the five FnBPA isotypes tested in this study and FnBPB were carried out in order to identify regions of amino acid sequence conservation (Fig 4.6A). Six sites were identified and mapped onto the crystal structure of FnBPA to assess if they are surface exposed and thus, available for interaction (Fig 4.6B). From these analyses, three sites; site 1, site 4 and site 6, were selected for alteration as they cover the largest areas of amino acid conservation and are surface exposed (Fig 4.6). Segments and not individual residues were altered to the equivalent region in ClfA (Fig 4.7). The variant proteins did not have a reduced ability to form FnBPA homophilic interactions (Fig 4.7) and from these analyses the dimerization sites of FnBPA were not identified. However, the data for the site 4 variant protein (His-FnBPA_{Site4}) is not reliable as this protein lost the ability to bind Fg (Fig 4.7B) and thus, may not be correctly folded or functional. To assess if His-FnBPA_{Site4} is correctly folded, nuclear magnetic resonance (NMR) experiments could be performed comparing the structure of native His-FnBPA_{N2N3} and His-FnBPA_{Site4}. There are several possible reasons why the dimerization sites were not identified in this study. Firstly, it is possible that none of the sites analysed are involved in FnBPA homophilic interactions. It is possible the alteration to ClfA sequence may not have been sufficient as several residues in each site were conserved in the ClfA sequence (Fig 4.7A). Thus, some of the residues were not altered in the sequence swaps. Further studies to identify the FnBPA-FnBPA binding sites are required. Phage display was used previously in the identification of SdrC-SdrC dimerization sites and thus, could be employed in this case (Barbu *et al.*, 2014). However, it is not always successful. Crystallization of the FnBPA N2 or N2N3 dimer would clearly allow the binding sites to be identified. Co-

crystallization of the small molecule FnBP biofilm inhibitors identified here (Table 3.2, Fig 4.10) in complex with FnBPA could also highlight at least one dimerization site.

A major aim of this study was to explore FnBP homophilic interactions as novel targets for anti-biofilm agents. Anti-biofilm agents against *S. aureus* are needed clinically. *S. aureus* is a major cause of indwelling device related infections which involve formation of a biofilm. Treatment of *S. aureus* infections is already complicated with the widespread emergence of antibiotic resistant *S. aureus* strains (Section 1.7.3, Foster, 2017). However, treatment of biofilm infections is more complex due to the nature of a mature biofilm. Once a biofilm is established, it is refractive to conventional antibiotics and resistant to host immune phagocytosis (Section 1.7). These infections also serve as foci for secondary infections with bacteria shedding from biofilms to other sites (Speziale *et al.*, 2014). Not surprisingly, treatment of biofilm infections typically involves removal of the device (Hogan *et al.*, 2015). Thus, the identification of novel targets for anti-biofilm agents and discovery of new agents is of great clinical importance.

Here, this study presents a novel strategy for prevention of biofilm through the disruption of FnBP homophilic interactions. This would be extremely advantageous as it would prevent the mature, difficult to treat biofilm from being established. In this study, *in silico* docking approaches targeting FnBPA led to the identification of several small molecule inhibitors which inhibit FnBPA homophilic interactions (Fig 4.12) and prevent biofilm formation by HA-MRSA clinical isolates *in vitro* (Fig 4.10) without affecting bacterial growth (Fig 4.11). A limitation is that binding of the small molecules to recombinant FnBPA_{N2N3} protein could not be demonstrated using DSF (Table 4.2). This may be due to a limitation of DSF as small molecule binding must infer stabilisation to the protein structure. Thus, further studies of small molecule protein binding could be carried out using more sensitive techniques such as Isothermal Titration calorimetry, NMR or co-crystallization of small molecule protein complexes. In particular, a study combining these techniques would allow binding affinities and binding sites of the small molecules to be elucidated.

This study also identified three inhibitors of FnBP-mediated adherence to Fg LH6, LH7 and LH10 (Figs 4.14, 4.15). FnBP-mediated adherence to Fg is an important virulence mechanism previously shown to promote *S. aureus* adhesion to thrombi, primary attachment to biotic surfaces and in promoting bacterial aggregation and biofilm formation in synovial fluid (Dastgheyb *et al.*, 2015). All three inhibitors are predicted to dock in the ligand binding trench overlapping the binding site of the Fg γ -chain peptide (Fig 4.14). Thus, the *in silico* predicted docking sites correlate well with the ability of all three inhibitors to prevent FnBP-mediated adherence of *S. aureus* to Fg *in vitro*. Furthermore, DSF data for LH7 supports its predicted binding site (Fig 4.18).

FnBPA and FnBPB also bind the host proteins elastin (Keane *et al.*, 2007, Roche *et al.*, 2004, Burke *et al.*, 2010) and plasminogen (Pietrocola *et al.*, 2016) through their N2 and N3 subdomains. Fg and elasin bind at the same site in the ligand binding trench of FnBPs (Keane *et al.*, 2007, Burke *et al.*, 2010). Thus, it is likely that LH6, LH7 and LH10, which are predicted to block Fg binding in the trench, will also inhibit FnBP-mediated adherence of *S. aureus* to elastin. The binding mechanism differs for FnBP-mediated adherence to plasminogen. FnBPB-plasminogen binding is mediated by the N3 subdomain alone and the binding site of plasminogen does not overlap with that of Fg (Pietrocola *et al.*, 2016). The plasminogen binding site of FnBPA remains unknown. Therefore, it is unlikely, at least in the case of FnBPB, that LH6, LH7 and LH10 would reduce the ability of FnBPB to bind plasminogen unless the inhibitors have a second binding site.

Thus, small molecules targeting two different functions of FnBPs have been identified in this study. LH1, LH2, LH3 and LH5 act as anti-biofilm agents inhibiting FnBP-mediated biofilm accumulation (Fig 4.10) and could be further investigated as leads in the development of non-antibiotic drugs for inhibiting *S. aureus* biofilm. LH6, LH7 and LH10 inhibit FnBP-mediated adherence of *S. aureus* to Fg (Fig 4.15) and could act as leads for the development of anti-adhesion agents. Detailed structure and activity relationships (SARs) analyses could be carried out to optimise and improve the potency of the inhibitors identified here to allow the development of a larger, more potent drug-like molecule. Notably, not all *S. aureus* biofilms are dependent upon FnBPs and *S. aureus* biofilm is a multifactorial process (Section 1.5). Thus, FnBP biofilm

inhibitors would likely be used in combination with other targeted inhibitors. A similar strategy would also be employed for inhibition of *S. aureus* adherence to Fg due to the functional redundancy among *S. aureus* cell wall-anchored proteins.

In conclusion, this study has contributed to our understanding of FnBP-FnBP interactions and evaluated these interactions as a target for anti-biofilm agents. **Further studies probing molecular interactions in *S. aureus* biofilm and targeted inhibitor studies** would allow these preventive therapies to be developed. Furthermore, small molecule inhibitors of FnBP-mediated biofilm and adherence to Fg have been identified here and may serve as leads in the further development of anti-biofilm and anti-adhesion agents.

Chapter 5

Discussion

5.1 Discussion

S. aureus is a leading cause of indwelling medical device related infections which typically involve formation of a biofilm. *S. aureus* biofilm formation is multifactorial and considered to occur in three distinct phases: primary attachment, accumulation and maturation followed by biofilm dispersal (Section 1.5, Speziale *et al.*, 2014). Biofilm infections are intrinsically difficult to treat. Once a mature biofilm is formed, it is refractive to conventional antibiotics and resistant to host immune phagocytosis (Section 1.7, Speziale *et al.*, 2014). More specifically, the bacteria are embedded in a multicellular community which in some instances is surrounded by a self-synthesized matrix where antibiotic and immune cell access is limited. Furthermore, bacteria in a mature biofilm lie in a dormant state. As most commonly used antibiotics target processes which are essential in actively dividing *S. aureus* cells, these compounds are not effective against dormant bacteria. Thus, biofilm infections cause a significant health burden where treatment often involves removal of the device (Hogan *et al.*, 2015). Another major health burden is the secondary infections which may occur as a result of a biofilm infection. Biofilms may act as foci of infection whereby bacterial cells can shed from the biofilm, migrate and establish infections at other sites of the body. For example, device related infections are a major cause of subsequent bloodstream infections (Hogan *et al.*, 2015). There is also the issue of widespread drug resistance among *S. aureus*, particularly the emergence of both hospital associated (HA)- and community associated (CA)-methicillin resistant *S. aureus* (MRSA) strains, which further complicates treatment (Section 1.7.3). Thus, there is a great need for novel preventive and treatment strategies to combat *S. aureus* biofilm infections.

In order to develop these novel strategies, further investigations into the molecular interactions and factors underpinning biofilm formation are required. These studies will aid in the identification of suitable, novel targets for anti-biofilm agents and the rational development of such agents. These *in vitro* studies should be combined with *in vivo* models of infection such as mouse (Vergara-Irigaray *et al.*, 2009) or rat (Schaeffer *et al.*, 2015) catheter models of infection or foreign body infection models such as the tissue cage model (Zimmerli *et al.*, 1982) to correlate findings to infection. Overall, a combined understanding of *S. aureus* biofilm formation, investigation of

bacterial targets and identification of anti-biofilm agents will allow the development of novel therapeutics for the treatment of biofilm infections.

The overall major aim of this thesis was to assess homophilic interactions of the *S. aureus* cell wall-anchored serine aspartate repeat (Sdr) C protein and the fibronectin binding proteins (FnBPs) as novel targets for anti-biofilm agents. The objective was to inhibit biofilm accumulation and thus, prevent a mature biofilm, which is refractive to antibiotic treatment, from forming. Such anti-biofilm agents would have many advantages. As the agents are targeting specific protein interactions but not inhibiting bacterial growth there would be considerably less selective pressure for drug resistance in comparison to antibiotics. This is an important concern with any preventive or treatment strategy as widespread antimicrobial drug resistance has become a major public health threat. There are a number of reasons for the reduction in selective pressure associated with anti-biofilm agents. Antibiotics target essential pathways in microbial growth such as protein synthesis and these pathways are well conserved across diverse bacterial species (Dickey *et al.*, 2017). Due to this, antibiotics provide major selective pressure on bacterial populations to resist killing. Furthermore, antimicrobial targets are typically conserved across many bacterial species and so, a mutated target or resistance mechanism may be transferred horizontally among many, unrelated bacterial species. In contrast, anti-biofilm agents have targets that are specific to a bacterial species or, at most, closely related bacteria. In the case of SdrC and FnBPs, they are only found in *S. aureus*.

Another advantage of this targeted anti-biofilm approach in this regard, is that, escape mutants are less likely to arise as the inhibitors target specific protein residues important in homophilic interactions in biofilm. Mutation of such sites would likely render the bacteria unable to form SdrC- or FnBP-mediated biofilm. The targets in this study are also surface exposed so penetration of the thick *S. aureus* cell wall is not required and efflux as a resistance mechanism does not apply. However, there is the possibility of the acquisition of other biofilm accumulation factors such as the *S. aureus* surface protein (Sas) X (Li *et al.*, 2012) or the *ica* locus (Jiang *et al.*, 2013, Fessler *et al.*, 2017) on mobile genetic elements which would provide an alternative way for the bacteria to accumulate. To augment this, a combination of specific inhibitors of

different biofilm factors could be employed although this adds further complexity to the development and implementation of such preventive therapy.

The use of anti-biofilm agents to prevent biofilm infections would also reduce the administration of antibiotics which, as mentioned, are largely unsuccessful in treating biofilm infections. Thus, these agents would alleviate at least some of the selective pressure imposed by antibiotics (Dickey *et al.*, 2017). Furthermore, anti-biofilm agents would be capable of preventing biofilm infections by *S. aureus* strains which have already acquired antibiotic resistance including widespread HA- and CA-MRSA strains.

There are several other advantages of the specificity of anti-biofilm agents. As the agents target specific *S. aureus* biofilm factors, in this case the cell wall-anchored proteins SdrC and FnBPs, they are unlikely to affect the host's microbiota which do not express these specific factors. This differs from broad spectrum antibiotics which affect essential pathways conserved among both the infecting pathogen and the host's microbiota. A major negative effect of the killing of host microbiota species by broad spectrum antibiotics has been the increase in *Clostridium difficile* infections in hospital settings (Dickey *et al.*, 2017). If an agent is highly specific this should also correlate with lower toxicity towards host cells as the specific target will only be associated with the infecting pathogen.

Although, anti-biofilm drugs have many favourable attributes, their development for prophylactic clinical use is not without several drawbacks. For the identification of an agent targeting a single, specific factor a lot more time, studies and cost is required in comparison to an antibiotic. Studies include in depth characterisation of each specific target, its role in biofilm both at the molecular level and *in vivo* and subsequent identification of novel agents. The identification of novel agents will most likely be followed by studies to improve the specific targeting, potency and toxicity of those agents. Furthermore, for anti-biofilm agents such as those identified in this study, a single agent would not be sufficient clinically to prevent *S. aureus* biofilm infections. This is because *S. aureus* biofilm formation is multifactorial (Section 1.5, Speziale *et al.*, 2014, Otto, 2008) and *S. aureus* displays a high level of functional redundancy among its cell wall-anchored proteins (Section 1.4, Foster *et al.*, 2014). Thus, a combination of

agents targeting different biofilm accumulation factors would be required. To improve such preventive strategies, these agents could be combined with anti-biofilm agents which prevent primary attachment of bacteria to the device. This would allow targeting of two important steps in biofilm formation; primary attachment and accumulation, prior to the formation of a mature biofilm.

Alternatively, an anti-biofilm agent with a wider spectrum of activity could be developed. Within this study itself, several of the small molecules identified were capable of inhibiting functions of both SdrC and FnBPs. LH1 and LH3 reduced SdrC-mediated biofilm of the surrogate host *L. lactis* and FnBP-dependent biofilm of the HA-MRSA strains BH1CC and DAR70. Thus, they may target both factors in biofilm accumulation. LH6, LH7 and LH10 inhibited SdrC-mediated biofilm of *L. lactis* and FnBP-mediated adherence to fibrinogen (Fg) with LH10 also inhibiting MRSA252 biofilm formation. Thus, these small molecules could act as inhibitors of primary attachment to devices coated with human Fg and SdrC-mediated biofilm accumulation. There is also potential for LH6, LH7 and LH10 to inhibit fibrin-dependent biofilm formation where fibrinogen and fibrin binding by cell wall-anchored proteins is important (Zapotoczna *et al.*, 2015, Dastgheyb *et al.*, 2015). This spectrum of activity is likely due to the conserved N2N3 subdomain structure adopted by members of the microbial surface components recognizing adhesive matrix molecules (MSCRAMM) family of *S. aureus* cell wall-anchored proteins of which SdrC and FnBPs are members (Section 1.4.1). Thus, there is potential for a pan-MSCRAMM inhibitor to be developed which may be of more interest clinically. This could be taken into account if a second generation of the molecules in this study are to be developed.

Finally, in the case of anti-biofilm agents which prevent biofilm accumulation, the agents will not eradicate the source of planktonic bacteria available to form biofilm. These bacteria would still have to be removed by the host immune system or antibiotics. However, treatment of such planktonic bacteria is more achievable than bacteria embedded in a biofilm which are largely refractive to antibiotics.

Alongside assessing novel targets for anti-biofilm agents and identifying agents themselves, it is important to further our understanding of the bacterial targets. Thus,

to support the assessment of SdrC and FnBPs as targets for anti-biofilm agents this study also aimed to further characterize SdrC and FnBPs roles in biofilm accumulation at the molecular level. In the case of SdrC, an important objective was to identify if SdrC's ability to mediate biofilm was of clinical relevance. To date, SdrC has been shown to promote biofilm in the *S. aureus* lab strain Newman (Barbu *et al.*, 2014). Here, we present data showing that SdrC promotes biofilm in the HA-MRSA clinical isolate MRSA252 and that adjacent MRSA252 cells interact through specific SdrC-SdrC interactions. MRSA252 is a member of the EMRSA-16 clone, an important *S. aureus* clone globally (Holden *et al.*, 2004). These data indicate that SdrC-mediated biofilm is clinically relevant. Further studies into the role of SdrC in biofilm formed by other clinically relevant *S. aureus* lineages would be required to assess the extent of SdrC's relevance. This has been somewhat assessed previously although the approach used was indirect. A panel of strains were assessed for inhibition of biofilm formation by addition of recombinant SdrC N2 *in vitro* (Barbu *et al.*, 2014). These data suggested that in approximately 50 % of the isolates tested SdrC promotes biofilm formation. Notably, the dimerization motifs 'RPGSV' and 'VQDYT' were conserved across 134 sequences assessed in the study (Barbu *et al.*, 2014). In order to directly assess a role for SdrC in a wider clinical context, isogenic *sdrC* deletion mutants of specific strains representative of important clinically relevant lineages worldwide could be constructed and compared to the parental strain for the ability to form biofilm. This would clearly address a role for SdrC across the most important *S. aureus* lineages. As these analyses would be *in vitro*, SdrC's role in biofilm should also be assessed in an *in vivo* animal model such as a mouse catheter model of infection.

In the case of FnBPs, this study aimed to further dissect the interactions occurring within biofilm accumulation to support the identification of inhibitors of FnBP-mediated biofilm. This study further localised FnBPA-FnBPA interactions to the N2 subdomain alone with the N3 subdomain not required *in vitro*. FnBPB N2N3 homophilic interactions were demonstrated in this study. In contrast to FnBPA, both recombinant FnBPB subdomains N2 and N3 bound GST-FnBPB_{N2N3} *in vitro* indicating a role for both subdomains in FnBPB-FnBPB interactions. FnBPs have a large amount of natural sequence diversity in their N2 and N3 subdomains with seven isotypes of

FnBPA (Loughman *et al.*, 2008) and FnBPB (Burke *et al.*, 2010) identified to date. Only isotype I of FnBPA has been assessed for the ability to form biofilm (Geoghegan *et al.*, 2013, O'Neill *et al.*, 2008). Here, data are presented showing that isotypes III, IV, V and VI along with isotype I also promote biofilm accumulation despite considerable amino acid sequence variation in their N2 subdomains. This suggests that the sites of FnBPA dimerization are likely to be conserved across the isotypes tested here. Data are also presented here showing that recombinant FnBPA and FnBPB proteins can form heterophilic interactions *in vitro*. This was an interesting observation as FnBPA and FnBPB share only 45 % amino acid identity in their N2 subdomains. The biological relevance of this interaction is yet to be assessed. Thus, several novel observations of FnBPA and FnBPB interactions have been identified here. However, attempts to elucidate the exact sites of FnBPA homophilic interactions in this study were unsuccessful. Resolution of a crystal structure of the FnBPA dimer would identify these sites. This would aid our understanding of FnBPA homophilic interactions in biofilm and allow further development of anti-biofilm agents.

This study has proposed protein homophilic interactions as targets in preventing biofilm *in vitro* with several small molecules identified. These small molecules may act as scaffolds in further drug development as improved potency would be required prior to *in vivo* testing. Further development of these inhibitors should involve a detailed structure and activity relationships (SARs) analysis approach. This could be carried out using a similar *in silico* approach whereby structural analogs of each inhibitor could be docked onto the structures of SdrC and FnBPA at the specified dimerization sites. Increased predicted binding affinities and interactions, particularly those involving hydrogen bonds to the dimerization sites, could then be assessed and compared to the leads for putative improved potency followed by *in vitro* assessment. Through such analyses, substructures will be identified which provide the observed anti-biofilm effects. These can then be optimized or joined with other anti-biofilm structures to improve the overall inhibitor potency or as mentioned previously, the range of activity, for example identifying inhibitors that inhibit several factors in *S. aureus* biofilm accumulation. Gathering further information on the protein-lead inhibitor interactions would also benefit these analyses. A binding affinity and co-crystal structure for each

inhibitor with its target would aid in the specification of the important residues to target, improving knowledge of the type of interaction required and allow comparison of structural analogs based on binding affinity to the target.

From the initial study here a few structural insights can be made which would feed into a SARs analyses study. A common substructure within LH3 (Fig 5.1A), the 2,3-dihydroxyquinoxaline, was observed in the majority of the *in silico* hits obtained when the Zinc lead-like library was docked onto SdrC targeting the 'VDQYT' motif. Notably, for these small molecule hits it was this substructure and not their variable regions which were predicted to interact with the protein. Thus, this substructure was flagged as potentially important and LH3 was selected as a representative small molecule. Thus, this substructure may serve as a starting point for further development. The remainder of the structure could be altered to optimize this small molecule and its potency. Another observation is the similarity in structure of small molecules LH6 and LH7 which have a similar spectrum of inhibition (Fig 5.1B). They both inhibit SdrC-mediated biofilm in the surrogate host *L. lactis* and FnBP-mediated adherence to Fg. Thus, the conserved substructure they share could serve as a useful scaffold and their variable regions could be further altered to improve potency.

Another important part of a SARs analysis would be to remove or replace undesirable functional groups. Small molecule biofilm inhibitors LH1, LH2, LH3 and LH5 all contain a sulphonamide group within their structure. Sulphonamide groups are known to cause allergies in some patients and thus, drugs with this group would never be used clinically. This group should be replaced or removed in any second generation inhibitors. SARs analysis should also examine the structures of the small molecules which had no observed inhibitory effect *in vitro*. Small molecules LH8, LH9, LH11 and LH14 did not inhibit SdrC-mediated biofilm formation. These compounds are all much larger than others in the screen and therefore are less likely to fit into the small pocket/binding trench of SdrC. LH8, LH11 and LH14 are also not linear, unlike LH6, LH7 and LH10, and therefore may not fit into the trench between subdomains N2 and N3. Another aspect not explored in this study was assessing small molecule combinations in order to test for additive or synergistic effects in biofilm inhibition. These tests would be of interest in further evaluating the small molecules identified here and

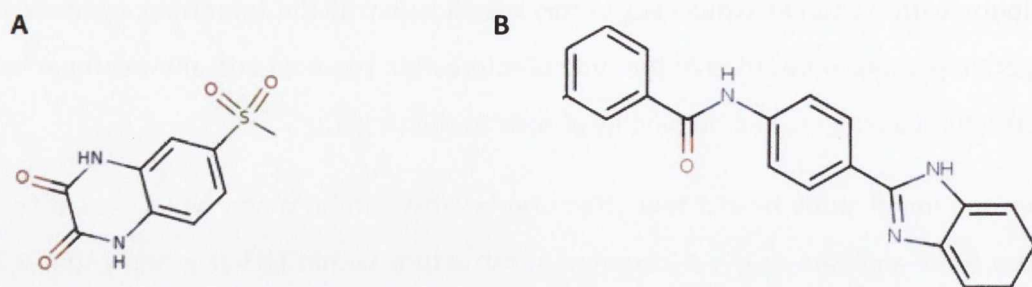


Fig 5.1. Shared small molecule substructures. A) LH3 substructure. Substructure within LH3 found in most docking hits from the Zinc lead-like library targeting the 'VDQYT' of SdrC. B) Common substructure shared between LH6 and LH7. Small molecules LH6 and LH7 share this common central structure with variable regions either side. Atoms are coloured by element with oxygens in red, nitrogens in blue, sulphur in brown, and carbons and hydrogens in black.

second generation molecules. Other essential factors which should be considered in the future development of more potent inhibitors are their solubility and toxicity.

Overall, this study has further characterised SdrC and FnBP interactions in *S. aureus* biofilm accumulation at the molecular level and highlighted these interactions as potential targets for anti-biofilm agents. Several small molecule inhibitors and a peptide inhibitor of *S. aureus* biofilm have been identified here which may be used as lead molecules for further drug design (Fig 5.2). These include inhibitors of primary attachment mediated by FnBP-Fg binding, SdrC-mediated biofilm accumulation and FnBP-mediated biofilm accumulation (Fig 5.2).

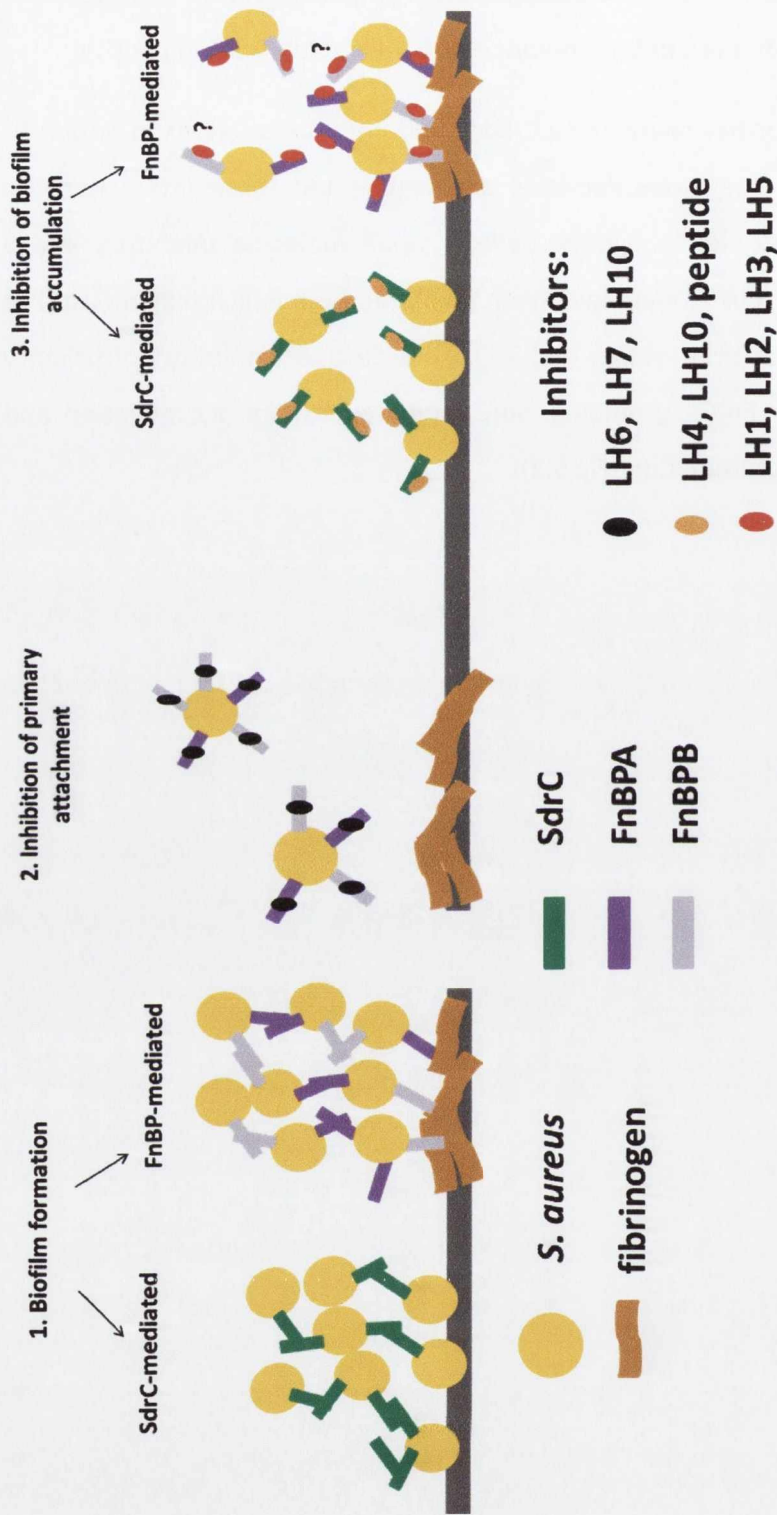


Fig 5.2 Summary model of biofilm inhibitors identified in this study. 1) *S. aureus* cells attach to abiotic surfaces or biotic surfaces. Attachment to biotic surfaces is mediated by MSCRAMM proteins including FnBPA and FnBPB binding host plasma proteins such as fibrinogen (Fg) coated on an indwelling device. SdrC, FnBPA and FnBPB proteins on adjacent bacteria form homophilic interactions promoting bacterial aggregation and biofilm formation. 2) Inhibition of primary attachment. Small molecules LH6, LH7 and LH10 inhibit FnBP-mediated adherence to Fig. 3) Inhibition of biofilm accumulation. Small molecules LH4 and LH10 and the peptide inhibitor inhibit SdrC-mediated biofilm accumulation. Small molecules LH1, LH2, LH3 and LH5 inhibit FnBP-mediated biofilm accumulation. LH1, LH3 and LH5 inhibit FnBPA homophilic interactions *in vitro*. It remains unknown if these small molecules inhibit FnBPB-FnBPB interactions.

References

- Abraham, N.M., and Jefferson, K.K. (2012) *Staphylococcus aureus* clumping factor B mediates biofilm formation in the absence of calcium. *Microbiology* **158**: 1504-1512.
- Abraham, N.M., Lamletthton, S., Fowler, V.G., and Jefferson, K.K. (2012) Chelating agents exert distinct effects on biofilm formation in *Staphylococcus aureus* depending on strain background: role for clumping factor B. *Journal of Medical Microbiology* **61**: 1062-1070.
- Agerer, F., Lux, S., Michel, A., Rohde, M., Ohlsen, K., and Hauck, C.R. (2005) Cellular invasion by *Staphylococcus aureus* reveals a functional link between focal adhesion kinase and cortactin in integrin-mediated internalisation. *Journal of Cell Science* **118**: 2189-2200.
- Aguinaga, A., Frances, M.L., Del Pozo, J.L., Alonso, M., Serrera, A., Lasa, I., and Leiva, J. (2011) Lysostaphin and clarithromycin: a promising combination for the eradication of *Staphylococcus aureus* biofilms. *International Journal of Antimicrobial Agents* **37**: 585-587.
- Alonzo, F., 3rd, and Torres, V.J. (2014) The bicomponent pore-forming leucocidins of *Staphylococcus aureus*. *Microbiology and Molecular Biology Reviews : MMBR* **78**: 199-230.
- Arciola, C.R., Campoccia, D., Ravaioli, S., and Montanaro, L. (2015) Polysaccharide intercellular adhesin in biofilm: structural and regulatory aspects. *Frontiers in Cellular and Infection Microbiology* **5**: 7.
- Arrecubieta, C., Asai, T., Bayern, M., Loughman, A., Fitzgerald, J.R., Shelton, C.E., Baron, H.M., Dang, N.C., Deng, M.C., Naka, Y., Foster, T.J., and Lowy, F.D. (2006) The role of *Staphylococcus aureus* adhesins in the pathogenesis of ventricular assist device-related infections. *The Journal of Infectious Diseases* **193**: 1109-1119.
- Arrecubieta, C., Lee, M.H., Macey, A., Foster, T.J., and Lowy, F.D. (2007) SdrF, a *Staphylococcus epidermidis* surface protein, binds type I collagen. *Journal of Biological Chemistry* **282**: 18767-18776.

- Arrizubieta, M.J., Toledo-Arana, A., Amorena, B., Penades, J.R., and Lasa, I. (2004) Calcium inhibits bap-dependent multicellular behavior in *Staphylococcus aureus*. *Journal of Bacteriology* **186**: 7490-7498.
- Askarian, F., Ajayi, C., Hanssen, A.M., van Sorge, N.M., Pettersen, I., Diep, D.B., Sollid, J.U., and Johannessen, M. (2016) The interaction between *Staphylococcus aureus* SdrD and desmoglein 1 is important for adhesion to host cells. *Scientific Reports* **6**: 22134.
- Atkin, K.E., MacDonald, S.J., Brentnall, A.S., Potts, J.R., and Thomas, G.H. (2014) A different path: revealing the function of staphylococcal proteins in biofilm formation. *FEBS letters* **588**: 1869-1872.
- Baird-Parker, A.C. (1965) Staphylococci and their classification. *Annals of the New York Academy of Sciences* **128**: 4-25.
- Barbu, E.M., Ganesh, V.K., Gurusiddappa, S., Mackenzie, R.C., Foster, T.J., Sudhof, T.C., and Hook, M. (2010) beta-Neurexin is a ligand for the *Staphylococcus aureus* MSCRAMM SdrC. *PLOS Pathogens* **6**: e1000726.
- Barbu, E.M., Mackenzie, C., Foster, T.J., and Hook, M. (2014) SdrC induces staphylococcal biofilm formation through a homophilic interaction. *Molecular Microbiology*.
- Baur, S., Rautenberg, M., Faulstich, M., Grau, T., Severin, Y., Unger, C., Hoffmann, W.H., Rudel, T., Autenrieth, I.B., and Weidenmaier, C. (2014) A nasal epithelial receptor for *Staphylococcus aureus* WTA governs adhesion to epithelial cells and modulates nasal colonization. *PLOS Pathogens* **10**: e1004089.
- Becker, K., Heilmann, C., and Peters, G. (2014a) Coagulase-negative staphylococci. *Clinical Microbiology Reviews* **27**: 870-926.
- Becker, K., and von Eiff, C., (2011) *Staphylococcus, Micrococcus, and Other Catalase-Positive Cocci**. In: Manual of Clinical Microbiology, 10th Edition. American Society of Microbiology, pp.
- Becker, S., Frankel, M.B., Schneewind, O., and Missiakas, D. (2014b) Release of protein A from the cell wall of *Staphylococcus aureus*. *Proceedings of the National Academy of Sciences of the United States of America* **111**: 1574-1579.
- Begier, E., Seiden, D.J., Patton, M., Zito, E., Severs, J., Cooper, D., Eiden, J., Gruber, W.C., Jansen, K.U., Anderson, A.S., and Gurtman, A. (2017) SA4Ag, a 4-antigen

- Staphylococcus aureus* vaccine, rapidly induces high levels of bacteria-killing antibodies. *Vaccine* **35**: 1132-1139.
- Bhattacharya, M., Wozniak, D.J., Stoodley, P., and Hall-Stoodley, L. (2015) Prevention and treatment of *Staphylococcus aureus* biofilms. *Expert Review of Anti-infective Therapy* **13**: 1499-1516.
- Biswas, R., Voggu, L., Simon, U.K., Hentschel, P., Thumm, G., and Gotz, F. (2006) Activity of the major staphylococcal autolysin Atl. *FEMS microbiology letters* **259**: 260-268.
- Boles, B.R., and Horswill, A.R. (2008) Agr-mediated dispersal of *Staphylococcus aureus* biofilms. *PLOS Pathogens* **4**: e1000052.
- Bookstaver, P.B., Williamson, J.C., Tucker, B.K., Raad, II, and Sherertz, R.J. (2009) Activity of novel antibiotic lock solutions in a model against isolates of catheter-related bloodstream infections. *The Annals of Pharmacotherapy* **43**: 210-219.
- Bowden, M.G., Heuck, A.P., Ponnuraj, K., Kolosova, E., Choe, D., Gurusiddappa, S., Narayana, S.V., Johnson, A.E., and Hook, M. (2008) Evidence for the "dock, lock, and latch" ligand binding mechanism of the staphylococcal microbial surface component recognizing adhesive matrix molecules (MSCRAMM) SdrG. *Journal of Biological Chemistry* **283**: 638-647.
- Brady, R.A., Leid, J.G., Camper, A.K., Costerton, J.W., and Shirtliff, M.E. (2006) Identification of *Staphylococcus aureus* proteins recognized by the antibody-mediated immune response to a biofilm infection. *Infection and Immunity* **74**: 3415-3426.
- Brady, R.A., O'May, G.A., Leid, J.G., Prior, M.L., Costerton, J.W., and Shirtliff, M.E. (2011) Resolution of *Staphylococcus aureus* biofilm infection using vaccination and antibiotic treatment. *Infection and Immunity* **79**: 1797-1803.
- Brown, A.F., Murphy, A.G., Lalor, S.J., Leech, J.M., O'Keeffe, K.M., Mac Aogain, M., O'Halloran, D.P., Lacey, K.A., Tavakol, M., Hearnden, C.H., Fitzgerald-Hughes, D., Humphreys, H., Fennell, J.P., van Wamel, W.J., Foster, T.J., Geoghegan, J.A., Lavelle, E.C., Rogers, T.R., and McLoughlin, R.M. (2015) Memory Th1 Cells Are Protective in Invasive *Staphylococcus aureus* Infection. *PLOS Pathogens* **11**: e1005226.

- Brown, S., Santa Maria, J.P., Jr., and Walker, S. (2013) Wall teichoic acids of Gram-positive bacteria. *Annual Review of Microbiology* **67**: 313-336.
- Burke, F.M., Di Poto, A., Speziale, P., and Foster, T.J. (2011) The A domain of fibronectin-binding protein B of *Staphylococcus aureus* contains a novel fibronectin binding site. *The FEBS journal* **278**: 2359-2371.
- Burke, F.M., McCormack, N., Rindi, S., Speziale, P., and Foster, T.J. (2010) Fibronectin-binding protein B variation in *Staphylococcus aureus*. *BMC Microbiology* **10**: 160.
- Buttner, H., Mack, D., and Rohde, H. (2015) Structural basis of *Staphylococcus epidermidis* biofilm formation: mechanisms and molecular interactions. *Frontiers in Cellular and Infection Microbiology* **5**: 14.
- Cedergren, L., Andersson, R., Jansson, B., Uhlen, M., and Nilsson, B. (1993) Mutational analysis of the interaction between staphylococcal protein A and human IgG1. *Protein Engineering* **6**: 441-448.
- Chambers, H.F., and Deleo, F.R. (2009) Waves of resistance: *Staphylococcus aureus* in the antibiotic era. *Nature Reviews Microbiology* **7**: 629-641.
- Chauhan, A., Lebeaux, D., Ghigo, J.M., and Beloin, C. (2012) Full and broad-spectrum *in vivo* eradication of catheter-associated biofilms using gentamicin-EDTA antibiotic lock therapy. *Antimicrobial Agents and Chemotherapy* **56**: 6310-6318.
- Chemical Computing Group Inc., S.S.W., Suite #910, Montreal, QC, Canada, H3A 2R7,, (2015.) *Molecular Operating Environment (MOE)*.
- Cheng, A.G., Kim, H.K., Burts, M.L., Krausz, T., Schneewind, O., and Missiakas, D.M. (2009) Genetic requirements for *Staphylococcus aureus* abscess formation and persistence in host tissues. *FASEB journal : official publication of the Federation of American Societies for Experimental Biology* **23**: 3393-3404.
- Claes, J., Liesenborghs, L., Peetermans, M., Veloso, T.R., Missiakas, D., Schneewind, O., Mancini, S., Entenza, J.M., Hoylaerts, M.F., Heying, R., Verhamme, P., and Vanassche, T. (2017) Clumping factor A, von Willebrand factor-binding protein and von Willebrand factor anchor *Staphylococcus aureus* to the vessel wall. *Journal of Thrombosis and Haemostasis : JTH* **15**: 1009-1019.

- Clarke, S.R., Andre, G., Walsh, E.J., Dufrêne, Y.F., Foster, T.J., and Foster, S.J. (2009) Iron-Regulated Surface Determinant Protein A Mediates Adhesion of *Staphylococcus aureus* to Human Corneocyte Envelope Proteins. *Infection and Immunity* **77**: 2408-2416.
- Clarke, S.R., Brummell, K.J., Horsburgh, M.J., McDowell, P.W., Mohamad, S.A., Stapleton, M.R., Acevedo, J., Read, R.C., Day, N.P., Peacock, S.J., Mond, J.J., Kokai-Kun, J.F., and Foster, S.J. (2006) Identification of *in vivo*-expressed antigens of *Staphylococcus aureus* and their use in vaccinations for protection against nasal carriage. *The Journal of Infectious Diseases* **193**: 1098-1108.
- Clarke, S.R., and Foster, S.J. (2008) IsdA Protects *Staphylococcus aureus* against the Bactericidal Protease Activity of Apolactoferrin. *Infection and Immunity* **76**: 1518-1526.
- Clarke, S.R., Mohamed, R., Bian, L., Routh, A.F., Kokai-Kun, J.F., Mond, J.J., Tarkowski, A., and Foster, S.J. (2007) The *Staphylococcus aureus* surface protein IsdA mediates resistance to innate defenses of human skin. *Cell Host & Microbe* **1**: 199-212.
- Conlon, B.P. (2014) *Staphylococcus aureus* chronic and relapsing infections: Evidence of a role for persister cells: An investigation of persister cells, their formation and their role in *S. aureus* disease. *BioEssays : News and Reviews in Molecular, Cellular and Developmental Biology* **36**: 991-996.
- Conlon, B.P., Geoghegan, J.A., Waters, E.M., McCarthy, H., Rowe, S.E., Davies, J.R., Schaeffer, C.R., Foster, T.J., Fey, P.D., and O'Gara, J.P. (2014) Role for the A domain of unprocessed accumulation-associated protein (Aap) in the attachment phase of the *Staphylococcus epidermidis* biofilm phenotype. *Journal of Bacteriology* **196**: 4268-4275.
- Conrady, D.G., Brescia, C.C., Horii, K., Weiss, A.A., Hassett, D.J., and Herr, A.B. (2008) A zinc-dependent adhesion module is responsible for intercellular adhesion in staphylococcal biofilms. *Proceedings of the National Academy of Sciences of the United States of America* **105**: 19456-19461.
- Conrady, D.G., Wilson, J.J., and Herr, A.B. (2013) Structural basis for Zn²⁺-dependent intercellular adhesion in staphylococcal biofilms. *Proceedings of the National Academy of Sciences of the United States of America* **110**: E202-211.

- Corrigan, R.M., Miajlovic, H., and Foster, T.J. (2009) Surface proteins that promote adherence of *Staphylococcus aureus* to human desquamated nasal epithelial cells. *BMC Microbiology* **9**: 22.
- Corrigan, R.M., Rigby, D., Handley, P., and Foster, T.J. (2007) The role of *Staphylococcus aureus* surface protein SasG in adherence and biofilm formation. *Microbiology* **153**: 2435-2446.
- Cramton, S.E., Gerke, C., Schnell, N.F., Nichols, W.W., and Gotz, F. (1999) The intercellular adhesion (*ica*) locus is present in *Staphylococcus aureus* and is required for biofilm formation. *Infection and Immunity* **67**: 5427-5433.
- Crosby, H.A., Kwiecinski, J., and Horswill, A.R. (2016) *Staphylococcus aureus* Aggregation and Coagulation Mechanisms, and Their Function in Host-Pathogen Interactions. *Advances in Applied Microbiology* **96**: 1-41.
- Cucarella, C., Solano, C., Valle, J., Amorena, B., Lasa, I., and Penades, J.R. (2001) Bap, a *Staphylococcus aureus* surface protein involved in biofilm formation. *Journal of Bacteriology* **183**: 2888-2896.
- Dantes, R., Mu, Y., Belflower, R., and *et al.* (2013) National burden of invasive methicillin-resistant *staphylococcus aureus* infections, united states, 2011. *JAMA Internal Medicine* **173**: 1970-1978.
- Dastgheyb, S., Parvizi, J., Shapiro, I.M., Hickok, N.J., and Otto, M. (2015) Effect of biofilms on recalcitrance of staphylococcal joint infection to antibiotic treatment. *The Journal of Infectious Diseases* **211**: 641-650.
- DeDent, A., Bae, T., Missiakas, D.M., and Schneewind, O. (2008) Signal peptides direct surface proteins to two distinct envelope locations of *Staphylococcus aureus*. *The EMBO Journal* **27**: 2656-2668.
- DeFrancesco, A.S., Masloboeva, N., Syed, A.K., DeLoughery, A., Bradshaw, N., Li, G.W., Gilmore, M.S., Walker, S., and Losick, R. (2017) Genome-wide screen for genes involved in eDNA release during biofilm formation by *Staphylococcus aureus*. *Proceedings of the National Academy of Sciences of the United States of America* **114**: E5969-e5978.
- Deisenhofer, J. (1981) Crystallographic refinement and atomic models of a human Fc fragment and its complex with fragment B of protein A from *Staphylococcus aureus* at 2.9- and 2.8-Å resolution. *Biochemistry* **20**: 2361-2370.

- Deivanayagam, C.C., Wann, E.R., Chen, W., Carson, M., Rajashankar, K.R., Hook, M., and Narayana, S.V. (2002) A novel variant of the immunoglobulin fold in surface adhesins of *Staphylococcus aureus*: crystal structure of the fibrinogen-binding MSCRAMM, clumping factor A. *The EMBO Journal* **21**: 6660-6672.
- DeLeo, F.R., Otto, M., Kreiswirth, B.N., and Chambers, H.F. (2010) Community-associated methicillin-resistant *Staphylococcus aureus*. *Lancet* **375**: 1557-1568.
- Desbois, A.P., and Smith, V.J. (2010) Antibacterial free fatty acids: activities, mechanisms of action and biotechnological potential. *Applied Microbiology and Biotechnology* **85**: 1629-1642.
- Dickey, S.W., Cheung, G.Y.C., and Otto, M. (2017) Different drugs for bad bugs: antivirulence strategies in the age of antibiotic resistance. *Nature Reviews. Drug Discovery* **16**: 457-471.
- Diep, B.A., Gill, S.R., Chang, R.F., Phan, T.H., Chen, J.H., Davidson, M.G., Lin, F., Lin, J., Carleton, H.A., Mongodin, E.F., Sensabaugh, G.F., and Perdreau-Remington, F. (2006) Complete genome sequence of USA300, an epidemic clone of community-acquired methicillin-resistant *Staphylococcus aureus*. *Lancet* **367**: 731-739.
- Diep, B.A., Stone, G.G., Basuino, L., Graber, C.J., Miller, A., des Etages, S.A., Jones, A., Palazzolo-Ballance, A.M., Perdreau-Remington, F., Sensabaugh, G.F., DeLeo, F.R., and Chambers, H.F. (2008) The arginine catabolic mobile element and staphylococcal chromosomal cassette mec linkage: convergence of virulence and resistance in the USA300 clone of methicillin-resistant *Staphylococcus aureus*. *The Journal of Infectious Diseases* **197**: 1523-1530.
- Edwards, A.M., Potter, U., Meenan, N.A., Potts, J.R., and Massey, R.C. (2011) *Staphylococcus aureus* keratinocyte invasion is dependent upon multiple high-affinity fibronectin-binding repeats within FnBPA. *PLOS One* **6**: e18899.
- Edwards, A.M., Potts, J.R., Josefsson, E., and Massey, R.C. (2010) *Staphylococcus aureus* host cell invasion and virulence in sepsis is facilitated by the multiple repeats within FnBPA. *PLOS Pathogens* **6**: e1000964.
- Falugi, F., Kim, H.K., Missiakas, D.M., and Schneewind, O. (2013) Role of Protein A in the Evasion of Host Adaptive Immune Responses by *Staphylococcus aureus*. *mBio* **4**.

- Feil, E.J., Cooper, J.E., Grundmann, H., Robinson, D.A., Enright, M.C., Berendt, T., Peacock, S.J., Smith, J.M., Murphy, M., Spratt, B.G., Moore, C.E., and Day, N.P. (2003) How clonal is *Staphylococcus aureus*? *Journal of Bacteriology* **185**: 3307-3316.
- Fessler, A.T., Zhao, Q., Schoenfelder, S., Kadlec, K., Brenner Michael, G., Wang, Y., Ziebuhr, W., Shen, J., and Schwarz, S. (2017) Complete sequence of a plasmid from a bovine methicillin-resistant *Staphylococcus aureus* harbouring a novel *ica*-like gene cluster in addition to antimicrobial and heavy metal resistance genes. *Veterinary Microbiology* **200**: 95-100.
- Feuillie, C., Formosa-Dague, C., Hays, L.M., Vervaeck, O., Derclaye, S., Brennan, M.P., Foster, T.J., Geoghegan, J.A., and Dufrene, Y.F. (2017) Molecular interactions and inhibition of the staphylococcal biofilm-forming protein SdrC. *Proceedings of the National Academy of Sciences of the United States of America* **114**: 3738-3743.
- Fleury, O.M., McAleer, M.A., Feuillie, C., Formosa-Dague, C., Sansevere, E., Bennett, D.E., Towell, A.M., McLean, W.H.I., Kezic, S., Robinson, D.A., Fallon, P.G., Foster, T.J., Dufrene, Y.F., Irvine, A.D., and Geoghegan, J.A. (2017) Clumping Factor B Promotes Adherence of *Staphylococcus aureus* to Corneocytes in Atopic Dermatitis. *Infection and Immunity* **85**.
- Flick, M.J., Du, X., Prasad, J.M., Raghu, H., Palumbo, J.S., Smeds, E., Hook, M., and Degen, J.L. (2013) Genetic elimination of the binding motif on fibrinogen for the *S. aureus* virulence factor ClfA improves host survival in septicemia. *Blood* **121**: 1783-1794.
- Formosa-Dague, C., Feuillie, C., Beaussart, A., Derclaye, S., Kucharikova, S., Lasa, I., Van Dijck, P., and Dufrene, Y.F. (2016a) Sticky Matrix: Adhesion Mechanism of the Staphylococcal Polysaccharide Intercellular Adhesin. *ACS Nano* **10**: 3443-3452.
- Formosa-Dague, C., Speziale, P., Foster, T.J., Geoghegan, J.A., and Dufrene, Y.F. (2016b) Zinc-dependent mechanical properties of *Staphylococcus aureus* biofilm-forming surface protein SasG. *Proceedings of the National Academy of Sciences of the United States of America* **113**: 410-415.
- Foster, T.J. (2016) The remarkably multifunctional fibronectin binding proteins of *Staphylococcus aureus*. *European journal of clinical microbiology & infectious*

- diseases : official publication of the European Society of Clinical Microbiology* **35**: 1923-1931.
- Foster, T.J. (2017) Antibiotic resistance in *Staphylococcus aureus*. Current status and future prospects. *FEMS Microbiology Reviews* **41**: 430-449.
- Foster, T.J., Geoghegan, J.A., Ganesh, V.K., and Hook, M. (2014) Adhesion, invasion and evasion: the many functions of the surface proteins of *Staphylococcus aureus*. *Nature Reviews Microbiology* **12**: 49-62.
- Foulston, L., Elsholz, A.K., DeFrancesco, A.S., and Losick, R. (2014) The extracellular matrix of *Staphylococcus aureus* biofilms comprises cytoplasmic proteins that associate with the cell surface in response to decreasing pH. *mBio* **5**: e01667-01614.
- Fowler, V.G., Jr., and Proctor, R.A. (2014) Where does a *Staphylococcus aureus* vaccine stand? *Clinical Microbiology and Infection : the official publication of the European Society of Clinical Microbiology and Infectious Diseases* **20 Suppl 5**: 66-75.
- Frenck, R.W., Jr., Creech, C.B., Sheldon, E.A., Seiden, D.J., Kankam, M.K., Baber, J., Zito, E., Hubler, R., Eiden, J., Severs, J.M., Sebastian, S., Nanra, J., Jansen, K.U., Gruber, W.C., Anderson, A.S., and Girgenti, D. (2017) Safety, tolerability, and immunogenicity of a 4-antigen *Staphylococcus aureus* vaccine (SA4Ag): Results from a first-in-human randomised, placebo-controlled phase 1/2 study. *Vaccine* **35**: 375-384.
- Ganesh, V.K., Barbu, E.M., Deivanayagam, C.C., Le, B., Anderson, A.S., Matsuka, Y.V., Lin, S.L., Foster, T.J., Narayana, S.V., and Hook, M. (2011) Structural and biochemical characterization of *Staphylococcus aureus* clumping factor B/ligand interactions. *Journal of Biological Chemistry* **286**: 25963-25972.
- Ganesh, V.K., Rivera, J.J., Smeds, E., Ko, Y.P., Bowden, M.G., Wann, E.R., Gurusiddappa, S., Fitzgerald, J.R., and Höök, M. (2008) A structural model of the *Staphylococcus aureus* ClfA-fibrinogen interaction opens new avenues for the design of anti-staphylococcal therapeutics. *PLOS Pathogens* **4**: e1000226.
- Gasson, M.J. (1983) Plasmid complements of *Streptococcus lactis* NCDO 712 and other lactic streptococci after protoplast-induced curing. *Journal of Bacteriology* **154**: 1-9.

- Geoghegan, J.A., Corrigan, R.M., Gruszka, D.T., Speziale, P., O'Gara, J.P., Potts, J.R., and Foster, T.J. (2010) Role of surface protein SasG in biofilm formation by *Staphylococcus aureus*. *Journal of Bacteriology* **192**: 5663-5673.
- Geoghegan, J.A., and Foster, T.J. (2015) Cell Wall-Anchored Surface Proteins of *Staphylococcus aureus*: Many Proteins, Multiple Functions. *Current Topics in Microbiology and Immunology*.
- Geoghegan, J.A., Monk, I.R., O'Gara, J.P., and Foster, T.J. (2013) Subdomains N2N3 of fibronectin binding protein A mediate *Staphylococcus aureus* biofilm formation and adherence to fibrinogen using distinct mechanisms. *Journal of Bacteriology* **195**: 2675-2683.
- Giersing, B.K., Dastgheyb, S.S., Modjarrad, K., and Moorthy, V. (2016) Status of vaccine research and development of vaccines for *Staphylococcus aureus*. *Vaccine* **34**: 2962-2966.
- Giesbrecht, P., Kersten, T., Maidhof, H., and Wecke, J. (1998) Staphylococcal cell wall: morphogenesis and fatal variations in the presence of penicillin. *Microbiology and Molecular Biology Reviews : MMBR* **62**: 1371-1414.
- Gomez, M.I., Lee, A., Reddy, B., Muir, A., Soong, G., Pitt, A., Cheung, A., and Prince, A. (2004) *Staphylococcus aureus* protein A induces airway epithelial inflammatory responses by activating TNFR1. *Nature Medicine* **10**: 842-848.
- Gomez, M.I., O'Seaghdha, M., Magargee, M., Foster, T.J., and Prince, A.S. (2006) *Staphylococcus aureus* protein A activates TNFR1 signaling through conserved IgG binding domains. *Journal of Biological Chemistry* **281**: 20190-20196.
- Graille, M., Stura, E.A., Corper, A.L., Sutton, B.J., Taussig, M.J., Charbonnier, J.B., and Silverman, G.J. (2000) Crystal structure of a *Staphylococcus aureus* protein A domain complexed with the Fab fragment of a human IgM antibody: structural basis for recognition of B-cell receptors and superantigen activity. *Proceedings of the National Academy of Sciences of the United States of America* **97**: 5399-5404.
- Greene, C., McDevitt, D., Francois, P., Vaudaux, P.E., Lew, D.P., and Foster, T.J. (1995) Adhesion properties of mutants of *Staphylococcus aureus* defective in fibronectin-binding proteins and studies on the expression of *fnb* genes. *Molecular Microbiology* **17**: 1143-1152.

- Gross, M., Cramton, S.E., Gotz, F., and Peschel, A. (2001) Key role of teichoic acid net charge in *Staphylococcus aureus* colonization of artificial surfaces. *Infection and Immunity* **69**: 3423-3426.
- Gruszka, D.T., Whelan, F., Farrance, O.E., Fung, H.K., Paci, E., Jeffries, C.M., Svergun, D.I., Baldock, C., Baumann, C.G., Brockwell, D.J., Potts, J.R., and Clarke, J. (2015) Cooperative folding of intrinsically disordered domains drives assembly of a strong elongated protein. *Nature Communications* **6**: 7271.
- Gruszka, D.T., Wojdyla, J.A., Bingham, R.J., Turkenburg, J.P., Manfield, I.W., Steward, A., Leech, A.P., Geoghegan, J.A., Foster, T.J., Clarke, J., and Potts, J.R. (2012) Staphylococcal biofilm-forming protein has a contiguous rod-like structure. *Proceedings of the National Academy of Sciences of the United States of America* **109**: E1011-1018.
- Hair, P.S., Echague, C.G., Sholl, A.M., Watkins, J.A., Geoghegan, J.A., Foster, T.J., and Cunnion, K.M. (2010) Clumping factor A interaction with complement factor I increases C3b cleavage on the bacterial surface of *Staphylococcus aureus* and decreases complement-mediated phagocytosis. *Infection and Immunity* **78**: 1717-1727.
- Hair, P.S., Foley, C.K., Krishna, N.K., Nyalwidhe, J.O., Geoghegan, J.A., Foster, T.J., and Cunnion, K.M. (2013) Complement regulator C4BP binds to *Staphylococcus aureus* surface proteins SdrE and Bbp inhibiting bacterial opsonization and killing. *Results in Immunology* **3**: 114-121.
- Hammer, N.D., and Skaar, E.P. (2011) Molecular mechanisms of *Staphylococcus aureus* iron acquisition. *Annual Review of Microbiology* **65**: 129-147.
- Harris, L.G., and Richards, R.G. (2004) *Staphylococcus aureus* adhesion to different treated titanium surfaces. *Journal of materials science. Materials in Medicine* **15**: 311-314.
- Hazenbos, W.L., Kajihara, K.K., Vandlen, R., Morisaki, J.H., Lehar, S.M., Kwakkenbos, M.J., Beaumont, T., Bakker, A.Q., Phung, Q., Swem, L.R., Ramakrishnan, S., Kim, J., Xu, M., Shah, I.M., Diep, B.A., Sai, T., Sebrell, A., Khalfin, Y., Oh, A., Koth, C., Lin, S.J., Lee, B.C., Strandh, M., Koefoed, K., Andersen, P.S., Spits, H., Brown, E.J., Tan, M.W., and Mariathasan, S. (2013) Novel staphylococcal

- glycosyltransferases SdgA and SdgB mediate immunogenicity and protection of virulence-associated cell wall proteins. *PLOS Pathogens* **9**: e1003653.
- Heilmann, C., Hussain, M., Peters, G., and Gotz, F. (1997) Evidence for autolysin-mediated primary attachment of *Staphylococcus epidermidis* to a polystyrene surface. *Molecular Microbiology* **24**: 1013-1024.
- Heilmann, C., Schweitzer, O., Gerke, C., Vanittanakom, N., Mack, D., and Gotz, F. (1996) Molecular basis of intercellular adhesion in the biofilm-forming *Staphylococcus epidermidis*. *Molecular Microbiology* **20**: 1083-1091.
- Herman-Bausier, P., El-Kirat-Chatel, S., Foster, T.J., Geoghegan, J.A., and Dufrene, Y.F. (2015) *Staphylococcus aureus* Fibronectin-Binding Protein A Mediates Cell-Cell Adhesion through Low-Affinity Homophilic Bonds. *mBio* **6**: e00413-00415.
- Hochbaum, A.I., Kolodkin-Gal, I., Foulston, L., Kolter, R., Aizenberg, J., and Losick, R. (2011) Inhibitory effects of D-amino acids on *Staphylococcus aureus* biofilm development. *Journal of Bacteriology* **193**: 5616-5622.
- Hogan, S., Stevens, N.T., Humphreys, H., O'Gara, J.P., and O'Neill, E. (2015) Current and future approaches to the prevention and treatment of staphylococcal medical device-related infections. *Current Pharmaceutical Design* **21**: 100-113.
- Holden, M.T., Feil, E.J., Lindsay, J.A., Peacock, S.J., Day, N.P., Enright, M.C., Foster, T.J., Moore, C.E., Hurst, L., Atkin, R., Barron, A., Bason, N., Bentley, S.D., Chillingworth, C., Chillingworth, T., Churcher, C., Clark, L., Corton, C., Cronin, A., Doggett, J., Dowd, L., Feltwell, T., Hance, Z., Harris, B., Hauser, H., Holroyd, S., Jagels, K., James, K.D., Lennard, N., Line, A., Mayes, R., Moule, S., Mungall, K., Ormond, D., Quail, M.A., Rabinowitsch, E., Rutherford, K., Sanders, M., Sharp, S., Simmonds, M., Stevens, K., Whitehead, S., Barrell, B.G., Spratt, B.G., and Parkhill, J. (2004) Complete genomes of two clinical *Staphylococcus aureus* strains: evidence for the rapid evolution of virulence and drug resistance. *Proceedings of the National Academy of Sciences of the United States of America* **101**: 9786-9791.
- Horsburgh, M.J., Aish, J.L., White, I.J., Shaw, L., Lithgow, J.K., and Foster, S.J. (2002) sigmaB modulates virulence determinant expression and stress resistance: characterization of a functional rsbU strain derived from *Staphylococcus aureus* 8325-4. *Journal of Bacteriology* **184**: 5457-5467.

- Houston, P., Rowe, S.E., Pozzi, C., Waters, E.M., and O'Gara, J.P. (2011) Essential role for the major autolysin in the fibronectin-binding protein-mediated *Staphylococcus aureus* biofilm phenotype. *Infection and Immunity* **79**: 1153-1165.
- HSPC, (2016) Data on *S. aureus*/MRSA bloodstream infections from acute hospitals, 2004 – Q4 2016 (including all public and private hospitals, complete datasets of historic data and trends). In. www.hspc.ie: Health Protection Surveillance Centre, pp.
- Hu, J., Xu, T., Zhu, T., Lou, Q., Wang, X., Wu, Y., Huang, R., Liu, J., Liu, H., Yu, F., Ding, B., Huang, Y., Tong, W., and Qu, D. (2011) Monoclonal antibodies against accumulation-associated protein affect EPS biosynthesis and enhance bacterial accumulation of *Staphylococcus epidermidis*. *PLOS One* **6**: e20918.
- Hu, X., Neoh, K.G., Shi, Z., Kang, E.T., Poh, C., and Wang, W. (2010) An *in vitro* assessment of titanium functionalized with polysaccharides conjugated with vascular endothelial growth factor for enhanced osseointegration and inhibition of bacterial adhesion. *Biomaterials* **31**: 8854-8863.
- Irwin, J.J., Shoichet, B.K., Mysinger, M.M., Huang, N., Colizzi, F., Wassam, P., and Cao, Y. (2009) Automated docking screens: a feasibility study. *Journal of Medicinal Chemistry* **52**: 5712-5720.
- Irwin, J.J., Sterling, T., Mysinger, M.M., Bolstad, E.S., and Coleman, R.G. (2012) ZINC: a free tool to discover chemistry for biology. *Journal of Chemical Information and Modeling* **52**: 1757-1768.
- Jansen, K.U., Girgenti, D.Q., Scully, I.L., and Anderson, A.S. (2013) Vaccine review: "Staphylococcus aureus vaccines: problems and prospects". *Vaccine* **31**: 2723-2730.
- Jennings, J.A., Courtney, H.S., and Haggard, W.O. (2012) Cis-2-decenoic acid inhibits *S. aureus* growth and biofilm *in vitro*: a pilot study. *Clinical Orthopaedics and Related Research* **470**: 2663-2670.
- Jiang, W., Maniv, I., Arain, F., Wang, Y., Levin, B.R., and Marraffini, L.A. (2013) Dealing with the Evolutionary Downside of CRISPR Immunity: Bacteria and Beneficial Plasmids. *PLOS Genetics* **9**.

- Josefsson, E., Hartford, O., O'Brien, L., Patti, J.M., and Foster, T. (2001) Protection against experimental *Staphylococcus aureus* arthritis by vaccination with clumping factor A, a novel virulence determinant. *The Journal of Infectious Diseases* **184**: 1572-1580.
- Joshi, G.S., Spontak, J.S., Klapper, D.G., and Richardson, A.R. (2011) Arginine catabolic mobile element encoded *speG* abrogates the unique hypersensitivity of *Staphylococcus aureus* to exogenous polyamines. *Molecular Microbiology* **82**: 9-20.
- Junter, G.A., Thebault, P., and Lebrun, L. (2016) Polysaccharide-based antibiofilm surfaces. *Acta biomaterialia* **30**: 13-25.
- Kaplan, J.B., Rangunath, C., Velliyagounder, K., Fine, D.H., and Ramasubbu, N. (2004) Enzymatic detachment of *Staphylococcus epidermidis* biofilms. *Antimicrobial Agents and Chemotherapy* **48**: 2633-2636.
- Keane, F.M., Loughman, A., Valtulina, V., Brennan, M., Speziale, P., and Foster, T.J. (2007) Fibrinogen and elastin bind to the same region within the A domain of fibronectin binding protein A, an MSCRAMM of *Staphylococcus aureus*. *Molecular Microbiology* **63**: 711-723.
- Kelley, L.A., Mezulis, S., Yates, C.M., Wass, M.N., and Sternberg, M.J. (2015) The Phyre2 web portal for protein modeling, prediction and analysis. *Nature Protocols* **10**: 845-858.
- Kelley, L.A., and Sternberg, M.J. (2009) Protein structure prediction on the Web: a case study using the Phyre server. *Nature Protocols* **4**: 363-371.
- Kiedrowski, M.R., Kavanaugh, J.S., Malone, C.L., Mootz, J.M., Voyich, J.M., Smeltzer, M.S., Bayles, K.W., and Horswill, A.R. (2011) Nuclease modulates biofilm formation in community-associated methicillin-resistant *Staphylococcus aureus*. *PLOS One* **6**: e26714.
- Kim, H.K., Falugi, F., Thomer, L., Missiakas, D.M., and Schneewind, O. (2015) Protein A Suppresses Immune Responses during *Staphylococcus aureus* Bloodstream Infection in Guinea Pigs. *mBio* **6**.
- Kokai-Kun, J.F., Chanturiya, T., and Mond, J.J. (2009) Lysostaphin eradicates established *Staphylococcus aureus* biofilms in jugular vein catheterized mice. *The Journal of Antimicrobial Chemotherapy* **64**: 94-100.

- Kolodkin-Gal, I., Romero, D., Cao, S., Clardy, J., Kolter, R., and Losick, R. (2010) D-amino acids trigger biofilm disassembly. *Science (New York, N.Y.)* **328**: 627-629.
- Kuroda, M., Ohta, T., Uchiyama, I., Baba, T., Yuzawa, H., Kobayashi, I., Cui, L., Oguchi, A., Aoki, K., Nagai, Y., Lian, J., Ito, T., Kanamori, M., Matsumaru, H., Maruyama, A., Murakami, H., Hosoyama, A., Mizutani-Ui, Y., Takahashi, N.K., Sawano, T., Inoue, R., Kaito, C., Sekimizu, K., Hirakawa, H., Kuhara, S., Goto, S., Yabuzaki, J., Kanehisa, M., Yamashita, A., Oshima, K., Furuya, K., Yoshino, C., Shiba, T., Hattori, M., Ogasawara, N., Hayashi, H., and Hiramatsu, K. (2001) Whole genome sequencing of methicillin-resistant *Staphylococcus aureus*. *Lancet* **357**: 1225-1240.
- Lacey, K.A., Geoghegan, J.A., and McLoughlin, R.M. (2016) The Role of *Staphylococcus aureus* Virulence Factors in Skin Infection and Their Potential as Vaccine Antigens. *Pathogens (Basel, Switzerland)* **5**.
- Lauderdale, K.J., Malone, C.L., Boles, B.R., Morcuende, J., and Horswill, A.R. (2010) Biofilm dispersal of community-associated methicillin-resistant *Staphylococcus aureus* on orthopedic implant material. *Journal of Orthopaedic Research : official publication of the Orthopaedic Research Society* **28**: 55-61.
- Le, K.Y., Dastgheyb, S., Ho, T.V., and Otto, M. (2014) Molecular determinants of staphylococcal biofilm dispersal and structuring. *Frontiers in Cellular and Infection Microbiology* **4**: 167.
- Le, K.Y., and Otto, M. (2015) Quorum-sensing regulation in staphylococci-an overview. *Frontiers in Microbiology* **6**: 1174.
- Li, M., Du, X., Villaruz, A.E., Diep, B.A., Wang, D., Song, Y., Tian, Y., Hu, J., Yu, F., Lu, Y., and Otto, M. (2012) MRSA epidemic linked to a quickly spreading colonization and virulence determinant. *Nature Medicine* **18**: 816-819.
- Li, M.Z., and Elledge, S.J. (2012) SLIC: a method for sequence- and ligation-independent cloning. *Methods in Molecular Biology* **852**: 51-59.
- Liang, X., Garcia, B.L., Visai, L., Prabhakaran, S., Meenan, N.A., Potts, J.R., Humphries, M.J., and Hook, M. (2016) Allosteric Regulation of Fibronectin/alpha5beta1 Interaction by Fibronectin-Binding MSCRAMMs. *PLOS One* **11**: e0159118.

- Lister, J.L., and Horswill, A.R. (2014) *Staphylococcus aureus* biofilms: recent developments in biofilm dispersal. *Frontiers in Cellular and Infection Microbiology* **4**: 178.
- Loughman, A., Sweeney, T., Keane, F.M., Pietrocola, G., Speziale, P., and Foster, T.J. (2008) Sequence diversity in the A domain of *Staphylococcus aureus* fibronectin-binding protein A. *BMC Microbiology* **8**: 74.
- Ludwig, W., Seewaldt, E., Kilpper-Balz, R., Schleifer, K.H., Magrum, L., Woese, C.R., Fox, G.E., and Stackebrandt, E. (1985) The phylogenetic position of *Streptococcus* and *Enterococcus*. *Journal of General Microbiology* **131**: 543-551.
- Luo, M., Zhang, X., Zhang, S., Zhang, H., Yang, W., Zhu, Z., Chen, K., Bai, L., Wei, J., Huang, A., and Wang, D. (2017) Crystal Structure of an Invasivity-Associated Domain of SdrE in *S. aureus*. *PLOS One* **12**: e0168814.
- Maira-Litran, T., Bentancor, L.V., Bozkurt-Guzel, C., O'Malley, J.M., Cywes-Bentley, C., and Pier, G.B. (2012) Synthesis and evaluation of a conjugate vaccine composed of *Staphylococcus aureus* poly-N-acetyl-glucosamine and clumping factor A. *PLOS One* **7**: e43813.
- Mann, E.E., Rice, K.C., Boles, B.R., Endres, J.L., Ranjit, D., Chandramohan, L., Tsang, L.H., Smeltzer, M.S., Horswill, A.R., and Bayles, K.W. (2009) Modulation of eDNA release and degradation affects *Staphylococcus aureus* biofilm maturation. *PLOS One* **4**: e5822.
- Mashalidis, E.H., Sledz, P., Lang, S., and Abell, C. (2013) A three-stage biophysical screening cascade for fragment-based drug discovery. *Nature Protocols* **8**: 2309-2324.
- Mashruwala, A.A., Gries, C.M., Scherr, T.D., Kielian, T., and Boyd, J.M. (2017) SaeRS Is Responsive to Cellular Respiratory Status and Regulates Fermentative Biofilm Formation in *Staphylococcus aureus*. *Infection and Immunity* **85**.
- Mazmanian, S.K., Ton-That, H., and Schneewind, O. (2001) Sortase-catalysed anchoring of surface proteins to the cell wall of *Staphylococcus aureus*. *Molecular Microbiology* **40**: 1049-1057.
- McCormack, N., Foster, T.J., and Geoghegan, J.A. (2014) A short sequence within subdomain N1 of region A of the *Staphylococcus aureus* MSCRAMM clumping factor A is required for export and surface display. *Microbiology* **160**: 659-670.

- McCourt, J., O'Halloran, D.P., McCarthy, H., O'Gara, J.P., and Geoghegan, J.A., (2014) Fibronectin binding proteins are required for biofilm formation by community-associated methicillin resistant *Staphylococcus aureus* strain LAC. . In. FEMS Microbiology Letters.
- McDonnell, G., and Russell, A.D. (1999) Antiseptics and disinfectants: activity, action, and resistance. *Clinical Microbiology Reviews* **12**: 147-179.
- Merino, N., Toledo-Arana, A., Vergara-Irigaray, M., Valle, J., Solano, C., Calvo, E., Lopez, J.A., Foster, T.J., Penadés, J.R., and Lasa, I. (2009) Protein A-mediated multicellular behavior in *Staphylococcus aureus*. *Journal of Bacteriology* **191**: 832-843.
- Mertz, D., Frei, R., Jaussi, B., Tietz, A., Stebler, C., Fluckiger, U., and Widmer, A.F. (2007) Throat swabs are necessary to reliably detect carriers of *Staphylococcus aureus*. *Clinical Infectious Diseases* **45**: 475-477.
- Missiakas, D., and Schneewind, O. (2016) *Staphylococcus aureus* vaccines: Deviating from the carol. *Journal of Experimental Medicine* **213**: 1645-1653.
- Misstear, K., McNeela, E.A., Murphy, A.G., Geoghegan, J.A., O'Keeffe, K.M., Fox, J., Chan, K., Heuking, S., Collin, N., Foster, T.J., McLoughlin, R.M., and Lavelle, E.C. (2014) Targeted nasal vaccination provides antibody-independent protection against *Staphylococcus aureus*. *The Journal of Infectious Diseases* **209**: 1479-1484.
- Monk, I.R., Shah, I.M., Xu, M., Tan, M.W., and Foster, T.J. (2012) Transforming the untransformable: application of direct transformation to manipulate genetically *Staphylococcus aureus* and *Staphylococcus epidermidis*. *mBio* **3**.
- Monk, I.R., Tree, J.J., Howden, B.P., Stinear, T.P., and Foster, T.J. (2015) Complete Bypass of Restriction Systems for Major *Staphylococcus aureus* Lineages. *mBio* **6**: e00308-00315.
- Montanaro, L., Poggi, A., Visai, L., Ravaioli, S., Campoccia, D., Speziale, P., and Arciola, C.R. (2011) Extracellular DNA in biofilms. *The International Journal of Artificial Organs* **34**: 824-831.
- Moreillon, P., Entenza, J.M., Francioli, P., McDevitt, D., Foster, T.J., Francois, P., and Vaudaux, P. (1995) Role of *Staphylococcus aureus* coagulase and clumping

- factor in pathogenesis of experimental endocarditis. *Infection and Immunity* **63**: 4738-4743.
- Mulcahy, M.E., Geoghegan, J.A., Monk, I.R., O'Keeffe, K.M., Walsh, E.J., Foster, T.J., and McLoughlin, R.M. (2012) Nasal colonisation by *Staphylococcus aureus* depends upon clumping factor B binding to the squamous epithelial cell envelope protein loricrin. *PLOS Pathogens* **8**: e1003092.
- Munoz, P., Hortal, J., Giannella, M., Barrio, J.M., Rodriguez-Creixems, M., Perez, M.J., Rincon, C., and Bouza, E. (2008) Nasal carriage of *S. aureus* increases the risk of surgical site infection after major heart surgery. *The Journal of Hospital Infection* **68**: 25-31.
- NCEC, (2013) National Clinical Effectiveness Committee Prevention and control methicillin-resistant *Staphylococcus aureus* (MRSA) national clinical guideline No. 2 2013. National Clinical Effectiveness Committee National Clinical Effectiveness Committee (NCEC).
- O'Brien, L., Kerrigan, S.W., Kaw, G., Hogan, M., Penadés, J., Litt, D., Fitzgerald, D.J., Foster, T.J., and Cox, D. (2002a) Multiple mechanisms for the activation of human platelet aggregation by *Staphylococcus aureus*: roles for the clumping factors ClfA and ClfB, the serine-aspartate repeat protein SdrE and protein A. *Molecular Microbiology* **44**: 1033-1044.
- O'Brien, L.M., Walsh, E.J., Massey, R.C., Peacock, S.J., and Foster, T.J. (2002b) *Staphylococcus aureus* clumping factor B (ClfB) promotes adherence to human type I cytokeratin 10: implications for nasal colonization. *Cellular Microbiology* **4**: 759-770.
- O'Halloran, D.P., Wynne, K., and Geoghegan, J.A. (2015) Protein A is released into the *Staphylococcus aureus* culture supernatant with an unprocessed sorting signal. *Infection and Immunity* **83**: 1598-1609.
- O'Neill, E., Pozzi, C., Houston, P., Humphreys, H., Robinson, D.A., Loughman, A., Foster, T.J., and O'Gara, J.P. (2008) A novel *Staphylococcus aureus* biofilm phenotype mediated by the fibronectin-binding proteins, FnBPA and FnBPB. *Journal of Bacteriology* **190**: 3835-3850.

- O'Neill, E., Pozzi, C., Houston, P., Smyth, D., Humphreys, H., Robinson, D.A., and O'Gara, J.P. (2007) Association between methicillin susceptibility and biofilm regulation in *Staphylococcus aureus* isolates from device-related infections. *Journal of Clinical Microbiology* **45**: 1379-1388.
- O'Riordan, K., and Lee, J.C. (2004) *Staphylococcus aureus* capsular polysaccharides. *Clinical Microbiology Reviews* **17**: 218-234.
- Olson, M.E., Ceri, H., Morck, D.W., Buret, A.G., and Read, R.R. (2002) Biofilm bacteria: formation and comparative susceptibility to antibiotics. *Canadian Journal of Veterinary Research* **66**: 86-92.
- Olson, M.E., Garvin, K.L., Fey, P.D., and Rupp, M.E. (2006) Adherence of *Staphylococcus epidermidis* to biomaterials is augmented by PIA. *Clinical Orthopaedics and Related Research* **451**: 21-24.
- Otto, M. (2008) Staphylococcal biofilms. *Current Topics in Microbiology and Immunology* **322**: 207-228.
- Paharik, A.E., and Horswill, A.R. (2016) The Staphylococcal Biofilm: Adhesins, Regulation, and Host Response. *Microbiology Spectrum* **4**.
- Palazzolo-Ballance, A.M., Reniere, M.L., Braughton, K.R., Sturdevant, D.E., Otto, M., Kreiswirth, B.N., Skaar, E.P., and DeLeo, F.R. (2008) Neutrophil microbicides induce a pathogen survival response in community-associated methicillin-resistant *Staphylococcus aureus*. *Journal of Immunology (Baltimore, Md. : 1950)* **180**: 500-509.
- Palumbo, F.S., Bavuso Volpe, A., Cusimano, M.G., Pitarresi, G., Giammona, G., and Schillaci, D. (2015) A polycarboxylic/amino functionalized hyaluronic acid derivative for the production of pH sensible hydrogels in the prevention of bacterial adhesion on biomedical surfaces. *International Journal of Pharmaceutics* **478**: 70-77.
- Parfentjev, I.A., and Catelli, A.R. (1964) TOLERANCE OF *STAPHYLOCOCCUS AUREUS* TO SODIUM CHLORIDE. *Journal of Bacteriology* **88**: 1-3.
- Park, H.Y., Kim, C.R., Huh, I.S., Jung, M.Y., Seo, E.Y., Park, J.H., Lee, D.Y., and Yang, J.M. (2013) *Staphylococcus aureus* Colonization in Acute and Chronic Skin Lesions of Patients with Atopic Dermatitis. *Annals of Dermatology* **25**: 410-416.

- Peacock, S.J., Day, N.P., Thomas, M.G., Berendt, A.R., and Foster, T.J. (2000) Clinical isolates of *Staphylococcus aureus* exhibit diversity in fnb genes and adhesion to human fibronectin. *The Journal of Infection* **41**: 23-31.
- Peacock, S.J., and Paterson, G.K. (2015) Mechanisms of Methicillin Resistance in *Staphylococcus aureus*. *Annual Review of Biochemistry* **84**: 577-601.
- Pelz, A., Wieland, K.P., Putzbach, K., Hentschel, P., Albert, K., and Gotz, F. (2005) Structure and biosynthesis of staphyloxanthin from *Staphylococcus aureus*. *Journal of Biological Chemistry* **280**: 32493-32498.
- Periasamy, S., Joo, H.S., Duong, A.C., Bach, T.H., Tan, V.Y., Chatterjee, S.S., Cheung, G.Y., and Otto, M. (2012) How *Staphylococcus aureus* biofilms develop their characteristic structure. *Proceedings of the National Academy of Sciences of the United States of America* **109**: 1281-1286.
- Pettersen, E.F., Goddard, T.D., Huang, C.C., Couch, G.S., Greenblatt, D.M., Meng, E.C., and Ferrin, T.E. (2004) UCSF Chimera--a visualization system for exploratory research and analysis. *Journal of Computational Chemistry* **25**: 1605-1612.
- Pietrocola, G., Nobile, G., Gianotti, V., Zapotoczna, M., Foster, T.J., Geoghegan, J.A., and Speziale, P. (2016) Molecular Interactions of Human Plasminogen with Fibronectin-binding Protein B (FnBPB), a Fibrinogen/Fibronectin-binding Protein from *Staphylococcus aureus*. *Journal of Biological Chemistry* **291**: 18148-18162.
- Pirnazar, P., Wolinsky, L., Nachnani, S., Haake, S., Pilloni, A., and Bernard, G.W. (1999) Bacteriostatic effects of hyaluronic acid. *Journal of Periodontology* **70**: 370-374.
- Planet, P.J., LaRussa, S.J., Dana, A., Smith, H., Xu, A., Ryan, C., Uhlemann, A.C., Boundy, S., Goldberg, J., Narechania, A., Kulkarni, R., Ratner, A.J., Geoghegan, J.A., Kolokotronis, S.O., and Prince, A. (2013) Emergence of the epidemic methicillin-resistant *Staphylococcus aureus* strain USA300 coincides with horizontal transfer of the arginine catabolic mobile element and speG-mediated adaptations for survival on skin. *mBio* **4**: e00889-00813.
- Ponnuraj, K., Bowden, M.G., Davis, S., Gurusiddappa, S., Moore, D., Choe, D., Xu, Y., Hook, M., and Narayana, S.V. (2003) A "dock, lock, and latch" structural model for a staphylococcal adhesin binding to fibrinogen. *Cell* **115**: 217-228.

- Powers, M.E., and Wardenburg, J.B. (2014) Igniting the Fire: *Staphylococcus aureus* Virulence Factors in the Pathogenesis of Sepsis. *PLOS Pathogens* **10**.
- Que, Y.A., Haefliger, J.A., Piroth, L., Francois, P., Widmer, E., Entenza, J.M., Sinha, B., Herrmann, M., Francioli, P., Vaudaux, P., and Moreillon, P. (2005) Fibrinogen and fibronectin binding cooperate for valve infection and invasion in *Staphylococcus aureus* experimental endocarditis. *Journal of Experimental Medicine* **201**: 1627-1635.
- Rice, K.C., Mann, E.E., Endres, J.L., Weiss, E.C., Cassat, J.E., Smeltzer, M.S., and Bayles, K.W. (2007) The *cidA* murein hydrolase regulator contributes to DNA release and biofilm development in *Staphylococcus aureus*. *Proceedings of the National Academy of Sciences of the United States of America* **104**: 8113-8118.
- Riethmuller, C., McAleer, M.A., Koppes, S.A., Abdayem, R., Franz, J., Haftek, M., Campbell, L.E., MacCallum, S.F., McLean, W.H.I., Irvine, A.D., and Kezic, S. (2015) Filaggrin breakdown products determine corneocyte conformation in patients with atopic dermatitis. *The Journal of Allergy and Clinical Immunology* **136**: 1573-1580.e1572.
- Roche, F.M., Downer, R., Keane, F., Speziale, P., Park, P.W., and Foster, T.J. (2004) The N-terminal A domain of fibronectin-binding proteins A and B promotes adhesion of *Staphylococcus aureus* to elastin. *Journal of Biological Chemistry* **279**: 38433-38440.
- Rohde, H., Burdelski, C., Bartscht, K., Hussain, M., Buck, F., Horstkotte, M.A., Knobloch, J.K., Heilmann, C., Herrmann, M., and Mack, D. (2005) Induction of *Staphylococcus epidermidis* biofilm formation via proteolytic processing of the accumulation-associated protein by staphylococcal and host proteases. *Molecular Microbiology* **55**: 1883-1895.
- Rudkin, J.K., Edwards, A.M., Bowden, M.G., Brown, E.L., Pozzi, C., Waters, E.M., Chan, W.C., Williams, P., O'Gara, J.P., and Massey, R.C. (2012) Methicillin resistance reduces the virulence of healthcare-associated methicillin-resistant *Staphylococcus aureus* by interfering with the agr quorum sensing system. *The Journal of Infectious Diseases* **205**: 798-806.
- Sanchez, C.J., Jr., Prieto, E.M., Krueger, C.A., Zienkiewicz, K.J., Romano, D.R., Ward, C.L., Akers, K.S., Guelcher, S.A., and Wenke, J.C. (2013) Effects of local delivery

- of D-amino acids from biofilm-dispersive scaffolds on infection in contaminated rat segmental defects. *Biomaterials* **34**: 7533-7543.
- Sanchez, C.J., Shivshankar, P., Stol, K., Trakhtenbroit, S., Sullam, P.M., Sauer, K., Hermans, P.W., and Orihuela, C.J. (2010) The pneumococcal serine-rich repeat protein is an intra-species bacterial adhesin that promotes bacterial aggregation *in vivo* and in biofilms. *PLOS Pathogens* **6**: e1001044.
- Sanford, B.A., Thomas, V.L., and Ramsay, M.A. (1989) Binding of staphylococci to mucus *in vivo* and *in vitro*. *Infection and Immunity* **57**: 3735-3742.
- Schaeffer, C.R., Woods, K.M., Longo, G.M., Kiedrowski, M.R., Paharik, A.E., Buttner, H., Christner, M., Boissy, R.J., Horswill, A.R., Rohde, H., and Fey, P.D. (2015) Accumulation-associated protein enhances *Staphylococcus epidermidis* biofilm formation under dynamic conditions and is required for infection in a rat catheter model. *Infection and Immunity* **83**: 214-226.
- Schaffer, A.C., Solinga, R.M., Cocchiario, J., Portoles, M., Kiser, K.B., Risley, A., Randall, S.M., Valtulina, V., Speziale, P., Walsh, E., Foster, T., and Lee, J.C. (2006) Immunization with *Staphylococcus aureus* clumping factor B, a major determinant in nasal carriage, reduces nasal colonization in a murine model. *Infection and Immunity* **74**: 2145-2153.
- Scherr, T.D., Heim, C.E., Morrison, J.M., and Kielian, T. (2014) Hiding in Plain Sight: Interplay between Staphylococcal Biofilms and Host Immunity. *Frontiers in Immunology* **5**: 37.
- Scherr, T.D., Roux, C.M., Hanke, M.L., Angle, A., Dunman, P.M., and Kielian, T. (2013) Global transcriptome analysis of *Staphylococcus aureus* biofilms in response to innate immune cells. *Infection and Immunity* **81**: 4363-4376.
- Schmidt, C.S., White, C.J., Ibrahim, A.S., Filler, S.G., Fu, Y., Yeaman, M.R., Edwards, J.E., Jr., and Hennessey, J.P., Jr. (2012) NDV-3, a recombinant alum-adjuvanted vaccine for *Candida* and *Staphylococcus aureus*, is safe and immunogenic in healthy adults. *Vaccine* **30**: 7594-7600.
- Schneewind, O., Mihaylova-Petkov, D., and Model, P. (1993) Cell wall sorting signals in surface proteins of Gram-positive bacteria. *The Embo Journal* **12**: 4803-4811.
- Schroeder, K., Jularic, M., Horsburgh, S.M., Hirschhausen, N., Neumann, C., Bertling, A., Schulte, A., Foster, S., Kehrel, B.E., Peters, G., and Heilmann, C. (2009)

- Molecular characterization of a novel *Staphylococcus aureus* surface protein (SasC) involved in cell aggregation and biofilm accumulation. *PLOS One* **4**: e7567.
- Shahrooei, M., Hira, V., Khodaparast, L., Khodaparast, L., Stijlemans, B., Kucharíková, S., Burghout, P., Hermans, P.W.M., and Van Eldere, J. (2012) Vaccination with SesC Decreases *Staphylococcus epidermidis* Biofilm Formation. *Infection and Immunity* **80**: 3660-3668.
- Sharp, J.A., Echague, C.G., Hair, P.S., Ward, M.D., Nyalwidhe, J.O., Geoghegan, J.A., Foster, T.J., and Cunnion, K.M. (2012) *Staphylococcus aureus* surface protein SdrE binds complement regulator factor H as an immune evasion tactic. *PLOS One* **7**: e38407.
- Siboo, I.R., Chaffin, D.O., Rubens, C.E., and Sullam, P.M. (2008) Characterization of the accessory Sec system of *Staphylococcus aureus*. *Journal of Bacteriology* **190**: 6188-6196.
- Sievers, F., Wilm, A., Dineen, D., Gibson, T.J., Karplus, K., Li, W., Lopez, R., McWilliam, H., Remmert, M., Soding, J., Thompson, J.D., and Higgins, D.G. (2011) Fast, scalable generation of high-quality protein multiple sequence alignments using Clustal Omega. *Molecular Systems Biology* **7**: 539.
- Singh, R., Ray, P., Das, A., and Sharma, M. (2009) Role of persisters and small-colony variants in antibiotic resistance of planktonic and biofilm-associated *Staphylococcus aureus*: an *in vitro* study. *Journal of Medical Microbiology* **58**: 1067-1073.
- Sinha, B., Francois, P., Que, Y.A., Hussain, M., Heilmann, C., Moreillon, P., Lew, D., Krause, K.H., Peters, G., and Herrmann, M. (2000) Heterologously expressed *Staphylococcus aureus* fibronectin-binding proteins are sufficient for invasion of host cells. *Infection and Immunity* **68**: 6871-6878.
- Spaan, A.N., Surewaard, B.G., Nijland, R., and van Strijp, J.A. (2013) Neutrophils versus *Staphylococcus aureus*: a biological tug of war. *Annu Rev Microbiol* **67**: 629-650.
- Spangenberg, T., Burrows, J.N., Kowalczyk, P., McDonald, S., Wells, T.N., and Willis, P. (2013) The open access malaria box: a drug discovery catalyst for neglected diseases. *PLOS One* **8**: e62906.

- Speziale, P., Pietrocola, G., Foster, T.J., and Geoghegan, J.A. (2014) Protein-based biofilm matrices in Staphylococci. *Frontiers in Cellular and Infection Microbiology* **4**: 171.
- Stackebrandt, E., and Teuber, M. (1988) Molecular taxonomy and phylogenetic position of lactic acid bacteria. *Biochimie* **70**: 317-324.
- Stemberk, V., Jones, R.P., Moroz, O., Atkin, K.E., Edwards, A.M., Turkenburg, J.P., Leech, A.P., Massey, R.C., and Potts, J.R. (2014) Evidence for steric regulation of fibrinogen binding to *Staphylococcus aureus* fibronectin-binding protein A (FnBPA). *Journal of Biological Chemistry* **289**: 12842-12851.
- Thammavongsa, V., Kim, H.K., Missiakas, D., and Schneewind, O. (2015) Staphylococcal manipulation of host immune responses. *Nature Reviews Microbiology* **13**: 529-543.
- Thurlow, L.R., Hanke, M.L., Fritz, T., Angle, A., Aldrich, A., Williams, S.H., Engebretsen, I.L., Bayles, K.W., Horswill, A.R., and Kielian, T. (2011) *Staphylococcus aureus* biofilms prevent macrophage phagocytosis and attenuate inflammation *in vivo*. *Journal of Immunology (Baltimore, Md. : 1950)* **186**: 6585-6596.
- Tong, S.Y., Davis, J.S., Eichenberger, E., Holland, T.L., and Fowler, V.G., Jr. (2015) *Staphylococcus aureus* infections: epidemiology, pathophysiology, clinical manifestations, and management. *Clinical Microbiology Reviews* **28**: 603-661.
- Tormo, M.A., Knecht, E., Gotz, F., Lasa, I., and Penades, J.R. (2005) Bap-dependent biofilm formation by pathogenic species of *Staphylococcus*: evidence of horizontal gene transfer? *Microbiology* **151**: 2465-2475.
- Trott, O., and Olson, A.J. (2010) AutoDock Vina: improving the speed and accuracy of docking with a new scoring function, efficient optimization, and multithreading. *Journal of Computational Chemistry* **31**: 455-461.
- Tzagoloff, H., and Novick, R. (1977) Geometry of cell division in *Staphylococcus aureus*. *Journal of Bacteriology* **129**: 343-350.
- van Belkum, A., Verkaik, N.J., de Vogel, C.P., Boelens, H.A., Verveer, J., Nouwen, J.L., Verbrugh, H.A., and Wertheim, H.F. (2009) Reclassification of *Staphylococcus aureus* nasal carriage types. *The Journal of Infectious Diseases* **199**: 1820-1826.
- Vanassche, T., Peetermans, M., Van Aelst, L.N., Peetermans, W.E., Verhaegen, J., Missiakas, D.M., Schneewind, O., Hoylaerts, M.F., and Verhamme, P. (2013)

- The role of staphylothrombin-mediated fibrin deposition in catheter-related *Staphylococcus aureus* infections. *The Journal of Infectious Diseases* **208**: 92-100.
- Vaudaux, P.E., Francois, P., Proctor, R.A., McDevitt, D., Foster, T.J., Albrecht, R.M., Lew, D.P., Wabers, H., and Cooper, S.L. (1995) Use of adhesion-defective mutants of *Staphylococcus aureus* to define the role of specific plasma proteins in promoting bacterial adhesion to canine arteriovenous shunts. *Infection and Immunity* **63**: 585-590.
- Vergara-Irigaray, M., Valle, J., Merino, N., Latasa, C., Garcia, B., Ruiz de Los Mozos, I., Solano, C., Toledo-Arana, A., Penades, J.R., and Lasa, I. (2009) Relevant role of fibronectin-binding proteins in *Staphylococcus aureus* biofilm-associated foreign-body infections. *Infection and Immunity* **77**: 3978-3991.
- Visai, L., Yanagisawa, N., Josefsson, E., Tarkowski, A., Pezzali, I., Rooijackers, S.H., Foster, T.J., and Speziale, P. (2009) Immune evasion by *Staphylococcus aureus* conferred by iron-regulated surface determinant protein IsdH. *Microbiology* **155**: 667-679.
- von Eiff, C., Becker, K., Machka, K., Stammer, H., and Peters, G. (2001) Nasal carriage as a source of *Staphylococcus aureus* bacteremia. Study Group. *New England Journal of Medicine* **344**: 11-16.
- Vuong, C., Voyich, J.M., Fischer, E.R., Braughton, K.R., Whitney, A.R., DeLeo, F.R., and Otto, M. (2004) Polysaccharide intercellular adhesin (PIA) protects *Staphylococcus epidermidis* against major components of the human innate immune system. *Cellular Microbiology* **6**: 269-275.
- Walsh, E.J., Miajlovic, H., Gorkun, O.V., and Foster, T.J. (2008) Identification of the *Staphylococcus aureus* MSCRAMM clumping factor B (ClfB) binding site in the alphaC-domain of human fibrinogen. *Microbiology* **154**: 550-558.
- Walsh, E.J., O'Brien, L.M., Liang, X., Hook, M., and Foster, T.J. (2004) Clumping factor B, a fibrinogen-binding MSCRAMM (microbial surface components recognizing adhesive matrix molecules) adhesin of *Staphylococcus aureus*, also binds to the tail region of type I cytokeratin 10. *Journal of Biological Chemistry* **279**: 50691-50699.

- Wang, R., Khan, B.A., Cheung, G.Y., Bach, T.H., Jameson-Lee, M., Kong, K.F., Queck, S.Y., and Otto, M. (2011) *Staphylococcus epidermidis* surfactant peptides promote biofilm maturation and dissemination of biofilm-associated infection in mice. *The Journal of Clinical Investigation* **121**: 238-248.
- Wang, X., Ge, J., Liu, B., Hu, Y., and Yang, M. (2013) Structures of SdrD from *Staphylococcus aureus* reveal the molecular mechanism of how the cell surface receptors recognize their ligands. *Protein & Cell* **4**: 277-285.
- Wann, E.R., Gurusiddappa, S., and Hook, M. (2000) The fibronectin-binding MSCRAMM FnBPA of *Staphylococcus aureus* is a bifunctional protein that also binds to fibrinogen. *Journal of Biological Chemistry* **275**: 13863-13871.
- Weidenmaier, C., Goerke, C., and Wolz, C. (2012) *Staphylococcus aureus* determinants for nasal colonization. *Trends in Microbiology* **20**: 243-250.
- Weidenmaier, C., Kokai-Kun, J.F., Kristian, S.A., Chanturiya, T., Kalbacher, H., Gross, M., Nicholson, G., Neumeister, B., Mond, J.J., and Peschel, A. (2004) Role of teichoic acids in *Staphylococcus aureus* nasal colonization, a major risk factor in nosocomial infections. *Nature Medicine* **10**: 243-245.
- Weidenmaier, C., Kokai-Kun, J.F., Kulauzovic, E., Kohler, T., Thumm, G., Stoll, H., Gotz, F., and Peschel, A. (2008) Differential roles of sortase-anchored surface proteins and wall teichoic acid in *Staphylococcus aureus* nasal colonization. *International Journal of Medical Microbiology : IJMM* **298**: 505-513.
- Wells, J.M., Robinson, K., Chamberlain, L.M., Schofield, K.M., and Le Page, R.W. (1996) Lactic acid bacteria as vaccine delivery vehicles. *Antonie Van Leeuwenhoek* **70**: 317-330.
- Wertheim, H.F., Vos, M.C., Ott, A., van Belkum, A., Voss, A., Kluytmans, J.A., van Keulen, P.H., Vandenbroucke-Grauls, C.M., Meester, M.H., and Verbrugh, H.A. (2004) Risk and outcome of nosocomial *Staphylococcus aureus* bacteraemia in nasal carriers versus non-carriers. *Lancet* **364**: 703-705.
- Wertheim, H.F., Walsh, E., Choudhury, R., Melles, D.C., Boelens, H.A., Miajlovic, H., Verbrugh, H.A., Foster, T., and van Belkum, A. (2008) Key role for clumping factor B in *Staphylococcus aureus* nasal colonization of humans. *PLOS Medicine* **5**: e17.

- WHO, (2014) Antimicrobial resistance: global report on surveillance 2014. <http://www.who.int>: World Health Organization.
- Wu, J.A., Kusuma, C., Mond, J.J., and Kokai-Kun, J.F. (2003) Lysothaphin disrupts *Staphylococcus aureus* and *Staphylococcus epidermidis* biofilms on artificial surfaces. *Antimicrobial Agents and Chemotherapy* **47**: 3407-3414.
- Xia, G., Kohler, T., and Peschel, A. (2010) The wall teichoic acid and lipoteichoic acid polymers of *Staphylococcus aureus*. *International Journal of Medical Microbiology : IJMM* **300**: 148-154.
- Xiang, H., Feng, Y., Wang, J., Liu, B., Chen, Y., Liu, L., Deng, X., and Yang, M. (2012) Crystal structures reveal the multi-ligand binding mechanism of *Staphylococcus aureus* ClfB. *PLOS Pathogens* **8**: e1002751.
- Yang, J., Yan, R., Roy, A., Xu, D., Poisson, J., and Zhang, Y. (2015) The I-TASSER Suite: protein structure and function prediction. *Nature Methods* **12**: 7-8.
- Yang, Y.H., Jiang, Y.L., Zhang, J., Wang, L., Bai, X.H., Zhang, S.J., Ren, Y.M., Li, N., Zhang, Y.H., Zhang, Z., Gong, Q., Mei, Y., Xue, T., Zhang, J.R., Chen, Y., and Zhou, C.Z. (2014) Structural insights into SraP-mediated *Staphylococcus aureus* adhesion to host cells. *PLOS Pathogens* **10**: e1004169.
- Zapotoczna, M., Jevnikar, Z., Miajlovic, H., Kos, J., and Foster, T.J. (2013) Iron-regulated surface determinant B (IsdB) promotes *Staphylococcus aureus* adherence to and internalization by non-phagocytic human cells. *Cellular Microbiology* **15**: 1026-1041.
- Zapotoczna, M., McCarthy, H., Rudkin, J.K., O'Gara, J.P., and O'Neill, E. (2015) An Essential Role for Coagulase in *Staphylococcus aureus* Biofilm Development Reveals New Therapeutic Possibilities for Device-Related Infections. *The Journal of Infectious Diseases* **212**: 1883-1893.
- Zapotoczna, M., O'Neill, E., and O'Gara, J.P. (2016) Untangling the Diverse and Redundant Mechanisms of *Staphylococcus aureus* Biofilm Formation. *PLOS Pathogens* **12**: e1005671.
- Zhang, J., Liu, H., Zhu, K., Gong, S., Dramsi, S., Wang, Y.T., Li, J., Chen, F., Zhang, R., Zhou, L., Lan, L., Jiang, H., Schneewind, O., Luo, C., and Yang, C.G. (2014) Antiinfective therapy with a small molecule inhibitor of *Staphylococcus aureus*

- sortase. *Proceedings of the National Academy of Sciences of the United States of America* **111**: 13517-13522.
- Zhang, X., Wu, M., Zhuo, W., Gu, J., Zhang, S., Ge, J., and Yang, M. (2015) Crystal structures of Bbp from *Staphylococcus aureus* reveal the ligand binding mechanism with Fibrinogen alpha. *Protein & Cell* **6**: 757-766.
- Zhang, Y. (2008) I-TASSER server for protein 3D structure prediction. *BMC Bioinformatics* **9**: 40.
- Zhang, Y., Wu, M., Hang, T., Wang, C., Yang, Y., Pan, W., Zang, J., Zhang, M., and Zhang, X. (2017) *Staphylococcus aureus* SdrE captures complement factor H's C-terminus via a novel 'close, dock, lock and latch' mechanism for complement evasion. *The Biochemical Journal* **474**: 1619-1631.
- Zimmerli, W., Waldvogel, F.A., Vaudaux, P., and Nydegger, U.E. (1982) Pathogenesis of foreign body infection: description and characteristics of an animal model. *The Journal of Infectious Diseases* **146**: 487-497.
- Zong, Y., Xu, Y., Liang, X., Keene, D.R., Hook, A., Gurusiddappa, S., Hook, M., and Narayana, S.V. (2005) A 'Collagen Hug' model for *Staphylococcus aureus* CNA binding to collagen. *The Embo Journal* **24**: 4224-4236.